SEISMIC RESPONSE OF PORT AND HARBOR FACILITIES

by

S.D. Werner
S.J. Hung

October 1982

AGBABIAN ASSOCIATES

El Segundo, California

50272-101

REPORT DOCUMENTATION PAGE	1. REPORT NO. NSF/CEE-82057	2.	3. Recipient's Accession No. PB8 3 145 49 0

4. Title and Subtitle
Seismic Response of Port and Harbor Facilities,
1982 Final Report

5. Report Date
October 1982

6.

7. Author(s)
S.D. Werner, S.J. Hung

8. Performing Organization Rept. No.
R-8122-5395

9. Performing Organization Name and Address
Agbabian Associates
250 North Nash Street
El Segundo, CA 90245

10. Project/Task/Work Unit No.

11. Contract(C) or Grant(G) No.
(C)
(G) CEE8012337

12. Sponsoring Organization Name and Address
Directorate for Engineering (ENG)
National Science Foundation
1800 G Street, N.W.
Washington, DC 20550

13. Type of Report & Period Covered

14.

15. Supplementary Notes
Submitted by: Communications Program (OPRM)
National Science Foundation
Washington, DC 20550

16. Abstract (Limit: 200 words)

This report evaluates the seismic response characteristics of port and harbor facilities in terms of: (1) the lessons to be learned from the observed behavior of such facilities during earthquakes; (2) the adequacy of their current seismic design provisions; and (3) the use of dynamic analysis to enhance these design provisions. It was found that: (1) the potential for damage to port and harbor facilities is most strongly related to porewater pressure buildup in the surrounding soil materials; (2) the current seismic design provisions for such facilities often fail to consider many of the possible effects of earthquake ground motions; (3) dynamic analysis can enhance the earthquake resistant design of port and harbor facilities; and (4) deterministic total stress methods of dynamic analysis are applicable to port and harbor facilities. The continuing development of deterministic effective stress methods and probabilistic methods should add significantly to these existing dynamic stress capabilities.

17. Document Analysis a. Descriptors

Earthquakes
Earthquake resistant structures
Ports
Harbors

Damage
Soils
Vibration

b. Identifiers/Open-Ended Terms

Ground motion
Porewater pressure

S.J. Hung, /PI

c. COSATI Field/Group

18. Availability Statement	19. Security Class (This Report)	21. No. of Pages
NTIS	20. Security Class (This Page)	22. Price

(See ANSI–Z39.18)   See Instructions on Reverse

OPTIONAL FORM 272 (4–77)
(Formerly NTIS–35)
Department of Commerce

SEISMIC RESPONSE OF PORT AND HARBOR FACILITIES

by

S.D. Werner
S.J. Hung

October 1982

AGBABIAN ASSOCIATES
El Segundo, California

i

ABSTRACT

Many port and harbor facilities throughout the world are located in highly seismic regions, and such facilities are susceptible to extensive damage from earthquake ground shaking. In view of this, and the serious consequences of the earthquake-related loss of a major port, this research program has investigated the seismic response characteristics of port and harbor facilities. The particular issues addressed by the program were (1) the lessons that can be learned from the extent, type, and causes of the damage induced to port and harbor facilities by prior earthquakes; (2) the adequacy of the current seismic design provisions for such facilities; and (3) the applicability of dynamic analysis as a means for enhancing these design provisions. The principle findings of the program were that (1) past earthquakes have shown that the potential for significant damage to port and harbor facilities is most strongly related to porewater pressure buildup in the surrounding soil materials; (2) the current seismic design provisions for such facilities often fail to take proper account of many of the possible effects of earthquake ground motions; (3) dynamic analysis can enhance the earthquake-resistant design of port and harbor facilities, and should be incorporated to a much greater extent into their seismic design provisions; and (4) deterministic total stress methods of dynamic analysis are applicable to port and harbor facilities at this time, and the continuing development of deterministic effective stress methods and probabilistic methods should add significantly to these existing dynamic analysis capabilities.

ACKNOWLEDGMENTS

v

Preceding page blank

- D.J. Leeds (engineering seismologist), Los Angeles

- Naval Civil Engineering Laboratory, Pt. Hueneme, California--J. Ferritto, S. Takahashi, and N.D. Albertsen

- Naval Facilities Engineering Command, San Bruno, California--D.A. Zignant and R. Beckwith

- Port of Los Angeles--E.K. Clark and M. Hirata

- Port of Long Beach--E.D. Allen and H. Fong

- Port of Oakland--J.F. Aidoo

- Port of San Francisco--V. Kiisk, J. Kellogg, J.C. Storer, and J.T.P. Louie

TABLE OF CONTENTS

TABLE OF CONTENTS (Concluded)

CHAPTER 1

OVERVIEW OF RESEARCH PROGRAM

1.1 PROGRAM OBJECTIVES

An important component of regional, national, and world-wide lifeline systems is port and harbor facilities. Such facilities function to load, unload, ship, and store cargoes of materiel and personnel, and to provide for repair and maintenance operations for support of this function. The interruption of this vital function, for any reason, could result in serious hardships and far-reaching economic consequences.

Many port and harbor facilities are located in highly seismic regions, and experience from past major earthquakes has shown that such facilities are susceptible to extensive earthquake-induced damage and property loss (e.g., Kuribayashi and Tazaki, 1979). In view of this, Agbabian Associates has carried out a multiyear research program to investigate how port and harbor facilities respond to strong earthquake motions, and how they can be designed and analyzed to resist these seismic effects. In particular, this program, carried out under National Science Foundation sponsorship, has addressed the following issues:

- How have port and harbor facilities been damaged during past earthquakes, and what lessons can be learned from these damage observations?

- How are port and harbor facilities currently designed to resist earthquakes, and what are the merits and limitations of these design procedures?

- How can current dynamic analysis procedures be used to enhance our ability to design port and harbor facilities against earthquake ground shaking effects?

• What future analytical development efforts should be undertaken to further improve our understanding of the behavior of port and harbor facilities during earthquakes, as well as our current seismic design capabilities?

This report presents the findings of this program in a form that can be disseminated to consulting engineers, port authority personnel, and government personnel engaged in the design and/or administration of port and harbor facilities. It is intended to provide guidance for appropriate enhancement of the seismic design and analysis procedures for these facilities, so that their vulnerability to earthquake-induced ground shaking can be reduced.

1.2 PROGRAM SCOPE

To fulfill the above objectives, this research program has involved the following technical efforts:

• A review and compilation of available documentation from the United States, Chile, and Japan regarding the susceptibility of port and harbor facilities to strong earthquakes.

• From this compilation, an identification of the primary modes and causes of damage suffered by port and harbor facilities during earthquakes.

• An evaluation of current seismic design provisions for port and harbor facilities.

• An assessment of the applicability of current dynamic analysis techniques to the seismic design of port and harbor facilities, and an identification of directions for additional development of such techniques that might enhance our seismic design capabilities in the future.

- Implementation of an illustrative dynamic analysis that shows the kinds of valuable design-related information that can be obtained from such analyses for port and harbor facilities.

It is noted that the above efforts pertain only to effects of dynamic earthquake-induced ground shaking on the behavior of structures and the surrounding soil media at ports and harbors. Consideration of the additional effects of earthquake-induced tsunamis, which are also important for port and harbor facilities, is beyond the scope of this research program.

1.3 REPORT ORGANIZATION

This report is divided into five main chapters. The remainder of this first chapter contains a summary of the results that are described in more detail in subsequent chapters. Chapter 2 contains results of our compilation and assessment of prior information pertaining to how port and harbor facilities have fared during past earthquakes. Our review and evaluation of current seismic design provisions for port and harbor facilities is provided in Chapter 3, and Chapter 4 explores how these design provisions can be enhanced by incorporating dynamic analysis techniques. Our illustrative dynamic analysis, carried out for an actual sheet-pile bulkhead structure in Japan, is contained in Chapter 5.

1.4 SUMMARY OF RESULTS

The results of this program, organized into the results from each chapter of the report, are summarized in the subsections that follow.

1.4.1 BEHAVIOR OF PORT AND HARBOR FACILITIES DURING PRIOR EARTHQUAKES (CHAPT. 2)

To identify the lessons that can be learned from the behavior of port and harbor facilities during past earthquakes, the first phase of this research program compiled and assessed available documented information pertaining to (1) the extent to which port and harbor facilities have been damaged during prior earthquakes; and (2) principal causes and modes of this damage. All available information that could be obtained within the resources of this program was used in carrying out this damage assessment. This information was primarily from Japan (much of which required Japanese-English translation) although significant information was also available from the United States and Chile. Results from our evaluation of this information is contained in Chapter 2 of this report.

The particular earthquakes from which documented damage to port and harbor facilities has been obtained are listed in Table 1-1, together with a summary of the damage that has occurred and possible causes of this damage. This information indicates the following important trends:

- By far the most significant source of earthquake-induced damage to port and harbor facilities has been porewater pressure buildup in the loose-to-medium dense, saturated, cohesionless soils that prevail at port and harbor sites. This has led to damage due to excessive lateral pressures applied to quay walls and bulkheads by backfill materials (Item A in Table 1-1), and to liquefaction (Item B), localized sliding (Item C), or massive submarine sliding of the site soil materials (Item D).

TABLE 1-1. SUMMARY OF EARTHQUAKE-INDUCED DAMAGE TO PORT AND HARBOR FACILITIES

| Earthquake | | | Port Location | Damage | Possible Cause(s) |
Location	Date	Magnitude		Description	
Kanto, Japan	Sep 1, 1923	8.2	Yokohama and Yokosuka	Concrete block quay walls: sliding, tilting, and/or collapse with some bearing capacity failure of rubble-stone foundation	A
				Steel bridge pier: buckling of pile supports	C,E
Kitaizu, Japan	Nov 26, 1930	7.0	Shimizu	Caisson quay wall (183 m long): tilting, outward sliding (8.3 m), and settlement (1.6 m)	A,B,C
				L-Shaped block quay wall (750 m long): outward sliding (4.5 m) and settlement (1.2 m)	
Shizuoka, Japan	Jul 11, 1935	6.3	Shimizu	Caisson quay wall: outward sliding (5.5 m) and settlement (0.9 m) accompanied by anchor system failure	A,B,C
Tonankai, Japan	Dec 7, 1944	8.3	Yokkaichi	Pile-supported concrete girder and deck: outward sliding (3.7 m) accompanied by extensive soil sliding	A,B,C
			Nagoya Osaka	Sheet-pile bulkhead with platform: outward bulging (4 m) Steel sheet-pile bulkhead: outward bulging (3 m)	
Nankai, Japan	Dec 21, 1946	8.1	Nagoya Yokkaichi	Sheet-pile bulkhead with platform: outward bulging (4 m) Pile-supported concrete girder and deck: outward sliding (3.7 m)	A,B,C
			Osaka	Steel sheet-pile bulkhead: outward bulging (3 m) and settlement (0.6 m)	
			Uno	Gravity-type concrete block and caisson quay wall: seaward sliding (0.4 m) accompanied by soil sliding	
Tokachi-Oki, Japan	Mar 4, 1952	8.1	Kushiro	Concrete caisson quay wall: tilting, outward sliding (6 m), and settlement (1 m)	A,B,C
Chile	May 22, 1960	8.4	Puerto Montt	Concrete caisson quay walls: overturning and extensive tilting	A,B,C
				Steel sheet-pile seawall: outward sliding (up to 1 m) and anchor failure	
				Gravity-type concrete seawall: complete overturning and sliding (1.5 m)	
			Talcuhuano	Concrete block quay wall: outward tilting	A,B
Alaska	Mar 27, 1964	8.4	Anchorage	Dock structures: extensive seaward tilting with bowing, buckling, and yielding of pile supports	B,D,E
			Valdez Whittier	Entire harbor: destroyed by massive submarine landslide Pile-supported piers and docks: buckling, bending, and twisting of steel pile supports	
				Steel sheet-pile bulkhead: extensive bulging	B,D
			Seward	Major portion of harbor: destroyed by massive submarine landslide	

TABLE 1-1. CONCLUDED)

Earthquake			Port Location	Damage		Possible Cause(s)
Location	Date	Magnitude		Description		
Niigata, Japan	Jun 16, 1964	7.5	Niigata	Extensive damage due to liquefaction and sliding of soil strata. Summary of damage is as follows: <u>Piers and landings</u>: sliding (up to 5 m), submergence, and tilting <u>Sheet-pile bulkheads</u>: sliding (over 2 m), submergence, settlement (up to 1 m), and tilting. Extensive anchor failure <u>Quay-walls</u>: sea sliding (up to 3 m) settlement (up to 4 m) with extensive anchor failure and wall tilting		A,B,C
Tokachi-Oki, Japan	May 16, 1968	7.8	Hachinohe	<u>Steel sheet-pile bulkheads</u>: outward sliding (0.9 m), tilting, and settlement, with anchor failure		A
			Aomori	<u>Gravity-type quay wall</u>: sliding and settlement (0.4 m) <u>Gravity-type breakwater</u>: sliding (0.9 m) and pavement settlement (0.9 m)		A
			Hakodate	<u>Steel sheet-pile bulkhead</u>: seaward tilting (0.6 m) and apron settlement (0.3 m) <u>Quay-wall</u>: settlement (0.6 m) and sliding (0.4 m)		A,B
Nemuro-Hanto-Oki, Japan	Jun 17, 1973	7.4	Hanasaki	<u>Gravity-type quay wall</u>: sliding (1.2 m) and settlement (0.3 m) with corresponding apron settlement (1.2 m) <u>Steel sheet-pile bulkhead</u>: sliding (2 m) and anchor failure		A,B
			Kiritappu	<u>Steel sheet-pile bulkhead</u>: relatively minor damage <u>Gravity-type quay walls</u>: relatively minor damage		
Miyagi-Ken-Oki, Japan	Jun 12, 1978	7.4	Shiogama	<u>Concrete gravity-type quay wall</u>: outward tilting (0.6 m) and apron pavement settlement (0.4 m)		
			Ishinomaki	<u>Steel sheet-pile bulkheads</u>: outward sliding (up to 1.2 m) and apron settlement (up to 1 m) <u>Concrete block retaining wall</u>: sliding, tilting, and cracking with corresponding pavement settlement (0.2 m) relative to wall		A,B
			Yuriage	<u>Concrete block gravity quay wall and steel sheet-pile bulkhead</u>: large horizontal displacements (up to 1.2 m)		
			Sendai	<u>Steel sheet-pile bulkheads</u>: cracking and settlement of apron and pavements		

<u>Legend</u>

    A: Excessive lateral pressure from backfill materials, in the absence of complete liquefaction, and possibly accompanied by reduction in water pressure on outside of wall
    B: Liquefaction
    C: Localized sliding
    D: Massive submarine sliding
    E: Vibrations of structure

● To substantiate the importance of these porewater
  pressure effects, Chapter 2 cites several cases
  involving similar port and harbor structures located
  on adjacent sites, in which one site experienced sig-
  nificant porewater pressure buildup during a given
  earthquake and the other did not. Invariably, the
  structures at the sites with significant porewater
  pressure buildup suffered severe damage, whereas the
  damage to structures at the other sites was much less
  substantial. In other such examples cited in Chapter 2,
  widespread liquefaction and massive soil sliding caused
  by porewater pressure buildup has resulted in complete
  destruction of entire port and harbor areas (e.g., the
  Niigata, 1964, and Alaska, 1964, earthquakes).

● There was very little, if any, evidence of damage
  directly related to the earthquake-induced vibrations
  of the structures (Item E in Table 1-1). This may be
  either because direct structural effects are overshadowed
  by the effects of porewater pressure buildup in the
  adjacent soils, or because the seismic design provisions
  related to structure vibratory effects are adequate or
  conservative. The more extensive use of dynamic analyses
  of the type described in Chapter 4 and carried out in
  Chapter 5 could provide important insights along these
  lines.

● Insights into the importance of the seismic coefficients
  used in the design of port and harbor facilities are
  provided by evidence from Japanese earthquakes. For
  example, in the earthquakes at Niigata (1964), Tokachi-
  Oki (1968), and Nemuro-Hanto-Oki (1973), affected port
  and harbor facilities were all designed using seismic

coefficients whose values were about half the values of the peak accelerations actually experienced during the earthquakes. Despite this similarity, these three earthquakes caused widely varying degrees of harbor damage. This damage appeared to be most closely related to the extent of liquefaction of the affected harbor sites, which was greatest during the Niigata earthquake and was least during the Tokachi-Oki event. This suggests that the seismic coefficients used in design of port and harbor facilities are of secondary importance, when compared to the potential for liquefaction of the site soil materials.

- Although the effects of porewater pressure buildup and liquefaction are predominant, there is evidence that the structure configurations, including the anchor system used for retaining wall structures, also plays an important role in the behavior of the port and harbor facilities during earthquakes. Chapter 2 cites several examples of the strong influence of the anchor system on the failure or survival of waterfront structures. Along these lines, the chapter also provides strong evidence that undesirable configurations of several structures at the Niigata Port contributed to the widespread damage that occurred at that port during the 1964 Niigata earthquake.

1.4.2 CURRENT SEISMIC DESIGN PROCEDURES (CHAPT. 3)

Having established the predominant factors that have contributed to the significant damage to port and harbor facilities during past earthquakes, the next phase of this program assessed how such facilities are designed against these factors, and whether these design procedures are adequate. To carry this out, seismic

design provisions used for port and harbor facilities in Japan and in the United States were compiled, reviewed, and evaluated. Results of these efforts are contained in Chapter 3 of this report, where the design procedure assessments are categorized as corresponding to geotechnical considerations and structure-specific considerations.

1.4.2.1 Geotechnical Considerations

The geotechnical phenomena addressed in this seismic design assessment pertain to (1) lateral earth pressures for retaining wall structures; (2) earthquake-induced dynamic water pressures; (3) earthquake effects on bearing capacity; (4) lateral and axial resistance of piles to seismic effects; (5) earthquake-induced slope instability; and (6) liquefaction. The port and harbor facility design practice pertaining to these phenomena is summarized in Table 1-2. This table indicates that most of these phenomena are either ignored or are treated using simplified pseudostatic techniques that have important limitations when used to represent dynamic effects from earthquakes. Dynamic analysis is now routinely carried out only for liquefaction investigations under free-field conditions; however even this is a relatively recent investigation and a potential major problem exists at many ports and harbors because possible liquefaction had been essentially ignored in past seismic design practice. In fact, when viewed in the context of the overall design requirements for port and harbor facilities, the geotechnical-related seismic effects summarized in Table 1-2 do not play nearly as major a role in the design process as would be desirable, in view of the extensive damage to such facilities that has occurred during prior earthquakes.

TABLE 1-2. GEOTECHNICAL-RELATED SEISMIC DESIGN PRACTICE
FOR PORT AND HARBOR FACILITIES (As of mid-1982)

Item	Predominant Design Practice
Earthquake-Induced Lateral Earth Pressures for Retaining Wall Structures	Mononobe-Okabe method most typically used, occasionally incorporating suggested simplifications by Seed and Whitman (1970).
Earthquake-Induced Dynamic Water Pressures	Usually ignored. Westergaard (1933) procedure occasionally used.
Earthquake Effects on Bearing Capacity	Usually ignored.
Lateral and Axial Resistance of Piles to Seismic Effects	Usually either ignored or considered using pseudostatic procedures.
Earthquake-Induced Slope Instability	Pseudostatic methods most typically used.
Liquefaction	Standard procedures described by Seed (1979a) most typically used, incorporating empirical and/or 1-D total stress dynamic analysis techniques. Occasional use of 1-D effective stress methods.

1.4.2.2 Structure-Specific Considerations

As part of this assessment effort, seismic design consid-erations have been summarized for three major types of port and harbor structures--gravity-type quay walls, sheet-pile bulkheads, and piers. These design considerations are summarized in Table 1-3.

1.4.3 DYNAMIC ANALYSIS PROCEDURES (CHAPT. 4)

In view of the susceptibility of port and harbor facilities to damage from earthquakes and the limitations in the current seismic design provisions, it would seem that dynamic analysis should play a greater role in the seismic design of such facili-ties than it has in the past. A dynamic analysis for use in the design process involves five main steps, which are (1) the measure-ment of reliable soils data; (2) the selection of an appropriate analysis procedure; (3) the development of a suitable model of the soil/structure system; (4) implementation of the dynamic response calculation; and (5) utilization of the analysis results in the design process. Sound engineering judgment must be exercised during each stage of such an analysis. It is particularly important to check that the results obtained and conclusions drawn are consistent with engineering experience and practice.

Keeping this overall analysis process in mind, Chapter 4 addressed one aspect of the process--the analytical procedures appropriate for application to port and harbor facilities. In particular, three general types of methods--deterministic total stress methods, deterministic effective stress methods, and probabilistic methods--were evaluated with regard to their ability to satisfy the following requirements for port and harbor facility applications.

1.   Through an appropriate soil/structure interaction analysis that accounts for the geometry and material properties

TABLE 1-3. STRUCTURE-SPECIFIC SEISMIC DESIGN CONSIDERATIONS
FOR PORT AND HARBOR FACILITIES

Facility	Seismic Forces Generally Considered in Design	Seismic Design Considerations
Gravity-Type Quay Walls	Pseudostatic lateral earth pressure forces and the inertia force of wall are most typically the only seismic design forces considered.	Quay walls are designed to avoid overturning and excessive sliding and tilting when subjected to seismic forces, although some horizontal wall movement is tolerated. Earthquake-induced slope instability is an important design consideration. Effects of lateral pressure are most important for caisson-type gravity quay walls because of their height. Remedial measures used to enhance the seismic resistance of quay walls include grouting of the backfill, widening the base of the wall, using pile supports, partially embedding the wall, and replacing underlying weak soils with more competent soil materials.
Sheet-Pile Bulkheads	A pseudostatic lateral earth pressure force is typically the only seismic design force considered.	Designs to resist lateral seismic forces are directed toward insuring (1) an adequate factor of safety against toe failure; (2) adequate bending resistance of the sheet pile; (3) adequate tensile resistance of the tie rod; and (4) adequate anchor resistance. Anchor design considerations include (1) placement of anchors at sufficient depths below ground surface to avoid weak near-surface soil deposits; (2) enhancement of anchor capacity by using deeply embedded piles or sheet piles; and (3) insuring an adequate distance between anchor and bulkhead wall, to avoid loss of passive pressure resistance of anchor.
Piers	Pseudostatic lateral forces, analogous to those used for building design, are most typically the only seismic design forces considered.	The relatively lightweight, pile-supported pier structures are less prone to seismic damage than are quay walls or bulkheads. The use of batter piles has resulted in damage to pier pile caps and decking, because of large lateral stiffness of such piles; therefore vertical pile supports are generally preferred.

of the site and the structure, the earthquake-induced stresses and deformations in the structure must be determined so as to guide the development of a suitable structure design.

2. Through a liquefaction analysis that accounts for the presence of the port and harbor structures as well as the material properties and topography of the surrounding site profile, the potential for significant porewater pressure buildup and its related effects (e.g., widespread liquefaction and slope instabilities) must be determined.

The evaluation of the ability of the three methods to satisfy these requirements considered the fundamental concepts on which each method is based (see Table 1-4), together with the current state of development of each method. Results from this evaluation indicated that

- Deterministic total stress methods are the only methods now sufficiently developed to satisfy Requirements 1 and 2 above for the seismic analysis of port and harbor facilities. For this reason, procedures and concepts pertaining to deterministic total stress methods are described in some detail in Chapter 4, so as to guide their application to seismic analyses of port and harbor facilities.

- Although deterministic total stress methods are the most applicable to port and harbor facilities at this time, they do not incorporate porewater pressure effects on the soil/structure system response (Requirement 1 above), nor do they directly incorporate effects of uncertainties in the seismic input or the soil properties. For this

TABLE 1-4. PROCEDURES FOR DYNAMIC ANALYSIS OF PORT AND HARBOR FACILITIES

Method	Description	Current Status for Applicability to Port and Harbor Facilities*
Deterministic Total Stress Methods	These methods involve dynamic analyses that compute the total state of stress in the soil. As applied to port and harbor facilities in accordance with Requirements 1 and 2, such methods involve the following steps: (1) computation of the soil/structure system response neglecting porewater pressure effects; (2) conversion of irregular soil shear stress histories from Step 1 to equivalent cyclic shear stresses; and (3) assessment of liquefaction potential of site through comparison of equivalent cyclic stresses from Step 2 to critical cyclic stresses that lead to liquefaction of the soil medium, as obtained from laboratory cyclic tests and/or empirical methods.	Applicable at this time
Deterministic Effective Stress Methods	These methods are based on the premise that the soil behavior is fundamentally controlled by effective stress rather than total stress. As applied to ports and harbor facilities in accordance with Requirements 1 and 2, such methods would involve the following steps: (1) use of laboratory tests to determine the necessary material parameters for the effective stress soil model; and (2) utilization of this soil model in a dynamic analysis of the coupled soil/structure system response, including effects of porewater pressure buildup and dissipation.	Under development
Probabilistic Methods	These methods (which conceivably can comprise either total stress or effective stress approaches) account for effects of uncertainties in defining seismic input motions, soil properties, etc. Such methods, as applied to port and harbor facilities in accordance with Requirements 1 and 2, would define the soil/structure system response in terms of probabilities of occurrence of a given event (e.g., liquefaction, a given state of stress in the structure, etc.)	Under development

*This current status evaluation pertains to the ability of each method to satisfy Requirements 1 and 2 for port and harbor facility analyses (Sec. 1.4.3) at this time.

reason, considerable research has been directed toward
the development of deterministic effective stress methods
and probabilistic methods. Neither of these methods are
yet sufficiently developed at this time to be applicable
to port and harbor facility analyses in accordance with
Requirements 1 and 2; however, the methods are included
in Chapter 4 in the context of promising dynamic
analysis procedures for the future.

- Deterministic effective stress methods have the advan-
  tage over total stress methods of including porewater
  pressure effects in the dynamic response analysis.
  However, such methods are now available primarily as
  one-dimensional techniques for analyzing the site lique-
  faction potential under free-field conditions involving
  vertically propagating shear waves in horizontally
  layered sites. The desirability of developing two-
  dimensional or three-dimensional effective stress
  methods that would satisfy Requirements 1 and 2 for
  port and harbor facilities is recognized by numerous
  geotechnical engineers, and work is proceeding in this
  area.

- Probabilistic methods have the advantage over deter-
  ministic methods of directly representing the effects
  of uncertainties in the seismic input motions and soil
  properties. Several probabilistic methods are now
  available for liquefaction analyses under free-field
  conditions; a very few methods for soil/structure inter-
  action analysis have also been developed. However with
  only a few exceptions, these procedures feature a proba-
  bilistic representation of the input motions and treat
  the soil properties deterministically. Furthermore,
  no probabilistic procedures yet treat the combined soil/
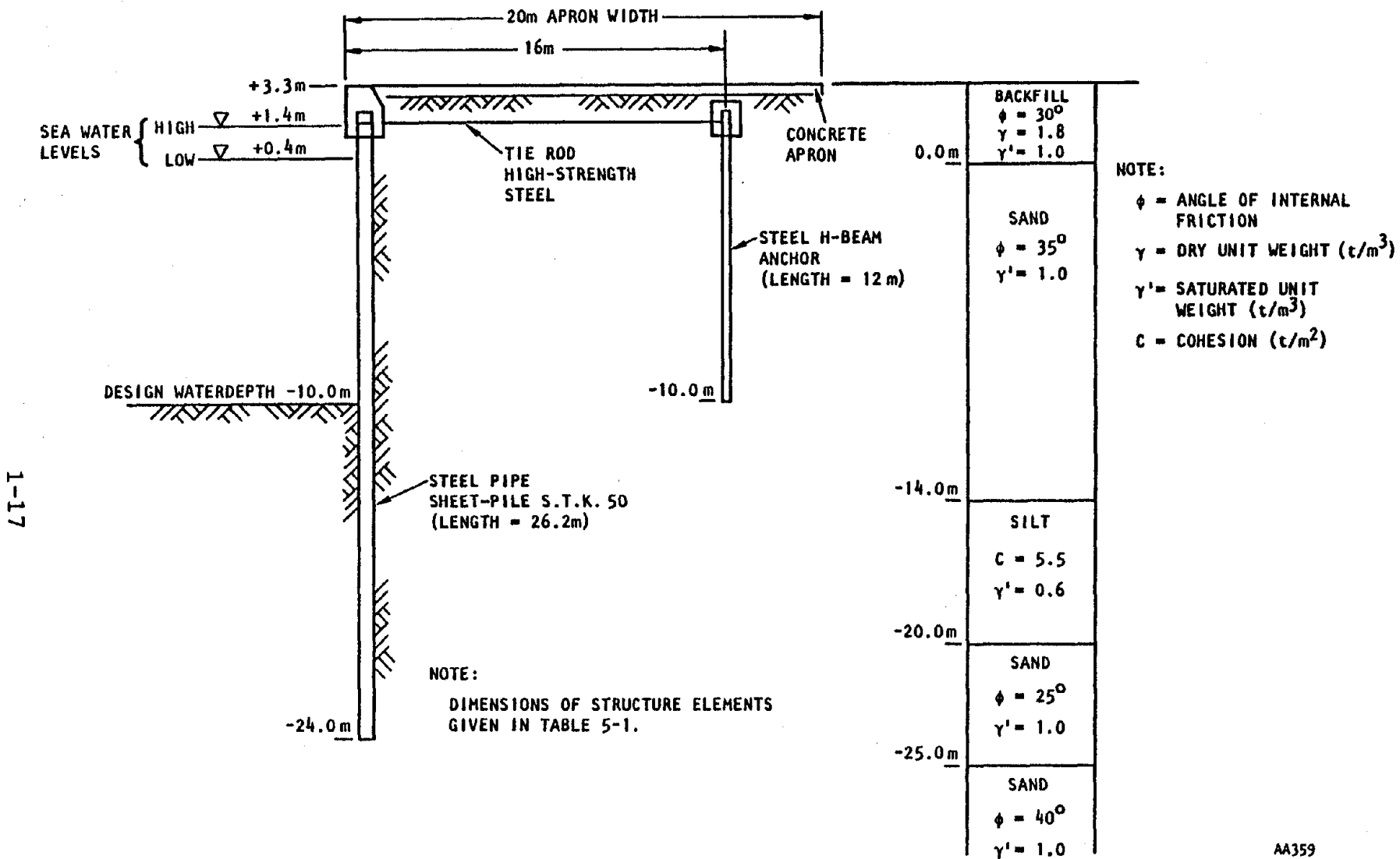 structure interaction and liquefaction problems, although

some existing techniques might possibly be combined as a promising first attempt along these lines.

- All of the above findings indicate that, when used with sound judgment, dynamic analysis represents a valuable means for enhancing the design of port and harbor facilities to resist earthquake ground motions. Deterministic total stress methods can be used at this time for this purpose, and continuing development of deterministic effective stress methods and probabilistic methods should add significantly to these existing dynamic analysis capabilities.

1.4.4   ILLUSTRATIVE DYNAMIC ANALYSIS (CHAPT. 5)

As a final phase of this research program, a dynamic analysis of an actual sheet-pile bulkhead struture in Japan was carried out in order to illustrate the applicability of dynamic analysis procedures to port and harbor facilities. During the 1978 Miyagi-Ken-Oki earthquake, this structure suffered damage in the form of settlement and cracking of its apron.

The bulkhead structure that was considered is comprised of a steel sheet pile supported by equally spaced steel pipes and anchored by a tie-rod/H-beam system. An unreinforced concrete apron rests on the ground surface and extends from the sheet pile to beyond the anchor (Fig. 1-1). The following two sets of soil conditions were considered in the dynamic analysis of this structure: (1) the original soil conditions at the site, which consist of a layer of loose fill underlain by saturated sands and silt; and (2) modifications to these original soil conditions due to the application of deep-compaction soil improvement techniques. Ground motions measured at a nearby site during the Miyagi-Ken-Oki earthquake were used as seismic input to the analysis.

20m APRON WIDTH

16m

+3.3m

SEA WATER LEVELS { HIGH ▽ +1.4m
LOW ▽ +0.4m

CONCRETE APRON

TIE ROD HIGH-STRENGTH STEEL

STEEL H-BEAM ANCHOR (LENGTH = 12 m)

DESIGN WATERDEPTH -10.0 m

-10.0 m

STEEL PIPE SHEET-PILE S.T.K. 50 (LENGTH = 26.2m)

NOTE:

DIMENSIONS OF STRUCTURE ELEMENTS GIVEN IN TABLE 5-1.

-24.0 m

Soil profile labels:

BACKFILL
ϕ = 30°
γ = 1.8
γ' = 1.0

0.0 m

SAND
ϕ = 35°
γ' = 1.0

-14.0 m

SILT
C = 5.5
γ' = 0.6

-20.0 m

SAND
ϕ = 25°
γ' = 1.0

-25.0 m

SAND
ϕ = 40°
γ' = 1.0

NOTE:

ϕ = ANGLE OF INTERNAL FRICTION

γ = DRY UNIT WEIGHT (t/m^3)

γ' = SATURATED UNIT WEIGHT (t/m^3)

C = COHESION (t/m^2)

AA359

(a) Soil/structure configuration   (b) Soil profile

FIGURE 1-1. SHEET-PILE BULKHEAD NO. 4 AT NAKANO WHARF, SENDAI HARBOR, JAPAN (Tsuchida et al., 1979)

The analytical procedure used in this illustrative example was a deterministic total stress method comprised of the following three steps: (1) a two-dimensional soil/structure interaction analysis carried out using the FLUSH code (Lysmer et al., 1975), which features an equivalent linear approach to represent the strain-dependence of the dynamic soil properties; (2) conversion of the irregular shear stress histories in the soil, as obtained from Step 1, to equivalent cyclic stresses using the empirical approach of Seed et al. (1975b); and (3) assessment of the liquefaction potential at the site, through comparison of these cyclic shear stresses to cyclic stresses shown by the Seed-Idriss (1981) empirical approach to lead to liquefaction.[*] The results obtained from this procedure showed the following trends:

- The calculations indicate that the site of this sheet-pile bulkhead is susceptible to porewater pressure effects. These effects, together with possible earthquake-induced settlement of the unsaturated loose fill above the water table, provide a plausible explanation for the observed damage to this structure from the earthquake--settlement and cracking of the apron.

- Upper bound estimates of the earthquake-induced internal stresses in the structure (in the absence of porewater pressure effects) indicate these structure stresses to be very low when compared to anticipated design values, although the stresses in the apron are probably sufficient to have caused some cracking.

---

[*]For this particular site, no laboratory cyclic test data were available which also would serve to assess the potential for liquefaction.

- Deep compaction soil improvement techniques, as represented in this analysis, substantially enhance the resistance of the upper portion of this site to porewater pressure buildup and liquefaction. This trend is in line with prior observations in Japan of the effects of soil improvement on the behavior of sand deposits during earthquakes.

- For these particular site conditions and seismic excitations, the dynamic analysis results produce lateral pressure distributions along the sheet-pile/soil interface that are markedly different from the pseudostatic pressure distributions computed from the Mononobe-Okabe equation and commonly used for design.

- Comparisons of the two-dimensional soil/structure system response with the one-dimensional free-field response showed that the peak shear stress in the near-surface regions of the soil backfill were affected by the topography of the site (and probably to a smaller degree by soil/structure interaction for this particular system). These effects on the soil/structure system response spectra and on the shear stresses in the deeper soil layers were much smaller.

1.5 CONCLUSIONS

The main findings of this research program are as follows:

- Earthquake Damage. The potential for significant earthquake damage to port and harbor facilities is most strongly affected by porewater pressure buildup in the site soil materials. Past earthquakes have shown that this damage is often very severe or catastrophic when

large-scale liquefaction and/or massive submarine slides induced by porewater pressure buildup have occurred. Porewater pressure buildup has also led to extensive damage due to excessive lateral pressures applied to quay walls and bulkheads along the structure/backfill interface.

- <u>Seismic Design Provisions</u>. Seismic effects are often not nearly as important a design consideration for port and harbor facilities as would be desirable, in view of the extensive damage to such facilities that has occurred during prior earthquakes. The seismic design provisions that do exist typically address some of the potential earthquake-induced phenomena in a simplified pseudostatic manner and ignore many of the others.

- <u>Dynamic Analysis Techniques</u>. Dynamic analysis, which is now routinely used only for liquefaction assessments under free-field conditions, should be incorporated to a much greater extent into seismic design provisions for port and harbor facilities. Deterministic total stress methods are applicable at this time to the dynamic analysis of port and harbor facilities, including the soil/structure system response and the potential for significant porewater pressure buildup in the surrounding soil medium. The continuing development of deterministic effective stress methods and probabilistic methods for such applications should add significantly to these existing dynamic analysis capabilities.

CHAPTER 2

BEHAVIOR OF PORT AND HARBOR FACILITIES
DURING PRIOR EARTHQUAKES

2.1 GENERAL DESCRIPTION

To provide insight regarding the vulnerability of port and
harbor facilities to earthquake effects and the important para-
meters to consider in the seismic design of such facilities, it
is important to consider how ports and harbors have fared during
prior earthquakes. Accordingly, this chapter contains results of
our detailed compilation and assessment of the considerable but
widely scattered information of this type that has been generated
by various researchers and engineers throughout the world (e.g.,
Duke and Leeds, 1963; Okamoto, 1973; NAS, 1973; Noda and Uwabe,
1975; Tsuchida et al., 1980). The earthquake events from which
information was obtained are primarily from Japan (Kanto, 1923;
Kitaizu, 1930; Shizouka, 1935; Ogahanto, 1939; Tonankai, 1944;
Nankai, 1946; Tokachi-Oki, 1952 and 1968; Niigata, 1964; Nemuro-
Hanto-Oki, 1973; and Miyagi-Ken-Oki, 1978) with additional
information from earthquakes in Chile (1960) and Alaska (1964).

2.2 1923 KANTO, JAPAN, EARTHQUAKE[*]

An extremely strong earthquake occurred in the southern part
of the Kanto region of Japan on September 1, 1923. The earthquake
was centered about 10 km south of Mt. Tanzawa at a depth of up to
10 km, and had an estimated magnitude of 8.2 (Fig. 2-1). Estimated
peak accelerations from this earthquake ranged from 0.33 to 0.39 g.

The most severe damage to port and harbor facilities during
this earthquake occurred at the Yokohama and Yokosuka Ports.
This damage is summarized in the paragraphs that follow.

---

[*]Primary reference for damage assessment from the 1923 Kanto
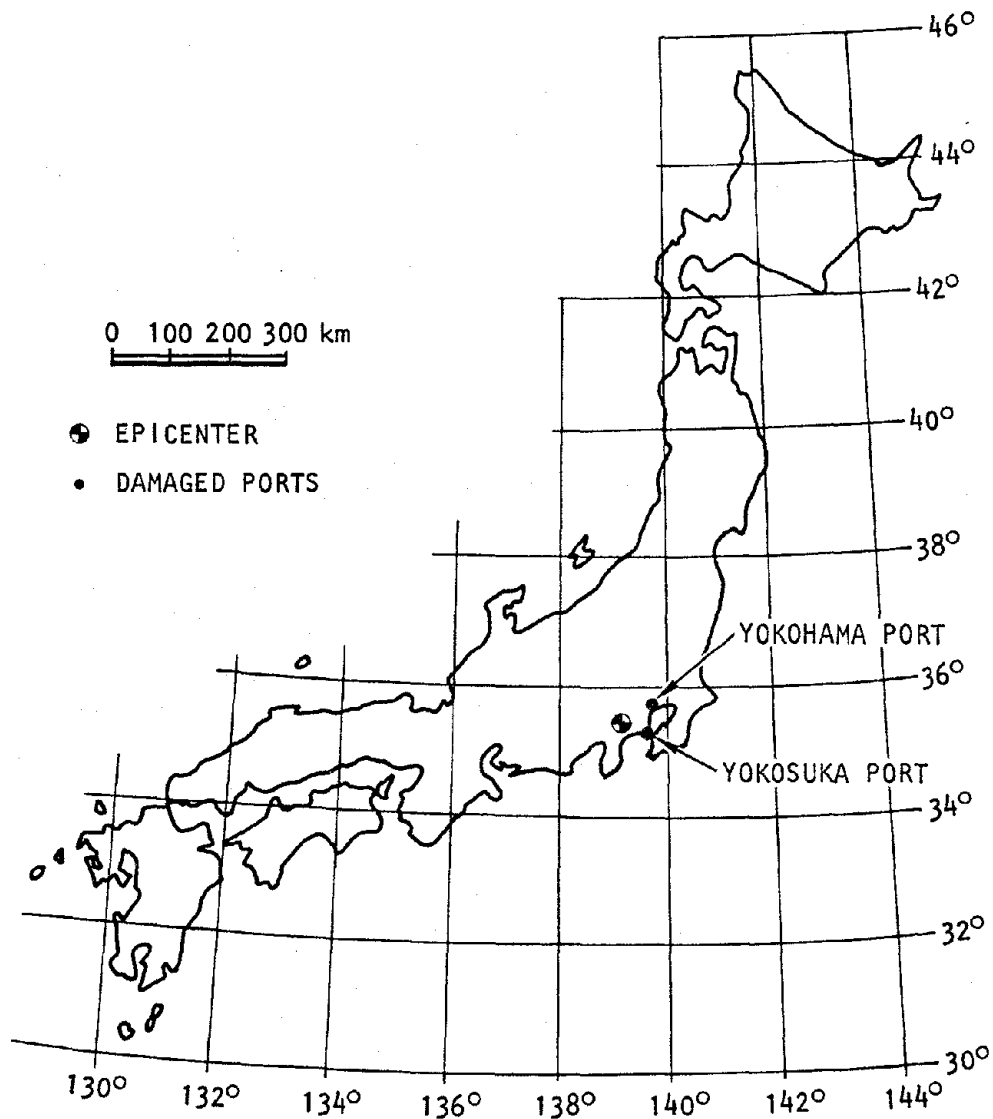earthquake was Noda and Uwabe (1975).

FIGURE 2-1.   EPICENTER AND DAMAGED PORTS FROM 1923 KANTO,
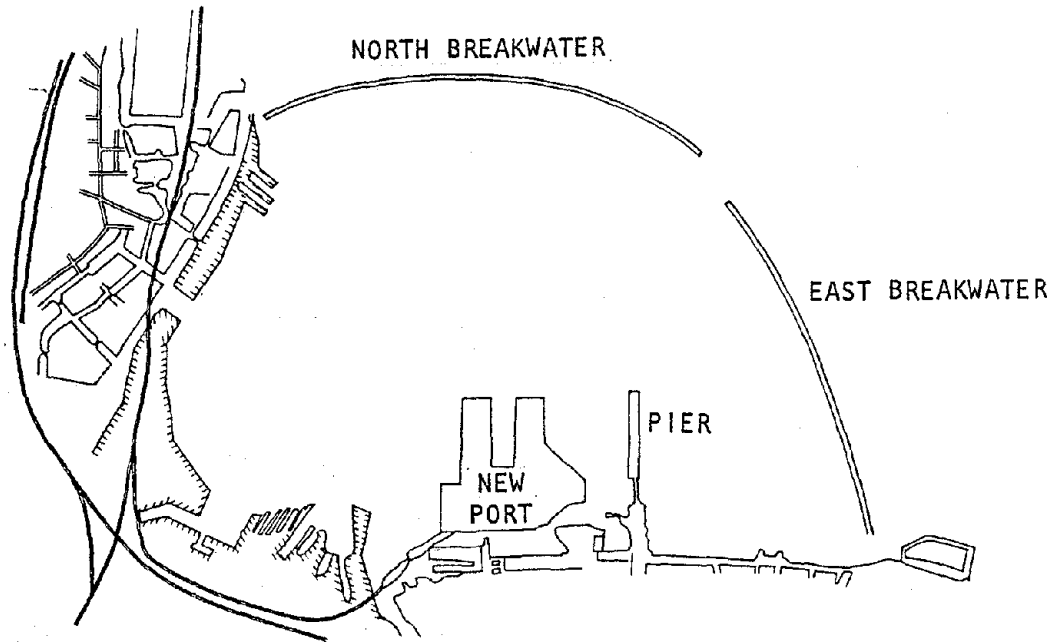JAPAN EARTHQUAKE (Noda and Uwabe, 1975)

2.2.1 YOKOHAMA PORT

The Yokohama Port is shown in Figure 2-2a. This port, which is underlain by mudstone, suffered extensive damage particularly in the New Port area where nearly 80% of the 2000 m of concrete block quay walls in that area were totally destroyed (Fig. 2-2b). These quay wall destruction modes featured predominantly outward sliding, overturning and collapse of the block elements, and tilting (Fig. 2-3a). From the available documentation, these failure modes appear to have been caused by excessive lateral pressure due to porewater pressure buildup in the backfill materials, possibly accompanied by a reduction in water pressure on the outside of the walls.

Another important aspect of the damage at the Yokohama Port was the buckling of a bridge in the central part of the main pier. This bridge was 490 m long and was comprised of a central steel core flanked along either side of its length by concrete extensions. This buckling caused complete failure of the steel core.

In addition to the quay wall and bridge pier damage, nearby warehouses and cargo handling equipment were rendered useless by extensive settlement of the underlying reclaimed land. However, those installations constructed on more solid soil materials survived the earthquake with much less damage.

2.2.2 YOKOSUKA PORT

In Yokosuka Port, the damage was less extensive than at Yokohama and was related to the nature of the underlying soil or rock medium. Those quay walls and other waterfront structures constructed on solid bedrock did not suffer damage from the earthquake shaking, whereas those revetments and quay walls constructed in backfilled areas were damaged severely, with
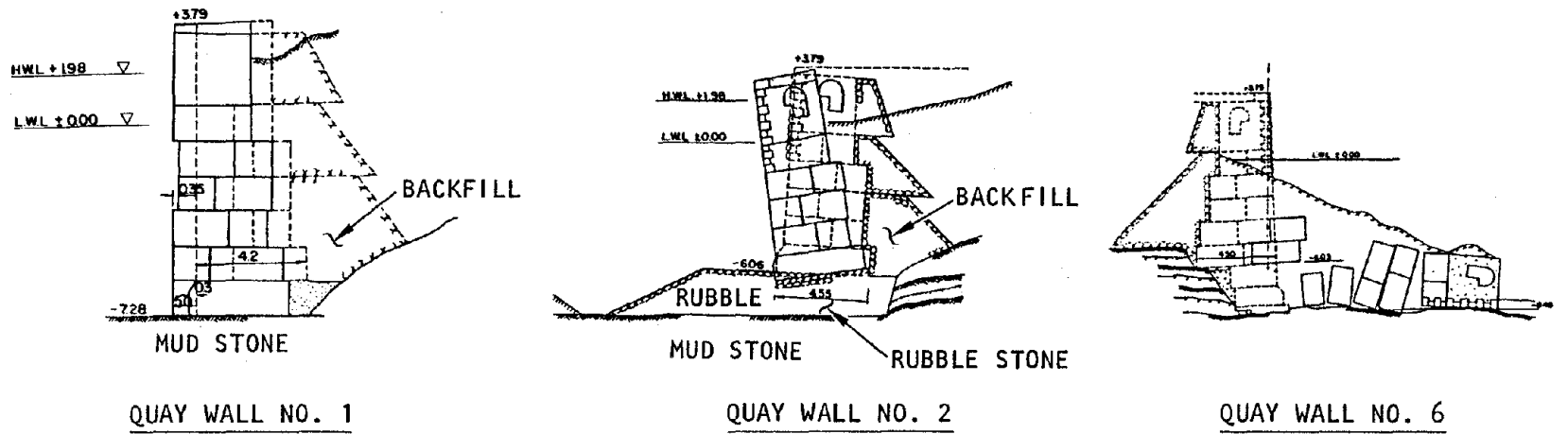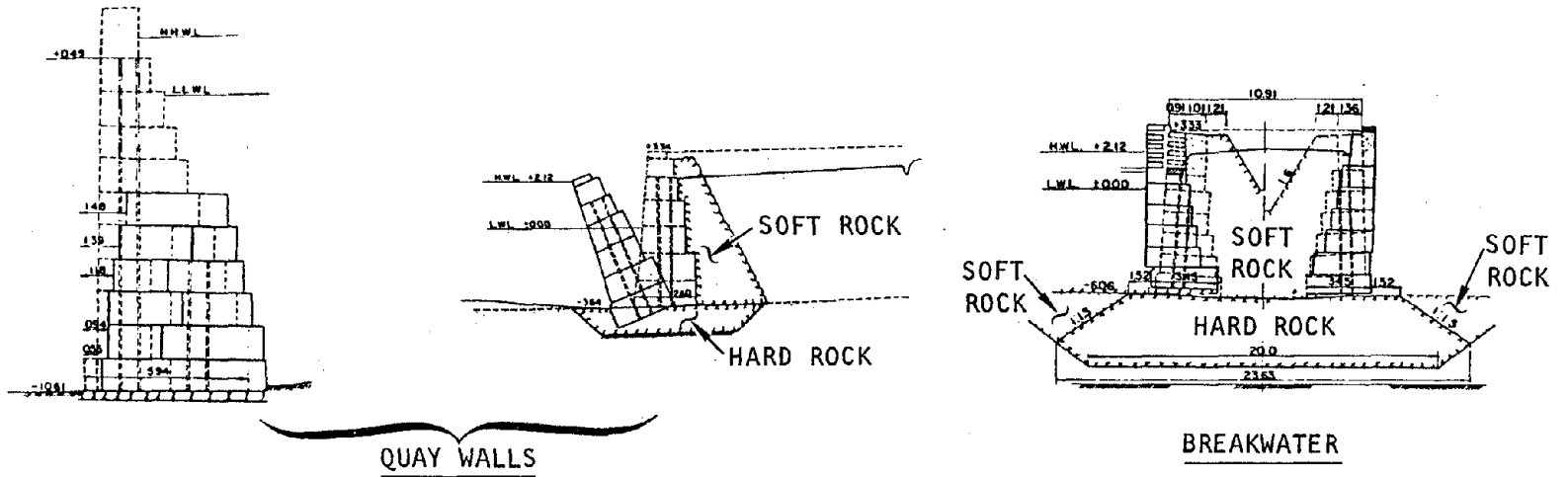
(a)   Port layout
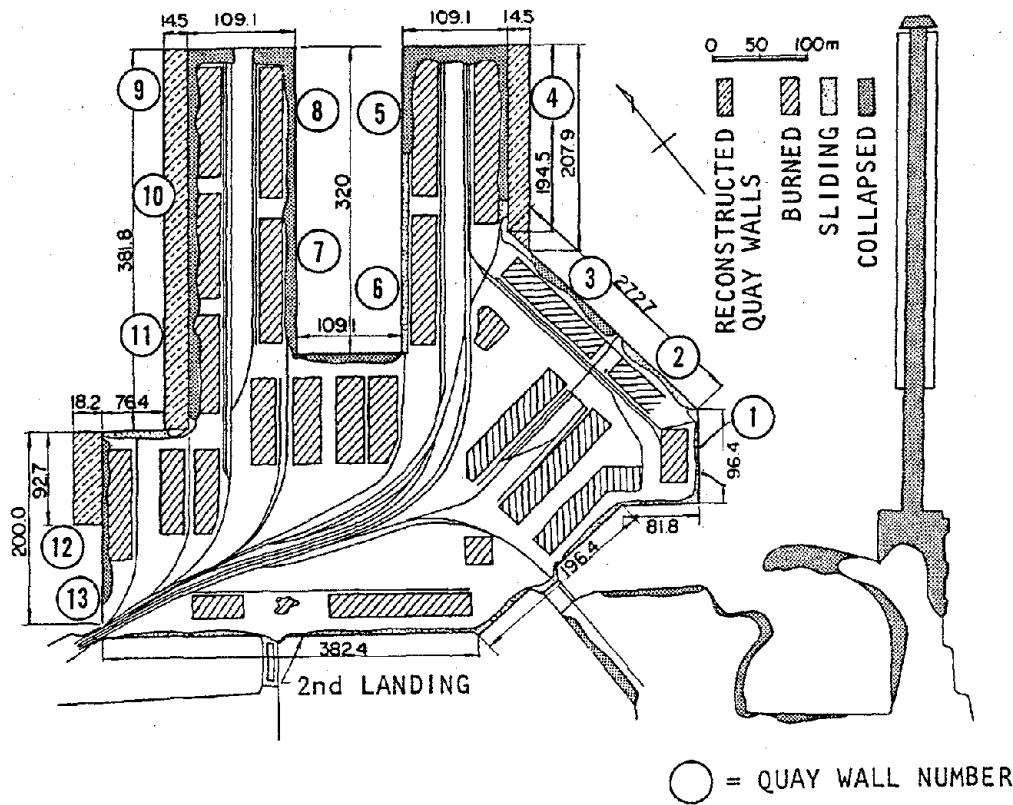
(b)   Damage at New Port

FIGURE 2-2.   YOKOHAMA PORT DURING 1923 KANTO, JAPAN EARTHQUAKE
(Node and Uwabe, 1975)

QUAY WALL NO. 1   QUAY WALL NO. 2   QUAY WALL NO. 6

(a)   At Yokohama Port

QUAY WALLS

BREAKWATER

(b)   At Yokosuka Port

NOTE:
-------- POSITION PRIOR TO EARTHQUAKE
———— POSITION AFTER EARTHQUAKE
NUMBERS = DIMENSIONS OR DEPTHS IN METERS

FIGURE 2-3.   QUAY WALL AND BREAKWATER DAMAGE — 1923 KANTO, JAPAN EARTHQUAKE
(Noda and Uwabe, 1975)

extensive sliding and overturning (Fig. 2-3b). The breakwaters were slightly displaced and damaged from the ground shaking (Fig. 2-3b) but remained functional.

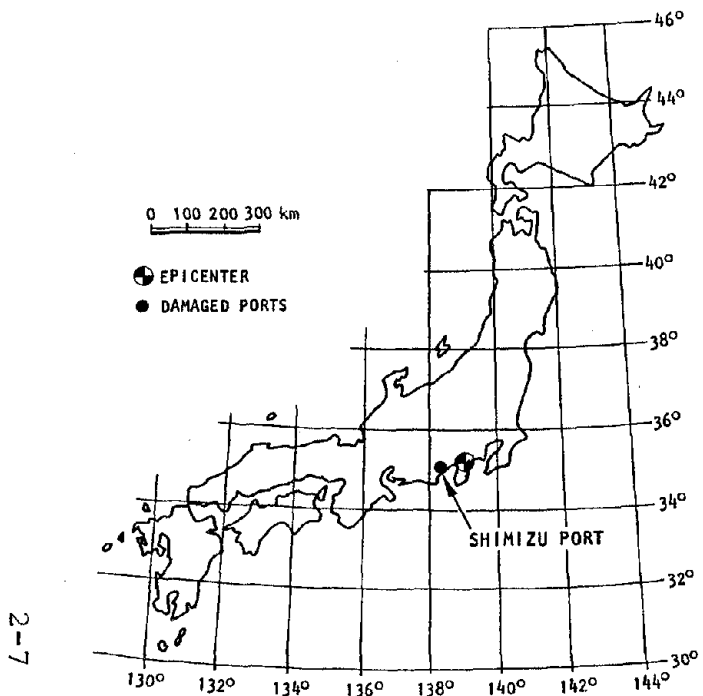## 2.3 1930 KITAIZU, JAPAN, EARTHQUAKE[*]

The Kitaizu earthquake occurred in the northern part of the Izu region of Japan on November 26, 1930 (Fig. 2-4a). This earthquake had a magnitude estimated at 7.0 and a focal depth of up to 5 km. The maximum acceleration was estimated to be about 0.15 g in Shimizu Port, where waterfront structures suffered severe damage.

The damage at Shimizu Port is depicted in Figure 2-4b. This figure shows that significant damage occurred at Berth B, where a 183-m caisson quay wall tilted substantially, slid outward about 8 m, and settled about 1.5 m (Fig. 2-4c). Substantial damage also occurred at Landing A, where an L-shaped concrete block quay wall, with a length of 750 m tilted, slid outward 4.5 m, and settled 1.2 m.
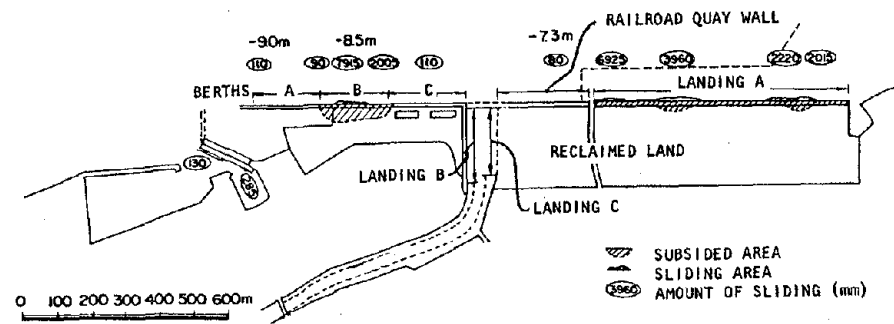
Typical soil conditions at Shimizu Port are shown in Figure 2-4d. Layers of weak clays and silts with very low blow-counts prevail within the entire 30 m depth at which soils data are given. This suggests that the damage at this port may have resulted from the combined effects of severe ground shaking, increased lateral pressures in the backfill behind the walls, a loss of strength of the underlying soft soil materials, and possibly a reduction in water pressure on the outside of the walls.

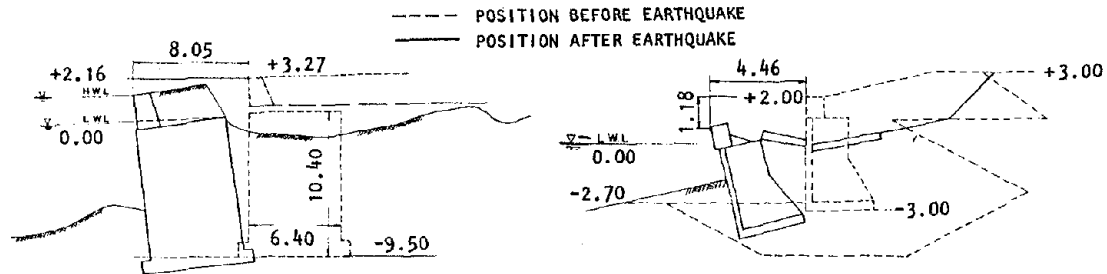[*]Primary reference for damage assessment from the 1930 Kitaizu earthquake was Noda and Uwabe (1975).

(a) Location of earthquake epicenter and Shimizu Port

(b) Damage at Shimizu Port

(c) Quay wall damage

AT BERTH B

AT LANDING A

(d) Soil properties at Shimizu Port

FIGURE 2-4. PORT AND HARBOR DAMAGE FROM 1930 KITAIZU EARTHQUAKE
(Noda and Uwabe, 1975)
(All dimensions and elevations in meters)

2.4 1935 SHIZUOKA, JAPAN, EARTHQUAKE[*]

On July 11, 1935, an earthquake of magnitude 6.3 occurred in the Shizuoka district of Japan, with an epicentral location just northwest of the Udo mountains southeast of the city of Shizuoka (Fig. 2-5a). The focal depth of this earthquake was about 10 km, and the peak acceleration in the Shimizu Port area was about 0.25 g. The area affected by this earthquake was small; however, within this area, damage was severe.

The behavior of the port and harbor facilities at Shimizu Port is noteworthy since many of these facilities had been strengthened and, where necessary, repaired after the 1930 Kitaizu earthquake. Despite this, significant damage was sustained during this 1935 event, primarily in the form of sliding and settlement of the quay walls (Fig. 2-5b,c). For example, the quay wall at Berth A, which had been strengthened to resist 0.15 g acceleration levels, suffered failure of the tie rods that connected the quay wall and anchor system. The quay walls at Berth C, at Landings A and B, and at the railroad were also damaged substantially, despite previous strengthening efforts. Retaining walls at Berth B, which had been designed and constructed after the 1930 Kitaizu earthquake incorporating seismic considerations, collapsed causing an outward sloughing and settlement of the back-fill and filled land.

The importance of the damage induced at Shimizu Port during the 1935 Shizuoka earthquake is that it occurred despite the use of modern (at that time) design procedures that incorporated seismic considerations in the strengthening of the waterfront facilities. This could be related to the fact that the damaged

---

[*]Primary reference for damage assessment from the 1935 Shizuoka earthquake was Noda and Uwabe (1975).
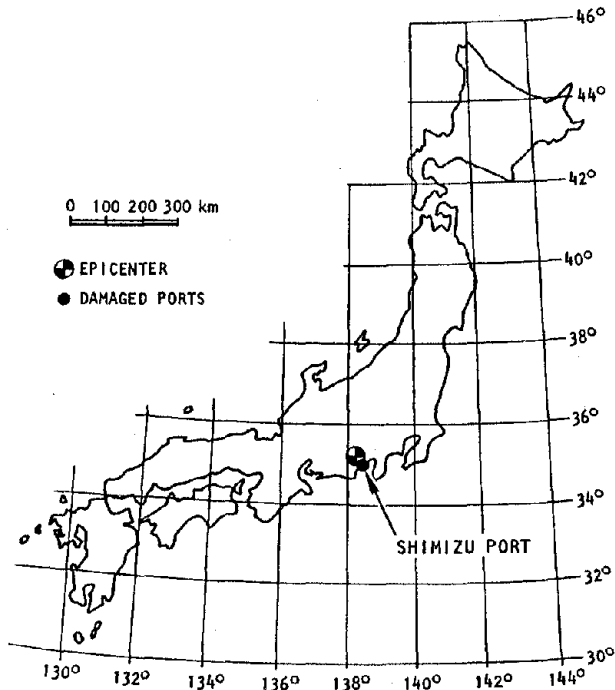
(a)   Location of earthquake epicenter
       and Shimizu Port

(b)   Damage at Shimizu Port

————— POSITION BEFORE EARTHQUAKE

——————— POSITION AFTER EARTHQUAKE
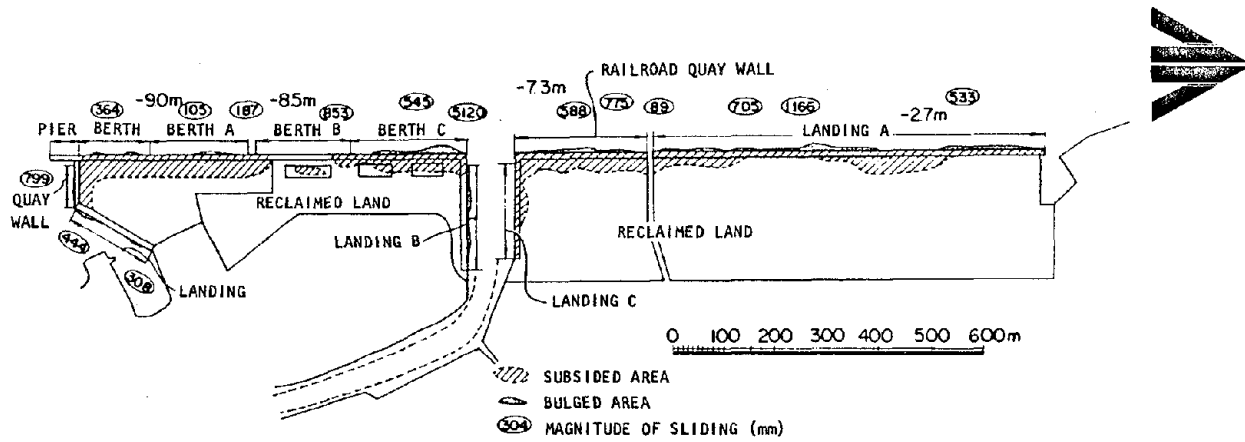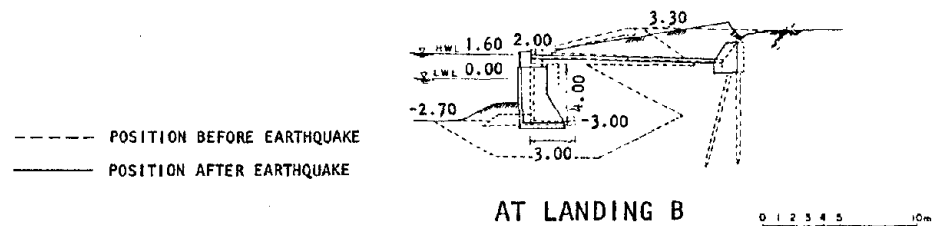
AT LANDING B
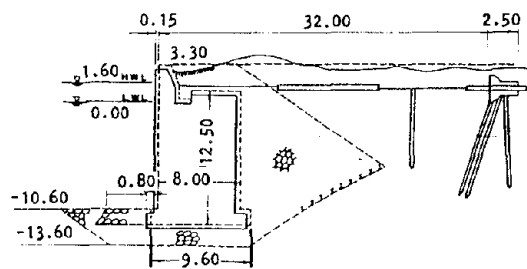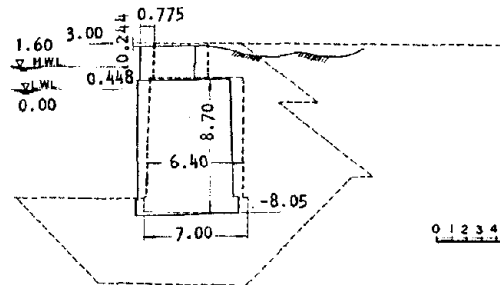
AT BERTH A

AT RAILROAD
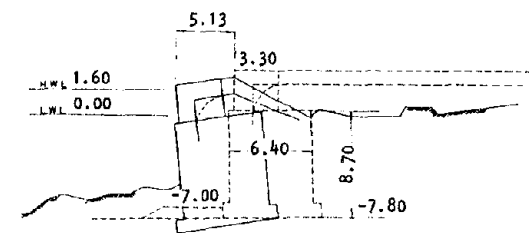
AT BERTH C

(c)   Quay wall damage (all dimensions and elevations in meters)

FIGURE 2-5.   PORT AND HARBOR DAMAGE FROM 1935 SHIZUOKA EARTHQUAKE
               (Noda and Uwabe, 1975)

quay walls at this port were constructed on soft alluvium whose bearing capacity could not be maintained during the ground shaking. Another possible contributing factor was that the adjacent backfill was comprised of reclaimed land with poorly graded gravel (Fig. 2-5b).

2.5 1939 OGAHANTO, JAPAN, EARTHQUAKE[*]

On May 1, 1939 a strong earthquake occurred off the Oga Peninsula of Japan (Fig. 2-6a). This earthquake had a magnitude of 7.0 and a very shallow focal depth. As in the 1935 Shizuoka earthquake, only a small area was affected by this event, within which damage was severe.

Structures at the Funakawa Port and the Akita Port were damaged to some extent during this earthquake. At Funakawa Port (peak acceleration $\cong 0.39$ g), minor damage occurred in the vicinity of concrete block quay walls, and consisted of a small degree of outward tilting of the quay walls and settlement of the backfill (Fig. 2-6b,c). This relatively slight damage may be attributed to the fact that the quay walls were supported on competent shale rock.

At Akita Port, (Fig. 2-7a) the subsurface materials were much less competent than at Funakawa Port, consisting primarily of very soft sands with blowcounts as low as 10, to a depth of 20 m. As a result, an L-shaped quay wall with a length of 142 m suffered substantial outward movement and tilting throughout its entire length (Fig. 2-7b), accompanied by large horizontal displacements (up to 1.5 m) and severe cracking in the concrete apron. This damage can probably be attributed to a porewater pressure buildup in these soft sandy materials, possibly leading to liquefaction and/or localized sliding of the soils in the vicinity of the quay wall.

---

[*]Primary reference for damage assessment from the 1939 Ogahanto earthquake was Noda and Uwabe (1975).
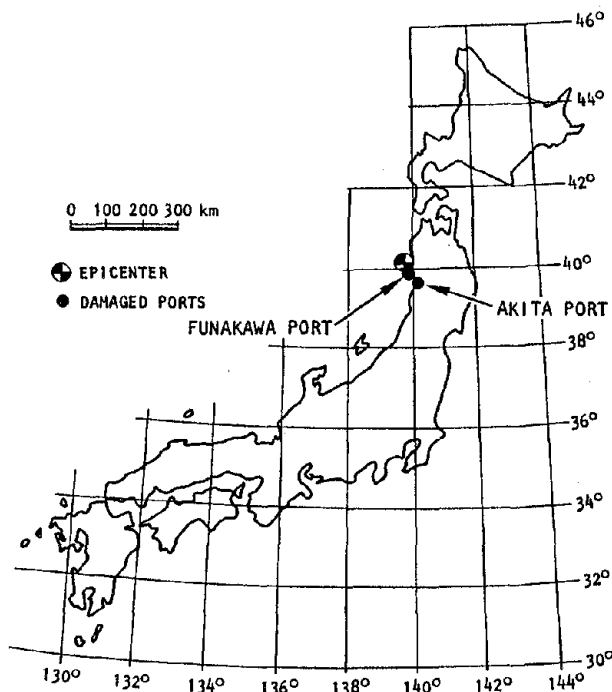
(a) Location of earthquake epicenter and Funakawa and Akita ports
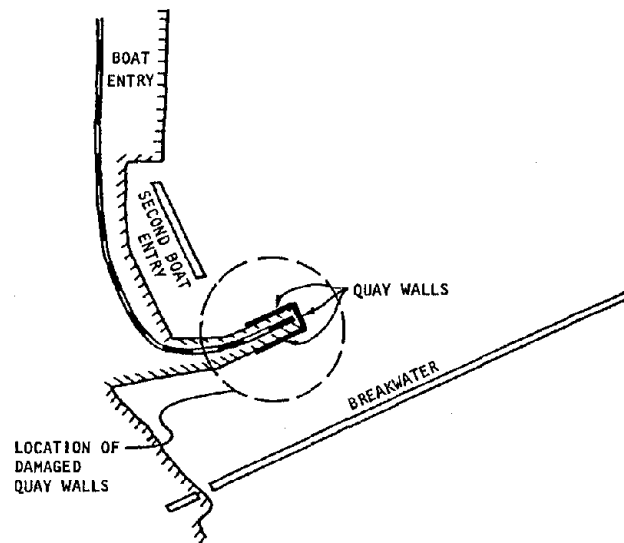
(b) Plan view of Funakawa Port showing location of damaged quay walls
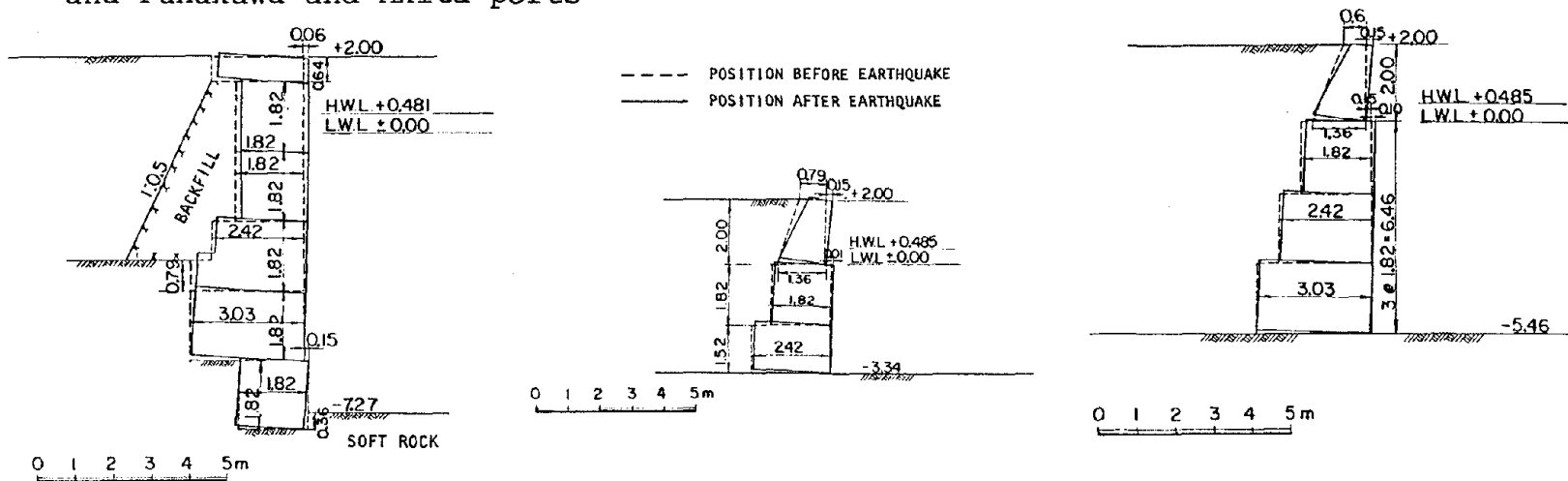
(c) Damaged quay walls at Funakawa Port (all dimensions and elevations in meters)

FIGURE 2-6. EPICENTRAL LOCATION AND DAMAGE AT FUNAKAWA PORT — 1939 OGAHANTO EARTHQUAKE (Noda and Uwabe, 1975)
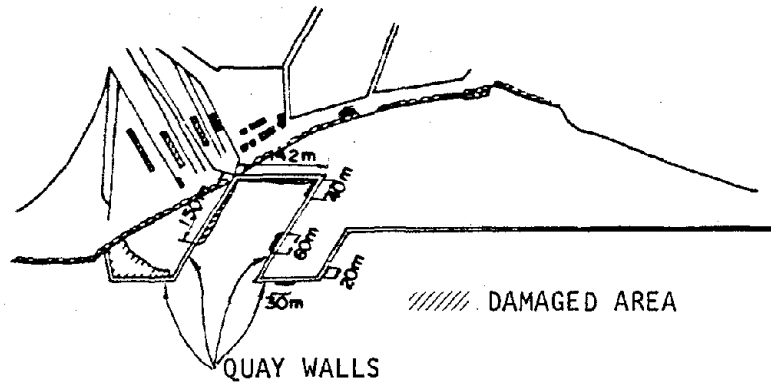
(a) Plan view of Akita Port showing location of damaged quay walls
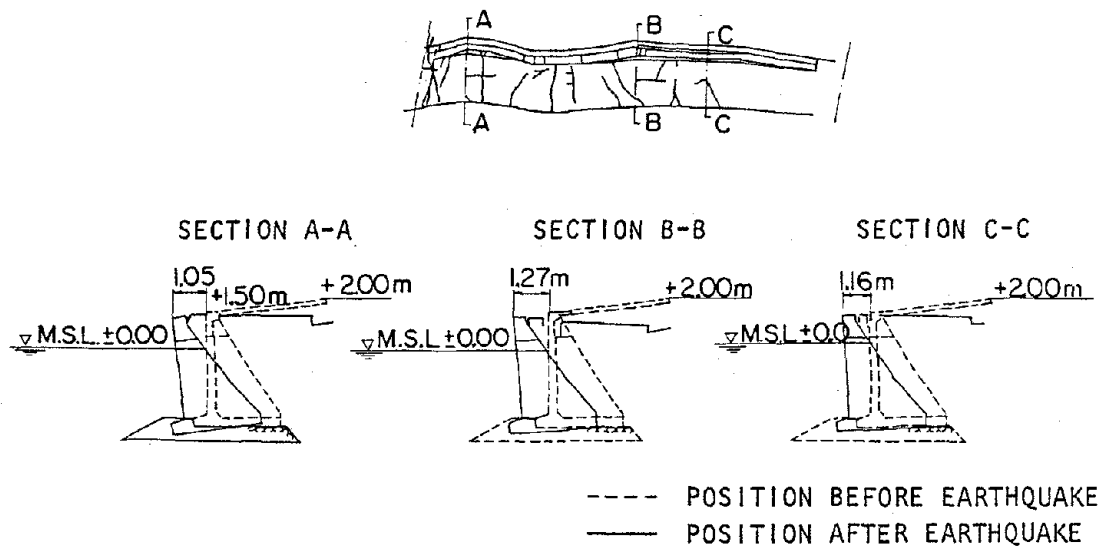
(b) Damage along length of L-shaped quay walls

FIGURE 2-7. DAMAGE AT AKITA PORT — 1939 OGAHANTO EARTHQUAKE (Noda and Uwabe, 1975)

2.6 1944 TONANKAI, JAPAN, EARTHQUAKE[*]

On December 7, 1944, a very strong earthquake of magnitude 8.3 occurred offshore of the Kii Peninsula with a hypocenter located very near the ground surface. This earthquake caused damage to structures at the Yokkaichi, Nagoya, and Osaka ports ((Fig. 2-8a).

At the Yokkaichi Port, a large trestle-type pier and quay wall suffered damage in the form of lateral movements (Fig. 2-8b). This damage has been attributed to earthquake-induced sliding of the soft clay slopes at this structure site, which are underlain by alternating layers of gravel and clay. At the Nagoya Port, almost all of the sheet pile bulkheads bulged seaward (Fig. 2-8c). No sliding at the lower part of the sheet-pile wall was observed, despite its rather short embedment length.

At the Osaka Port, retaining-wall structures along the central pier, which were comprised of sheet-pile bulkheads and subsurface pile-supported platforms, suffered substantial seaward bulging (about 3 m) and slight vertical settlement (Fig. 2-8d). This damage was attributed to the poor subsurface conditions at this port, which are comprised of sludge to a depth of 33 m, underlain by alternating layers of gravel and sludge. It occurred despite the fact that the structures were supported by wood piles that extended to the gravel layer.

2.7 1946 NANKAI, JAPAN, EARTHQUAKE[†]

On December 21, 1946, a major earthquake of magnitude 8.1 occurred 60 km offshore of the Kii Peninsula, with a focal depth of 30 km (Fig. 2-9a). Damage from this earthquake was spread

---

[*]Primary references for damage assessment from the 1944 Tonankai earthquake were Amano et al. (1956) and Okamoto (1973).

[†]Primary references for damage assessment from the 1946 Nankai earthquake were Amano et al. (1956), JPHRI (1980), and Noda and Uwabe (1975).

0 100 200 300 km

● EPICENTER
● DAMAGED PORTS

YOKKAICHI
PORT

NAGOYA PORT
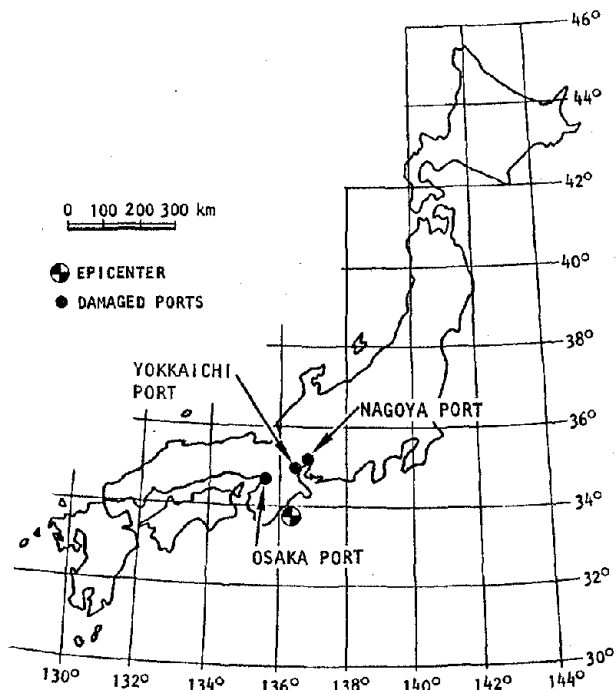
OSAKA PORT

(a) Location of earthquake epicenter
and damaged ports
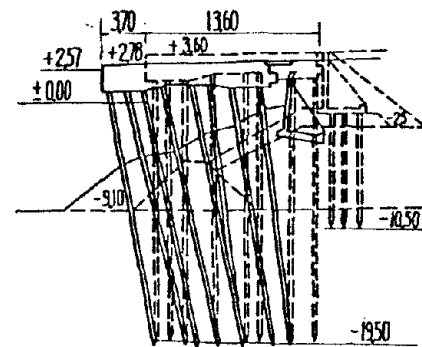
(b) Trestle-type pier and quay
wall at Yokkaichi Port
(Amano, et al., 1956)

+3.5 m

±0.0 m   Tie rod

21.2 m

−7.5 m

l = 16m Steel sheet pile

ℓ = 20cm, l = 30m

Wooden pile
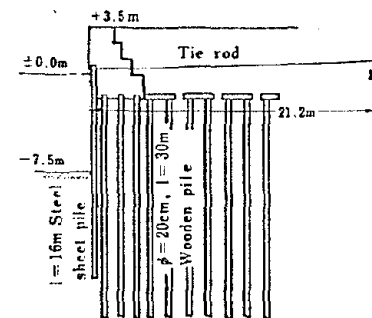
(d) Central pier at Osaka Port
(Okamoto, 1973)

4.0

+4.10 +4.80

H.W.L +2.70

L.W.L ±0.00

Larssen V

Wooden Pile

−9.1

−13.8

0   5   10m
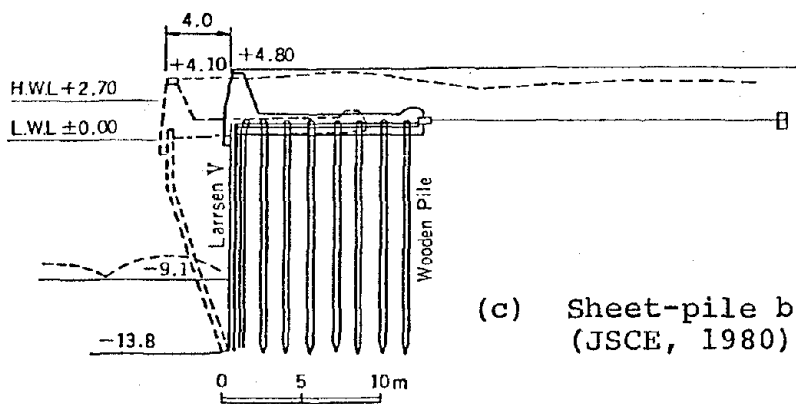
(c) Sheet-pile bulkhead in Nagoya Port
(JSCE, 1980)

FIGURE 2-8. PORT AND HARBOR STRUCTURES DAMAGED DURING
1944 TONAKAI EARTHQUAKE
(All dimensions and elevations in meters)

R-8122-5395
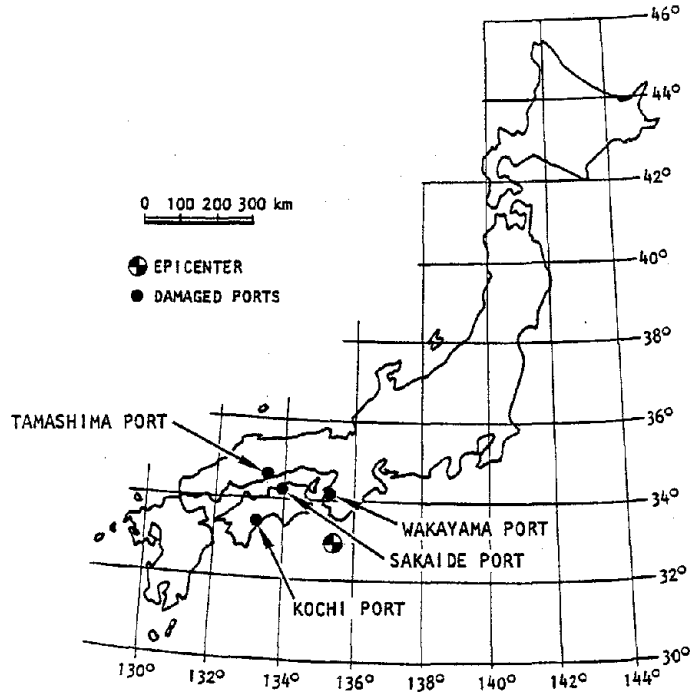
(a) Location of earthquake epicenter
     and damaged ports
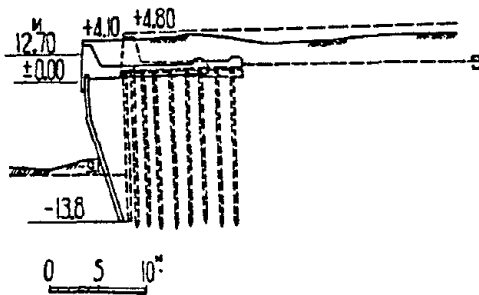
(b) Sheet-pile bulkhead at
     Nagoya Port
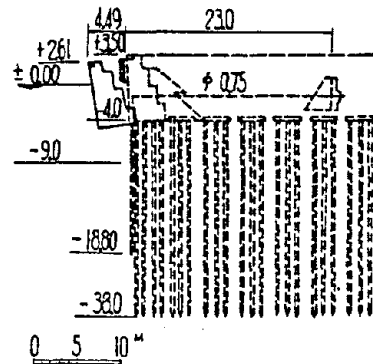
(c) Central pier at
     Osaka Port

FIGURE 2-9. PORT AND HARBOR STRUCTURES DAMAGED DURING 1946
             NANKAI EARTHQUAKE (Amano, et al., 1956)
             (All dimensions and elevations in meters)

over a very wide area, with the greatest damage at alluvial sandy soil deposits along rivers and at sites with poor soil along shorelines, even when these sites were far from the epicenter. Therefore, this damage was undoubtedly soils-related, and probably due to porewater pressure buildup in these soil materials.

The most significant damage at port and harbor locations involved the collapse and shifting of quay walls at the Sakaide, Wakayama, Kochi, and Tamashima Ports, and the outward bulging of a sheet-pile bulkhead and a retaining wall at the Nagoya Port and the Osaka Port, respectively (Fig. 2-9b,c). The Central Pier at Osaka Port, which was also damaged during the 1944 Tonankai earthquake, suffered the most extensive damage of any structure in that port. The degree of bulging of this wall was about the same as that of the 1944 event, although its settlement was somewhat greater and was accompanied by prominent cracking. Also the anchor system for this wall displaced seaward, and the fill behind the earthquake settled substantially.

2.8 1952 TOKACHI-OKI, JAPAN, EARTHQUAKE[*]

On March 4, 1952, a major earthquake of magnitude 8.1 occurred 70 km east of Cape Erimo (Fig. 2-10a). This earthquake had a focal depth of about 45 km, and caused substantial damage in the Hidaka, Tokachi, and Kushiro prefectures of Hokkaido, particularly in the coastal alluvium and in peat bogs and reclaimed marshland.

The port that suffered the most damage from this earthquake was that at Kushiro (Figs. 2-10b). The subsurface soil deposits at that port are comprised of coarse sands and gravels with low

_____

[*]Primary reference for damage assessment from the 1952 Tokachi-Oki earthquake was Noda and Uwabe (1975).
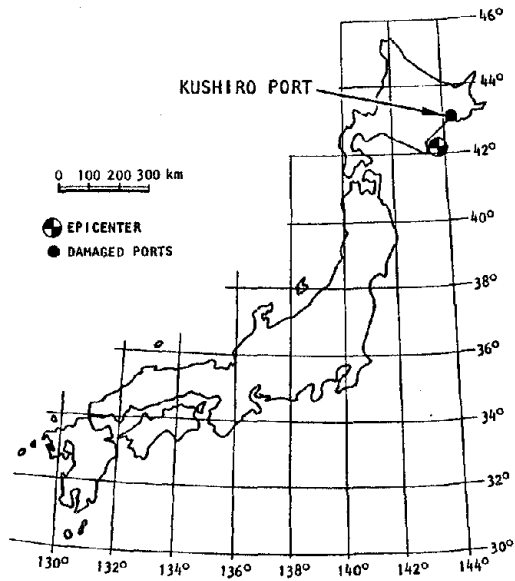
(a) Location of earthquake epi-
    center and Kushiro Port
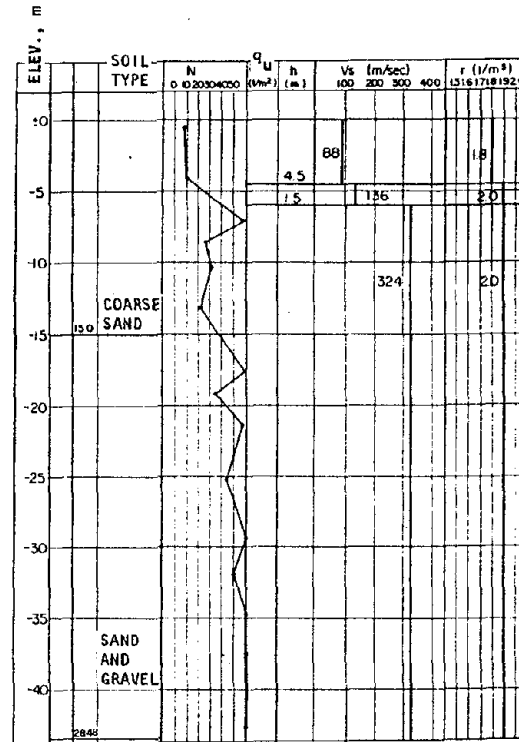
(c) Soil profile at Kushiro Port
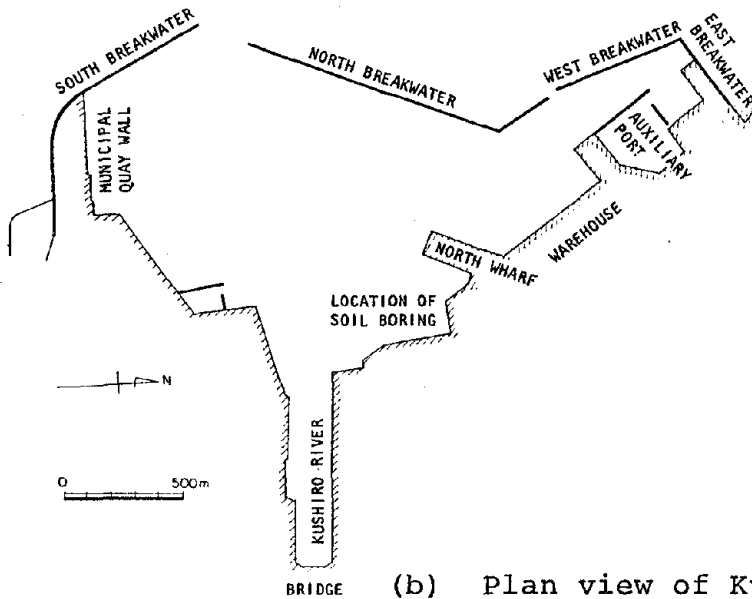
(b) Plan view of Kushiro Port

FIGURE 2-10. EPICENTER OF 1952 TOKACHI-OKI EARTHQUAKE AND DESCRIPTION
OF KUSHIRO PORT (Noda and Uwabe, 1975)

blowcounts over the first 5 m of depth, and moderate-to-high blowcounts thereafter (Fig. 2-10c). Quay walls at Kushiro Port, particularly those of the caisson type along the North Wharf, suffered substantial sliding (of up to 3 m), settlement (of up to 0.7 m), and tilting (Fig. 2-11). This probably was related to porewater pressure buildup in the subsurface soil materials, which led to sliding along shallow slip surfaces and to bearing capacity failures due to high toe pressures.

2.9 1960 CHILE EARTHQUAKES[*]

A series of several strong earthquakes, shook South Central Chile within about a one-month time period starting on May 21, 1960. Within this time period, Chile experienced no less than 13 earthquakes of magnitude 6 or greater, with one being at least as large as the 1906 San Francisco event (magnitude 8.3). Many cities between Concepción to the north and Puerto Montt to the south were subjected to severe shaking at least once during this series of earthquakes (Fig. 2-12a). The epicenters of the major events within this series were located near but not directly at any major city.

The most substantial damage to port and harbor facilities during these earthquakes occurred at Puerto Montt and was primarily soils related. This port was underlain by an artificial fill material comprised of gravel, sand, silt, and some masonry fragments and organic matter (see Fig. 2-12b). The fill was typically placed by dumping, except in the new harbor area where it was placed hydraulically by dredging from the harbor bottom. Throughout the harbor, it served either as an underlying support medium or as backfill to the quay walls and

---

[*]Primary references for damage assessment from the 1960 Chile earthquakes were Duke and Leeds (1963) and Noda and Uwabe (1975).
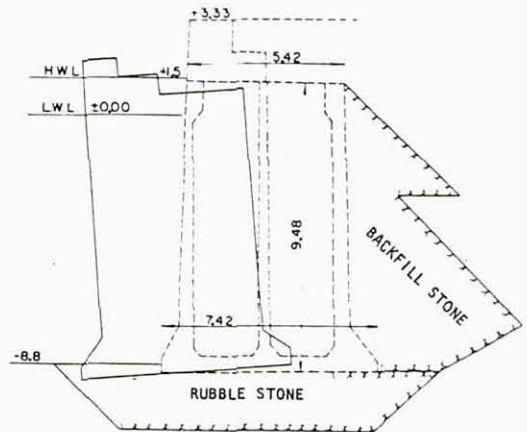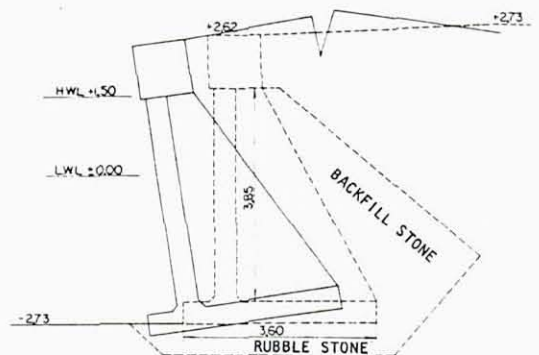
(a) Plan view

NOTE:

HORIZONTAL DISPLACEMENTS RANGE
FROM 1.8 m to 3.3 m

VERTICAL SETTLEMENTS RANGE
UP TO 1 m

LEGEND

- - - - POSITION BEFORE EARTHQUAKE
——— POSITION AFTER EARTHQUAKE

SECTION A-A

SECTION B-B

SECTION C-C

(b) Cross sections

FIGURE 2-11. DISPLACEMENTS OF QUAY WALLS AT NORTH WHARF OF
KUSHIRO PORT — 1952 TOKACHI OKI EARTHQUAKE
(Noda and Uwabe, 1975)

(All dimensions and elevations in meters)

Photograph courtesy of D.J. Leeds
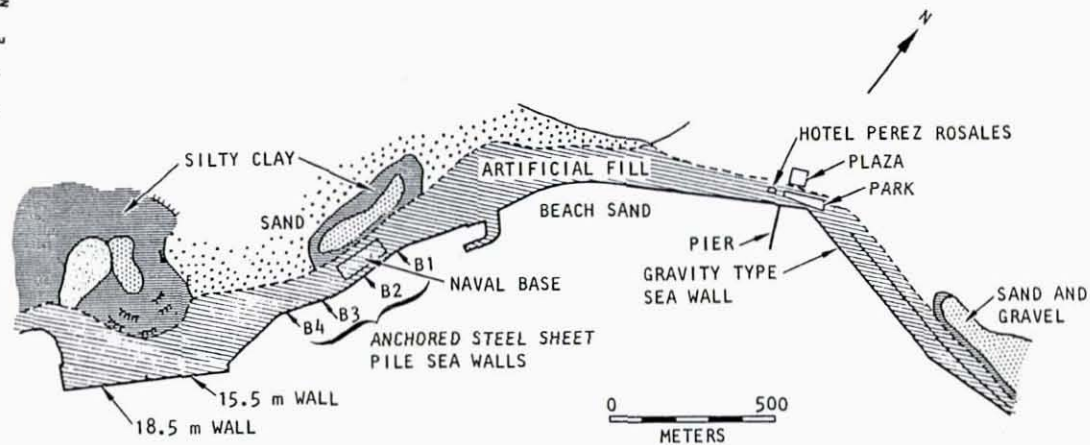
(a) Affected region

(b) Puerto Montt waterfront zone

FIGURE 2-12.   1960 CHILI EARTHQUAKES — AFFECTED REGION AND PUERTO
MONTT WATERFRONT ZONE (Duke and Leeds, 1963)

other retaining wall structures. Widespread and substantial liquefaction of this artificial fill during the earthquakes was the primary cause of the extensive damage and failures of the port and harbor structures at Puerto Montt.

As an example of the port and harbor facility destruction at Puerto Montt, more than 500 m of a gravity-type sea wall failed or were severely damaged. A 15.5-m wall overturned completely along its full length of 300 m, and the concrete segments of an 18.5-m wall overturned along nearly its entire length of 226 m (Fig. 2-13). In addition, most of the supporting caissons slid up to 1 m and tipped seaward. It is noted that the backfill material for these quay walls, which was comprised of the hydraulically placed artificial fill material described above, was in practically a quick condition when inspected following the earthquake.

Another example of the extensive failures along the Puerto Montt harbor was along the naval base, which was faced with anchored steel sheet-pile sea walls (Fig. 2-14a). The four wall segments that failed are depicted in Figures 2-14b as B1, B2, B3, and B4. Segment B1 slid seaward up to 1 m, and Segment B2 failed in flexure at the base of its cantilevered portion; this latter failure was attributed to corrosion which reduced the 5/16-in. webs of Segment B2 to about 1/8 in. At Segments B2, B3, and B4, the tie rods of the anchored portion broke in tension at the threaded portion. The railway track on the fill behind Segments B2, B3, and B4 was severely distorted due to the seaward flow of the backfill accompanying these failures. Details of these failures are given in Figure 2-14b.

Still other examples of failure at Puerto Montt can be cited. The downtown pier at this harbor suffered severe distortion of its decking and piling (Fig. 2-15a), and most of the remaining major waterfront structures suffered damage or destruction due to the earthquake-induced failure of the underlying fill.
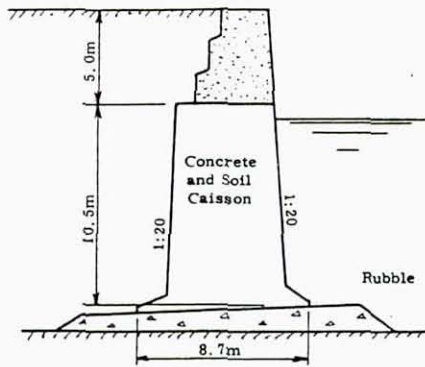
15.5 METER QUAY WALL
(after Chile Dept. of Ports)
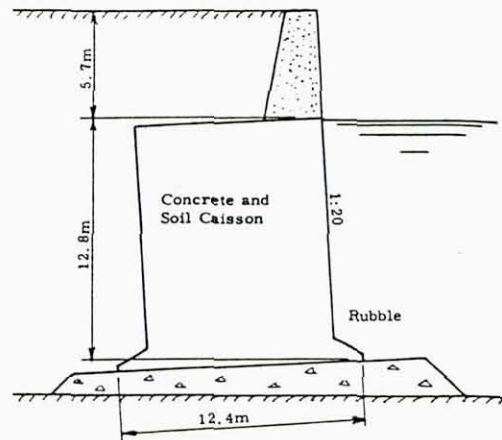
18.5 METER QUAY WALL
(after Chile Dept. of Ports)

(a)   Cross-sections prior to earthquake

Photograph courtesy of D.J. Leeds

(b)   Failure of 15.5 m gravity wall

FIGURE 2-13.   QUAY WALL FAILURES AT PUERTO MONTT
(Duke and Leeds, 1963)
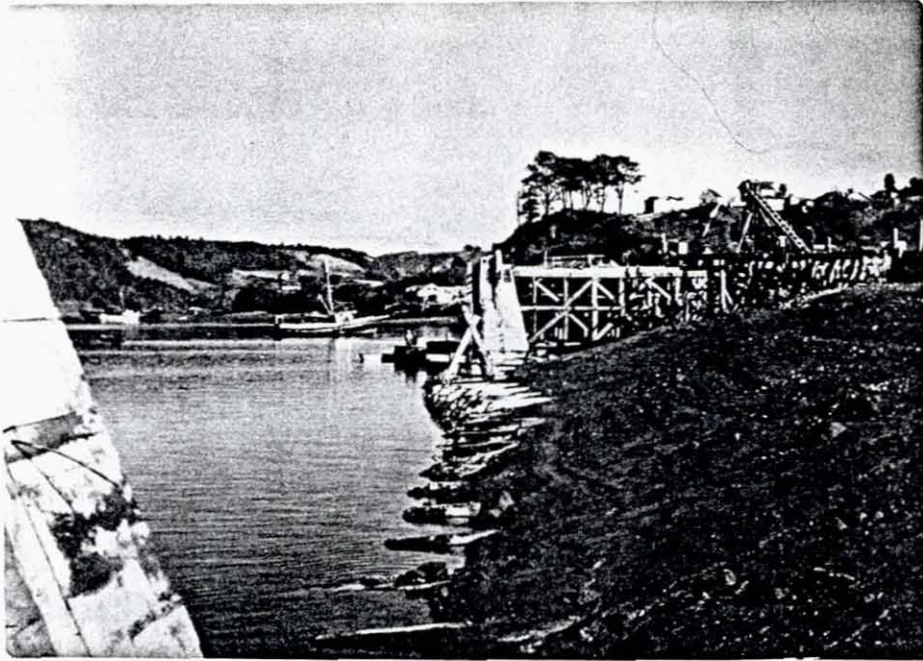
Photograph courtesy of D.J. Leeds

(c) Failure of 18.5 m gravity wall
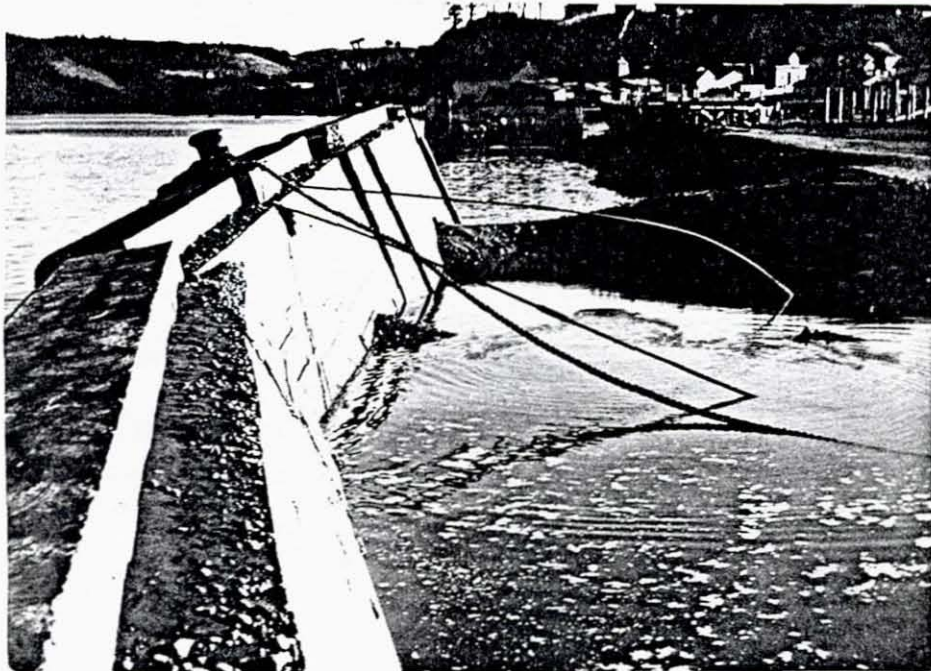
Photograph courtesy of D.J. Leeds

(d) Failure of gravity-type sea wall

FIGURE 2-13. (CONCLUDED)

2-23
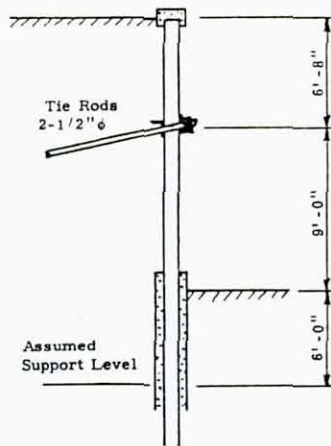
(a) Cross section of
    sheet pile sea
    wall

SEA WALL	TIE-ROD SPACING, ft	LENGTH OF FAILED SEGMENT, ft	NATURE OF FAILURE
B1	5.0	EXTENSIVE	ANCHOR YIELDED (?)
B2	7.5	70	RUSTED CANTILEVER SECTION FAILED
B3	7.5	80	TIE-RODS BROKE
B4	7.5	150	TIE-RODS BROKE

(b) Details of wall failures

FIGURE 2-14. FAILURES OF SEA WALL SEGMENTS B1, B2, B3, AND B4
(Duke and Leeds, 1963)
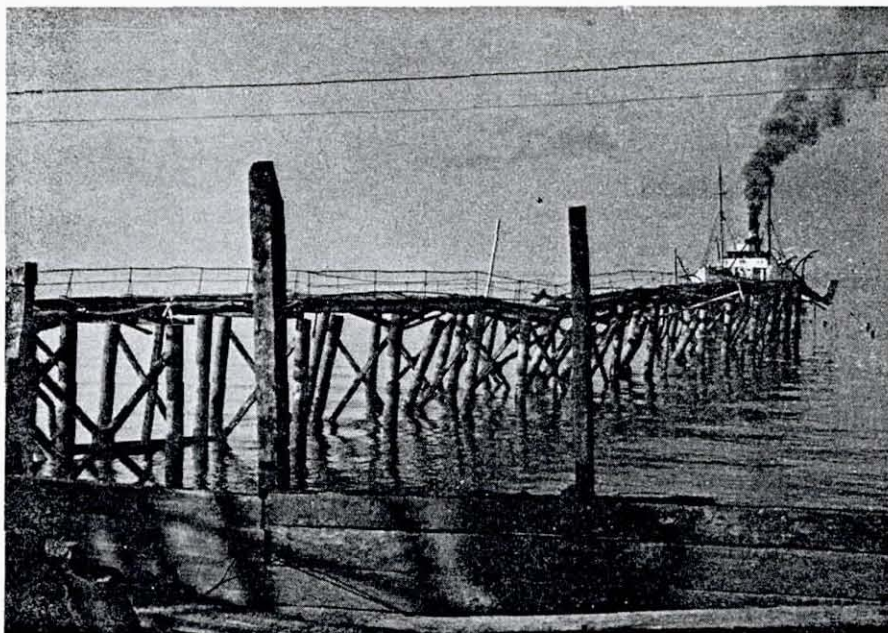
Photograph courtesy of D.J. Leeds

(a) Downtown pier at Puerto Montt
(Duke and Leeds, 1963)
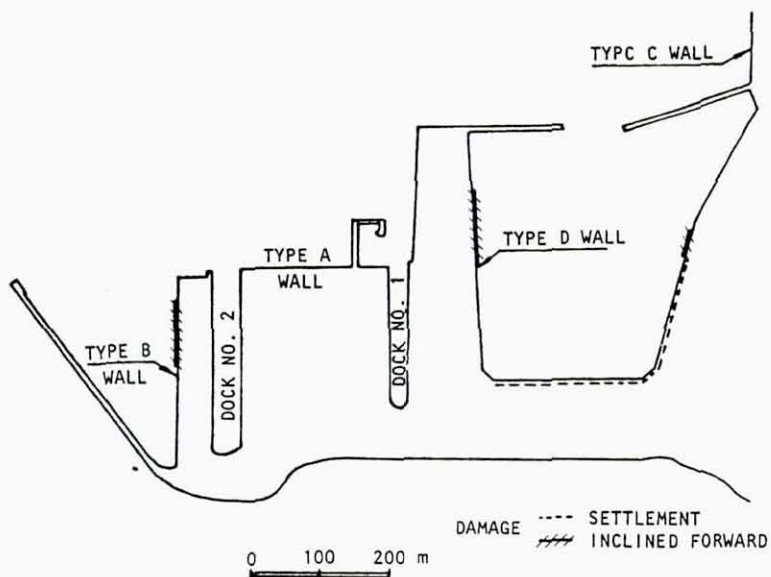
(b) Displacements of quay walls at Talcahuano
Port (Noda and Uwabe, 1975)

FIGURE 2-15. OTHER EXAMPLES OF PORT AND HARBOR FACILITY
DAMAGE — 1960 CHILE EARTHQUAKES

Some examples of port and harbor facility damage at other ports besides Puerto Montt are also noteworthy. In Talcahuano Port near Concepción (at the northern end of the affected area, Fig. 2-12a) concrete block quay walls suffered pronounced tilting and settlement (Fig. 2-15b).

2.10 1961 HYUGANADA, JAPAN, EARTHQUAKE[*]

A strong earthquake of magnitude 7.0 struck the southern part of Japan off Miyazaki prefecture on February 27, 1961 (Fig. 2-16a). The focal depth was about 40 km. The maximum horizontal acceleration was estimated to be in the range of 0.25 to 0.30 g in the vicinity of the city of Miyazaki.

The most severe effects of this earthquake were felt at Aburatsu Port (Fig. 2-16b). However, because of the relatively favorable soil conditions at this port (Fig. 2-16c), none of the waterfront structures at this port suffered a loss of function as a result of this earthquake. Typical damage incurred at this port is shown in Figure 2-16d for two quay walls that were under construction at the time of the earthquake. The -7.5 m quay wall shown in this figure experienced a maximum horizontal displacement of 20 cm, a maximum settlement of 18 cm, and a settlement of the backfill materials behind the wall of 60 cm. The -5.0 m quay wall shown in this figure displaced horizontally 24 cm and settled 39 cm.

2.11 1964 ALASKA, USA, EARTHQUAKE

A series of six strong earthquakes struck the Gulf of Alaska on March 27, 1964 (Fig. 2-17). The magnitude of the largest of these events was 8.4, and its focal depth was estimated at

---

[*]Primary reference for damage assessment from the 1961 Hyuganada earthquake was Noda and Uwabe (1975).
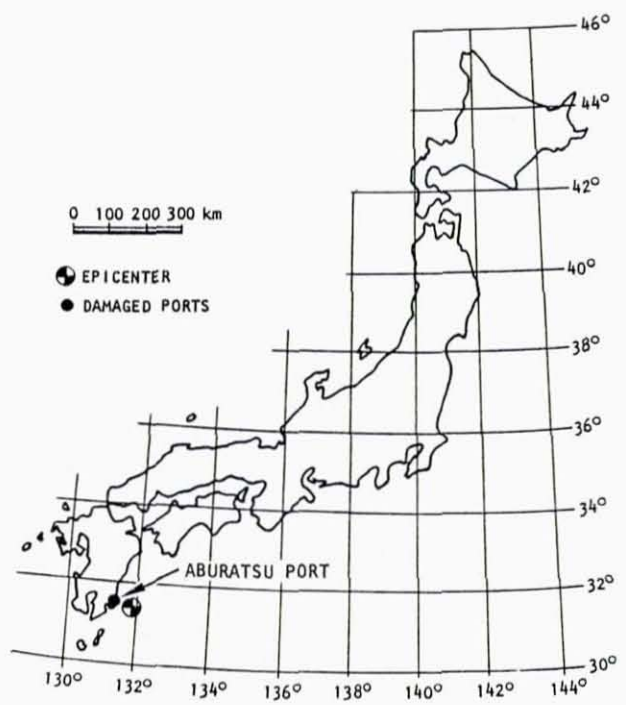
(a) Location of earthquake epicenter
     and Aburatsu Port
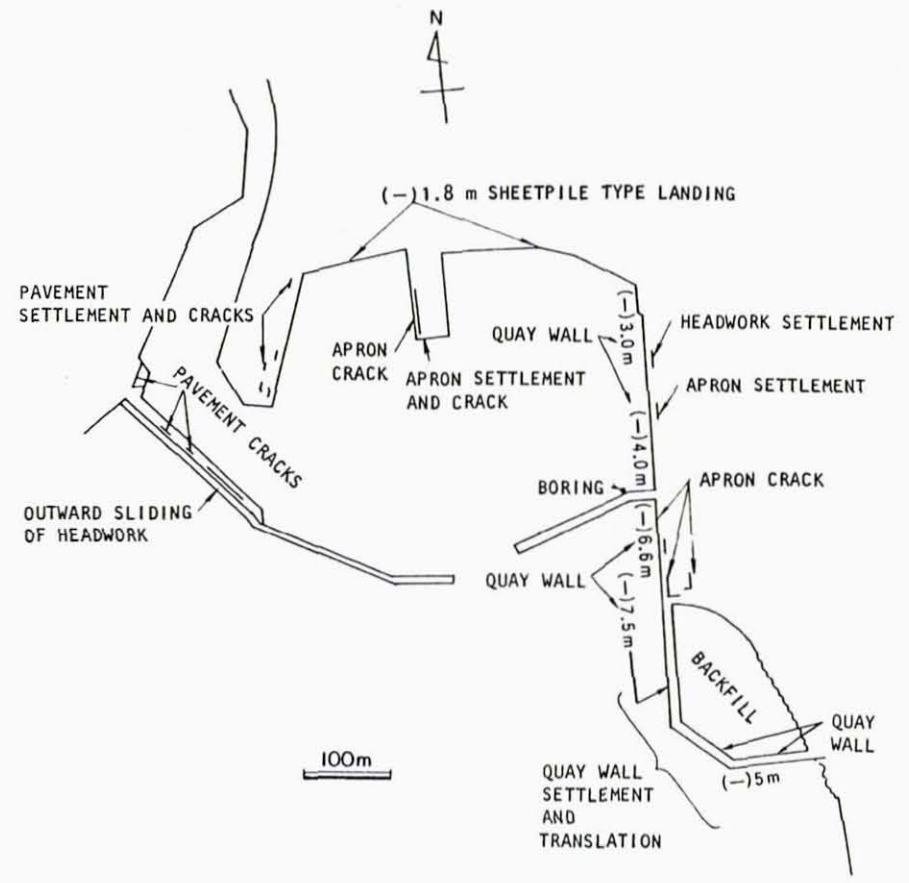
(b) Earthquake damage at Aburatsu Port

FIGURE 2-16.   PORT AND HARBOR DAMAGE FROM 1961 HYUGANADA
               EARTHQUAKE (Noda and Uwabe, 1975)
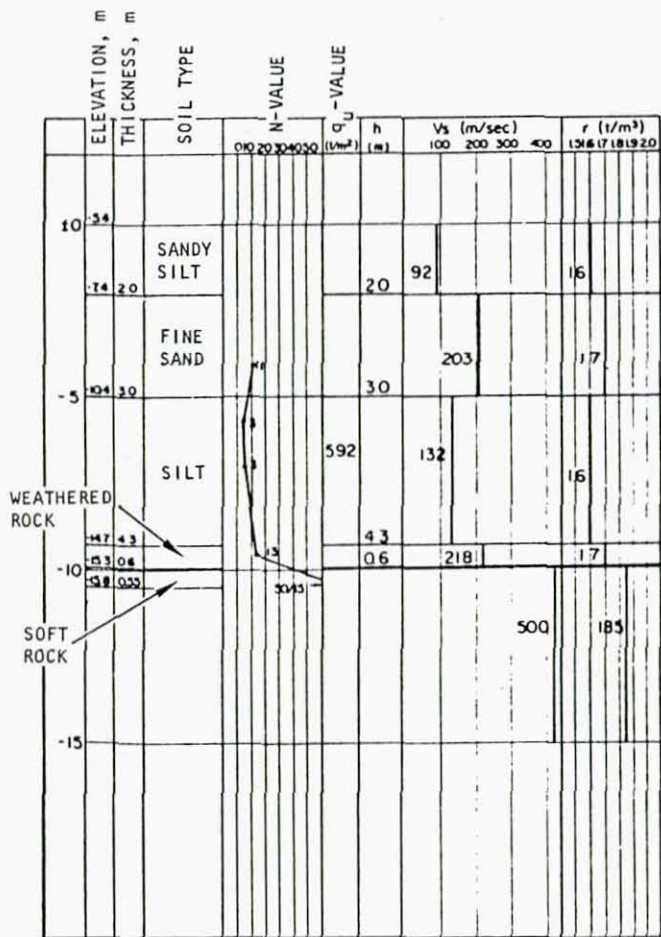
(c) Soil profile at Aburatsu Port
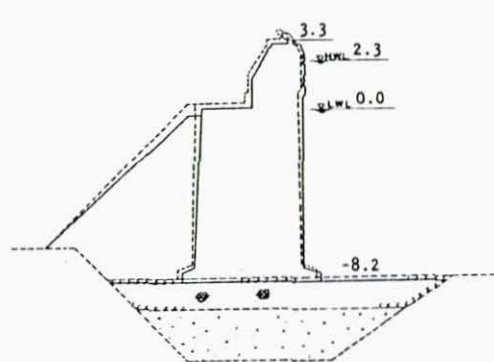
-7.5 m QUAY WALL
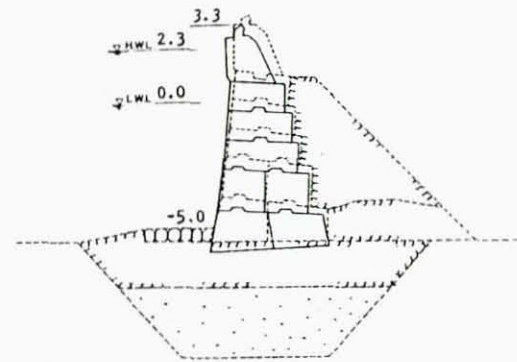
-5.0 m QUAY WALL

(d) Damaged quay walls at Aburatsu Port
(all dimensions and elevations in meters)

FIGURE 2-16.   (CONCLUDED)
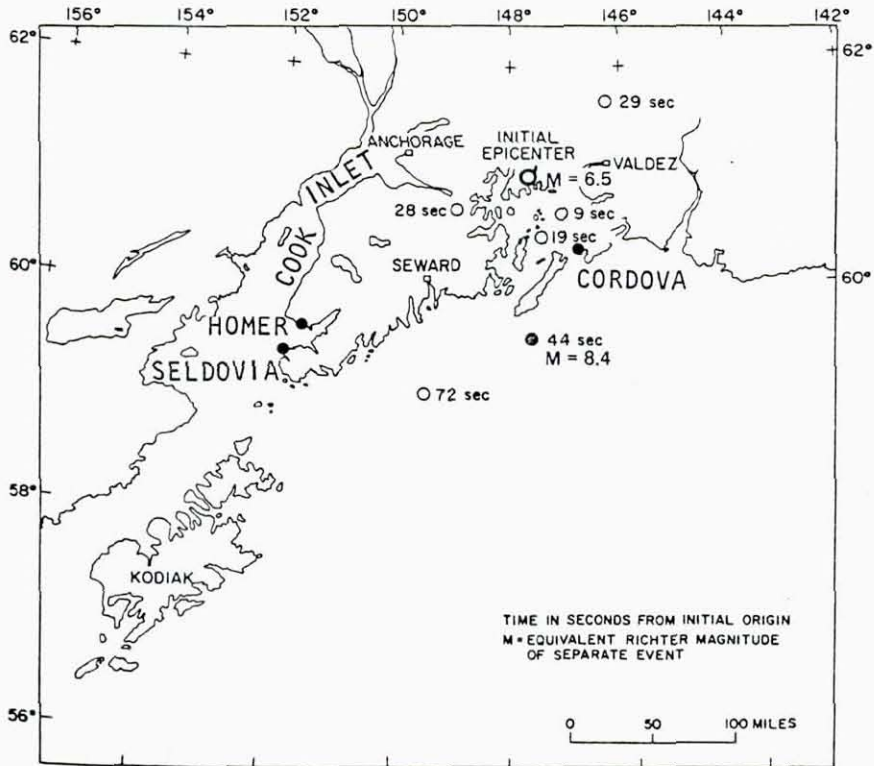
FIGURE 2-17.   MULTIPLE EVENTS OF MAIN SHOCK OF THE
ALASKA EARTHQUAKE (Wyss and Brune,
1967)

between 10 to 30 miles. The damage and destruction caused by these earthquakes at ports and harbors was extremely widespread particularly at Anchorage, Seward, Valdez, and Whittier. This damage is described in the subsections that follow.

2.11.1 ANCHORAGE HARBOR[*]

2.11.1.1 Soil Conditions

The soil conditions throughout much of the Anchorage area consists of a surface layer of relatively dense sandy gravel that is underlain by silty clay and then by layers and lenses of silt, sand, and sandy gravel to depths as great as 200 ft to 300 ft in some locations. This surface gravel layer is typically 20 to 70 ft deep, but becomes thinner to the southwest of Anchorage and disappears northeast of the airport and west of Turnagain Heights; at Turnagain Heights the surface layer is comprised of fine-to-medium sand. Groundwater in the Anchorage area flows from the mountains to the east and through the permeable soil layers to the ocean.

Porewater pressures in the sand and gravel layers affected the stability of the bluffs and slopes in the Anchorage area, most notably at Turnagain Heights where landslides and slope failures led to large scale ground movements. Such movements at Turnagain Heights as well as at other regions in Anchorage were the primary source of damage to structures in the area. In general, the earthquake-induced soil response throughout Anchorage was dependent on the soil properties, topography, layer geometry, depth of water table, and the intensity and duration of the ground shaking.

---

[*] Primary references for damage assessment at Anchorage Harbor were Arno and McKinney (1973) and Scott (1973a).

2.11.1.2 Harbor Damage

The Anchorage Harbor facilities (Fig. 2-18) are comprised of several dock structures. Of these, the Ocean Dock and City Dock suffered particularly substantial damage, summarized as follows:

- Ocean Dock. This 77 ft by 355 ft open-pile dock structure with its 30 ft by 300 ft approach and its 48 ft by 200 ft warehouse was almost completely destroyed. The approach suffered considerable heaving and lateral breakage, particularly near the rock fill. The dock itself deformed substantially, and suffered fractures up to 3 ft wide along the junctions with the dock extensions.

- City Dock. This 600 ft by 300 ft pile-supported dock structure consisted of a 212 ft wide dock, a 98 ft wide earth fill berm, a 150 ft by 500 ft transit shed, and two approach structures on the south end. The piles showed bowing, buckling, and yielding under large horizontal seismic forces. The west approach trestle exhibited concrete rupture at its expansion joints, tilting, and relative vertical displacement, while the east approach trestle suffered little damage. Widespread subsidence of the land mass in the Anchorage area caused a lowering of dock relative to water level, and destruction of the facility protection devices against the effects of floating and submerged ice.
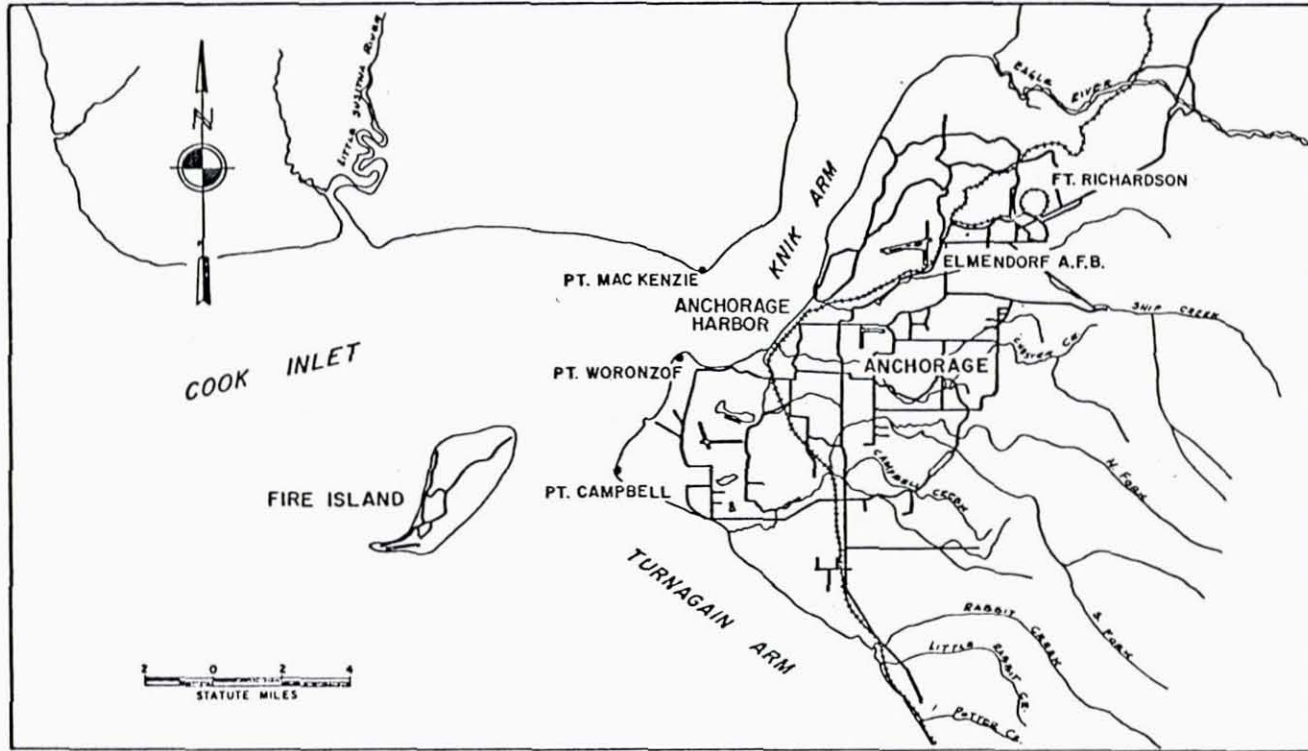
(a)   Locations

FIGURE 2-18.   HARBOR FACILITIES AT ANCHORAGE
(Arno and McKinney, 1973)
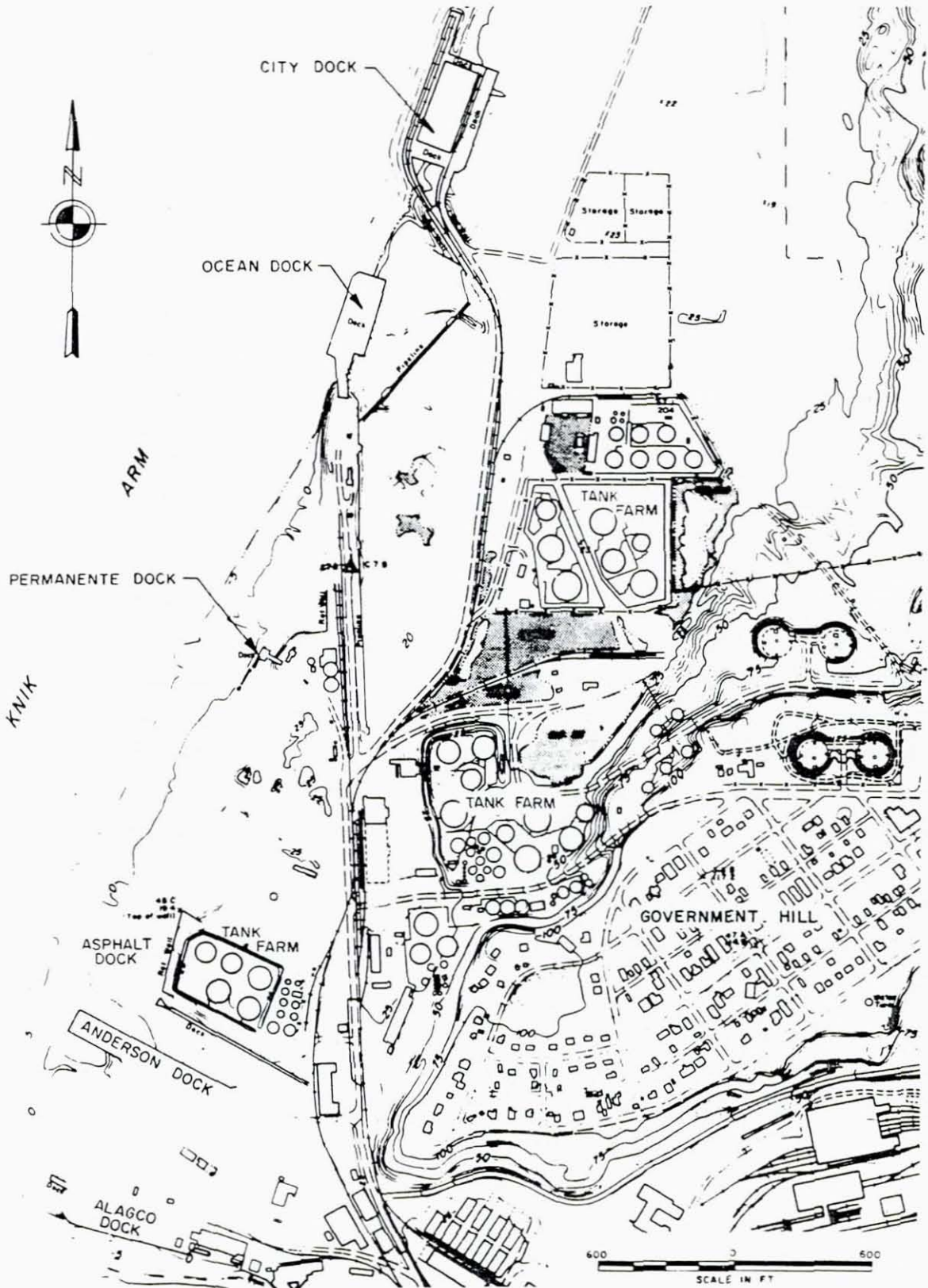
(b) Layout

FIGURE 2-18. (CONCLUDED)

2.11.2 SEWARD HARBOR[*]

2.11.2.1 General Description

Seward is located at the northern end of the western shore of Resurrection Bay (Figs. 2-19a,b), a narrow arm of the Pacific Ocean that extends about 12 miles north into the mountainous Kenai Peninsula. The city of Seward developed on the alluvial fan deposited by Lowell Creek. Seward is a major port and has highly developed harbor facilities. Facilities include railroad marshaling yards, several marginal wharfs, petroleum product unloading docks, a cannery dock, and a small-boat basin (Fig. 2-20).

The soils in and around Seward are both glacial and non-glacial in origin, and consist mainly of glacial till and associated compact glaciofluvial deposits of sand and gravel, alluvial fan and valley deposits of sand and gravel, marine deposits of organic fine sand and silt, and recent alluvium composed of stream-deposited sand and gravel. In the waterfront area of Seward, loose sands and gravels in alluvial fan deposits overlie dense glacial deposits; the thickness of these sands and gravels increases appreciably toward the distal edge of the fan.

2.11.2.2 Description of Damage

The primary damage to the Seward Harbor was caused by massive submarine landslides which induced large portions of the waterfront to slide into Resurrection Bay (Fig. 2-21). Damage was also induced by tsunamis and recessions that swept the waterfront at irregular intervals throughout the night

---

[*]Primary references for damage assessment at Seward Harbor were Shannon and Hilts (1973), Arno and McKinney (1973), Long (1973), Tanaka (1973), Seed (1973), and Lemke (1971).
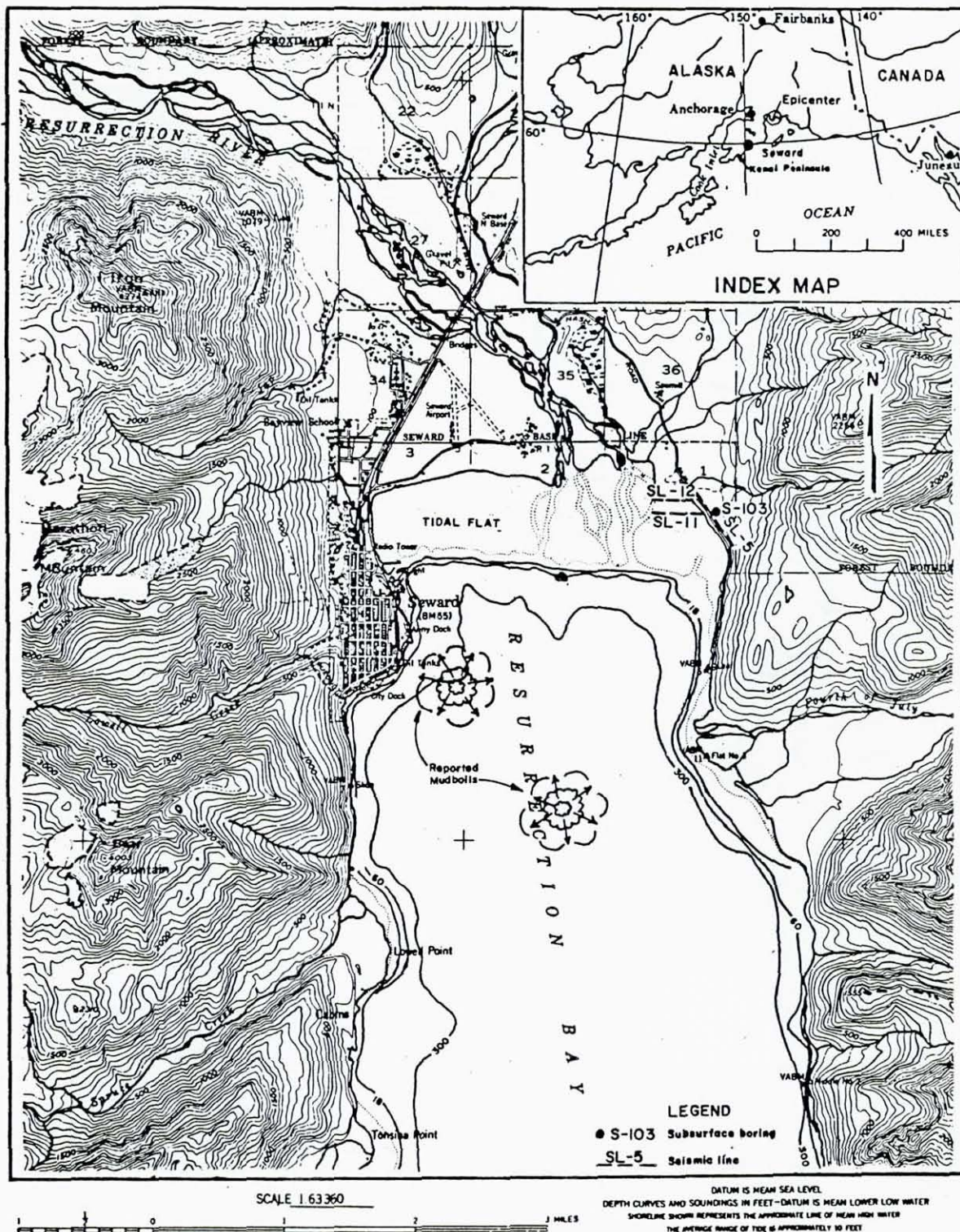
(a) Map of Seward and surrounding area

FIGURE 2-19. LOCATION OF SEWARD HARBOR
(Shannon and Hilts, 1973)
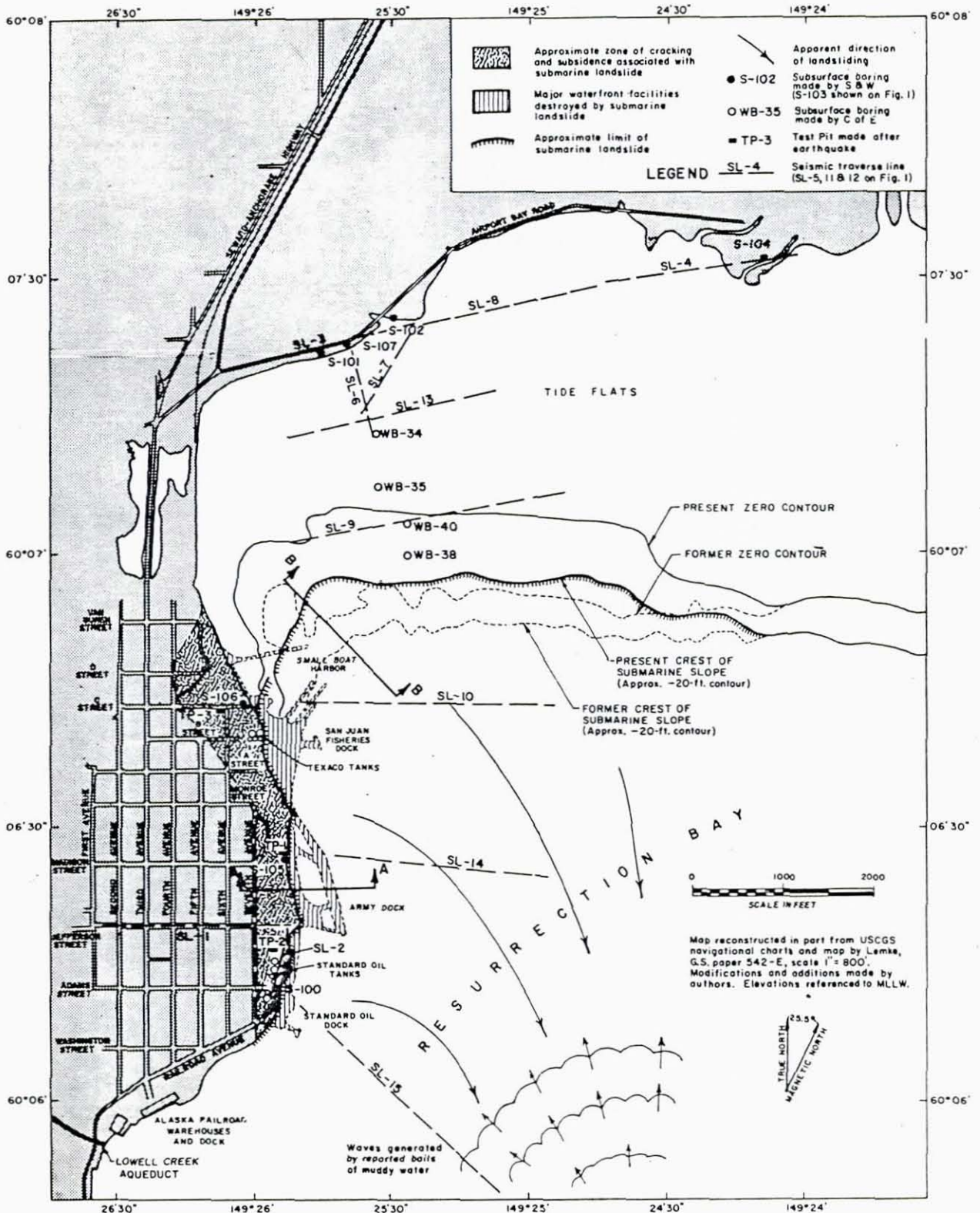
(b) Proximity of landslide to city of Seward

FIGURE 2-19. (CONCLUDED)
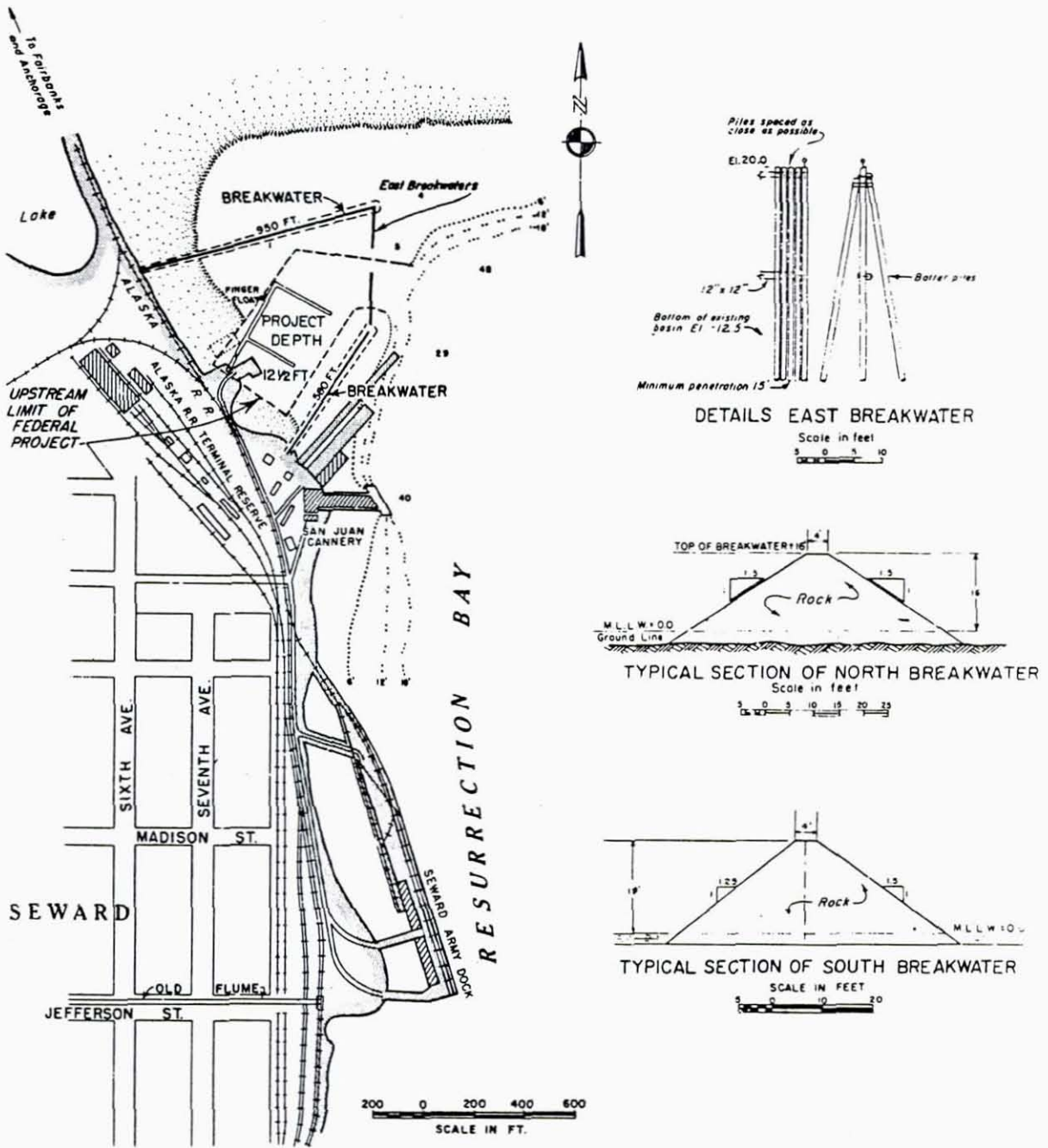
(a)   Small-boat basin

FIGURE 2-20.   SEWARD HARBOR (Arno and McKinney, 1973)
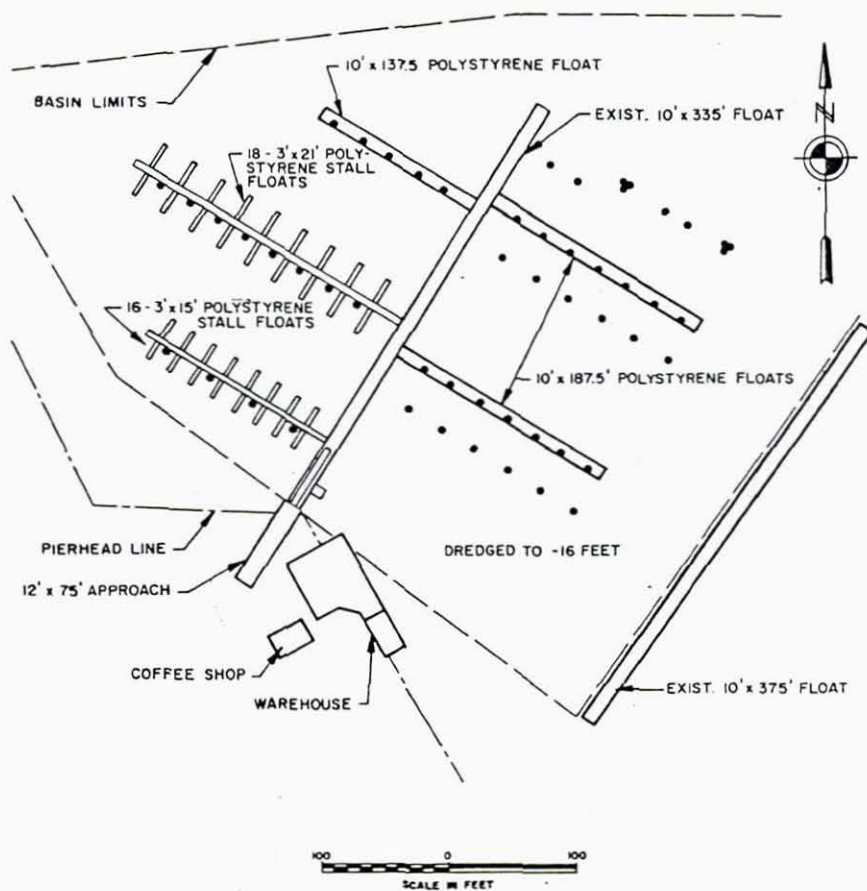
(b) Inner-harbor facilities of
small-boat harbor

FIGURE 2-20. (CONCLUDED)
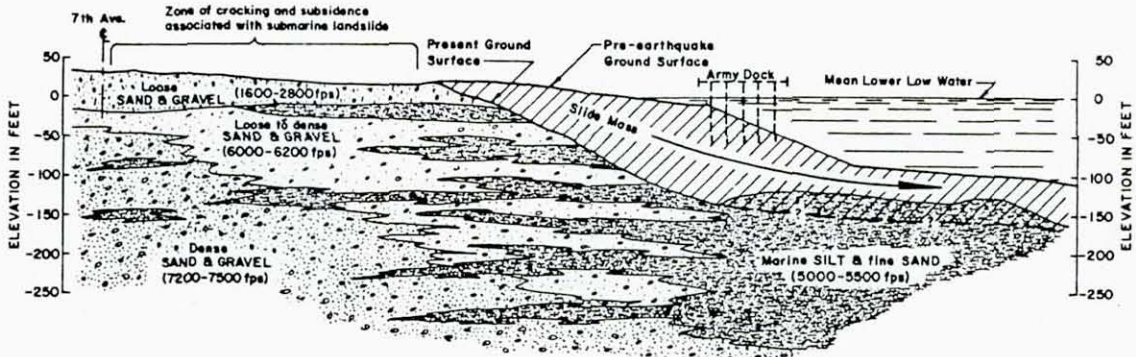
PROFILE A-A (Fig. 2-19b)
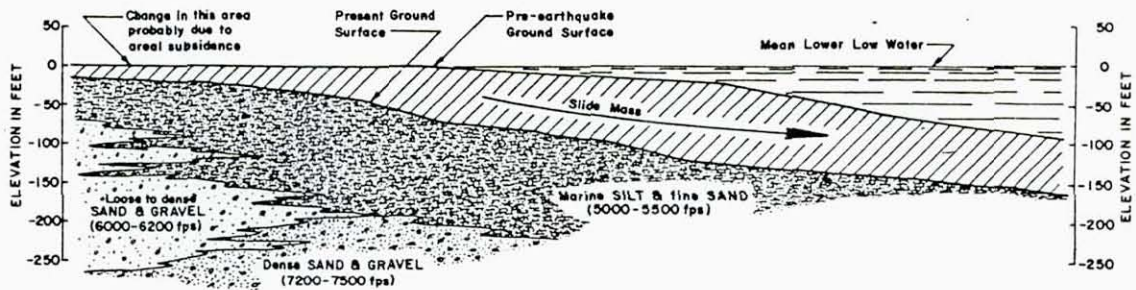
PROFILE B-B (Fig. 2-19b)

NOTES

1. Present Ground Surface from soundings by Corps of Engineers, April, 1964.

2. Pre-earthquake Ground Surface from USCGS Navigational Charts, 1932, and Alaska R.R. Maps, 1953.

3. Subsurface soils generalized from borings and seismic velocity profiles.

4. Elevation datum: MLLW

5. Location of sections on Fig. 2.

6. Numbers in parenthesis below soil description are seismic velocities.

FIGURE 2-21.   SUBMARINE LANDSLIDE AT SEWARD
(Shannon and Hilts, 1973)

following the earthquake. Relatively minor damage was induced directly by structural vibratory effects.

The massive submarine landslides began shortly after the initiation of the earthquake shaking. This initial stage was characterized by a drop in the water level from 20 to 30 ft. A strip of waterfront 50 to 400 ft wide and 4000 ft long then slid into Resurrection Bay, carrying with it oil tanks, docks, warehouses, and other harbor facilities (Fig. 2-19b). At the later stages of ground shaking, a large mud boil was observed offshore. Large (15 ft) waves radiating from the boil struck sides of Seward waterfront and Resurrection Bay and spread burning fuel from ruptured storage tanks. The ground failure was believed to have been initially induced offshore, followed by a spreading of the onshore area.

2.11.2.3 Analysis of Slide Mechanics

The occurrence of the massive submarine landslides in Seward was attributable to the extended duration of the strong shaking (3 to 4 min) and the corresponding response of the subsurface soil deposits. The loose sands and gravels that comprise the alluvial fan deposits at the waterfront area of Seward were initially deposited at close to their natural angle of repose, and were of marginal static stability to begin with, particularly near the south end of the slide where slopes are the steepest. When subjected to additional dynamic effects from the earthquakes, these slopes failed. Stability decreased further by foreset bedding, which in some areas was almost parallel to slopes. No submarine landsliding was detected in the extreme northeast corner of the bay where bedrock overlain by dense glacial deposits is within 100 to 200 ft of ground surface, and the thickness of the marine deposits and recent alluvium is generally less than 100 ft.

The spreading of the landslide from its offshore origin to
the onshore area in the tide flats to the north, may be related
to the thick marine deposits and flat slopes that exist in this
region. This situation is particularly susceptible to liquefac-
tion when subjected to stress reversals; Seed (1979a) has indicated
that flat slopes are more susceptible to liquefaction than are
steep slopes, because relatively small initial shear stresses on
flat slopes are more likely to undergo complete reversal under
dynamic excitation.

Artesian pressures observed at the head of Resurrection Bay
were probably a significant factor in decreasing the stability of
the slopes in this area. Groundwater conditions beneath the Seward
waterfront were probably different before the earthquake, and
failure to detect the presence of artesian pressures after the
earthquake does not preclude their possible existence before the
earthquake, particularly in areas interfingered with marine silt.
It is also possible that, in these areas, confining layers were
removed by prior landslides.

2.11.3 VALDEZ HARBOR[*]

2.11.3.1 General Description

The port of Valdez is the ocean terminus of the Richardson
Highway, and is a major port serving the interior of Alaska
(Fig. 2-22a). The port, which is comprised of numerous docks,
piers, terminals, small-boat facilities, and fuel storage tanks,
is protected by two large breakwaters (Fig. 2-22b).

---

[*]Primary references for damage assessment at Valdez Harbor were
Seed (1973), Scott (1973a), Arno and McKinney (1973), Long (1973),
and Coulter and Migliaccio (1971).
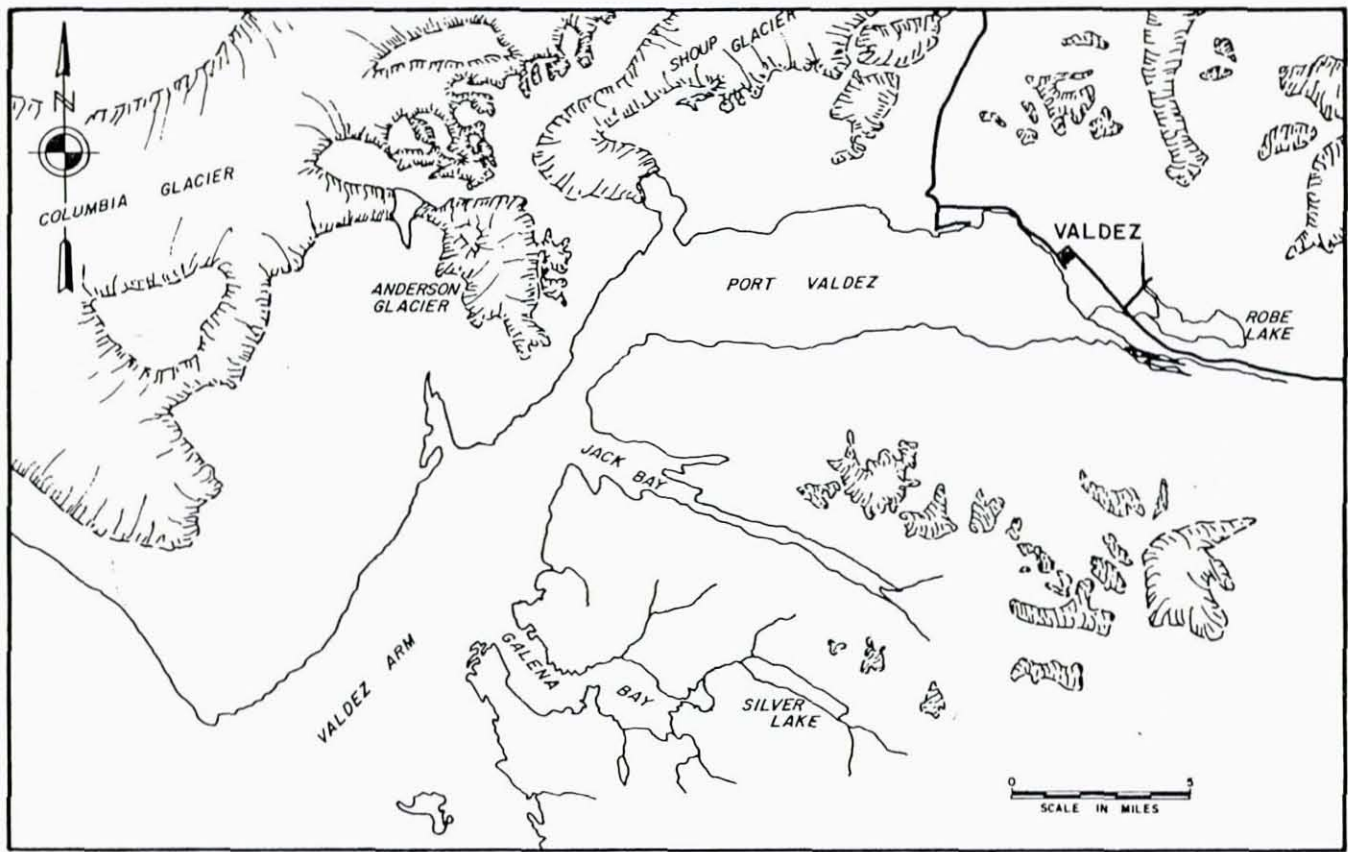
(a) Vicinity map

FIGURE 2-22. VALDEZ HARBOR (Arno and McKinney, 1973)
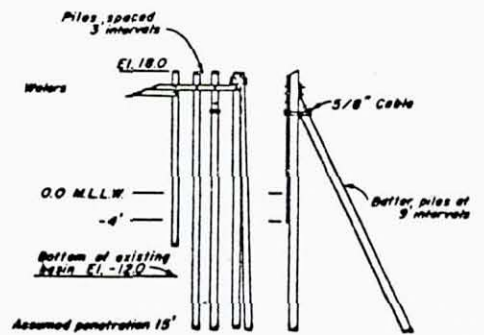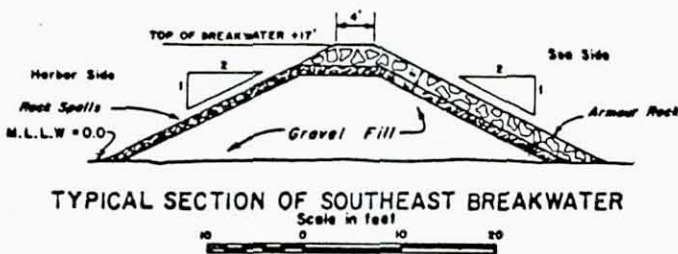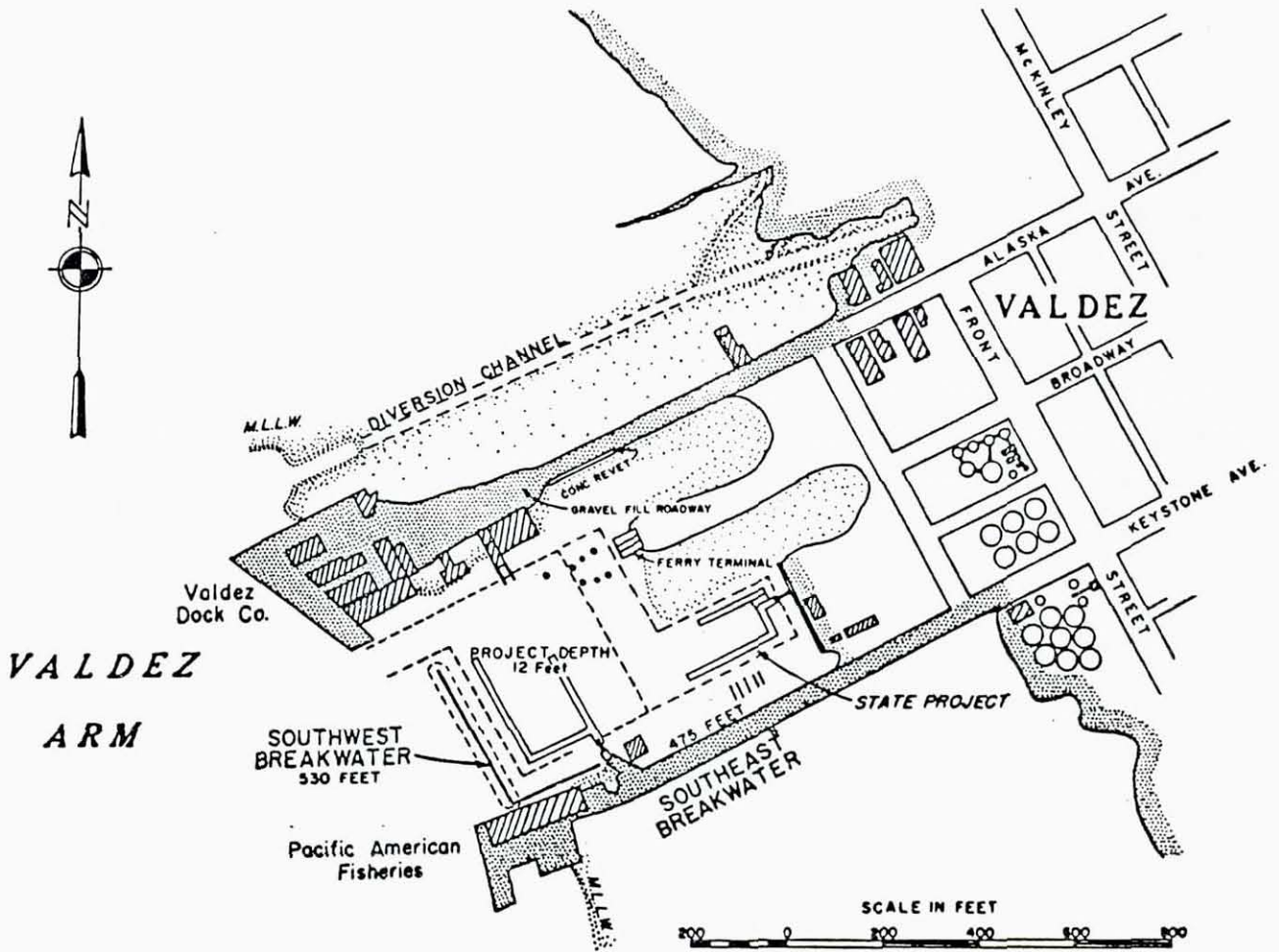
(b) Harbor layout

FIGURE 2-22. (CONCLUDED)

The city of Valdez is situated at tidewater on the seaward edge of a glacial-outwash delta. The delta, which slopes westward from elevation 300 ft at the toe of the glacier to sea level at a 4 mile distance, is comprised of poorly consolidated silt, fine sand, and gravel (Fig. 2-23). The water table was within a few feet of ground surface throughout the delta.

Borings in the dock area were carried out by the Alaska Department of Highways to depths of up to 132 ft, and indicate the following two distinct layers:

- Surface Layer. This layer consists of loose-to-medium-dense sandy gravels with cobbles and silt. It is 20 to 30 ft thick and apparently corresponds to fill placed during the development of the harbor facilities.

- Underlying Layer. This lower layer is comprised of loose-to-medium dense gravelly sand with thin lenses of silt. It persists to the maximum depths drilled and corresponds to the above indicated outwash delta.

2.11.3.2 Description of Damage

The principal source of damage at Valdez was a massive submarine landslide along the waterfront. This slide occurred over an area 4000 ft long by 600 ft wide (Fig. 2-24) and completely destroyed all docks, piers, terminals, and small-boat facilities. Power, sewer, and water systems were totally disrupted. Fires broke out in fuel storage tanks immediately east of the small-boat basin and destroyed a tank farm. The water depth at the dock face increased from 35 to 110 ft, and the area near the small-boat basin, formerly exposed at low tide, was covered by about 70 ft of water. Large waves generated by the subaqueous slide swept onto the Valdez waterfront and also caused significant damage. The waves were of sufficient size to lift a large 400 ft long cargo ship 30 ft above the pier.
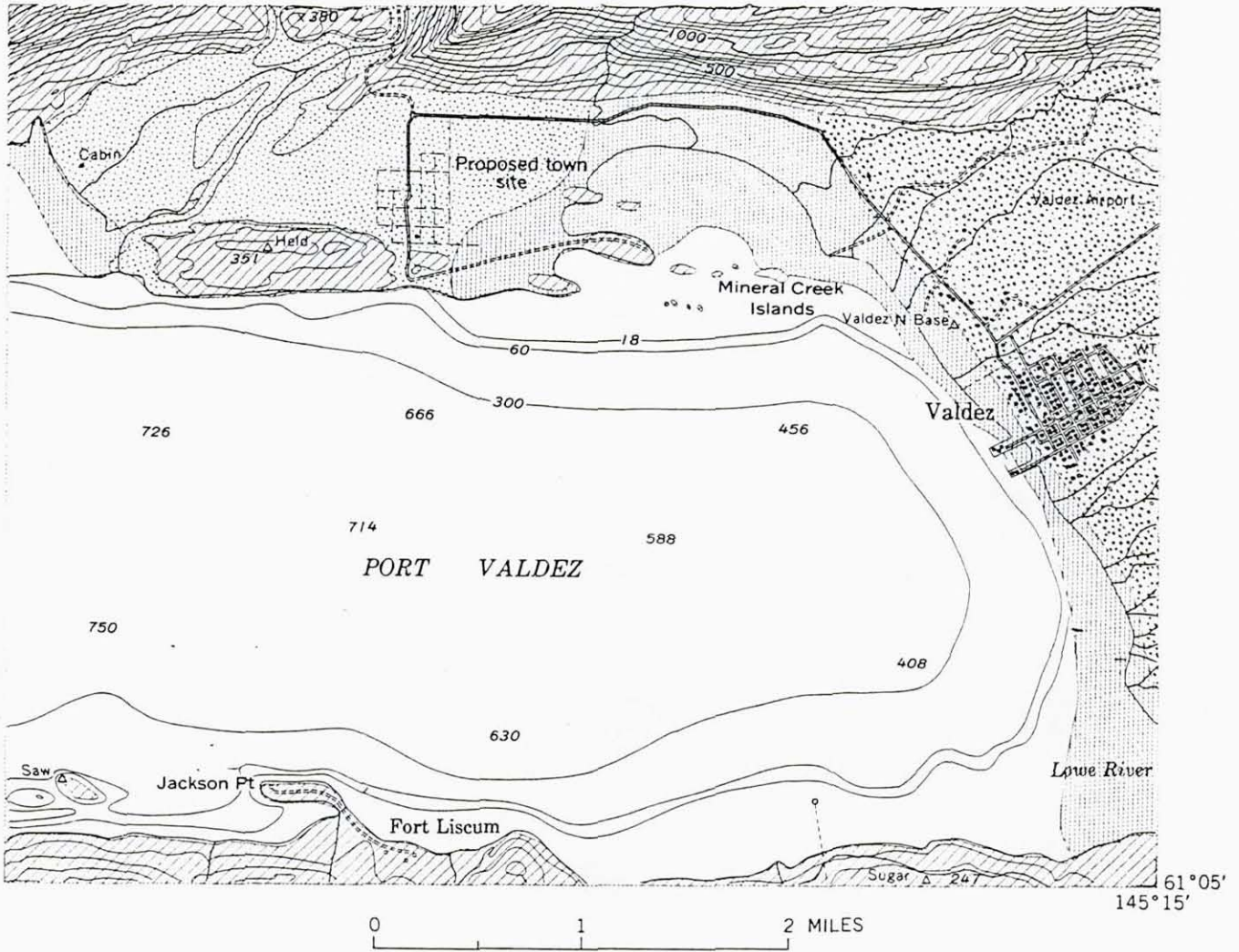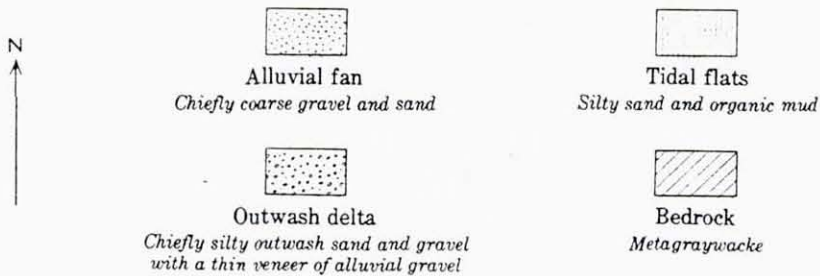
FIGURE 2-23.   SOIL CONDITIONS AT VALDEZ HARBOR (Coulter and
              Migliaccio, 1971)
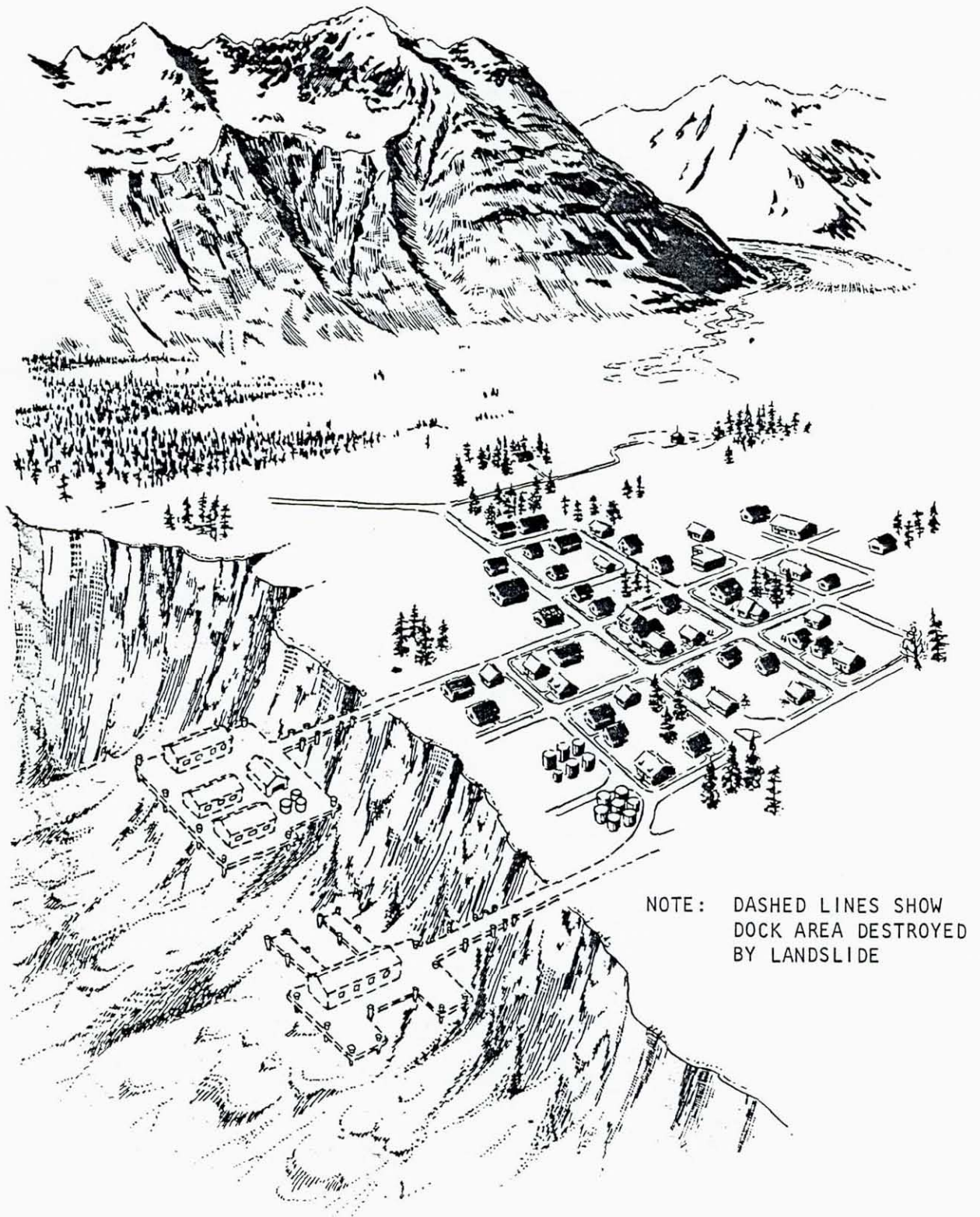
NOTE: DASHED LINES SHOW DOCK AREA DESTROYED BY LANDSLIDE

FIGURE 2-24. ARTIST'S CONCEPT OF FLOW SLIDE AT VALDEZ, 1964. SKETCH BY DAVID LANEVILLE, ALASKA DEPARTMENT OF HIGHWAYS. (Seed, 1973)

2.11.3.3 Analysis of Slide

The severe landslides at Valdez have been attributed to the intensity and duration of the ground shaking. This shaking was sufficient to cause liquefaction in loose-to-medium dense saturated sand. Furthermore, during the earthquake, water withdrew from beaches almost simultaneously with the initial shocks. This withdrawal may have been accompanied by a sudden decrease in hydrostatic head which, in turn, would have resulted in an immediate increase in the weight of upper soil layers and a decrease in support at the toe of the slide due to the sudden drop in sea level. Also, this situation was aggravated by the slide occurring at low tide.

2.11.4 WHITTIER HARBOR[*]

2.11.4.1 General Description

The town of Whittier is situated 40 miles southeast of Anchorage and 33 miles southwest of the earthquake epicenter, at the western end of Passage Canal, and is an ocean terminal of the Alaska Railroad (Fig. 2-25). Permanent dock facilities at Whittier Harbor include a 60 by 1000 ft steel and concrete wharf, a 130 by 900 ft storage warehouse, and the Marginal Wharf (Fig. 2-26).

The subsurface conditions in the Whittier area consist of slate and graywacke of probable Cretaceous age, overlain by unconsolidated Quaternary deposits consisting of glacial morraine, reworked outwash and stream gravel, and artificial fill. Artificial fill covered the easternmost 500 ft of an airstrip area near the Union Oil Company fuel tanks, and an extensive area

---

[*]Primary references for damage assessment at Whittier Harbor were Belanger (1973) and Kachadoorian (1971).
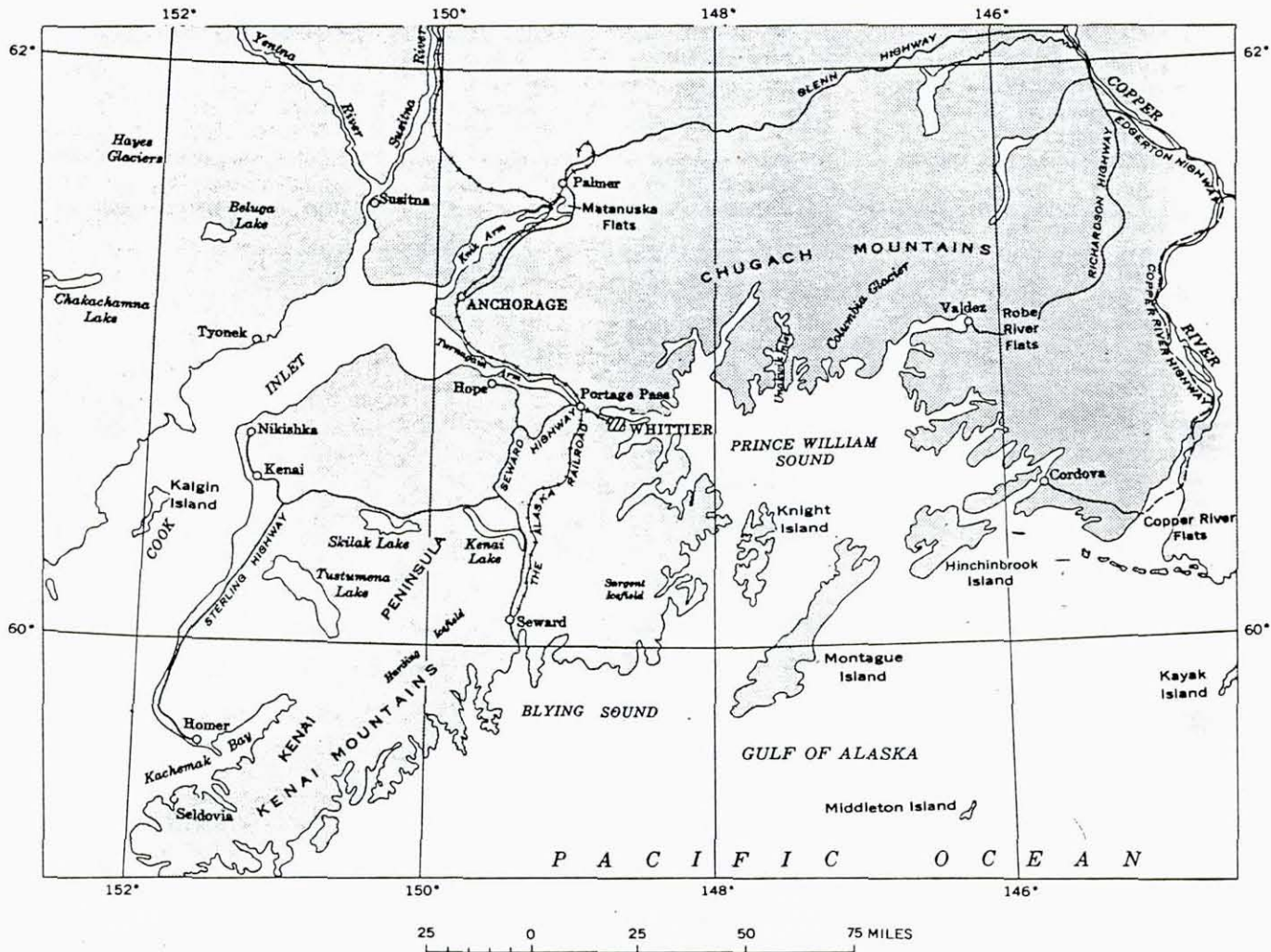
FIGURE 2-25.   INDEX MAP SHOWING LOCATION OF WHITTIER AREA
(Kachadoorian, 1971)
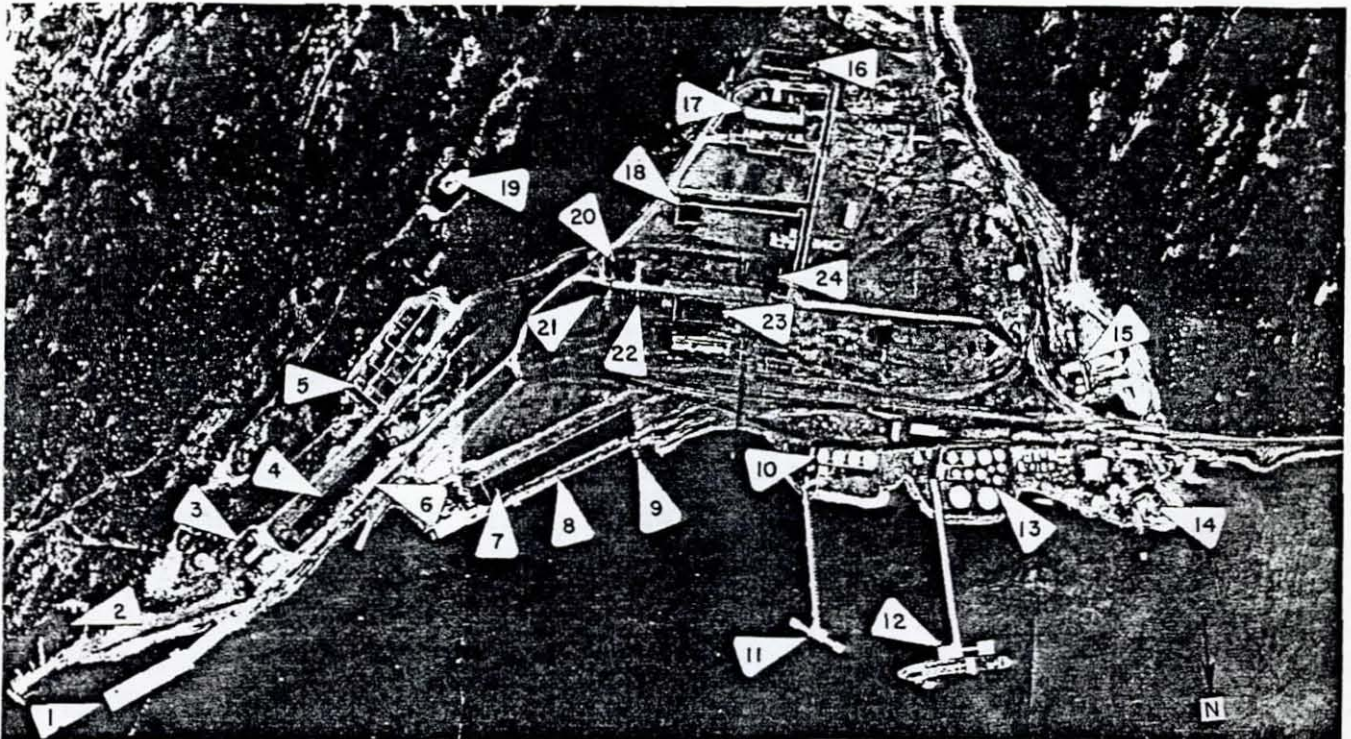
(1) DELONG DOCK
(2) SMALL-BOAT HARBOR
(3) POWER PLANT
(4) SPORTSMAN'S INN
(5) BUCKNER BUILDING
(6) RAILROAD DEPOT
(7) TRANSIT WAREHOUSE
(8) MARGINAL WHARF
(9) CAR-BARGE SLIP
(10) U.S. ARMY POL TANK FARM
(11) U.S. ARMY POL DOCK
(12) UNION OIL COMPANY DOCK
(13) UNION OIL COMPANY COMPLEX
(14) COLUMBIA LUMBER CO.
(15) KOPPERS CO. INC.
(16) SCHOOL
(17) HODGE BUILDING
(18) GYMNASIUM
(19) UNDERGROUND WATER RESERVOIR
(20) FIRE STATION
(21) ALASKA COMMUNICATIONS BUILDING
(22) HEADQUARTERS BUILDING
(23) COLD-STORAGE WAREHOUSE
(24) COMPOSITE SHOP

(a) Preearthquake photo of Whittier showing major facilities and glacial delta of townsite
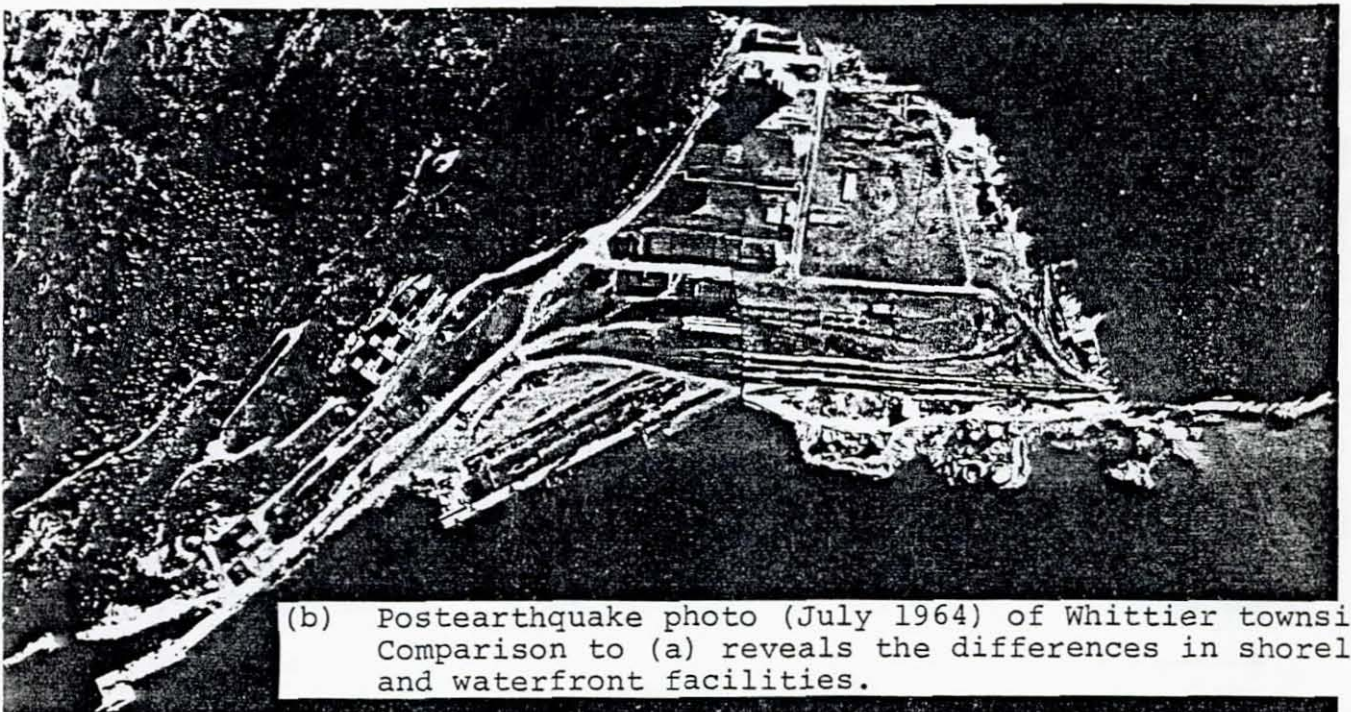
(b) Postearthquake photo (July 1964) of Whittier townsite. Comparison to (a) reveals the differences in shoreline and waterfront facilities.

FIGURE 2-26. WHITTIER BEFORE AND AFTER EARTHQUAKE (Belanger, 1973)

around the Marginal Wharf. Fill materials were obtained locally
and thus consisted of delta deposits or glacial outwash and
stream deposits.

2.11.4.2 Description of Damage

The principal sources of damage to the Whittier Harbor were
large scale subsidence, compaction, and landslides of the under-
lying soil medium. Compaction of unconsolidated sediments and
differential subsidence damaged the DeLong Dock, an intransit
storage shed, and the Marginal Wharf, with a maximum subsidence
of 1-1/2 ft recorded near the Marginal Wharf. Landslides occurred
in delta sediments at the head of the Passage Canal, at the
Whittier waterfront, and along the northshore of the Passage Canal.
They also damaged a small pier near the FAA station, and may have
destroyed a slip tower at car-barge slip dock.

Landslide-generated waves reached altitudes of 30 to 50 ft
and caused significant damage. These waves completely destroyed
the small-boat harbor, stub pier, and car-barge slip dock at
Whittier Harbor; in addition, they contributed to the damage to
DeLong Dock (also damaged by subsidence) and to an intransit
storage shed (also damaged by subsidence and seismic shaking).
Wave-induced damage to the Marginal Wharf included buckling,
bending, and twisting of steel pilings on the warehouse side
of the wharf, and outward bulging of steel sheet pilings beneath
the warehouse face.

2.12 1964 NIIGATA, JAPAN, EARTHQUAKE[*]

2.12.1 EARTHQUAKE EVENT

On June 16, 1964, a large earthquake of magnitude 7.5
occurred near Niigata City on the west coast of the Japan Sea

---

[*]Primary references for damage assessment from the 1964 Niigata
  earthquake were Kawakami and Asada (1966), Hayashi et al. (1966),
  Seed and Idriss (1967), Hakuno (1968), and JPHRI (1964).

(Fig. 2-27). The epicenter of the earthquake was about 55 km
north of Niigata, and its focal depth was approximately 40 km.
This earthquake, which was the largest ever recorded in the
coastal area of the Japan Sea, caused very severe damage to
structures over extensive inland and coastal areas. The primary
cause of damage to these structures was widespread and extensive
liquefaction of the sandy soils on which they were supported, and
tsunamis caused further destruction of facilities located near
the coastline. Peak ground accelerations recorded in Niigata
were on the order of 0.16 g. At the port area, these accelera-
tion levels were probably in the 0.15 g to 0.20 g range.

2.12.2 SOIL CONDITIONS

The city of Niigata straddles the Shinano River (Fig. 2-28a),
which has deposited alluvial sands that, at the coast, have been
overlain by deposits of dune sand. The older parts of Niigata
were constructed on dune sand and, in the early 1900's, the
city expanded toward the lowland areas near the river which
are comprised of recent sediments and reclaimed land.

The sand deposits underlying the city are relatively loose
near the ground surface but become more dense with increasing
depth (Fig. 2-28b). These sands extend to a depth of about
100 ft below the ground surface, and the alluvial deposits to
depths of 200 ft to 300 ft. The water table in the vicinity of
the river is about 3 ft below the ground surface and, in the sand
dune area, the water table is 10 ft or more below the ground
surface (Seed and Idriss, 1967).

2.12.3 DESCRIPTION OF NIIGATA PORT

The port of Niigata (West Harbor) functions as a major
harbor area for the west coast of Japan. It is situated at
the mouth of the Shinano River and has the layout shown in
Figure 2-29.

2-51
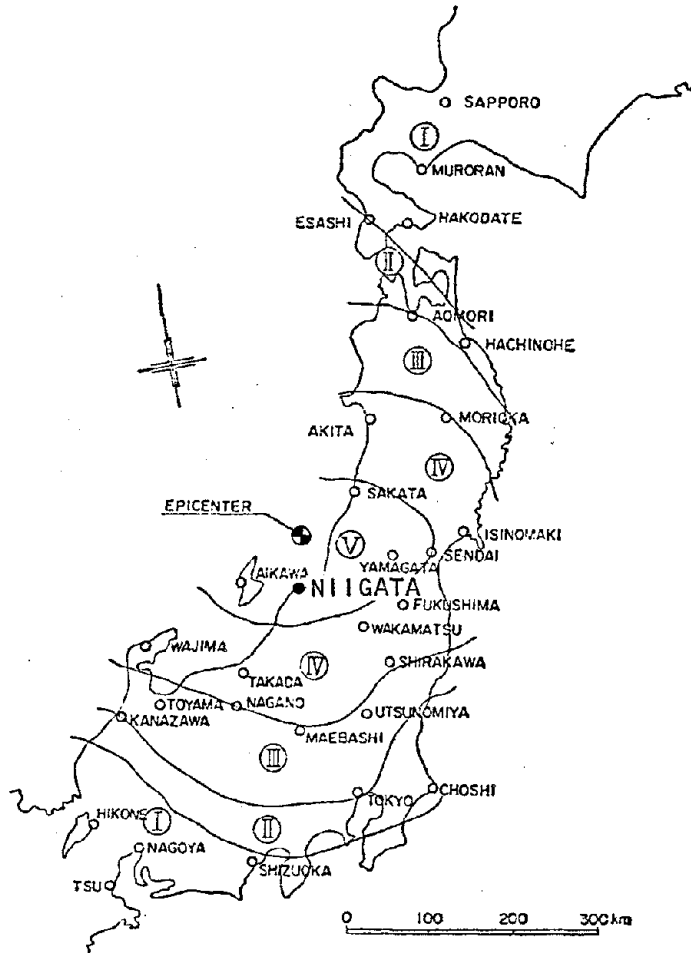
FIGURE 2-27. ISOSEISMAL MAP OF 1964 NIIGATA EARTHQUAKE,
JMA SCALE (Kawakami and Asada, 1966)
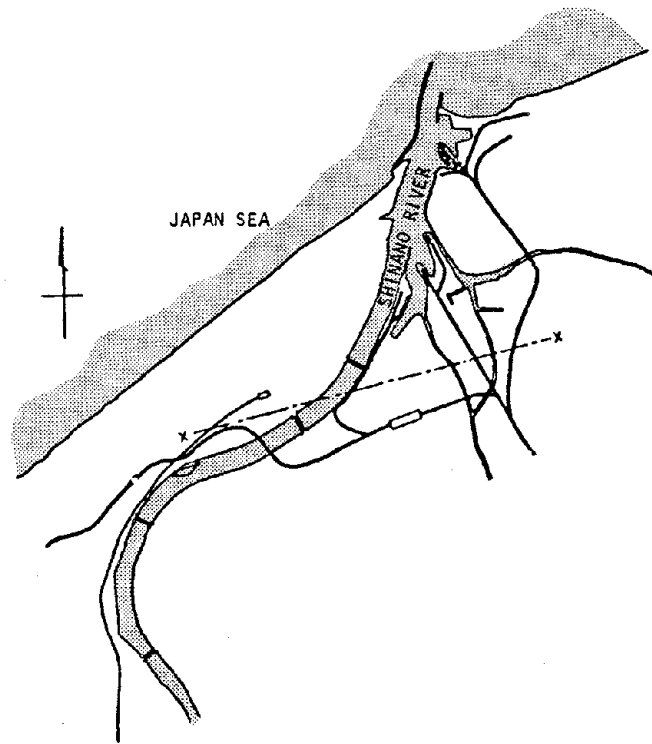
(a)   Plan of Niigata Port area
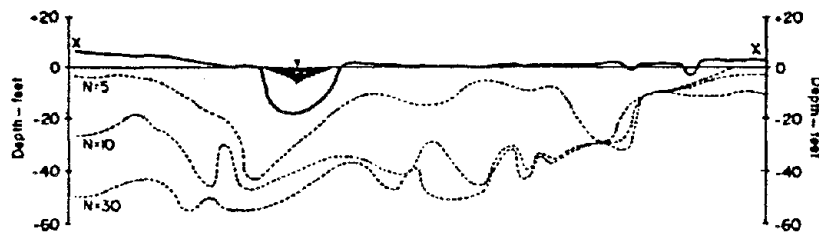
(b)   Soil profile along XX

FIGURE 2-28.   PLAN OF NIIGATA PORT AND SOIL PROFILE
(Seed and Idriss, 1967)
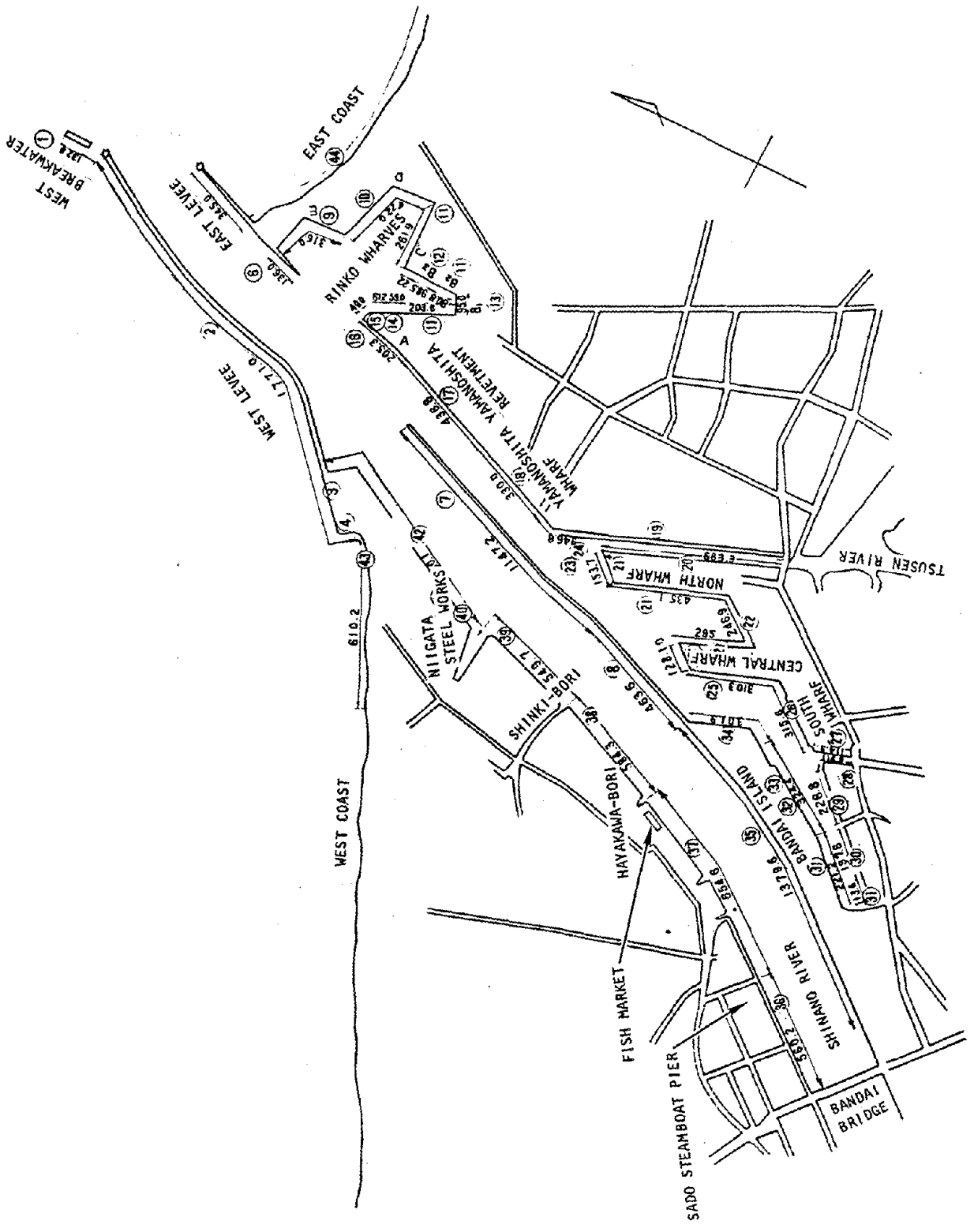
FIGURE 2-29. NIIGATA PORT (JPHRI, 1964)

It is noted that, prior to the 1964 earthquake, many Niigata port facilities had subsided more than 2 m, as part of an overall pattern of ground subsidence experienced throughout much of the city. This extensive subsidence hampered the function of many of the port facilities. Therefore, in the late 1950s, many of these port facilities were modified as countermeasures to these subsidence effects so as to restore their ability to function. Most of these modifications, which were somewhat urgent because of the widespread subsidence that had occurred, involved configurational changes of the facilities so as to increase their height. These involved substantial modifications of the cross sections of the port and harbor facilities and, in some cases, the original structure was completely contained within the new structure.

Although these structure modifications were beneficial in overcoming the effects of the ground subsidence that had occurred, they often increased the susceptibility of the structure to earthquake ground shaking. For example, the height increases imparted to quay wall structures, which raised their center of mass, were often not accompanied by corresponding strengthening of the foundations of these structures. Therefore, this increased the susceptibility of the structures to damage from increased earthquake-induced lateral pressures that often resulted from porewater pressure buildup in the backfill.

Another aspect of the Niigata port and harbor facilities that warrants mention is the seismic coefficients used in their redesign. These seismic coefficients (typically 0.10 to 0.12) were smaller than the peak acceleration levels estimated for the port area (0.15 to 0.20 g). However, although this could have contributed to the earthquake-induced damage that occurred, the most predominant cause of the severe damage and destruction that occurred at

Niigata Port due to the ground shaking was extensive porewater pressure buildup and liquefaction.[*]

2.12.4 DESCRIPTION OF DAMAGE

The damage to port and harbor facilities caused by the Niigata earthquake was extremely severe, particularly at the Niigata Port. As shown in Figures 2-30a, this port is located in the most heavily damaged region of Niigata. The damage at Niigata Port was primarily caused by liquefaction of the very loose sandy sediments and reclaimed land that prevail there (Fig. 2-30b,c). Descriptions of this damage to the various port facilities are provided in the paragraphs that follow.

2.12.4.1 Rinko Wharves

The effects of the earthquake-induced ground shaking and subsequent liquefaction of the soil medium caused significant damage at the Rinko Wharves of Niigata Port, particularly in the form of large scale sliding, tilting, and settlement of the quay walls at Berths A, B, C, and D (located as shown in Fig. 2-31a). Furthermore, because the ground surface at Rinko Wharves was near sea level, these failures, together with the effects of a sub-sequent tsunami, caused the areas behind the quay walls to be

---

[*]As discussed subsequently in connection with later earthquakes in Japan (i.e., the 1968 Tokachi-Oki and 1973 Nemuro-Hanto-Oki events), other port facilities were designed with similarly low seismic coefficients when compared to peak ground accelera-tions, but suffered less damage during these earthquake events. This is because these structures were sited on more competent soils than existed at Niigata Port, and were less prone to wide-spread liquefaction.
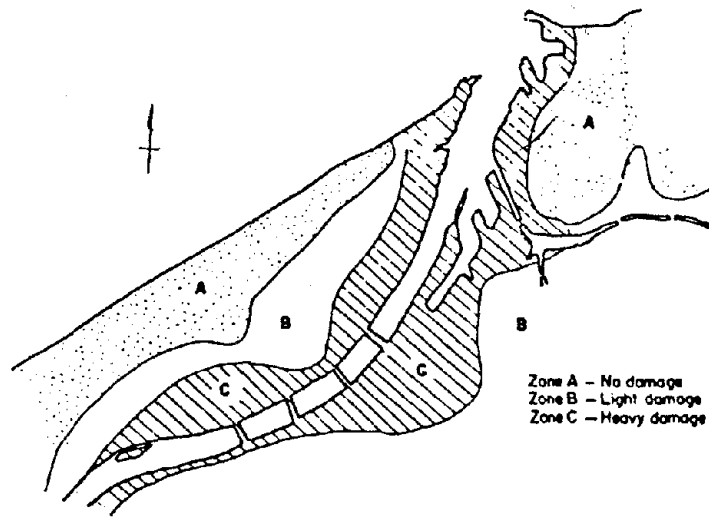
(a)   Damage zones in Niigata port area
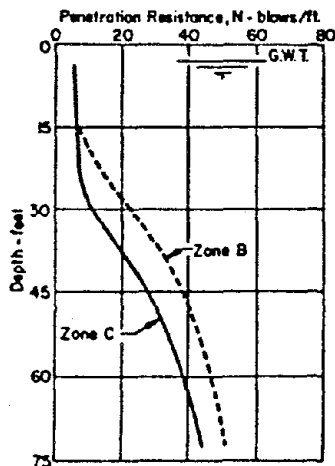
(b)   Comparison of soil
conditions in Zone B
(light damage) and
Zone C (heavy
damage
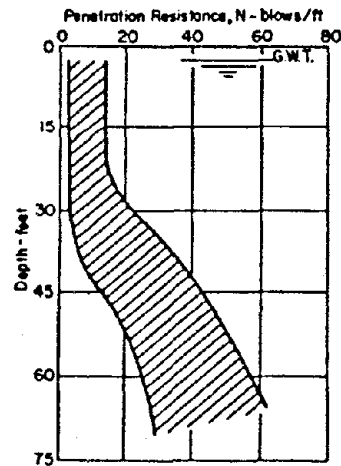
(c)   Range of penetration
resistance values in
heavy damage zone

FIGURE 2-30.   DAMAGE AT NIIGATA PORT (Seed and Idriss, 1967)
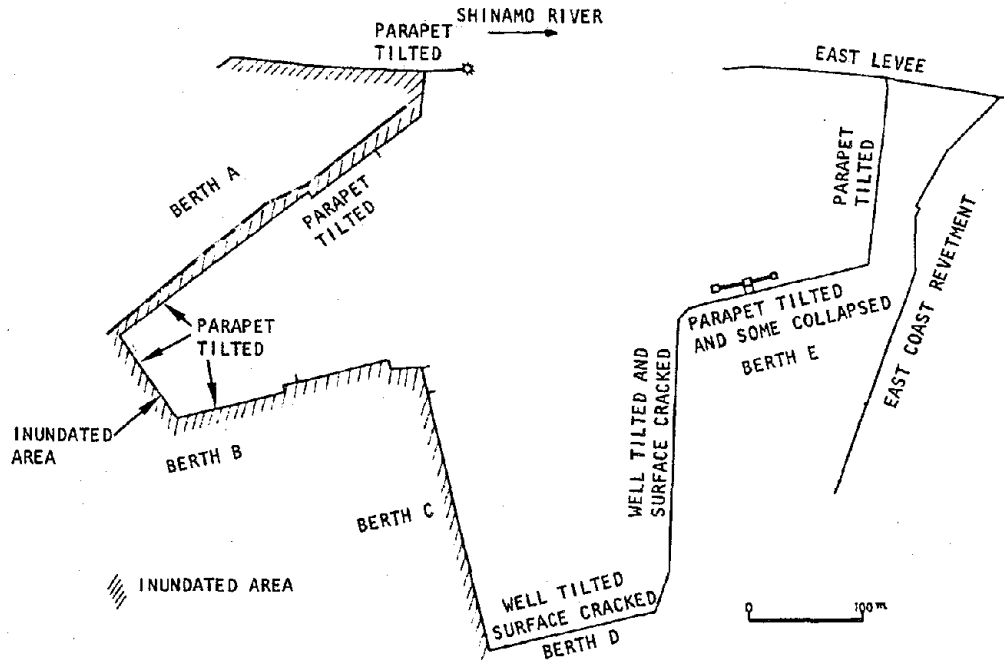
(a)   Plan view of damage (JPHRI, 1964)
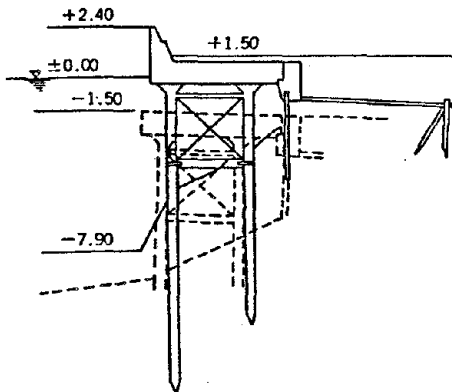
(b)   Trestle type pier,
      Berth B
      (JSCE, 1980)

────────── POSITION PRIOR TO EARTHQUAKE
────── ── POSITION AFTER EARTHQUAKE
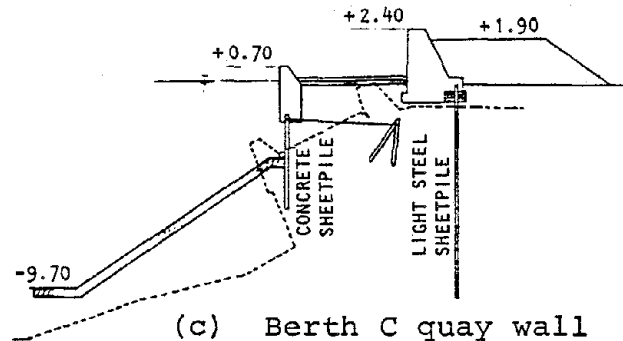
(c)   Berth C quay wall
      (JPHRI, 1964)
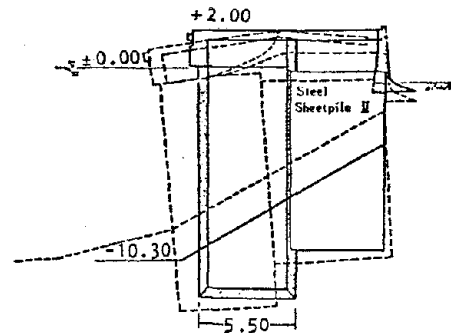
(d)   Berth D quay wall
      (JSCE, 1980)

FIGURE 2-31.   DAMAGE AT RINKO WHARVES, NIIGATA PORT
               (All dimensions and elevations in meters)

submerged below the ocean water level. These effects were particu-
larly pronounced at Berths A, B, and C. A further description of
the damage at these ports is as follows:

a.   Berth A. At this berth, a section of a concrete
     gravity-type quay wall sank and submerged into the
     water. A section of a concrete block quay wall sank
     more than 4 m, accompanied by tilting seaward. This
     also resulted in a complete submergence into the sea
     water. A section of quay wall with well-type con-
     struction sank vertically with no apparent tilting.
     The concrete cap of the adjacent concrete sheet pile
     bulkhead also submerged completely.

b.   Berth B. This berth is comprised of a concrete trestle
     type pier and a concrete sheet-pile quay wall. The pier
     tilted slightly away from the water and sank severely.
     The entire pier structure submerged below the water
     because of excessive loosening of sand stratum as a
     result of liquefaction (Fig. 2-31b). The parapet of
     the quay wall also tilted seaward and sank flush with
     the embankment.

c.   Berth C. This berth consists of concrete sheet-pile
     type quay wall construction. The earthquake caused the
     entire quay wall to submerge into the water. Apparently,
     the inclined embankment in front of the quay wall and
     the shallow concrete sheet piles failed together
     (Fig. 2-31c).

d.   Berth D. The quay wall at this berth suffered severe
     seaward tilting that, in turn, caused tilting of the
     neighboring concrete piles and cracking of the concrete
     slabs (Fig. 2-31d).

2.12.4.2 Yamanoshita Wharf and Revetment

The ground shaking that occurred during the Niigata earthquake resulted in varying degrees of damage to sheet-pile bulkheads at the Yamanoshita Wharf and the Yamanoshita Revetment. At the Yamanoshita Wharf, a sheet-pile bulkhead suffered no appreciable damage, except for a local settlement of the fill behind the anchor system (Fig. 2-32a). However, in the immediately adjacent Yamanoshita Revetment, a similar sheet-pile bulkhead settled (up to 1 m) over its entire length. In addition, its concrete parapet tilted substantially, to the extent that some segments of the parapet were completely submerged into the sea water (Fig. 2-32b).

The significant differences in the earthquake-induced behavior of these two adjacent bulkheads can be attributed to three causes. First, the bulkhead at the Yamanoshita Wharf (which suffered no significant damage) was constructed only about a year before the Niigata earthquake, without the subsidence countermeasures that had been employed in a redesign of the older bulkhead at the Yamanoshita Revetment (which suffered appreciable damage). Second, the anchor for the bulkhead at the Yamanoshita Revetment was designed with a much lower factor of safety than that at the Yamonoshita Wharf. Finally, the Yamanoshita Revetment was constructed on fill materials judged to be relatively vulnerable to strong ground shaking.

2.12.4.3 North Wharf

As shown in Figure 2-33a, the North Wharf consists of the Backside Landing, North-Tip Landing, North Wharf Quay Wall, and North Wharf Landings A and B. Because the types of construction are different at each of these facilities, they experienced different degrees of damage.
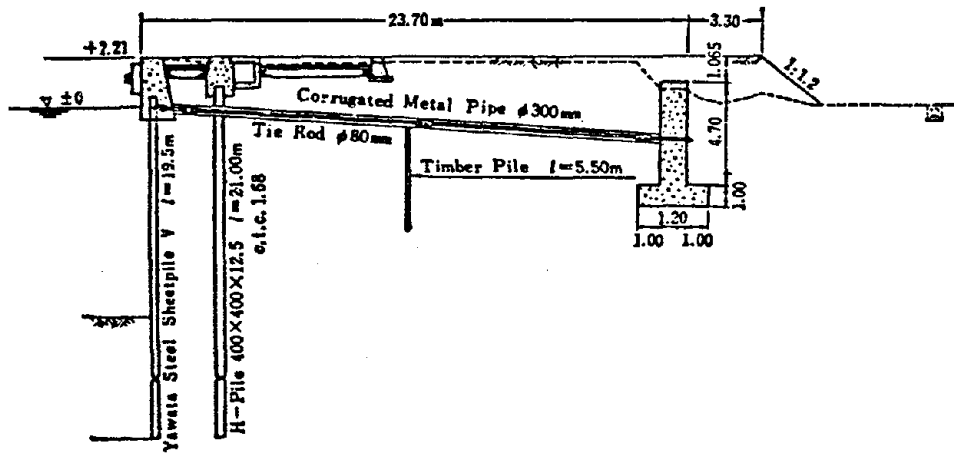
(a)   Sheet-pile bulkhead at
      Yamanoshita Wharf
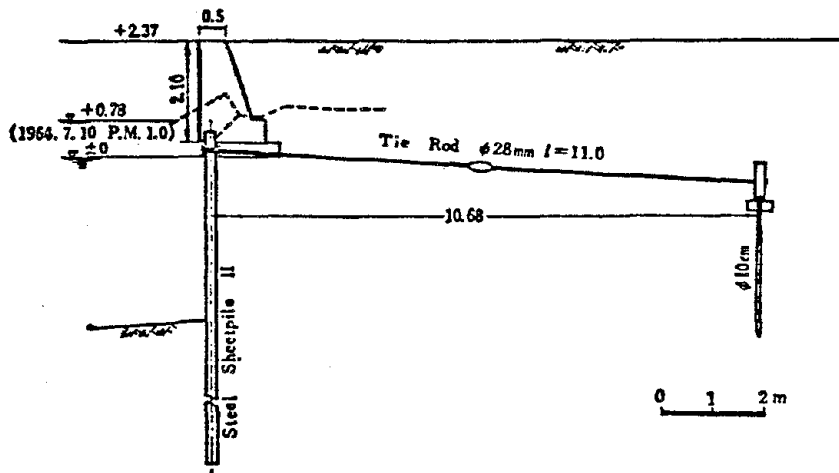
(b)   Sheet-pile bulkhead at
      Yamanoshita revetment

FIGURE 2-32.   DAMAGE AT YAMANOSHITA WHARF AND REVETMENT,
               NIIGATA PORT (JPHRI, 1980)

               (All dimensions and elevations in meters
                unless otherwise shown)

EAST WHARF

CONCRETE BLOCK
QUAY WALLS ON
TIMBER PILES

SHEET-PILE
BULKHEAD

CONCRETE BLOCK QUAY
WALLS ON STEEL PILES

LANDING B   LANDING A   NORTH WHARF QUAY WALL

CONCRETE BLOCK QUAY WALLS

NORTH TIP LANDING

N

NORTH WHARF BACKSIDE LANDING

SHEET-PILE BULKHEAD

TSUSEN RIVER

////// INUNDATED AREA

------ POSTEARTHQUAKE POSITION
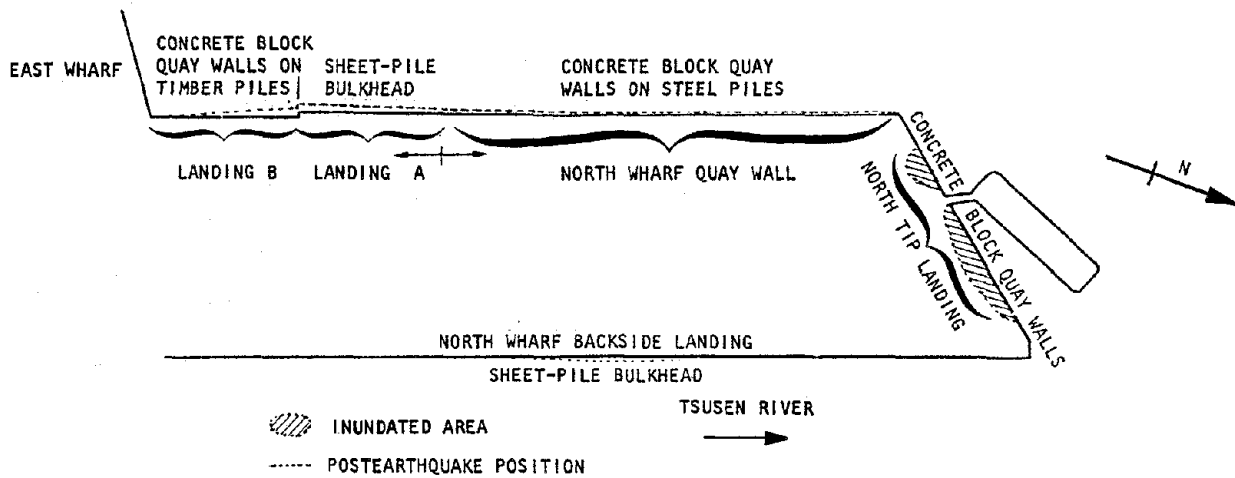
(a) Plan view (JPHRI, 1964)
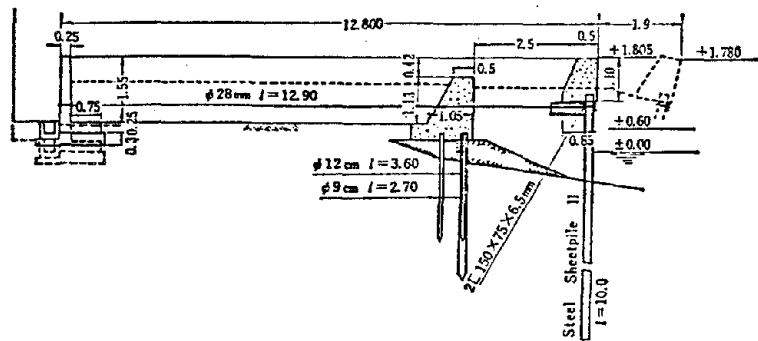
(b) Sheet-pile bulkhead at backside landing
      (JPHRI, 1980)

FIGURE 2-33. DAMAGE AT NORTH WHARF, NIIGATA PORT

(All dimensions and elevations in meters
unless otherwise shown)
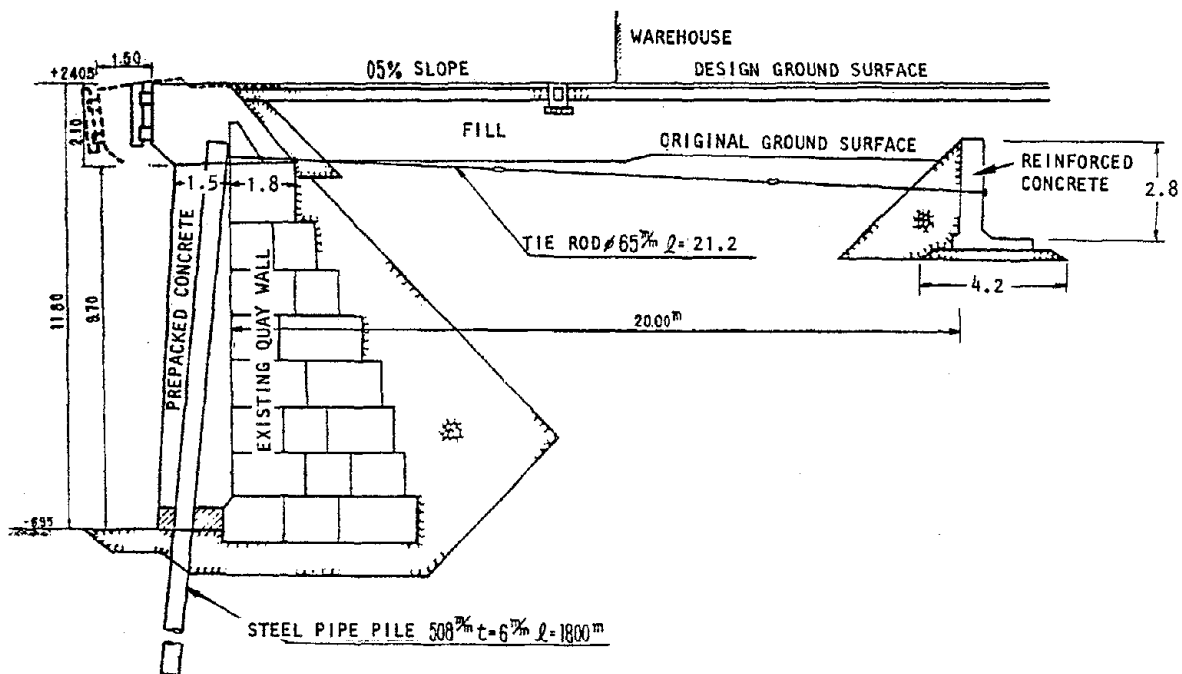
(c) North Wharf quay wall
(JPHRI, 1964)
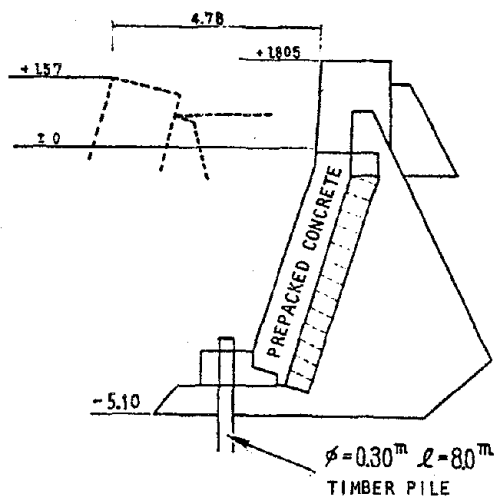
(d) North Wharf Landing B
(JPHRI, 1964)

FIGURE 2-33. (CONCLUDED)

2.12.4.3.1 *Backside Landing*

The Backside Landing is located on the left bank of Tsusen River. The earthquake caused the 680-m steel sheet-pile bulkhead at that landing to tilt seaward throughout its entire length with a maximum horizontal displacement of about 2 m occurring near the midlength of the bulkhead (Fig. 2-33b). The settlement of the backfill sands was about 50 to 70 cm, and has been attributed to the large horizontal displacement of the bulkhead and to consolidation of these sands that resulted from the ground shaking and from porewater pressure effects. The horizontal displacement of the anchor wall was small compared to that of the bulkhead, probably because of a failure of the tie rods that connected the bulkhead and the anchor wall.

The bulkhead on the right bank of the Tsusen River experienced practically no damage, despite the fact that (1) its configuration is almost identical to that of the bulkhead on the left side of the river; and (2) the pre- and post-earthquake boring logs obtained from each bank of the river showed no significant difference in soil conditions. The differences in the earthquake behavior of these two bulkheads have been attributed to the fact that the anchor wall on the left bank was constructed much closer to the sheet pile than that on the right bank. As discussed in Chapter 3 (Sec. 3.3.2), this could have resulted in all or part of the dynamic passive pressure zone in the anchor along the left bank falling within the active pressure zone of the sheet pile, causing a loss of passive pressure resistance of the anchor.

2.12.4.3.2 *North-Tip Landing*

As a result of the earthquake ground shaking, the bulkhead and the pavement of North-Tip Landing was completely submerged along the entire 150 m length of the landing. In addition, the concrete cap of the bulkhead tilted landward along one section

of the landing and seaward at another. This damage to the North-Tip Landing structures was attributable to its weak subsurface sandy soil properties, its reconstructed complex structural cross section, and an unexpected increase in water depth in the vicinity of the landing just prior to the earthquake. Boring logs at this landing showed that the blowcounts are 5 or less to a depth of 8 m, and are below 10 for the soil layers down to 11 m deep; therefore these sandy soil materials were particularly susceptible to porewater pressure buildup.

2.12.4.3.3 *North Wharf Quay Wall*

The North Wharf Quay Wall (Fig. 2-33c) underwent a large scale reconstruction in 1960 as a remedy to the earlier subsidence of the structure. During the 1964 earthquake, the concrete cap of the quay wall experienced large (1.5 m) horizontal displacement; however the body of the quay wall managed to remain intact, probably because of the steel pipe piles installed at the time of the reconstruction. However, the earthquake-induced damage to the paved apron and the warehouse buildings adjacent to the quay wall was severe, particularly above the reinforced concrete anchor walls. As a result, it is believed that the anchor walls and the quay wall displaced seaward as a unit, probably because of widespread porewater-pressure-induced liquefaction and sliding of the entire soil region at the site of these walls and the adjacent buildings. The blowcounts of the sandy soils in this area ranged from 7 to 20 at the depths of the pile foundations, and were lower at depths closer to the ground surface.

2.12.4.3.4 *North Wharf Landings A and B*

The bulkhead at North Wharf Landing A is comprised of a steel sheet pile constructed in front of an existing concrete block gravity wall. It suffered damage of a similar type to that observed at the adjacent North Wharf Quay Wall, but with

a greater degree of severity. The concrete slabs and warehouse buildings behind the bulkhead also suffered substantial damage. The saturated sandy soil conditions in this area were even less competent than those at North Wharf Quay Wall, with blowcounts of less than 10 to a depth of 15 m. Therefore the damage to this sheet-pile bulkhead probably resulted from extensive porewater pressure buildup and liquefaction.

Figure 2-33d shows a cross section of the North Wharf Landing B bulkhead. The entire length of this bulkhead suffered extensive horizontal displacement, and the degree of damage to the slabs and warehouse buildings was similar to that at Landing A. The soil conditions in this area were also very poor. Layers of silty clayey mud occupied 15 m of the upper strata, and the blowcounts for the soils at the pile foundation level were in the neighborhood of 5. Therefore, the failure of the bulkhead has been attributed to large scale sliding of the entire upper soil strata.

2.12.4.4 East Wharf

The sea wall at the East Wharf of Niigata Port was changed from a sheet-pile type to a trestle type at the time its height was increased in the 1950's as a countermeasure to subsidence effects. Anchor walls were used to help resist the earth pressures applied to the sea wall (Fig. 2-34).

The earthquake-induced damage to the sea wall was very severe, featuring a large outward displacement (3 m) of its concrete cap, and a substantial settlement (1 m) of the concrete pavement slabs behind the quay wall. The adjacent warehouse buildings at the East Wharf also suffered severe damage. This failure seemed to have been caused by sliding of the anchor walls and settlement of the foundation soils. This, in turn, was probably caused by the poor soil conditions in the area, with blowcounts of less than 10
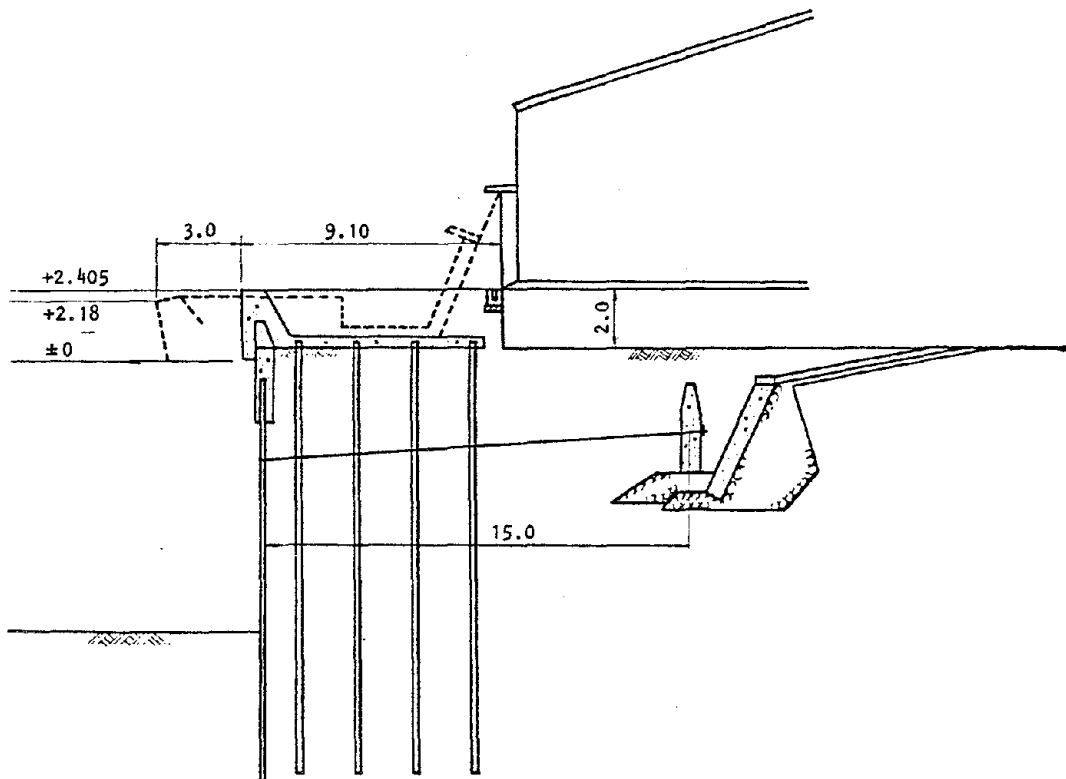
FIGURE 2-34.   SEA WALL AT EAST WHARF, NIIGATA PORT (JPHRI, 1964)
              (All dimensions and elevations in meters)

within the 14 m depth of the soil stratum. The sheet piles that supported the East Wharf sea wall were situated in this poor soil medium.

2.12.4.5 Central Wharf

The quay walls at Central Wharf are the same configuration as that of North Wharf Quay Wall (Fig. 2-33c). The damage was also similar to that experienced at North Wharf. As in that case, the warehouse buildings suffered tremendous damage, while the configurations of the quay walls remained fairly intact despite their extremely large horizontal displacements (up to 2.3 m). For the same reasons mentioned earlier (Sec. 2.12.4.3.3), the movement of the anchor walls contributed to the failure of warehouse buildings and concrete slabs.

The structural configurations of the quay walls on the south and north sides of the wharf are practically identical with only minor differences in their dimensions (Figs. 2-33c, 2-35). Despite this, they suffered distinctly different degrees of damage, with the quay wall on the south side displacing 2.1 m seaward, and the quay wall on the north side sustaining only a slight, barely noticeable displacement. This can be primarily attributed to the different safety factors used in the design of the anchor for these quay walls, although the differences in the soil conditions and the distribution of the potentially liquefiable soils in the vicinity of the quay wall foundations on the south side may also have contributed to these different degrees of damage.

2.12.4.6 South Wharf

The configuration of South Wharf, originally a concrete block gravity-type quay wall with timber piers, was later reconstructed to correspond to a steel sheet-pile quay wall (Fig. 2-36). During the 1964 earthquake, the quay wall suffered uneven swelling and
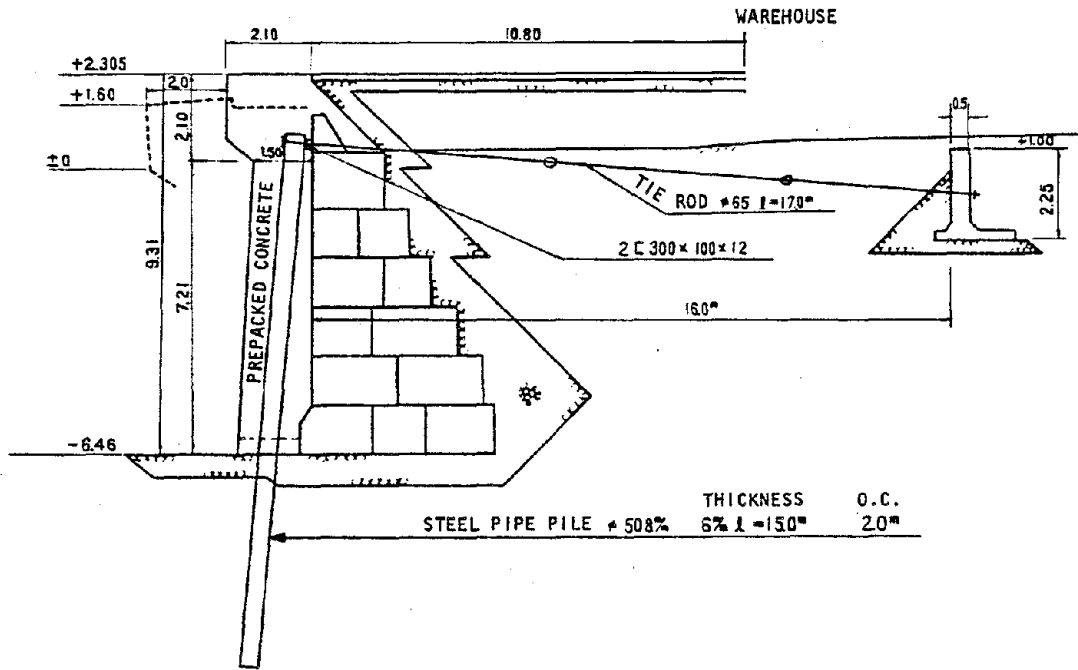
FIGURE 2-35. SOUTH QUAY WALL AT CENTRAL WHARF, NIIGATA PORT
(JPHRI, 1964)

(All dimensions and elevations in meters unless
otherwise shown)
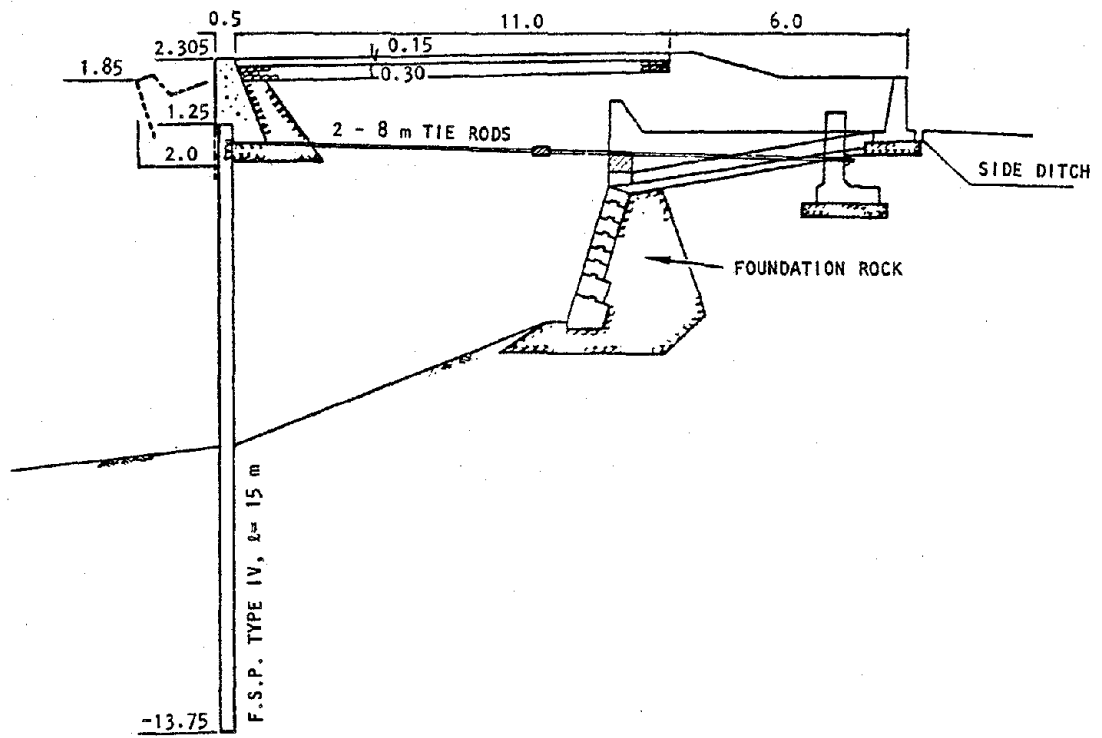
FIGURE 2-36. QUAY WALL AT SOUTH WHARF, NIIGATA PORT
(JPHRI, 1964)

(All dimensions and elevations in meters)

settlement, with a maximum horizontal displacement at the concrete cap of about 2 m and a settlement of the concrete slabs behind the quay wall of about 1 m. The soils in this area have blowcounts in the range of 5 to 20 at the sheet-pile foundation level; these blowcounts drop to about 5 at the locations where the quay wall suffered the most severe damage.

2.12.4.7. Kurinoki River Landings

The right bank of Kurinoki River is the site of a concrete block quay wall structure that suffered large slippage and tilting, together with about a 1-m settlement. The concrete cap of this structure submerged completely below the water surface at some locations. The left bank of the river suffered similar damage but to a lesser degree.

2.12.4.8. Bandai Island Wharf

Almost the entire quay wall and bulkhead that surround Bandai Island submerged into the water, because of liquefaction of the subsurface and backfill soil materials at the locations of these structures. The quay wall tilted seaward and its apron settled nearly 1 m. The bulkhead, comprised of a steel sheet pile filled with dredged soils, settled severely without much horizontal movement and sank into the water.

2.12.4.9. Shinano River Left Bank Bulkhead

This bulkhead extends over a length of 3 km from the Bandai Bridge to the ocean (Fig. 2-37a), and virtually its entire length was damaged by the earthquake. This, in turn, resulted in very heavy damage to the buildings along the river bank. In addition, large scale sliding of the river bank, which resulted in catastrophic structural failures, was observed in a number of locations.
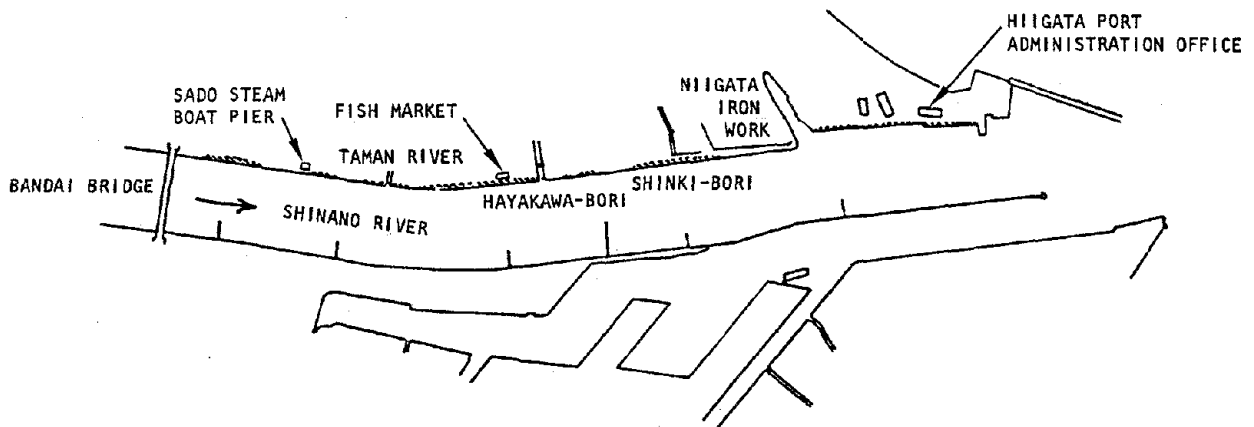
(a)   Extent of bulkhead
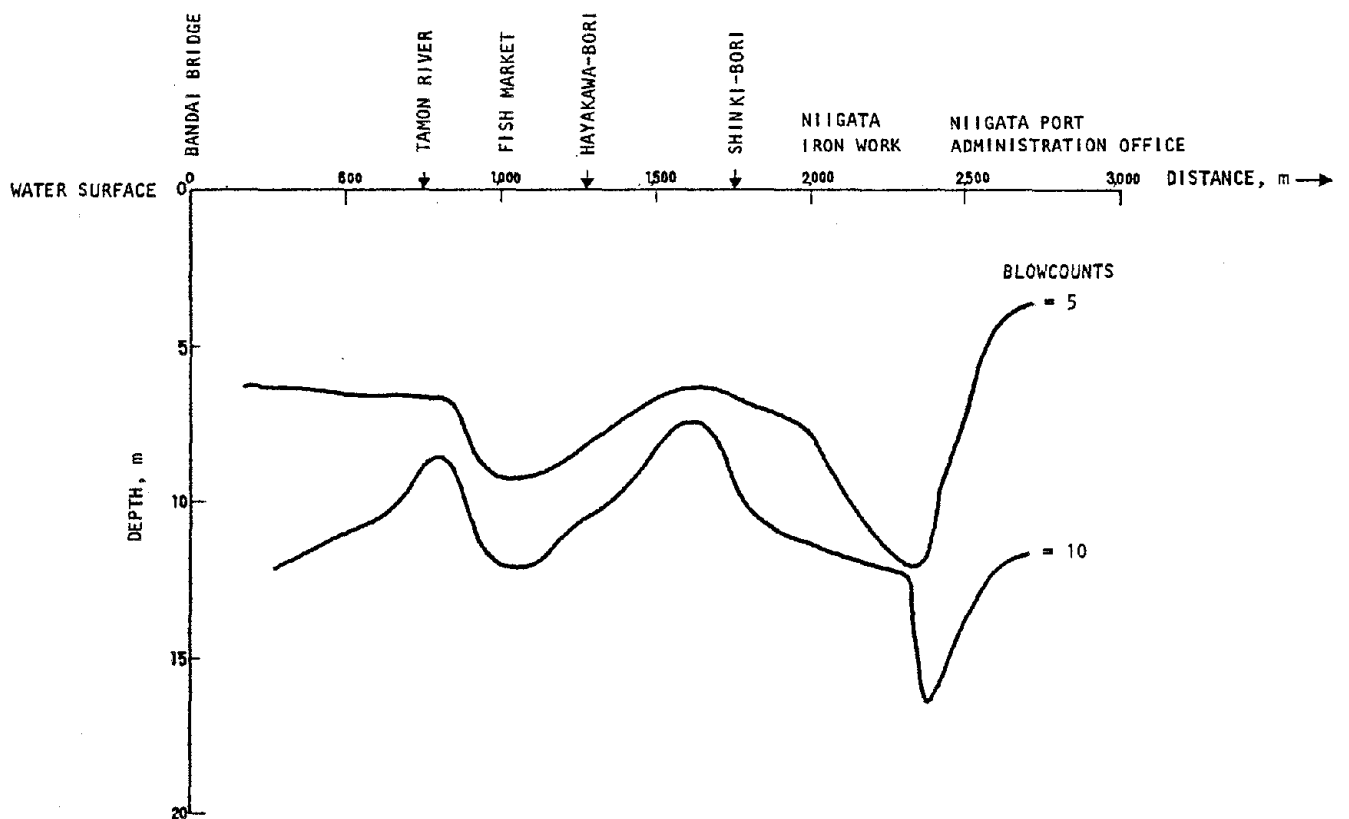
(b)   Profile of blowcounts along bulkhead

FIGURE 2-37.   SHINANO RIVER LEFT BANK BULKHEAD (JPHRI, 1964)

2-72

The bulkhead in the section between Bandai Bridge and Hayakawa-bori was entirely submerged as a result of the ground shaking, except at the areas near Bandai Bridge and Sado Steam Boat Pier. The area near the Fish Market was the hardest hit due to its poor soil conditions (Fig. 2-37b). At that area, the bulkhead was completely submerged and the major bulkhead damage, in the form of tilting and settlement, was caused by the failure of tie-rods, by foundation sliding, and by movement of the anchor walls.

The section of the bulkhead between Hayakawa-bori and Shinki-bori suffered relatively minor damage due to the fact that the soil conditions in this area are much more competent (Fig. 2-37b). Most of the bulkhead in the section between Shinki-bori and Niigata Steel Work settled, to the extent that the concrete cap became flush with the water surface. Within this section, uneven landward and seaward tilting of the concrete cap also occurred throughout the entire length of the bulkhead. The section of the bulkhead downstream from the Niigata Steel Work was completely submerged and destroyed, due to the poor soil conditions within this section and an insufficient bulkhead freeboard.

2.12.4.10 West Coast Bulkheads

The West Coast Bulkheads are of a gravity type with tetrapods protecting the embankment and timber piles supporting the foundation (Fig. 2-38). The damage to these bulkheads was most severe along its eastern section (610 m long). Within this section, damage was particularly severe in the vicinity of the West Breakwater, where severe settlement (up to 3 m) occurred at the bulkhead itself, at the soil behind the bulkhead, at the embankment, and at the neighboring breakwater. However, the bulkhead located to the east of this 610-m eastern section sustained only minor damage.
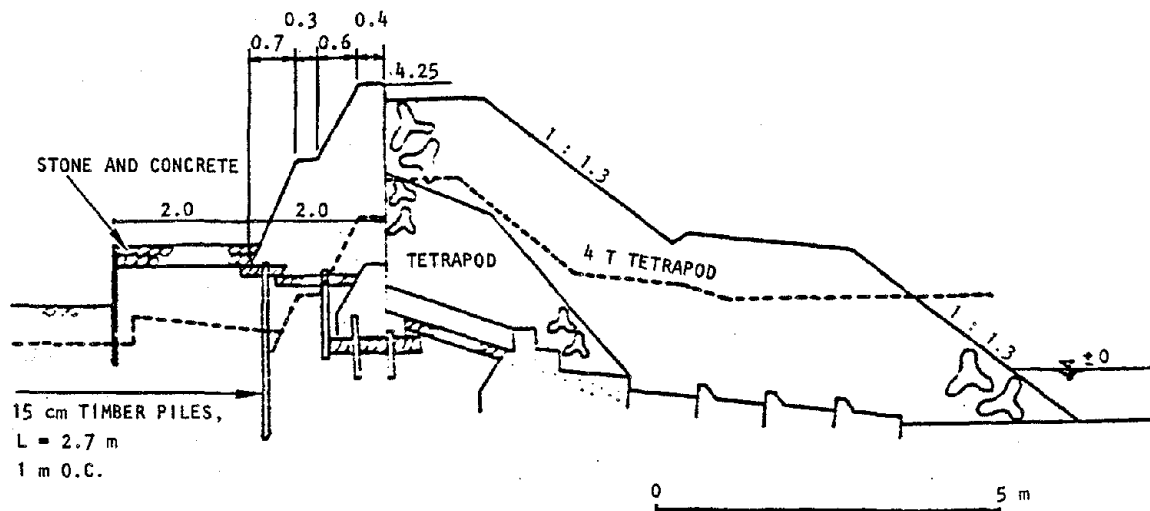
FIGURE 2-38.   WEST COAST BULKHEADS, HIIGATA PORT (JPHRI, 1964)
             (All dimensions and elevations in meters)

The distinctly different behavior demonstrated by these two sections of the West Coast Bulkheads is attributable primarily to the difference in the subsurface soil conditions. The eastern section, where major damage of the bulkheads took place, is located near the mouth of Shinano River where the soils are predominantly weak sands with a low penetration resistance. However, at the western section where only minor damage occurred, the subsurface soils are comprised of dense coastal sands with a high shear strength.

2.12.4.11 East Niigata Port

East Niigata Port is located about 15 km east of Niigata Port (West Harbor). In contrast to the severe damage observed at Niigata Port, the 1964 earthquake caused practically no damage at East Niigata Port. This was primarily due to (1) the much more favorable soil conditions that exist at East Niigata Port, with blowcounts exceeding 20 over the upper 10 m and exceeding 30 thereafter; and (2) the much more favorable structure configurations at East Niigata Port, due to the fact that the facilities at this port did not undergo the height increases and other subsidence countermeasures that were implemented at Niigata Port (Sec. 2.12.3).

2.13 1968 TOKACHI-OKI, JAPAN, EARTHQUAKE[*]

2.13.1 GENERAL DESCRIPTION

On May 16, 1968, an earthquake of magnitude 7.8 struck the southern part of Hokkaido and the Pacific Coast of Tohoku in Japan (Fig. 2-39). This earthquake, which had a focal depth of

_____

[*]Primary reference for damage assessment from the 1968 Tokachi-Oki earthquake was JPHRI (1968).
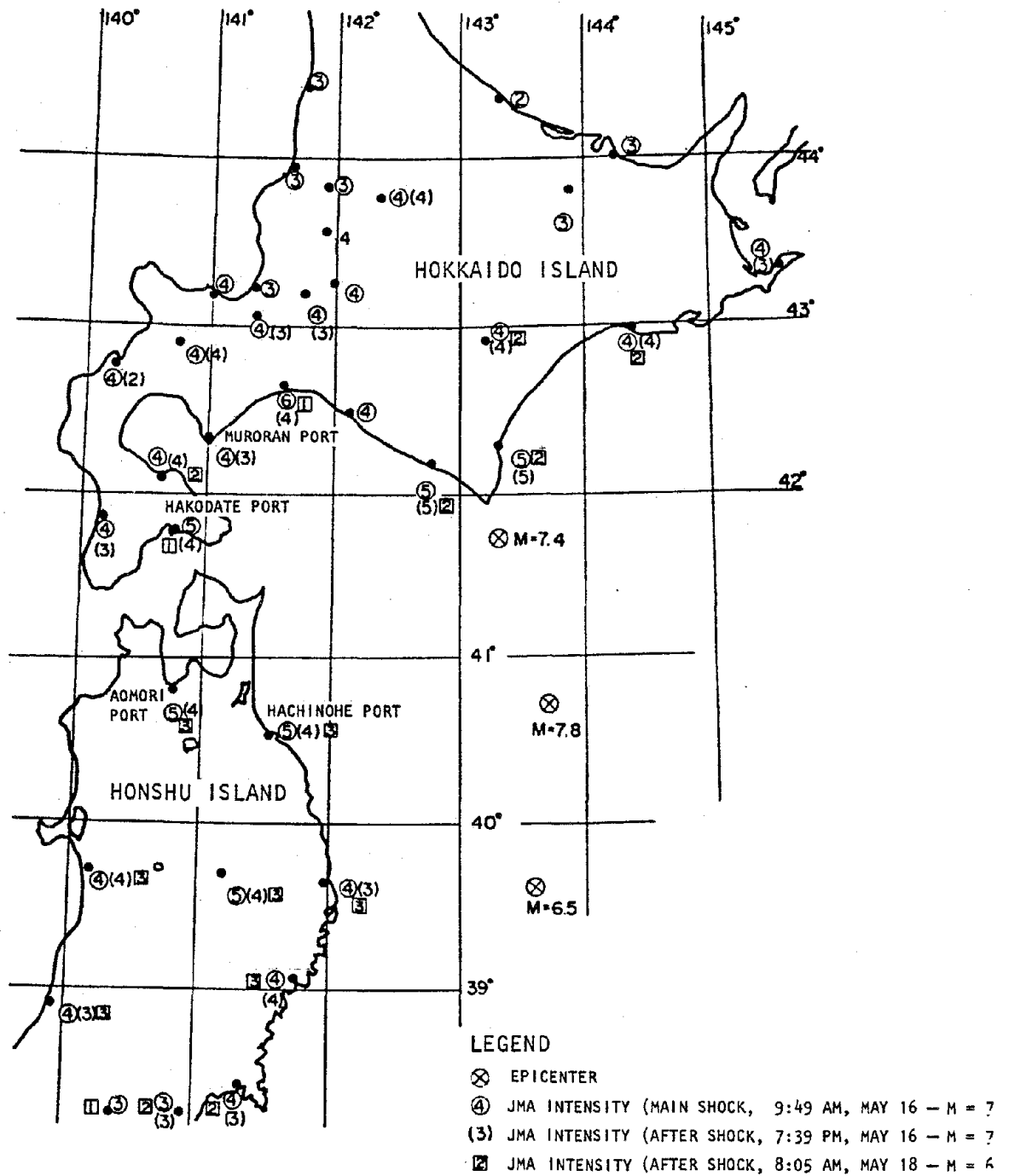
FIGURE 2-39. LOCATION OF 1968 TOKACHI-OKI EARTHQUAKE EPICENTER AND AFFECTED HARBOR AREAS (JPHRI, 1968)

20 km, induced peak accelerations (measured at Hachinohe Port in Tohoku) of 0.24 g horizontal and 0.08 g vertical.

The 1968 Tokachi-Oki earthquake affected port and harbor facilities over a widespread area within the Tohoku coastal region, with the most prominent effects at Hachinohe, Aomori, Hakodate, and Muroran Ports (Fig. 2-39). The following port and harbor facility response characteristics were induced by this earthquake.

- Not many large waterfront structures suffered severe damage, although some moderate damage was observed.

- The gravity type structures with concrete caissons were not damaged. A number of quay walls built with concrete blocks or cast-in-place concrete tilted, some critically.

- Many steel sheet-pile bulkheads suffered small deformations. Some tilting of the sheet pile was attributed to insufficient anchor resistance.

- None of the cellular bulkheads, built either on a sandy soil foundation or a clayey soil foundation, was affected by the earthquake. The trestle-type piers suffered no damage.

- No sheet-pile bulkhead damage was observed that could be attributed to insufficient embedment or bending moment resistance capacity.

- Uneven settlement and cracking of paved aprons behind the waterfront structures were common to all types of facilities, due to settlement or subsidence of the underlying backfill. Sand boils were also observed at several locations near these damaged aprons.

The above response characteristics indicate that only moderate damage was induced at harbor locations by the 1968 Tokachi-Oki earthquake, despite the fact that the design of many of the structures was based on seismic coefficients that were small (0.05 to 0.15) in comparison with the peak ground accelerations (0.24 g measured at Hachinohe Port). This is in marked contrast to the effects of the 1964 Niigata earthquake, which caused substantial destruction to structures at Niigata Port that were also designed using seismic coefficients (0.10 to 0.12) that were somewhat less than the estimated peak accelerations from that earthquake (0.15 g to 0.20 g). These differences between the behavior of waterfront structures during the Niigata and Tokachi-Oki earthquakes can be attributed to the following.

- The soil conditions at the ports affected by the 1968 Tokachi-Oki earthquake are much more favorable than those at Niigata Port. The soils at Niigata Port are primarily loose sands, with near-surface blowcounts typically in the range of 5 to 10; these soils were particularly susceptible to porewater pressure buildup and liquefaction. In contrast, the soil conditions at ports affected by the Tokachi-Oki earthquake are primarily dense sand layers with blowcounts exceeding 40.

- Prior to the 1964 Niigata earthquake, a majority of the waterfront structures at Niigata Port had undergone various degrees of modification in an attempt to countermeasure earlier soil subsidence effects. The rather complicated structural configurations that resulted from these modifications contributed to the increased vulnerability of the structures in Niigata Port to seismic excitations. No such structure modifications were carried out at the ports affected by the 1968 Tokachi-Oki earthquake.

With this as background, the remainder of this section describes the effects of the Tokachi-Oki earthquake at the Hachinohe, Aomori, Hakodate, and Muroran Ports.

2.13.2 HACHINOHE PORT

The most substantial effects of the 1968 Tokachi-Oki earthquake on port and harbor facilities occurred at Hachinohe Port, where about half of the total damage costs to such facilities was incurred. Seismic coefficients used in the design of the newer facilities at this port ranged from 0.05 to 0.10, which was well below the peak acceleration level measured at Hachinohe (0.24 g); no information was available regarding the seismic coefficients of the older ports. Subsurface soils at Hachinohe Port are comprised of sands, with blowcounts ranging from 10 to 20 at shallow depths and 40 to 50 at deeper locations (Fig. 2-40).

The most significant damage at Hachinohe Port was the collapse of the Kawaragi Estuary Breakwater (which represented about two-thirds of the damage costs at this port); however this breakwater collapse was caused by a subsequent tsunami rather than by the ground shaking. Damage more directly related to earthquake ground motion effects occurred at the First Industrial Harbor, where 5 sheet-pile bulkheads out of 25 suffered damage that included apron settlement and tilting. Quay walls in the Kanbi District suffered similar damage (Fig. 2-41).

2.13.3 AOMORI PORT

The Aomori Port is sited on alluvial deposits comprised of sandy soils with blowcounts of about 10 at shallow depths and dense sandy gravels with blowcounts ranging from 30 to 50 at deeper depths. The waterfront structures at this port were designed using seismic coefficients of from 0.05 to 0.075, which
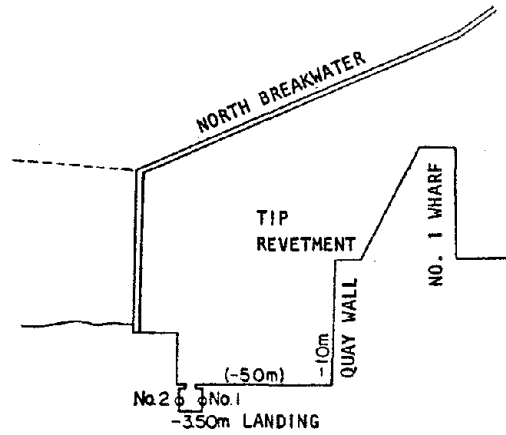
(a)   Plan view of harbor
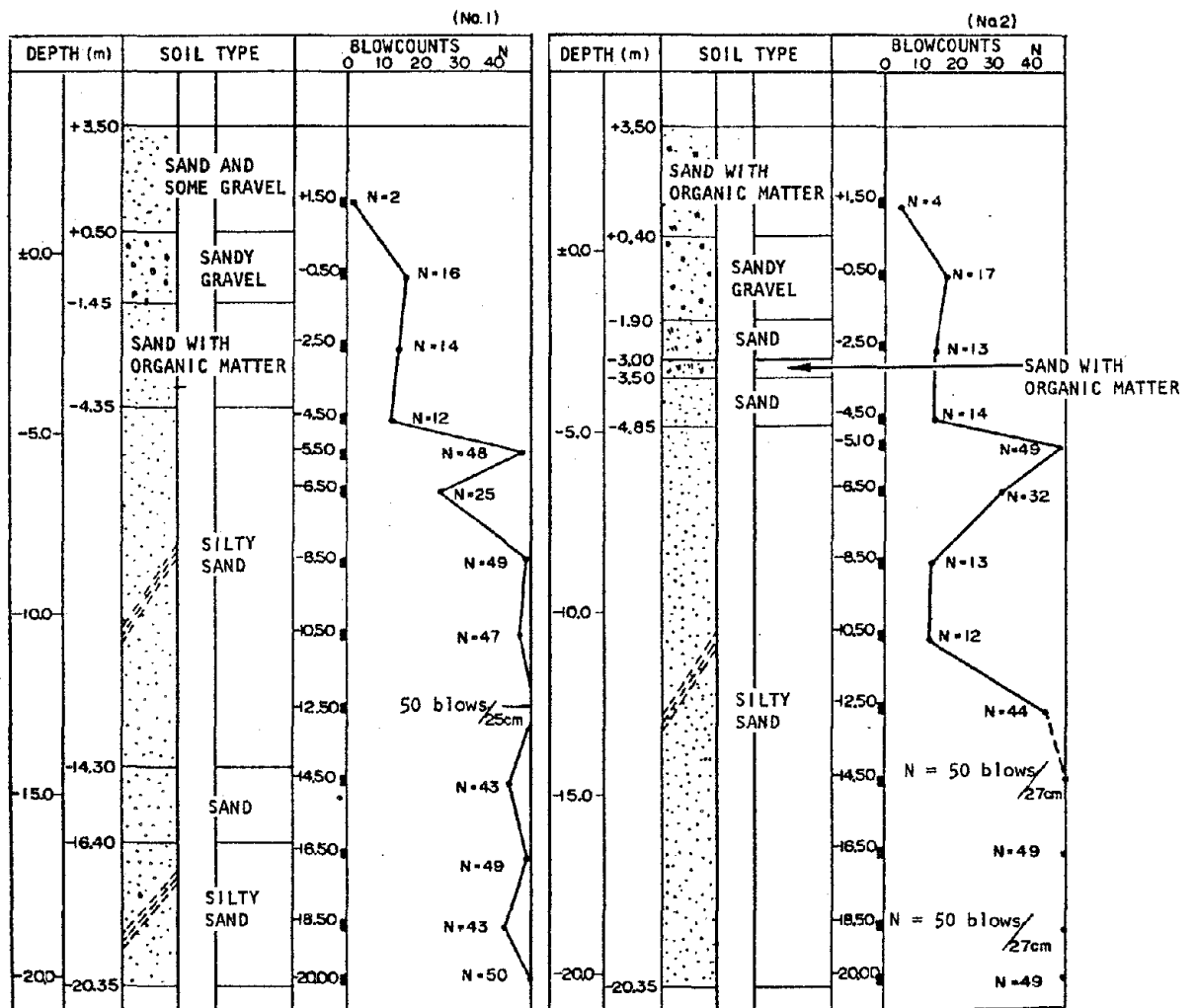
(b)   Soil profile

FIGURE 2-40.   HACHINOHE PORT (JPHRI, 1968)
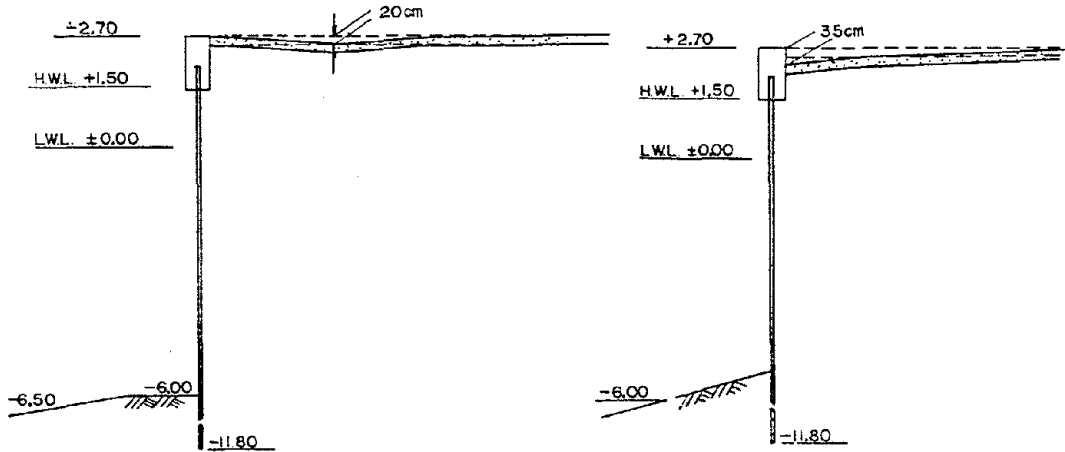
(a)   Quay Wall No. 2, first industrial harbor

(c)   Kanbi Fishing Port
      quay wall
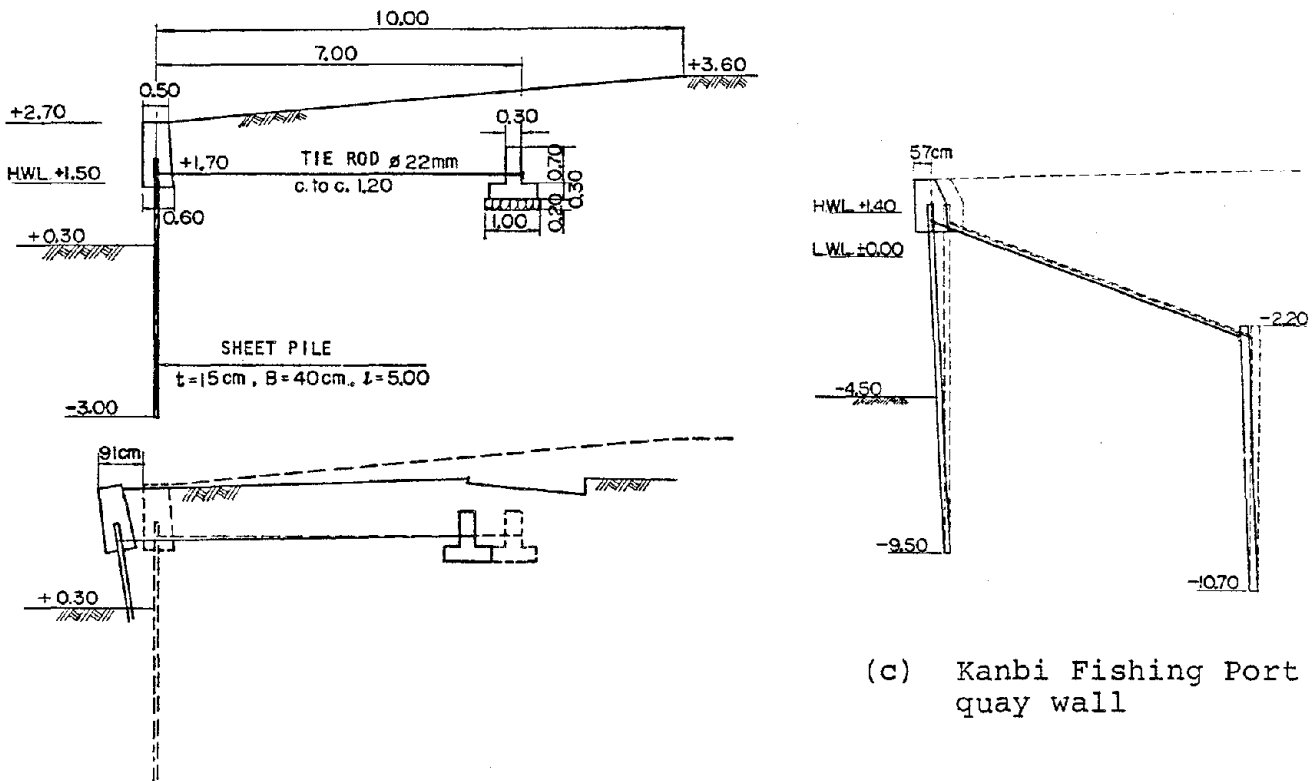
(b)   Quay wall at steam
      generating plant

FIGURE 2-41.   DAMAGED QUAY WALLS AT HACHINOHE PORT, 1968
               TOKACHI-OKI EARTHQUAKE (JPHRI, 1968)

               (All dimensions and elevations in meters)

are substantially lower than the peak accelerations recorded at Aomori (0.22 g). However, despite these low seismic coefficients, large structures such as cellular and caisson bulkheads sustained no damage, and damage to quay walls and wharves was limited to pavement settlement and cracking and relatively minor sliding and tilting. Few structures lost their function as a result of the earthquake shaking.

2.13.4 HAKODATE PORT

Hakodate Port, whose layout is shown in Figure 2-42a, is situated in a region having complex soil conditions with abruptly changing properties over very short distances. For example, the Wakamatsu-cho Wharf area is dominated by thick clay layers, while the soils at Kitahama Wharf are comprised of a mixture of sandy clay layers and intermittent sand layers. Seismic coefficients used in the design of the Hakodate Port structures are not well documented, except at Kitahama Wharf where a value of 0.1 was used.

The Kitahama and Wakamatsu-cho wharves at Hakodate Port were most severely damaged by the earthquake. At Kitahama Wharf, a steel sheet-pile bulkhead designed with batter piles suffered seaward tilting and settlement of its apron all along its 330 m length. This was attributed to shear failures in the welded connections of the batter pile and headwork, and to possible liquefaction of the surrounding soil, as evidenced by sandboils observed in the waterfront area near the bulkhead (Fig. 2-42b). Quay Wall No. 2 at Wakamatsu-cho Wharf slid (0.4 m) and settled (0.6 m) all along its 100 m length, due to relative horizontal displacements between the lower caisson structure and the upper concrete region (Fig. 2-42c). This resulted in severe settlement in the densely populated areas behind the quay wall which, together with subsequent flooding due to this foundation failure, caused significant property damage.

(a)   Port layout

DAMAGE ALONG LENGTH OF BULKHEAD

SHEAR FAILURE AT
PILE/HEADWORK
INTERFACE AT
155.0 m SECTION
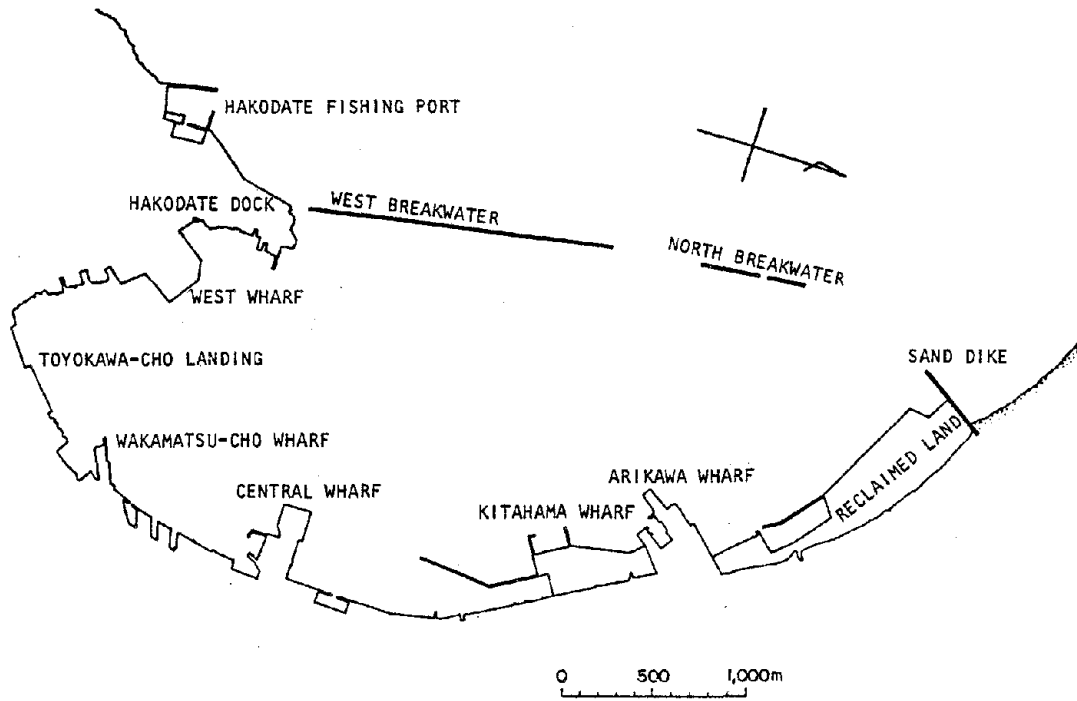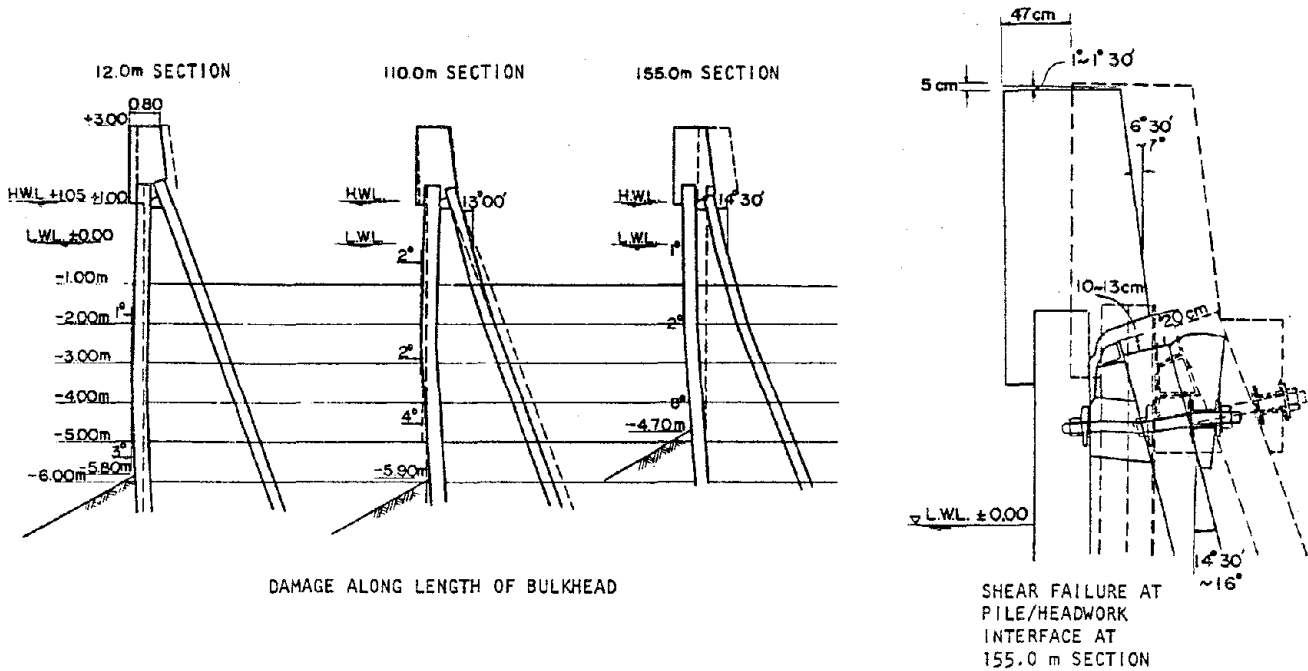
(b)   Damage to -5.5 m bulkhead at Kitahama Wharf

FIGURE 2-42.   DAMAGE AT HAKODATE PORT, 1968 TOKACHI-OKI
EARTHQUAKE (JPHRI, 1968)

2-83
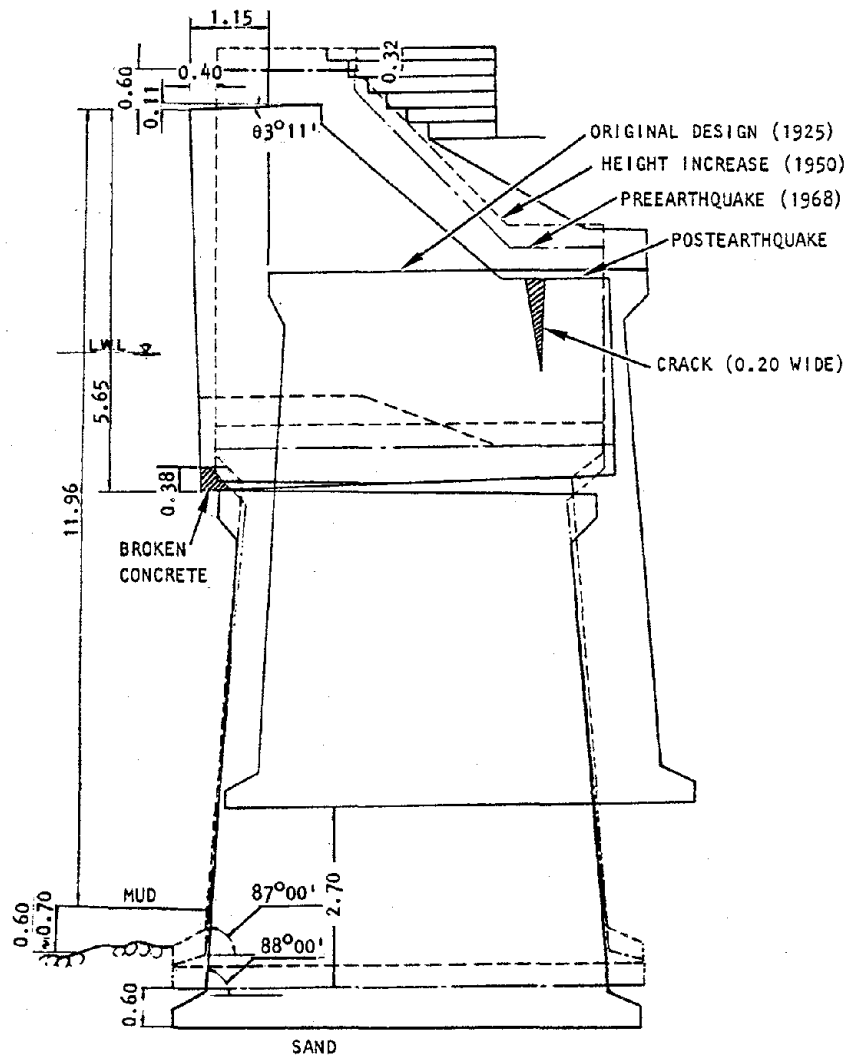
(c)   Damage to Quay Wall No. 2 at Wakamatsu-cho Wharf
       (all dimensions and elevations in meters)

FIGURE 2-42.   (CONCLUDED)

2.13.5 MURORAN PORT

The Muroran Port is the most important industrial port in northern Japan (Fig. 2-43a). It is situated on soil deposits whose top 1-to-2 m are comprised of silty clays with very low blowcounts (less than 2) and whose underlying soils are soft volcanic ash and sand from 2 to 5 m (blowcounts less than 10) and dense volcanic ash at depths of 5 to 10 m (blowcounts exceed 50). Competent bedrock exists at depths below 10 m (Fig. 2-43b). Limited available information on seismic coefficients used in the design of structures at Muroran Port indicates coefficients of 0.10 to 0.15 were used, as compared with a peak acceleration of 0.21 g recorded at this port during the earthquake.

Despite the recorded peak accelerations being somewhat higher than the design seismic coefficients, the damage to waterfront structures at Muroran Port was limited to some tilting of sea walls and settlement of paved aprons. Sandboils observed in this port area after the earthquake suggest that this minor damage could have been caused by some degree of porewater pressure buildup in the underlying sand layers. An example of an undamaged structure is the sheet-pile bulkhead at the West Wharf No. 3 (Fig. 2-43c) which is similar to a severely damaged bulkhead at Hakodate Port (Fig. 2-42b).

2.14 1973 NEMURO-HANTO-OKI, JAPAN, EARTHQUAKE[*]

2.14.1 GENERAL DISCUSSION

An earthquake of magnitude 7.4 struck the eastern area of Hokkaido off the Numuro Peninsula (Fig. 2-44) on June 17, 1973. This earthquake had a focal depth of 40 km, and induced JMA seismic intensities in Nemuro and Kushiro cities of as high as V.

---

[*] Primary reference for damage assessment from the 1973 Nemuro-Hanto-Oki earthquake was JPHRI (1973).
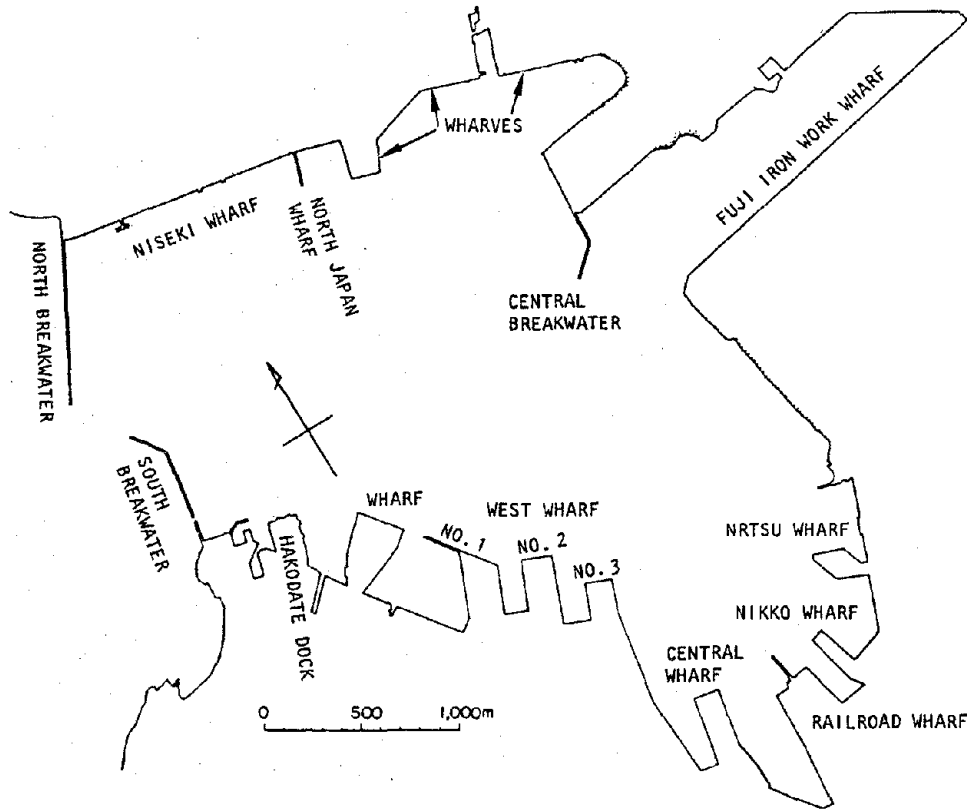
(a) Plan view
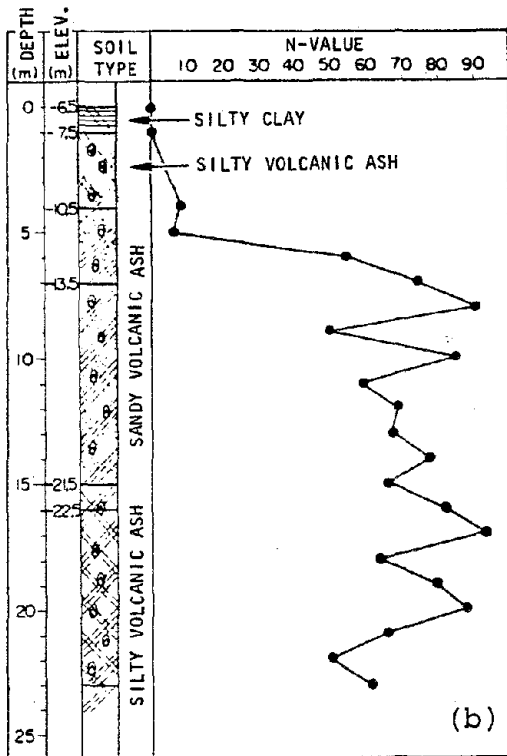
(b) Soil profile
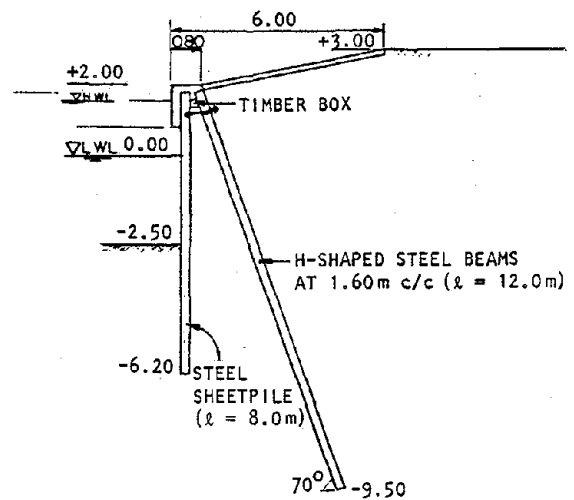
(c) Undamaged bulkhead
West Wharf No. 3

FIGURE 2-43. MURORAN PORT LAYOUT, SOIL PROFILE, AND TYPICAL UN-
DAMAGED STRUCTURE, 1968 TOKACHI-OKI EARTHQUAKE
(JPHRI, 1968)
(All dimensions and elevations in meters)

2-86
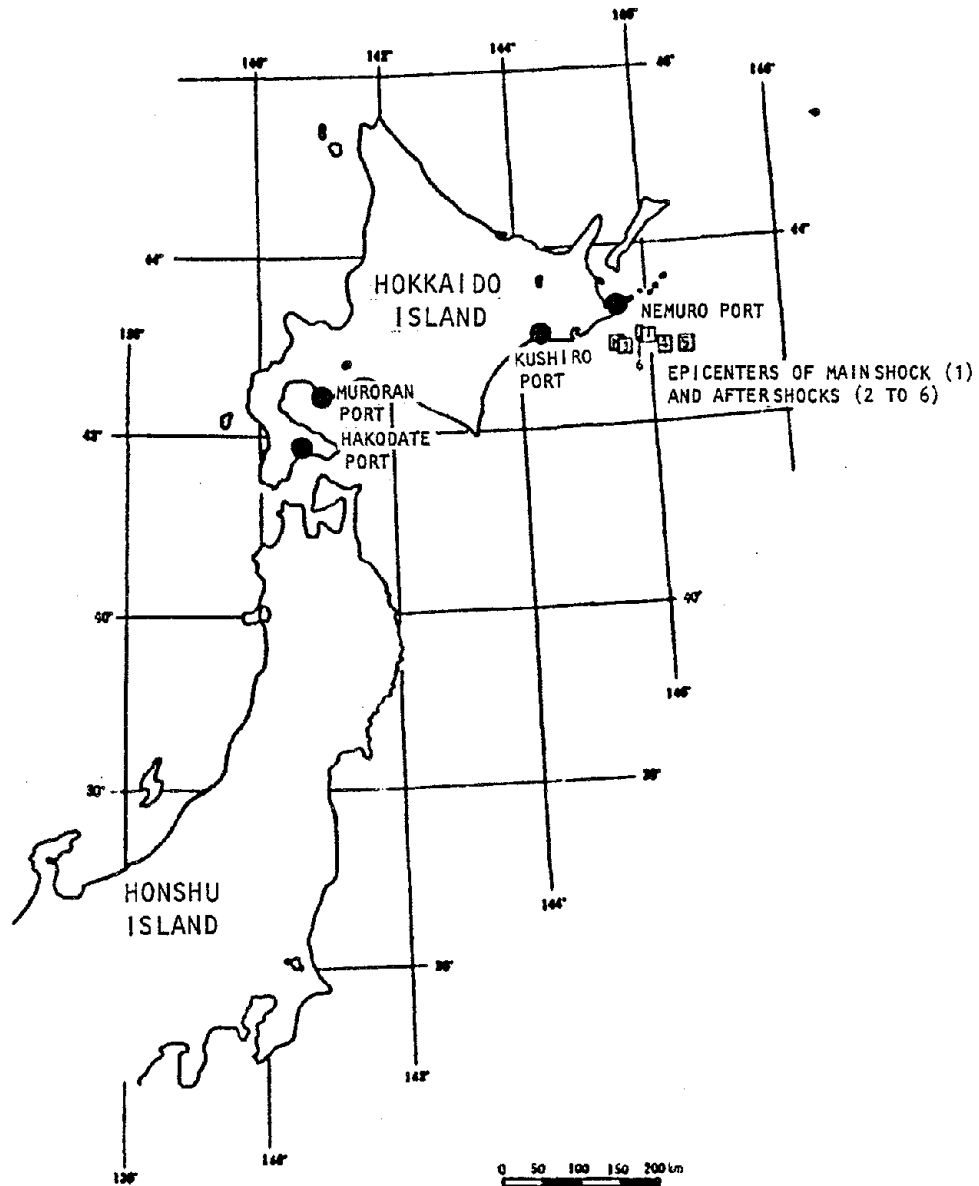
FIGURE 2-44. LOCATION OF EARTHQUAKE EPICENTER AND PORTS AFFECTED BY 1973 NEMURO-HANTO-OKI EARTHQUAKE (JPHRI, 1973)

Many aftershocks followed, the largest of which took place on
June 24 and had a magnitude of 7.3. A strong-motion accelerogram
of the main shock was obtained at Kushiro Port, and had a peak
horizontal acceleration of 0.17 g. The maximum accelerations
at Hanasaki and Kiritappu Ports were estimated to be about 0.29 g
and 0.26 g, respectively.

In the remainder of this section, the earthquake-induced
effects on port and harbor facilities at four main ports--Hanasaki,
Kiritappu, Kushiro, and Nemuro--are summarized. Of these, Hanasaki
Port suffered the most severe damage, and moderate damage was
induced at Kiritappu. Kurshiro Port and Nemuro Port (which are
only 6 km away from Hanasaki Port) sustained only very slight
damage during the Nemuro-Hanto-Oki earthquake.

2.14.2 HANASAKI PORT

The Hanasaki Port (Fig. 2-45a) is situated on soil deposits
comprised of sandy soils with blowcounts ranging from about 5 to
more than 50. At several borehole locations, however, the blow-
counts of these sands do not steadily increase with depth; instead,
at depths as great as 13 m, sand layers with blowcounts of less
than 20 are encountered between layers with much greater blowcounts
(Fig. 2-45b).

Severe damage was suffered by sheet-pile bulkheads and by
gravity-type quay walls. This damage is further described as
follows:

- Sheet-Pile Bulkheads along Fisherman's Wharf. Lique-
  faction of the sandy alluvium along the southern tip of
  the steel sheet-pile bulkhead at the southwest side of
  Fisherman's Wharf caused much larger horizontal displace-
  ments at that location than elsewhere along its length
  (Fig. 2-46a). An insufficient anchoring capacity of
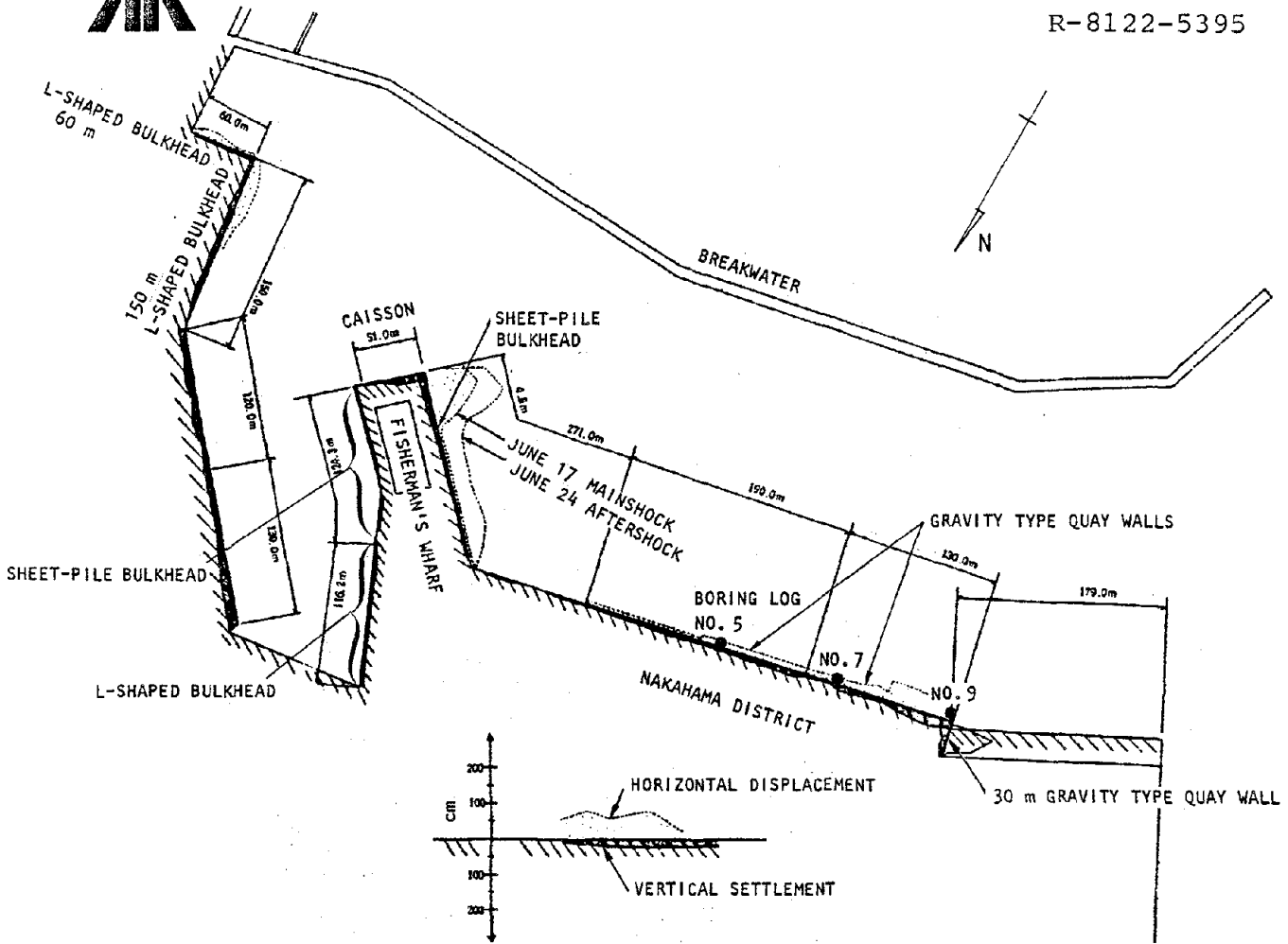
(a)   Plan view of harbor showing earthquake-induced displacements
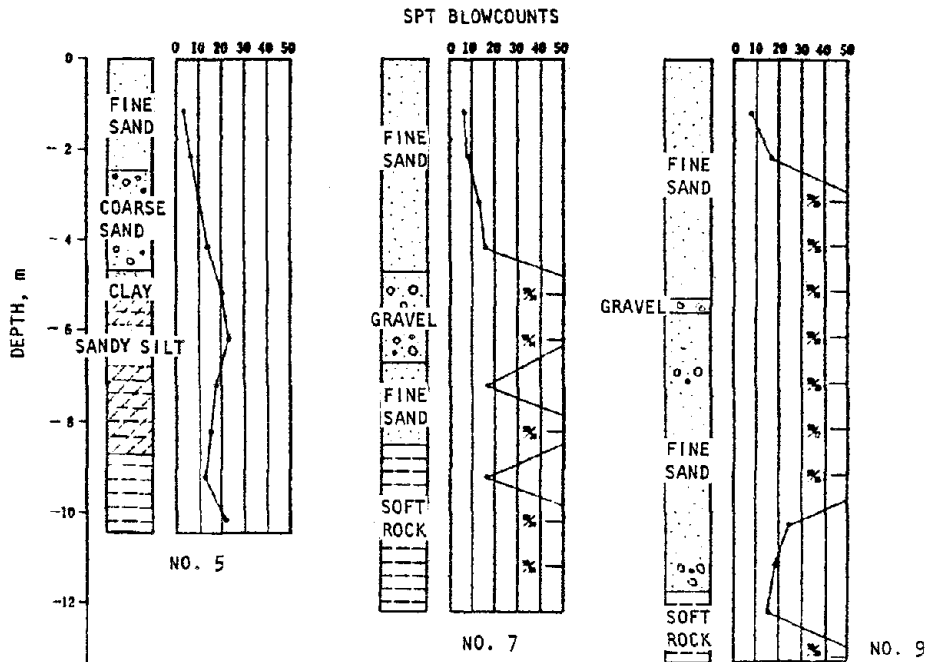
(b)   Example soil boring logs

FIGURE 2-45.   HANASAKI PORT LAYOUT AND SOIL PROFILE (JPHRI, 1973)
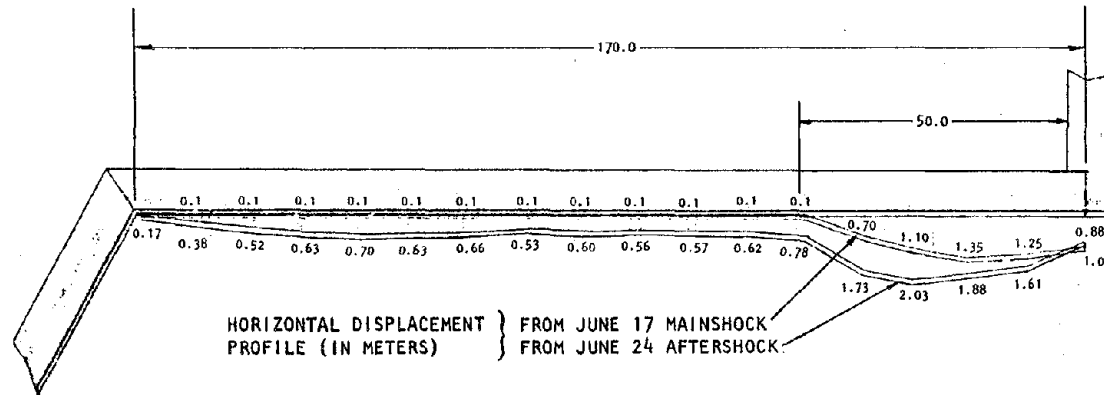
(a) Plan view of sheet-pile bulkhead along southwest
side of Fisherman's Wharf
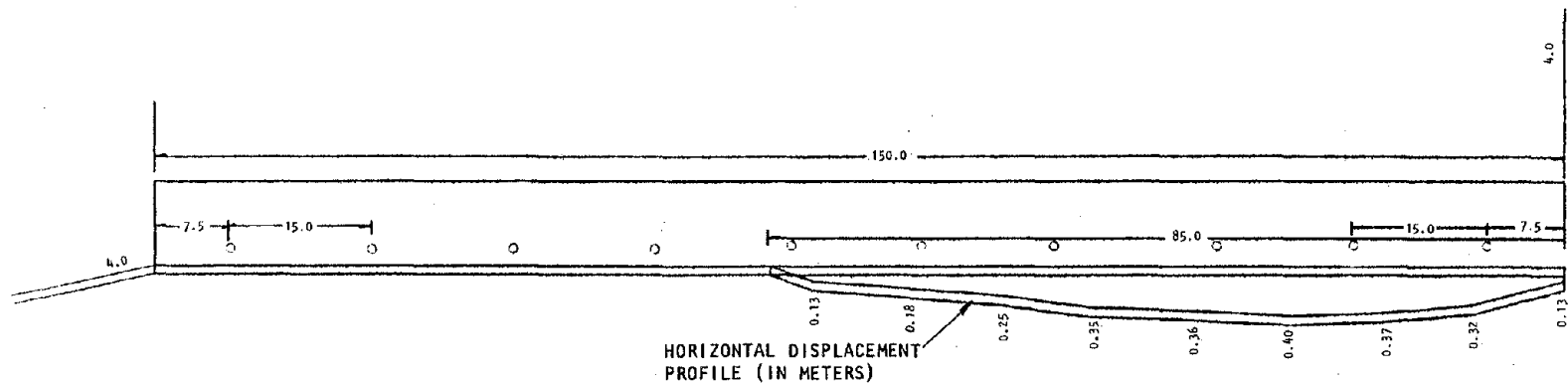
(b) Plan view of L-shaped bulkhead near east end of port

FIGURE 2-46. EARTHQUAKE DAMAGE AT HANASAKI PORT, 1973 NEMURO-HANTO-OKI
EARTHQUAKE (JPHRI, 1973)
(All dimensions and elevations in meters)
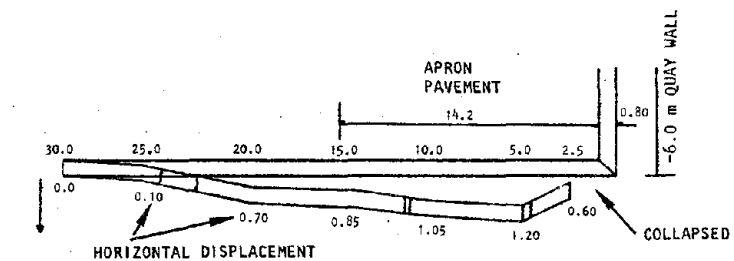
PLAN
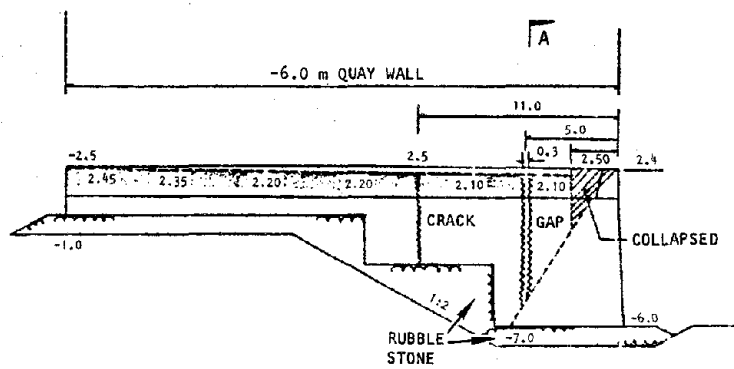
ELEVATION
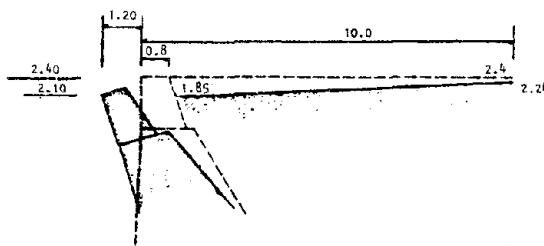
SECTION A-A

(c)   30 m quay wall at
      west end of port

FIGURE 2-46.   (CONTINUED)
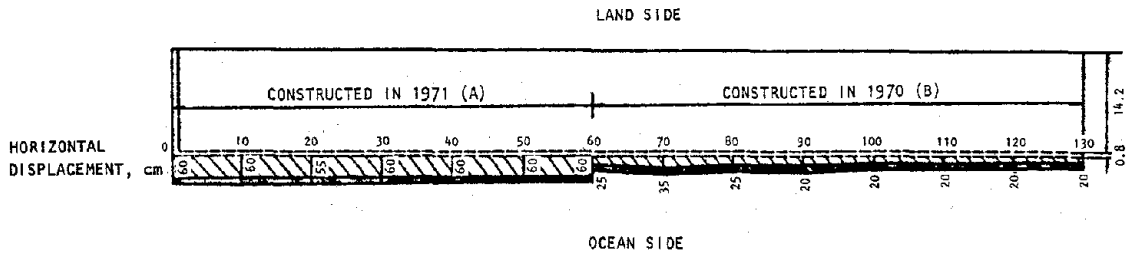
QUAY WALL HORIZONTAL DISPLACEMENT PROFILE
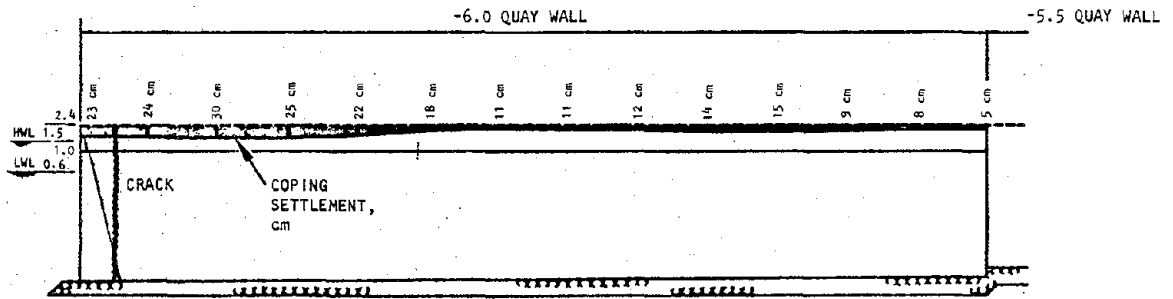
QUAY WALL ELEVATION
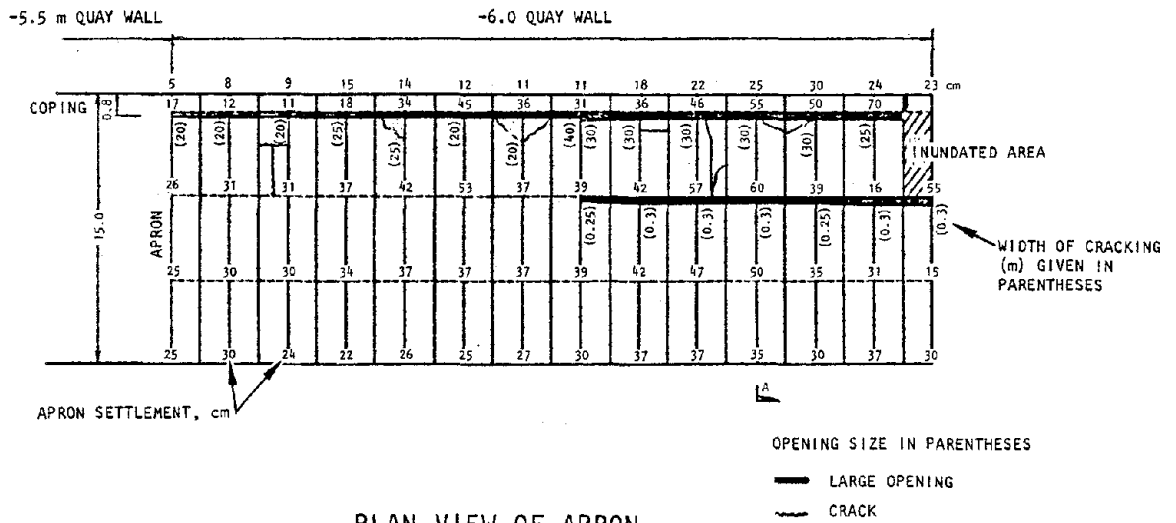
PLAN VIEW OF APRON

(d)   130 m section of gravity quay wall in Nakahama district

FIGURE 2-46.   (CONCLUDED)

the anchor system at this bulkhead also contributed to this damage. In contrast to this, a similar steel sheet-pile bulkhead along the northeast side of Fisherman's Wharf experienced virtually no sliding displacement, primarily because it made use of an existing gravity-type breakwater as an anchor that retained its anchoring capacity throughout the ground shaking. For both of these bulkheads, the settlements were very small.

• <u>Sheet-Pile Bulkheads at East End of Port</u>. These L-shaped bulkheads (of lengths 150 m and 60 m) experienced horizontal displacement and bulging (of up to 0.4 m) as well as apron settlements (0.4 m). Sand boils found in the area suggest that porewater pressure buildup contributed to this damage (Fig. 2-46b).

• <u>Gravity Type Quay Wall at West End of Port</u>. This 30 m quay wall experienced a maximum horizontal displacement of 1.2 m and a maximum settlement of 0.3 m. Prominent vertical cracking was induced at two locations in the wall, and the adjacent paved apron sank up to 1.2 m because of backfill settlement resulting from ground shaking and later from tsunami effects (Fig. 2-46c).

• <u>Gravity Type Quay Wall in Nakahama District</u>. (130-m section). The west 130-m section of this quay wall suffered horizontal displacement and settlement throughout its length. However, these effects were much more prominent in Segment A of this quay wall section, constructed in 1971, than in Segment B, constructed 1 yr earlier (Fig. 2-46d). This has been attributed to the backfill sand materials along Segment A being weaker and more liquefiable than along

Segment B, possibly because the structural and backfill
materials used for the construction of the quay wall at
Segment A were stored upon the Segment B backfills; this
apparently preloaded the Segment B backfill sands,
making them more resistant to the effects of earth-
quake ground shaking.

2.14.3 KIRITAPPU PORT

Kiritappu Port is situated on fine silty sands and sandy
silts together with coarse sand deposits. Although there was
some evidence of liquefaction of these deposits during the ground
shaking, the damage at Kiritappu Port was less severe than at
Hanasaki Port. This damage was restricted to uneven settlement
of the pavement apron, with a maximum apron settlement of 0.3 m.

2.14.4 KUSHIRO PORT

Kushiro Port is situated on generally favorable soil condi-
tions comprised of intermittent layers of gravelly clay, coarse
sands, and mud overlying bedrock at a depth of 6 to 8 m. Because
of these favorable conditions, the earthquake-induced damage at
this port was very light and the operation of the port was not
affected by the ground shaking.

2.14.5 NEMURO PORT

Nemuro Port is situated on very shallow soil deposits of
gravelly silty sands and clays overlying bedrock at depths below
the ground surface ranging from 2 m to 8 m. Because of these
excellent soil conditions, no significant earthquake damage was
induced at Nemuro Port, despite the fact that it is located only
6 km north of Hanasaki Port where significant damage took place.

2.15 1974 IZUHANTO-OKI, JAPAN, EARTHQUAKE[*]

The Izuhanto-Oki earthquake occurred on May 9, 1974, off
the Izu Peninsula in central Japan (Fig. 2-47). The magnitude of
this earthquake was 6.9 and its focal depth approximately 10 km.
The earthquake-induced damage to port and harbor facilities was
light even though the earthquake magnitude and the ground motion
intensities were significant. For example, the Mera Fishing Port
located 10 km from the epicenter suffered only slight damage
despite its strong ground accelerations, whose peak value was
estimated to be in the order of 0.4 g. This damage included some
settlement and sliding of the 80 m long -6.5 m breakwater, and
slight seaward displacement and apron settlement at a 60 m long
-3.0 m concrete block quay wall. The excellent behavior of water-
front structures at the Mera Fishing Port has been attributed to
the favorable site conditions at this port, which are comprised
of shallow outcroppings of competent rock (at depths of approxi-
mately -5.0 m).

Rather light earthquake-induced damage also occurred at the
Shimoda Port and the Inatori Fishing Port, located 20 and 30 km
from the epicenter respectively, even though the peak ground
acceleration at these ports were estimated to be 0.25 g and 0.1 g
to 0.15 g respectively in these two ports. As at the Mera Fishing
Port, this light damage was attributable to the favorable site
conditions at Shimoda and Inatori, which are comprised of sound
bedrock at depths of about 10 m.

---

[*]Primary reference for damage assessment from the 1974 Izuhanto-Oki
earthquake was Noda and Uwabe (1975).
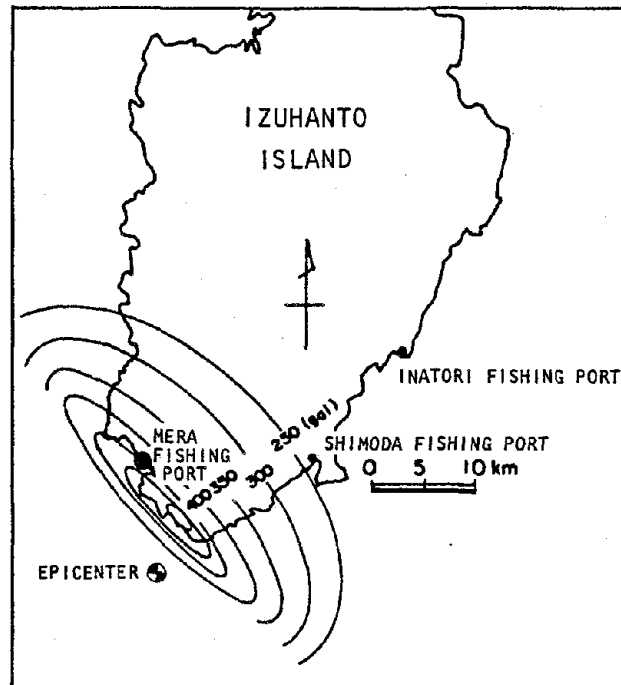
FIGURE 2-47. LOCATION OF 1974 IZUHANTO-OKI EARTHQUAKE
EPICENTERS AND AFFECTED AREAS (Noda and
Uwabe, 1975)

2.16 1978 MIYAGI-KEN-OKI, JAPAN, EARTHQUAKE[*]

2.16.1 GENERAL DISCUSSION

On June 12, 1978 an earthquake of magnitude 7.4 and focal depth 30 km occurred with an epicenter in the Pacific Ocean off the Miyagi Prefecture (Fig. 2-48). Motions recorded at Shiogama, Sendai, and Ishinomaki Ports during this earthquake were the strongest ever measured at port and harbor sites in Japan. For example, even though Shiogama Port was 104 km from the center of the Miyagi-Ken-Oki earthquake, peak accelerations of 0.29 g (horizontal) and 0.17 g (vertical) were recorded there.

The Miyagi-Ken-Oki earthquake caused particularly severe damage to gravity-type quay walls and piers and to sheet-pile bulkheads. This damage was particularly severe at sites where liquefaction occurred, and was usually only minor at sites with no apparent liquefaction.

The most significant effects of the Miyagi-Ken-Oki earthquake on port and harbor structures occurred at Shiogama, Sendai, and Isinomaki Ports and at the Ishinomaki and Yuriage Fishing Ports. These effects are described in the remainder of this section.

2.16.2 SHIOGAMA PORT

The Shiogama Port (Fig. 2-49) is situated in a region generally comprised of bedrock at a shallow depth (10 m or less at the Central Pier) overlain by a thin surface layer of sand

---

[*]Primary reference for damage assessment from the 1978 Miyagi-Ken-Oki earthquake was Tsuchida, et al. (1979).

NOTE: NUMBERS SHOWN CORRESPOND TO JMA INTENSITIES
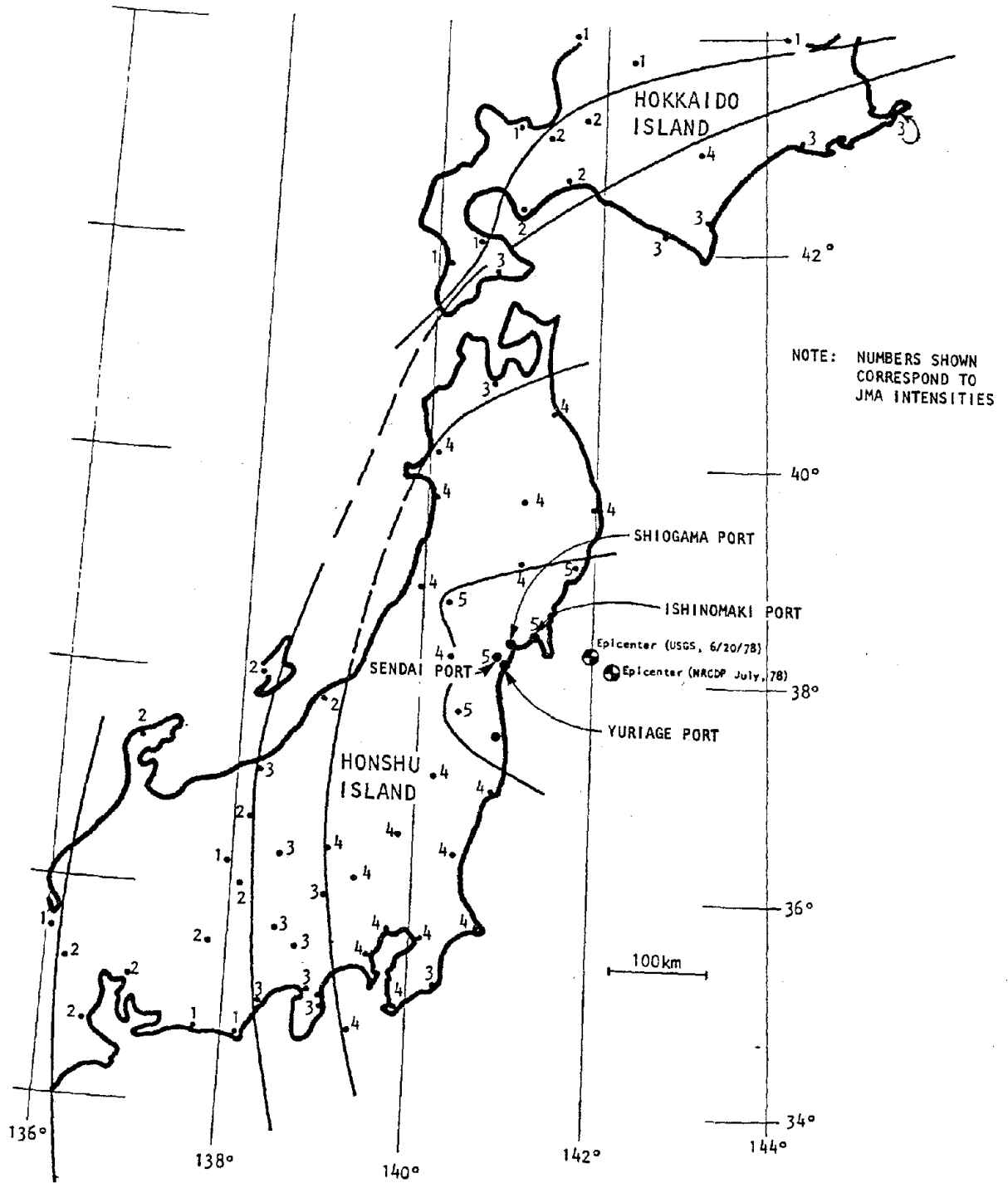
FIGURE 2-48.   JMA INTENSITY MAP SHOWING EARTHQUAKE EPICENTER AND HARBOR LOCATIONS, 1978 MIYAGI-KEN-OKI EARTHQUAKE (Brady, 1978)
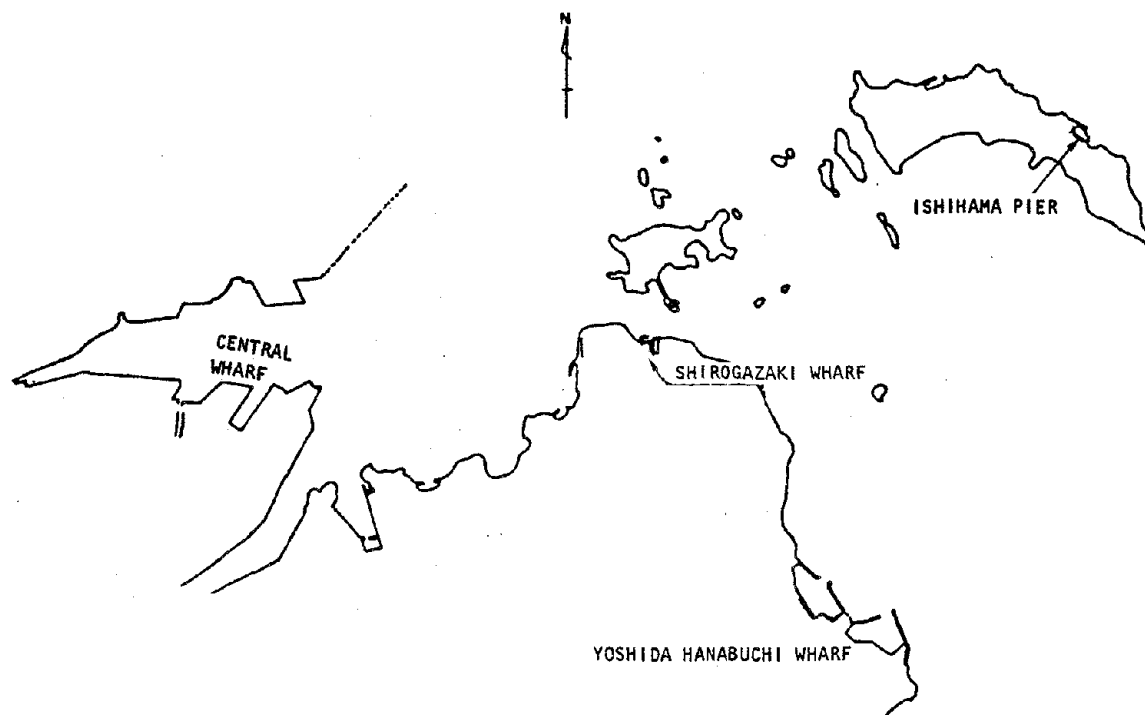
FIGURE 2-49.   SHIOGAMA PORT (Tsuchida et al., 1979)

and 20 to 25 m of clays. The earthquake caused the following damage at this port:

- **Yoshida Hanabuchi Wharf.** This wharf is comprised of two different sections of concrete block quay wall. About half of the 178 m west section suffered seaward tilting of the headworks and settlement of the apron. The relative displacements between the headwork and the apron were 0.5 m (horizontal) and 0.2 m (vertical). About one-third of the 246 m east section of this quay wall suffered damage of a similar type but of less severity (Fig. 2-50a).

- **Ishihama Pier.** This concrete block gravity type pier was constructed on a layer of rubblestone overlying bedrock, and included small stone fill within its interior. Outward tilting of the concrete blocks during the earthquake resulted in bulging of the pier cross section and settlement of the apron (Fig. 2-50b).

- **Shirogazaki Wharf.** The concrete block quay wall was undamaged by the Miyagi-Ken-Oki earthquake. A contributing factor to the excellent performance of this quay wall during the earthquake was that its lower layer of concrete blocks was embedded into the bedrock (Fig. 2-50c), rather than resting on a layer of rubblestone as was the case at Ishihama Pier (Fig. 2-50b).

- **Central Wharf.** The 60-m concrete gravity type quay wall at this wharf suffered significant seaward tilting of the headwork along the entire length of the quay wall (0.6-m displacement) and severe cracking and settlement (up to 0.4 m) of the apron and concrete pavement (Fig. 2-50d).
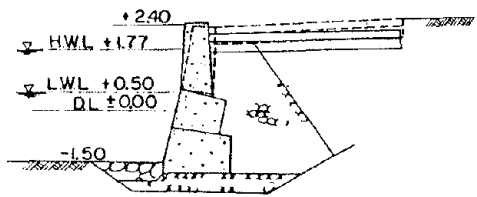
WEST SECTION
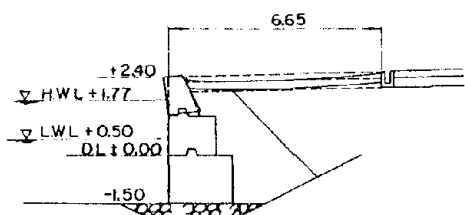
EAST SECTION

(a) Yoshida Hanabuchi Wharf
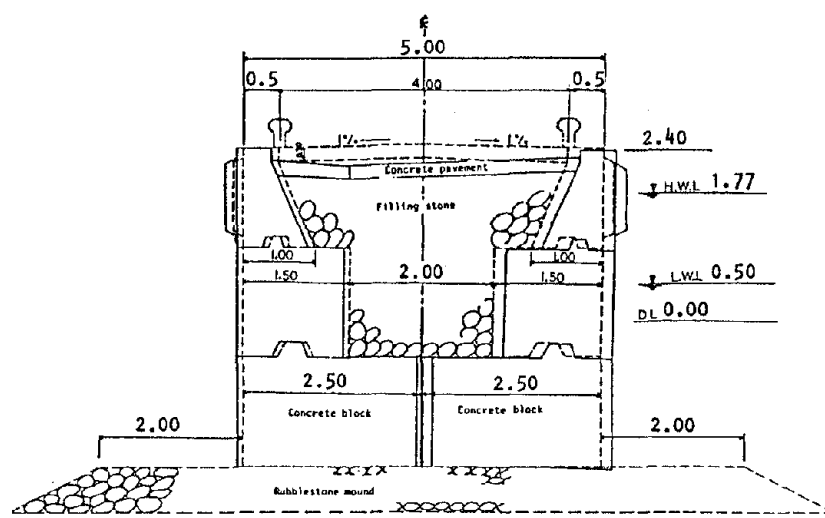
(b) Ishihama Pier
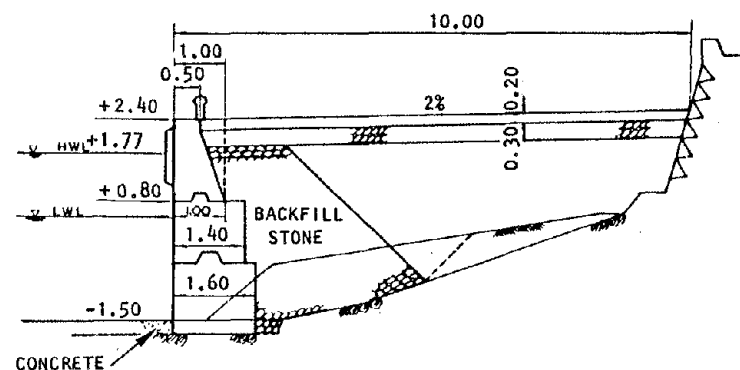
(c) Shirogazaki Pier
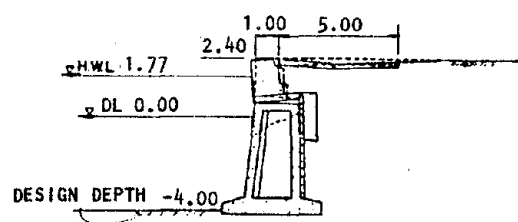
(d) Central Wharf

FIGURE 2-50.   DAMAGED QUAY WALLS AT SHIOGAMA PORT, 1978 MIYAGI-KEN-OKI
EARTHQUAKE (Tsuchida et al., 1979)
(All dimensions and elevations in meters)

2.16.3 SENDAI PORT

The Sendai Port has soil conditions comprised of a surface layer of sand (3 m to 20 m thick) underlain by layers of medium coarse sand and silty loam. Dense sand and bedrock underlie the silty loam layer. All waterfront facilities at Sendai Port were designed using a seismic coefficient of 0.1, except for a quay wall in the Central Waterway that was designed using 0.15.

The most noteworthy earthquake effects at Sendai Port involve comparisons between response characteristics of two practically identical adjacent steel sheet-pile bulkheads at Nakano Wharf (Fig. 2-51). Bulkhead No. 4, which was anchored using vertical H-beams experienced cracking and settlement of its apron and pavements (Fig. 2-52a), while Bulkhead No. 5, which was anchored using batter piles, remained intact with no apparent damage (Fig. 2-52b). Comparable trends were exhibited by other bulkheads at Sendai Port designed with these two different anchor systems.

The differences in behavior between Bulkheads 4 and 5 can be attributed to the nature of the soil properties at each bulkhead, as well as to the differences in anchor systems. Figure 2-52 shows that, even though Bulkheads 4 and 5 are adjacent to one another, there are differences in the soil properties of the two sites. This is particularly true near the ground surface, where the fill materials at Bulkhead No. 4 exhibit a much lower SPT resistance than do the near-surface sand materials at Bulkhead No. 5. However, the differences in anchor support systems for these two bulkheads could also have contributed to their differing response to the ground shaking in accordance with the following possible mechanism: (1) the batter-pile-supported anchor system at Bulkhead No. 5 would presumably have had a greater resistance to increased lateral pressures that could result from porewater
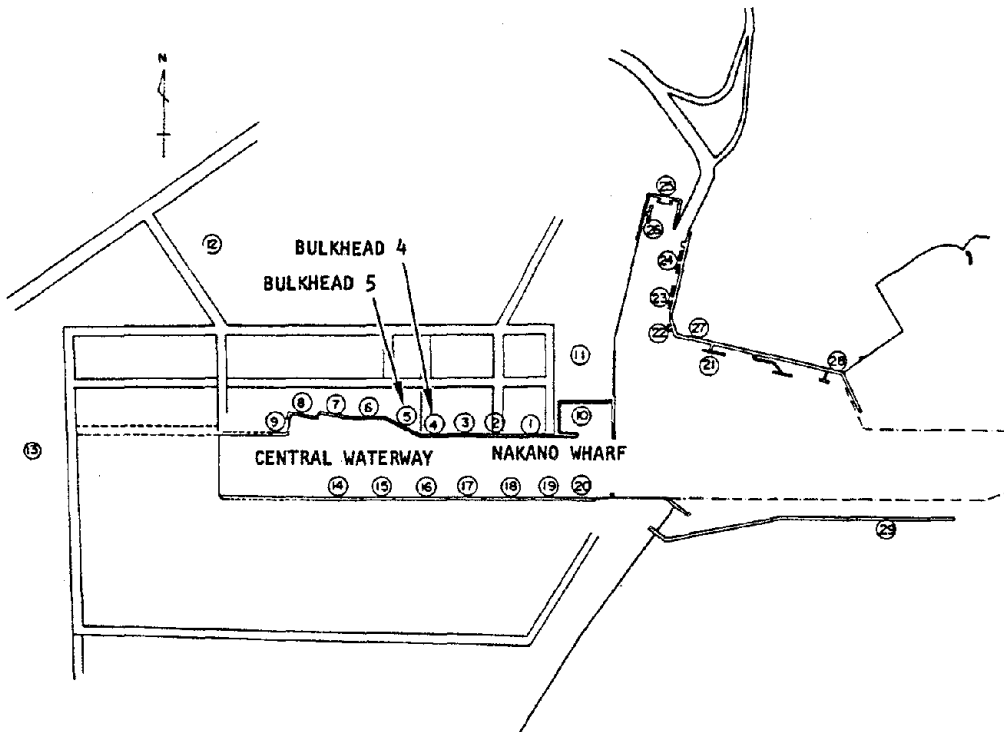
FIGURE 2-51. SENDAI PORT LAYOUT (Tsuchida et al., 1979)

(a) Cross section and soil properties, Bulkhead 4

(b) Cross section and soil properties, Bulkhead 5
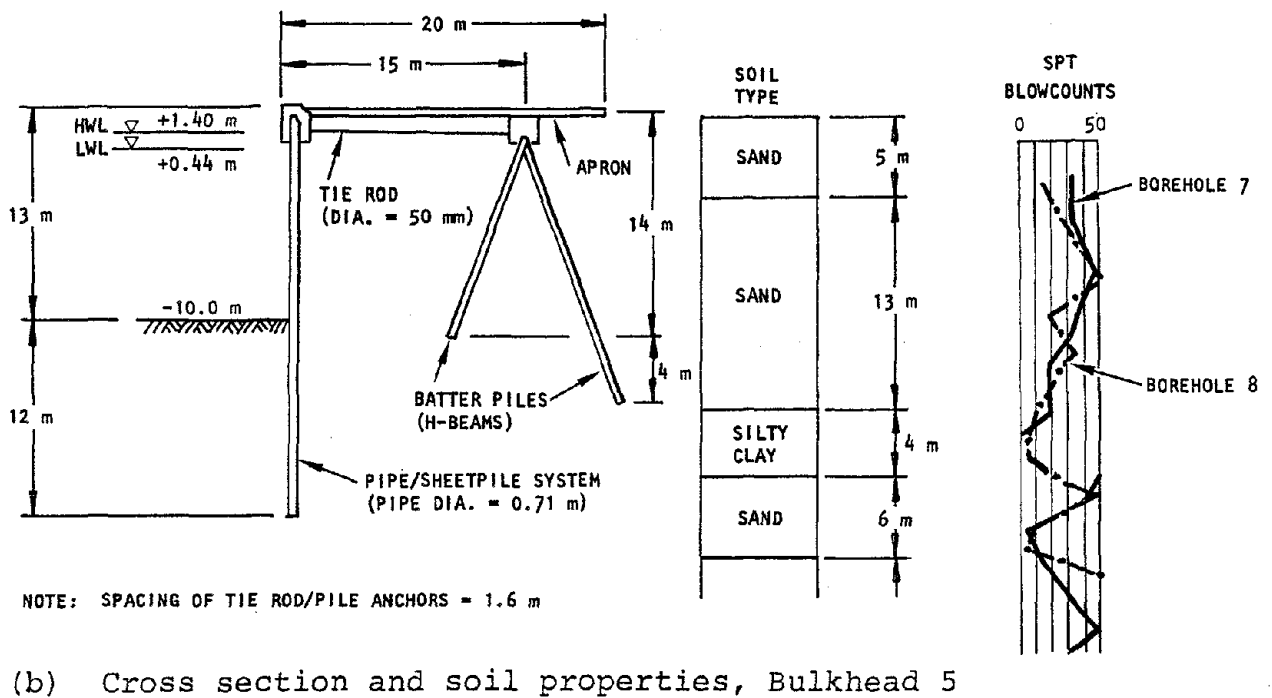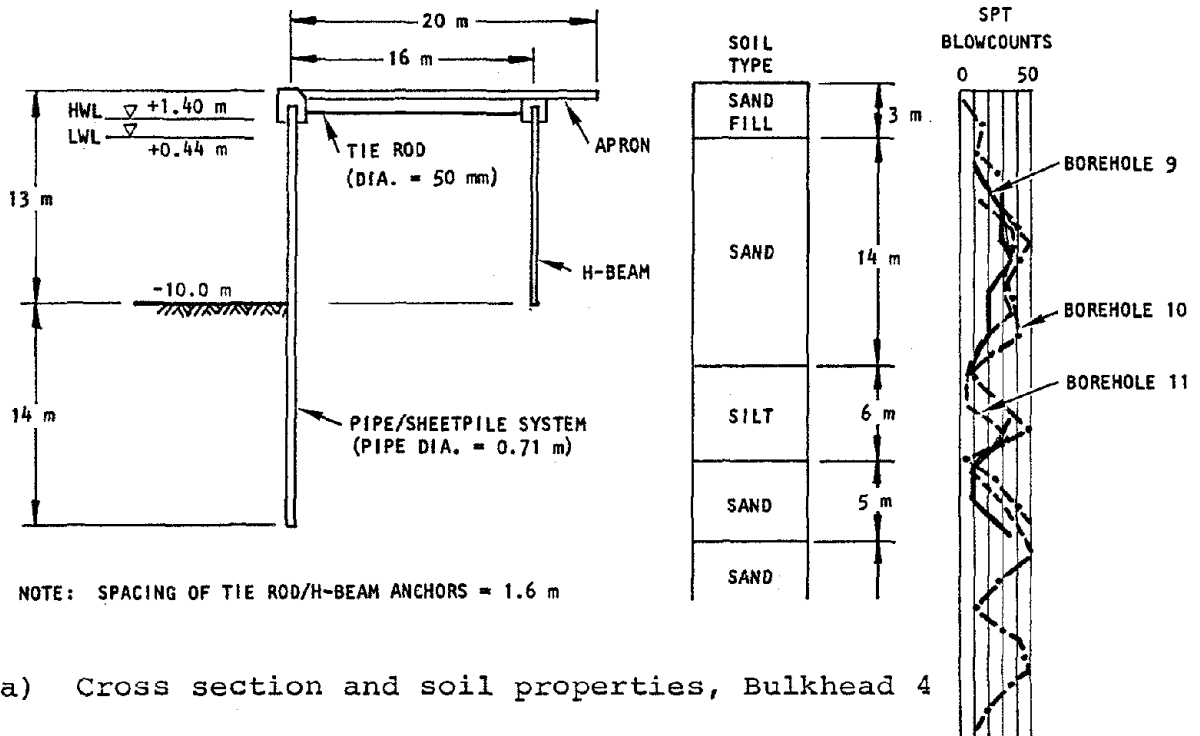
FIGURE 2-52.   BULKHEADS 4 AND 5 AT NAKANO WHARF, SENDAI PORT
               (Tsuchida et al., 1979)

pressure buildup in the soil along its interface with the sheet pile; (2) this would reduce the tendency of the sheet pile and the soil to displace laterally due to these increased pressures; and (3) as a result, any reduction in confinement of the soil layers (particularly those near the ground surface) would be minimized which, in turn, would minimize the tendency of these layers to settle and to thereby damage the overlying apron. The behavior of these two sheet-pile bulkhead systems is discussed further in Chapter 5, in the context of a dynamic analysis of Bulkhead No. 4 that was carried out as part of this research program.

2.16.4 ISHINOMAKI PORT

The Ishinomaki Port (Fig. 2-53a) is situated on essentially uniform soils comprised of a 12 m thick surface layer of soft sands (blowcounts 10 to 15) underlain by a 13 m thick soft clay layer (blowcounts 5 to 10), a 15 m thick segment of medium to coarse sands, and gravel at depths below 40 m. The earthquake-induced damage at Ishinomaki Port was very severe, accounting for about 90% of the total damage costs incurred by port and harbor facilities as a result of the Miyagi-Ken-Oki earthquake.

General trends from observations of the damage at Ishinomaki Port during this earthquake were:

- The damage to quay walls and sheet-pile bulkheads correlated strongly with the ocurrence of liquefaction at adjacent backfill areas; i.e., significant damage occurred at sites with strong evidence of liquefaction, whereas no such evidence was apparent at sites of undamaged structures.

- Steel-pipe quay walls and breakwaters sustained very little damage during this earthquake.
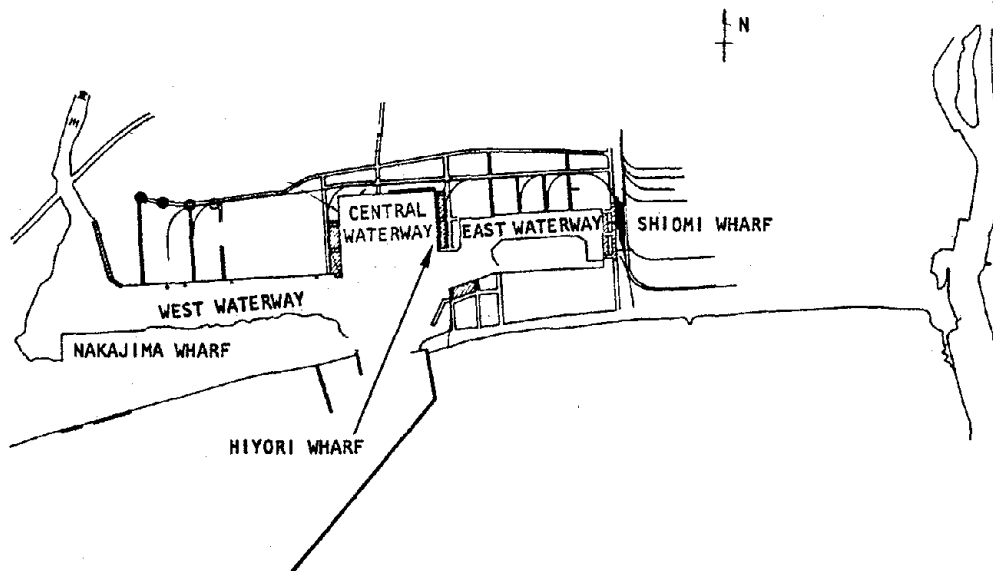
(a) Port layout, Isinomaki Port

CROSS SECTION, UNDAMAGED

CROSS SECTION, DAMAGED
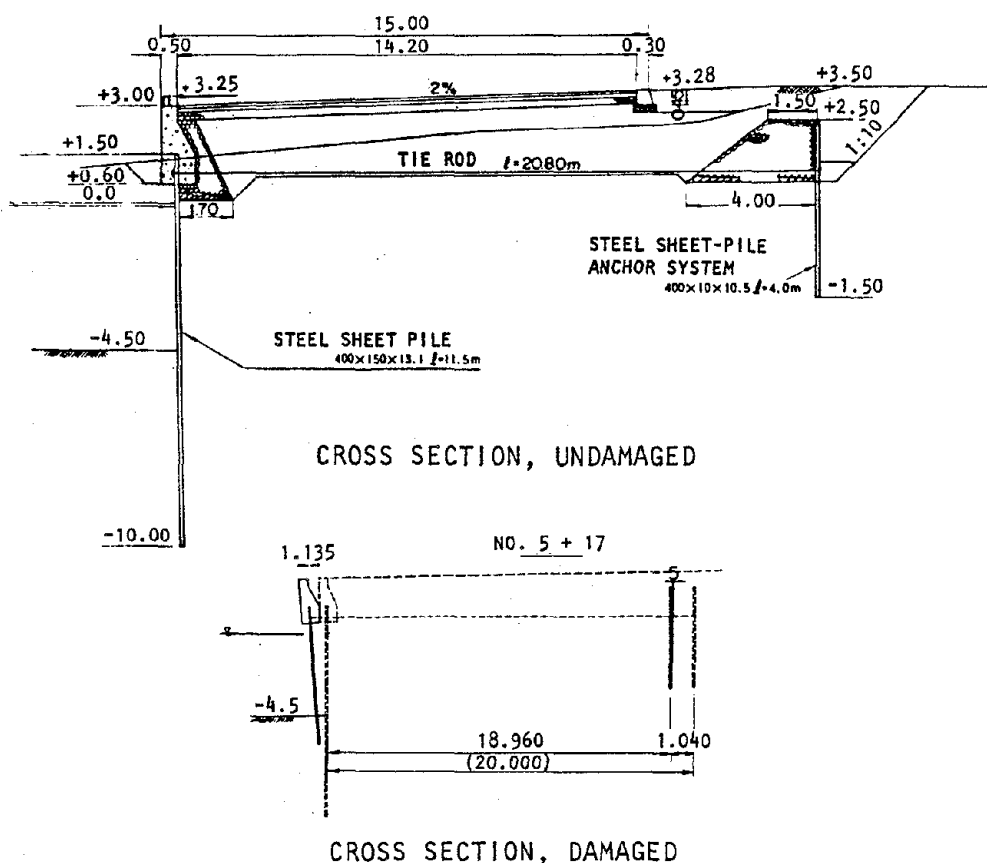
(b) Damaged sheet-pile bulkhead at Shiomi Wharf

FIGURE 2-53. DAMAGE AT ISHINOMAKI PORT DURING MIYAGI-KEN-
OKI EARTHQUAKE (Tsuchida et al., 1979)
(All dimensions and elevations in meters)

Additional discussion of damage at specific locations within Ishinomaki Port is as follows:

- <u>Nakajima Wharf</u>. A 400-m vertical sheet-pile bulkhead at this wharf suffered substantial seaward sliding and tilting, (with horizontal displacements as high as 0.6 m) as well as a significant settlement of the apron (up to 1 m). There was widespread evidence of liquefaction of the sandy soils at this bulkhead site, in the form of sand spouting that continued well after the earthquake.

- <u>Hiyori Wharf</u>. A quay wall at this wharf experienced damage in the form of displacements of the headwork of 0.6 m (horizontal) and 0.2 m (vertical). There was evidence of liquefaction at this wharf, in the form of sand spouts from cracks within the apron.

- <u>Shiomi Wharf</u>. A 300-m sheet-pile bulkhead (Fig. 2-53b) and its auxiliary structures suffered significant seaward horizontal displacement (1.2 m) at its midlength but only small settlement (0.1 m). Subsequent inspections of the tie rod connecting the wall to its anchor system indicated that this rod was not damaged; this suggests that the entire sheet-pile bulkhead including its anchor displaced as a unit, possibly due to liquefaction of the sandy backfill and underlying soil deposits.

2.16.5 ISHINOMAKI FISHING PORT

The Ishinomaki Fishing Port is located east of the Ishinomaki Port at the mouth of the Kitakami River (Fig. 2-54). The subsurface conditions at this port correspond to 25 m of alluvium (alternating layers of sand and silt) underlain by bedrock. SPT
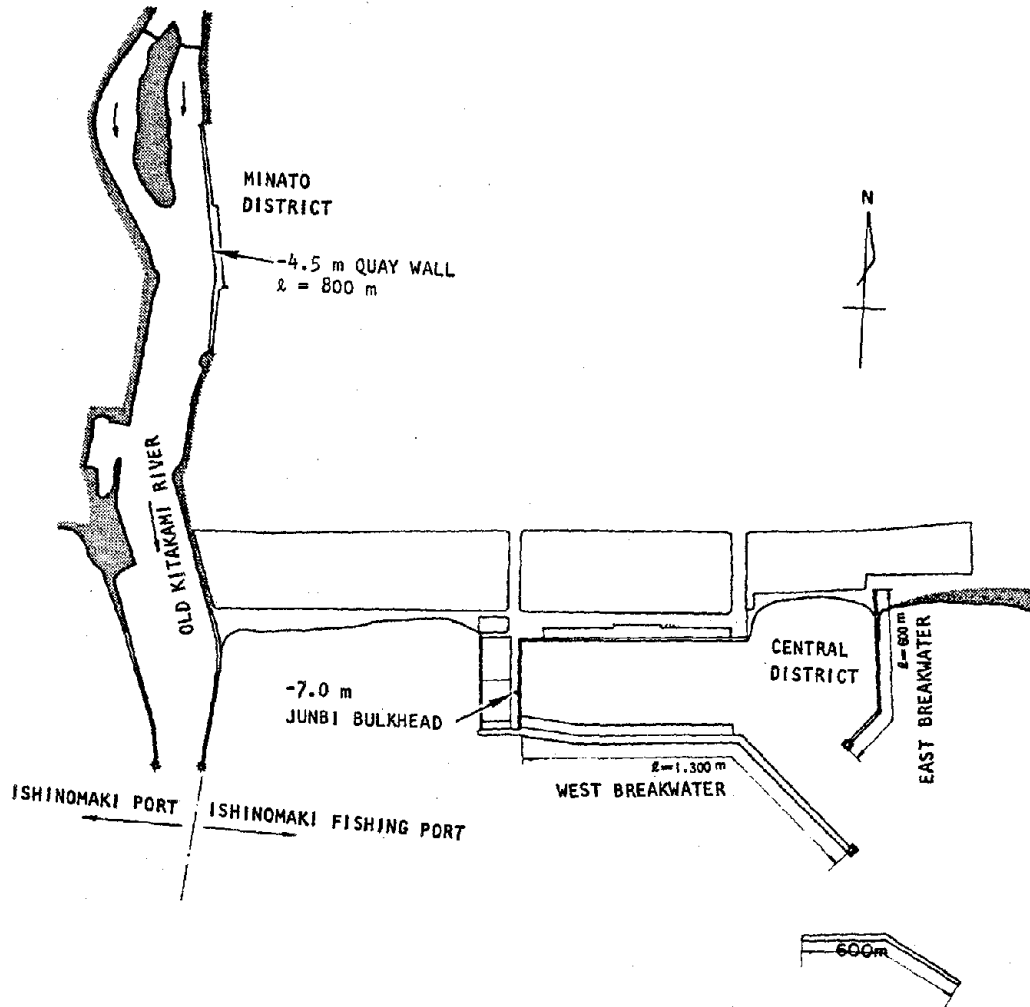
FIGURE 2-54. LAYOUT OF ISHINOMAKI FISHING PORT
(Tsuchida et al., 1979)

blowcounts within the alluvium fluctuate considerably with depth, but generally fall below 10 to 20 throughout most of the alluvium. Waterfront facilities at this fishing port were designed using a seismic coefficient of 0.1.

The Miyagi-Ken-Oki earthquake caused damage to the Ishinomaki Fishing Port in the form of horizontal displacements of quay walls and cracking and settlement of aprons. Liquefaction was evident in the alluvial sands that prevail at this site, in the form of sandboils and spouting of sand deposits, particularly within the Central District of the port. Further discussion of the waterfront facility damage is as follows:

- Junbi Bulkhead. Almost two-thirds of a 300-m steel sheet-pile bulkhead in the Central District of this port was damaged. This damage took the form of seaward displacements of the steel sheet piles (up to about 0.3 m) and cracking and some settlement of the apron (about 0.1 m). Water and sand spouted from cracks in the apron, indicating porewater pressure buildup and possible liquefaction.

- Minato District. About three-quarters of a 750-m quay wall suffered damage in the form of wall tilting and apron settlement (up to about 0.2 m).

2.16.6 YURIAGE FISHING PORT

The Yuriage Fishing Port (Fig. 2-55a) is situated on about 20 m of alluvial sands underlain by dense gravels. Blowcounts of the sand materials range from less than 10 near the ground surface to up to 40 at deeper depths. The seismic coefficient used in the design of waterfront facilities at the Yuriage Fishing Port was 0.1.
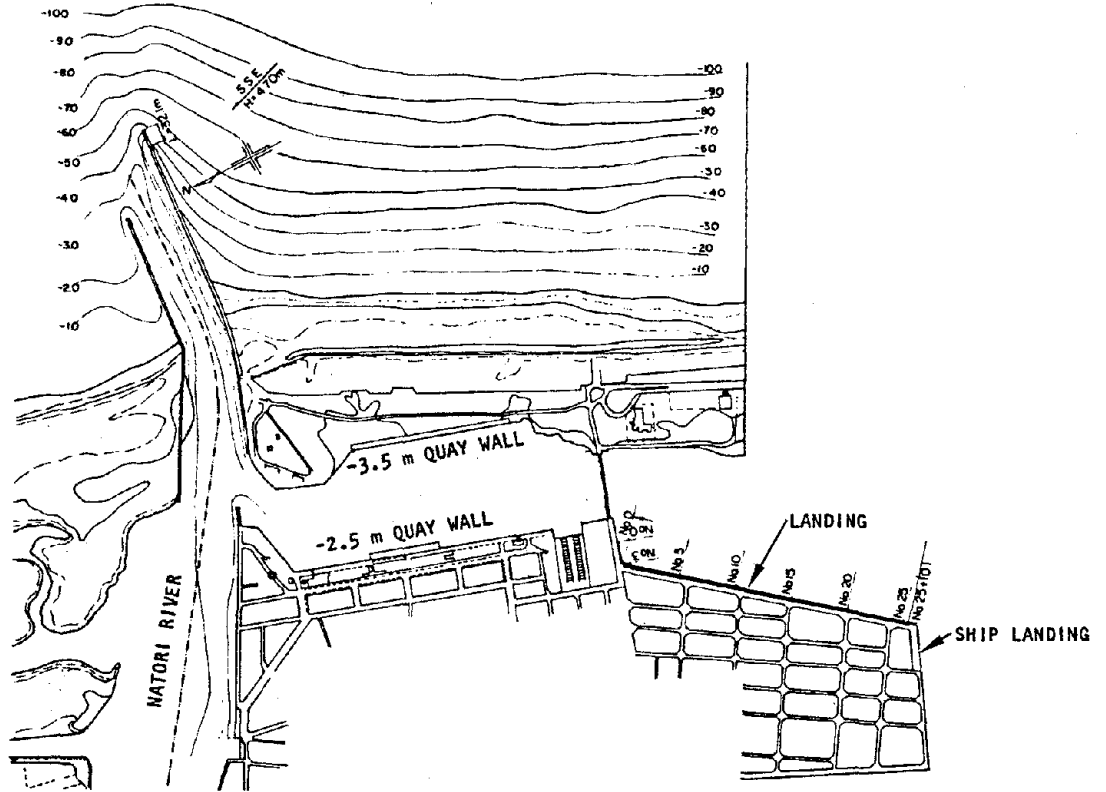
(a)   Port layout (Tsuchida et al., 1979)
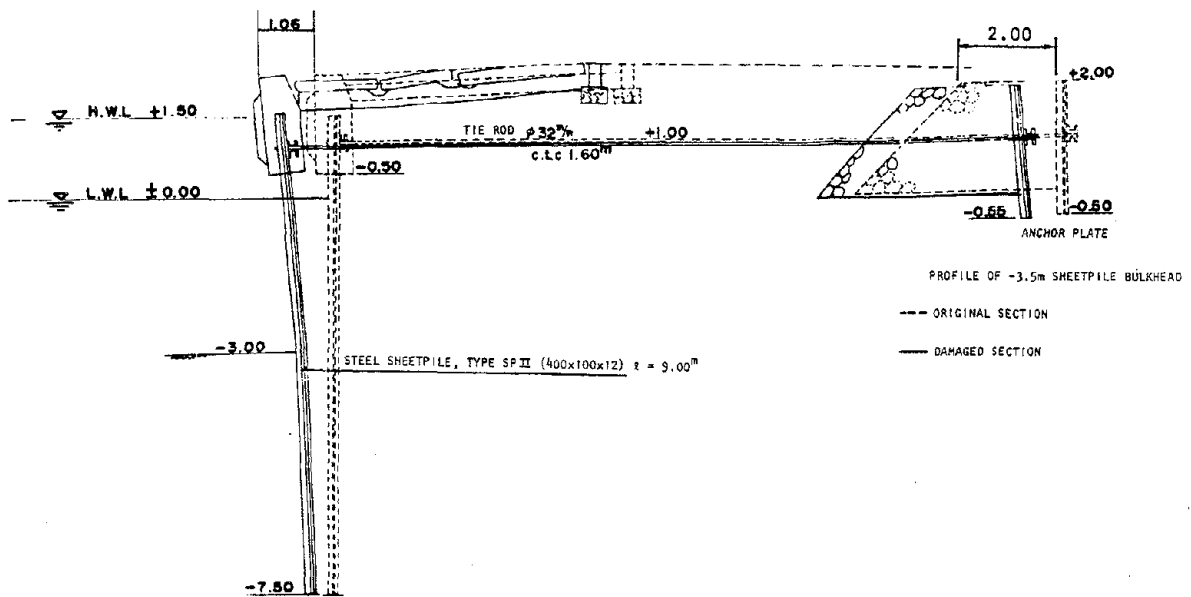
(b)   Damaged quay wall on east side of port
      (Tsuchida and Noda, 1979)

FIGURE 2-55.   DAMAGE AT YURIAGE FISHING PORT, 1978 MIYAGI-KEN-
               OKI EARTHQUAKE (All dimensions and elevations
               in meters)

The Miyagi-Ken-Oki earthquake induced widespread and severe damage at this port. For example, a concrete block quay wall on the west bank of the port suffered severe wall translations and rotations (with a maximum horizontal displacement of 1.2 m) and apron cracking and settlement (up to about 0.3 m). In addition, almost 300 m of a sheet-pile bulkhead on the east bank of the port underwent severe damage that featured maximum horizontal displacements of the headwork of about 1.2 m (Fig. 2-55b). In this latter case, the sheet pile and anchor system displaced horizontally as a unit, suggesting overall movement of the sandy soil deposits, possibly as a result of liquefaction.

In addition to quay walls and bulkheads, docks at this port were also subjected to substantial damage. A landing for ships on the south end of the port experienced a horizontal sliding of almost 1 m and a settlement of 1.1 m. An adjacent landing slid up to 0.7 m and settled up to 0.5 m over almost half of its 550 m length.

2.17 SUMMARY OF RESULTS

This chapter contains results from our extensive compilation and assessment of the dynamic response characteristics of ports and harbors during prior earthquakes. These results not only clearly demonstrate the extreme susceptibility of port and harbor facilities to widespread damage from earthquake ground shaking, but also provide important details regarding the nature of significant port and harbor response characteristics and damage modes that should be of value in future seismic design applications.

Our compilation and assessment of seismic response characteristics and damage modes for port and harbor facilities (summarized in Table 2-1) indicates the following trends:

- By far the most significant source of earthquake-induced damage to port and harbor facilities has been porewater pressure buildup in the loose-to-medium dense, saturated, cohesionless soils that prevail at port and harbor sites. This has led to damage due to excessive lateral pressures applied to quay walls and bulkheads by backfill materials (Item A in Table 2-1), and to liquefaction (Item B), localized sliding (Item C), or massive submarine sliding of the site soil materials (Item D).

- To substantiate the importance of these porewater pressure effects, this chapter cites several cases involving similar port and harbor structures located on adjacent sites, in which one site experienced significant porewater pressure buildup during a given earthquake and the other did not. Invariably, the structures at the sites with significant porewater pressure buildup suffered severe damage, whereas the damage to structures at the other sites was much less substantial. In other such examples cited in this chapter, widespread liquefaction and massive soil sliding caused by porewater pressure buildup has resulted in complete destruction of entire port and harbor areas (e.g., the Niigata, 1964, and Alaska, 1964, earthquakes).

- There was very little, if any, evidence of damage directly related to the earthquake-induced vibrations of the structures (Item E in Table 2-1). This may be

TABLE 2-1. SUMMARY OF EARTHQUAKE-INDUCED DAMAGE TO PORT AND HARBOR FACILITIES

Earthquake			Port Location	Damage	Possible Cause(s)
Location	Date	Magnitude		Description	
Kanto, Japan	Sep 1, 1923	8.2	Yokohama and Yokosuka	Concrete block quay walls: sliding, tilting, and/or collapse with some bearing capacity failure of rubble-stone foundation	A
				Steel bridge pier: buckling of pile supports	C,E
Kitaizu, Japan	Nov 26, 1930	7.0	Shimizu	Caisson quay wall (183 m long): tilting, outward sliding (8.3 m), and settlement (1.6 m)	A,B,C
				L-Shaped block quay wall (750 m long): outward sliding (4.5 m) and settlement (1.2 m)	
Shizuoka, Japan	Jul 11, 1935	6.3	Shimizu	Caisson quay wall: outward sliding (5.5 m) and settlement (0.9 m) accompanied by anchor system failure	A,B,C
Tonankai, Japan	Dec 7, 1944	8.3	Yokkaichi	Pile-supported concrete girder and deck: outward sliding (3.7 m) accompanied by extensive soil sliding	A,B,C
			Nagoya Osaka	Sheet-pile bulkhead with platform: outward bulging (4 m) Steel sheet-pile bulkhead: outward bulging (3 m)	
Nankai, Japan	Dec 21, 1946	8.1	Nagoya Yokkaichi	Sheet-pile bulkhead with platform: outward bulging (4 m) Pile-supported concrete girder and deck: outward sliding (3.7 m)	
			Osaka	Steel sheet-pile bulkhead: outward bulging (3 m) and settlement (0.6 m)	A,B,C
			Uno	Gravity-type concrete block and caisson quay wall: seaward sliding (0.4 m) accompanied by soil sliding	
Tokachi-Oki, Japan	Mar 4, 1952	8.1	Kushiro	Concrete caisson quay wall: tilting, outward sliding (6 m), and settlement (1 m)	A,B,C
Chile	May 22, 1960	8.4	Puerto Montt	Concrete caisson quay walls: overturning and extensive tilting	
				Steel sheet-pile seawall: outward sliding (up to 1 m) and anchor failure	A,B,C
				Gravity-type concrete seawall: complete overturning and sliding (1.5 m)	
			Talcuhuano	Concrete block quay wall: outward tilting	A,B
Alaska	Mar 27, 1964	8.4	Anchorage	Dock structures: extensive seaward tilting with bowing, buckling, and yielding of pile supports	B,D,E
			Valdez	Entire harbor: destroyed by massive submarine landslide	
			Whittier	Pile-supported piers and docks: buckling, bending, and twisting of steel pile supports	
				Steel sheet-pile bulkhead: extensive bulging	B,D
			Seward	Major portion of harbor: destroyed by massive submarine landslide	

TABLE 2-1. CONCLUDED)

Earthquake			Port Location	Damage	
Location	Date	Magnitude		Description	Possible Cause(s)
Niigata, Japan	Jun 16, 1964	7.5	Niigata	Extensive damage due to liquefaction and sliding of soil strata. Summary of damage is as follows: Piers and landings: sliding (up to 5 m), submergence, and tilting Sheet-pile bulkheads: sliding (over 2 m), submergence, settlement (up to 1 m), and tilting. Extensive anchor failure Quay-walls: sea sliding (up to 3 m) settlement (up to 4 m) with extensive anchor failure and wall tilting	A,B,C
Tokachi-Oki, Japan	May 16, 1968	7.8	Hachinohe	Steel sheet-pile bulkheads: outward sliding (0.9 m), tilting, and settlement, with anchor failure	A
			Aomori	Gravity-type quay wall: sliding and settlement (0.4 m) Gravity-type breakwater: sliding (0.9 m) and pavement settlement (0.9 m)	A
			Hakodate	Steel sheet-pile bulkhead: seaward tilting (0.6 m) and apron settlement (0.3 m) Quay-wall: settlement (0.6 m) and sliding (0.4 m)	A,B
Nemuro-Hanto-Oki, Japan	Jun 17, 1973	7.4	Hanasaki	Gravity-type quay wall: sliding (1.2 m) and settlement (0.3 m) with corresponding apron settlement (1.2 m) Steel sheet-pile bulkhead: sliding (2 m) and anchor failure	A,B
			Kiritappu	Steel sheet-pile bulkhead: relatively minor damage Gravity-type quay walls: relatively minor damage	
Miyagi-Ken-Oki, Japan	Jun 12, 1978	7.4	Shiogama	Concrete gravity-type quay wall: outward tilting (0.6 m) and apron pavement settlement (0.4 m)	
			Ishinomaki	Steel sheet-pile bulkheads: outward sliding (up to 1.2 m) and apron settlement (up to 1 m) Concrete block retaining wall: sliding, tilting, and cracking with corresponding pavement settlement (0.2 m) relative to wall	A,B
			Yuriage	Concrete block gravity quay wall and steel sheet-pile bulkhead: large horizontal displacements (up to 1.2 m)	
			Sendai	Steel sheet-pile bulkheads: cracking and settlement of apron and pavements	

Legend

A: Excessive lateral pressure from backfill materials, in the absence of complete liquefaction, and possibly accompanied by reduction in water pressure on outside of wall
B: Liquefaction
C: Localized sliding
D: Massive submarine sliding
E: Vibrations of structure

either because direct structural effects are overshadowed by the effects of porewater pressure buildup in the adjacent soils, or because the seismic design provisions related to structure vibratory effects are adequate or conservative. The more extensive use of dynamic analyses of the type described in Chapter 4 and carried out in Chapter 5 could provide important insights along these lines.

• Insights into the importance of the seismic coefficients used in the design of port and harbor facilities are provided by evidence from Japanese earthquakes. For example, in the earthquakes at Niigata (1964), Tokachi-Oki (1968), and Nemuro-Hanto-Oki (1973), affected port and harbor facilities were all designed using seismic coefficients whose values were about half the values of the peak accelerations actually experienced during the earthquakes. Despite this similarity, these three earthquakes caused widely varying degrees of harbor damage. This damage appeared to be most closely related to the extent of liquefaction of the affected harbor sites, which was greatest during the Niigata earthquake and was least during the Tokachi-Oki event. This suggests that the seismic coefficients used in design of port and harbor facilities are of secondary importance, when compared to the potential for liquefaction of the site soil materials.

• Although the effects of porewater pressure buildup and liquefaction are predominant, there is evidence that the structure configurations, including the anchor system used for retaining wall structures, also plays an important role in the behavior of the port and harbor facilities during earthquakes. This chapter cites several

examples of the strong influence of the anchor system
on the failure or survival of waterfront structures.
Along these lines, the chapter also provides strong
evidence that undesirable configurations of several
structures at the Niigata Port contributed to the
widespread damage that occurred at that port during
the 1964 Niigata earthquake.

CHAPTER 3

CURRENT SEISMIC DESIGN PROCEDURES

3.1 OVERVIEW

In Chapter 2, not only has the significant vulnerability of
port and harbor facilities to earthquake motions been demonstrated
but, where possible, the causes of the significant damage that
has been imparted to such facilities has also been interpreted.
In view of this, it is important to now consider how these various
causes are considered in the design of port and harbor facilities
to resist earthquakes, and to evaluate the adequacy of these
seismic design procedures.

The results of our compilation and evaluation of seismic
design procedures for port and harbor facilities is presented
in this chapter. These results are based on (1) our review and
assessment of available and pertinent documentation from Japan
and the United States;* and (2) interviews and discussions with
port and harbor authority personnel, consulting engineers, and
government agency representatives experienced in port and harbor
design and maintenance (see Acknowledgements). Results of these

---

*The pertinent references from Japan reviewed in this design
procedure assessment included Okabe (1926), Mononobe (1929),
JPHRI (1965 and 1980), Okamoto (1973), Hayashi et al. (1975),
Noda and Uwabe (1976), Kitajima and Uwabe (1979), and Noda
and Hayashi (1980). From the United States, design-related
references that were reviewed included Westergaard (1933), USN
(1968-1971), DANAF (1973), Seed and Whitman (1970), Chakrabarti
et al. (1978), Pyke et al. (1978), Seed (1979a, 1979b), and Pita
et al. (1982) as well as other references cited in the text to
this chapter. In addition, geotechnical and structural design
reports for particular port facilities were furnished by several
of the consulting engineers and port authority representatives
with whom we visited, and provided valuable background for this
seismic design evaluation.

efforts are presented, not as detailed descriptions of seismic design procedures on an individual basis, but rather as a brief description and assessment of overall trends that emerged as our work in this area proceeded.

The remainder of this chapter is divided into two main sections that address geotechnical design considerations and structure-specific seismic design considerations respectively. In this regard, it is noted that seismic design practice in Japan for port and harbor facilities in general does not appear to differ markedly from that in the United States; however the Japanese have developed much more thorough and complete documentation of their seismic design procedures.

3.2   GEOTECHNICAL CONSIDERATIONS

The geotechnical considerations addressed in this seismic design assessment pertain to (1) lateral earth pressures for retaining wall structures; (2) earthquake-induced dynamic water pressures; (3) earthquake effects on bearing capacity; (4) lateral and axial resistance of piles to seismic effects; (5) earthquake-induced slope instability; and (6) liquefaction. The port and harbor facility design practice pertaining to these considerations is summarized briefly in Table 3-1 and more fully in the paragraphs that follow.

3.2.1   LATERAL EARTH PRESSURES FOR RETAINING WALL STRUCTURES

The Mononobe-Okabe equation is the predominant approach in the United States and Japan for calculating earthquake-induced lateral earth pressures which, when superimposed onto lateral pressures from static conditions, form the basis for the design of port and harbor retaining wall structures such as quay walls, sheet-pile bulkheads, etc. (Mononobe, 1929; Okabe, 1926). As discussed by Seed and Whitman (1970), this approach was developed

TABLE 3-1.   GEOTECHNICAL-RELATED SEISMIC DESIGN PRACTICE
FOR PORT AND HARBOR FACILITIES (As of mid-1982)

Item	Predominant Design Practice
Earthquake-Induced Lateral Earth Pressures for Retaining Wall Structures	Mononobe-Okabe method most typically used, occasionally incorporating suggested simplifications by Seed and Whitman (1970).
Earthquake-Induced Dynamic Water Pressures	Usually ignored. Westergaard (1933) procedure occasionally used.
Earthquake Effects on Bearing Capacity	Usually ignored.
Lateral and Axial Resistance of Piles to Seismic Effects	Usually either ignored or considered using pseudostatic procedures.
Earthquake-Induced Slope Instability	Pseudostatic methods most typically used.
Liquefaction	Standard procedures described by Seed (1979a) most typically used, incorporating empirical and/or 1-D total stress dynamic analysis techniques. Occasional use of 1-D effective stress methods.

for dry cohesionless soils and was based on the assumptions that (1) the wall moves sufficiently to mobilize the minimum active pressure; (2) when the minimum active pressure acts against the wall, a wedged-shaped soil mass is at the point of incipient failure with the maximum shearing resistance mobilized all along the plane sliding surface; and (3) the soil wedge acts as a rigid body with earthquake accelerations acting uniformly throughout the wedge. Based on these assumptions, Mononobe and Okabe used the Coulomb sliding wedge method to obtain an expression for the total pseudostatic horizonal earthquake force as a function of the horizontal and vertical ground accelerations and various parameters related to the soil, wall, and backfill (Fig. 3-1). Seed and Whitman (1970) evaluated the sensitivity of the Mononobe-Okabe equation to these parameters and, from this, developed a simplified form of this equation.

Despite its almost universal use in the design of port and harbor facilities, the Mononobe-Okabe equation has the following important limitations when used for this purpose.

- Because the Mononobe-Okabe equation has been developed for dry, cohesionless soils, it does not account for the potentially important increases in lateral pressure that may occur because of porewater pressure buildup in loose, saturated cohesionless soils below the water table, nor does it allow for the presence of cohesive soil materials.

- The flexibility of the retaining wall, which may be important for sheet-pile bulkheads and even for certain quay wall configurations, is neglected in the Mononobe-Okabe approach.

- The dynamic phenomena that occur during the ground shaking cannot be represented by a pseudostatic approach.

3-4
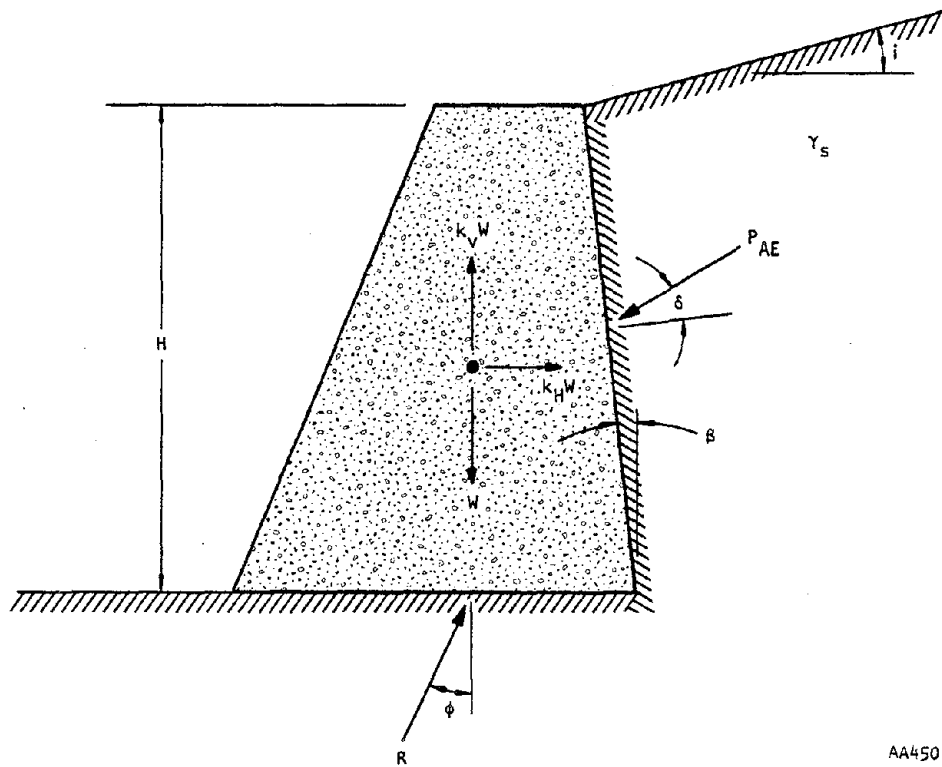
Variables:

P_{AE} = Active pressure during earthquake

γ_s = Unit weight of soil

H = Height of wall

ϕ = Angle of friction of soil

δ = Angle of wall friction

i = Slope of ground surface behind wall

β = Slope of back of wall

W = Weight of wall

k_H = Horizontal acceleration of wall, g's

k_v = Vertical acceleration of wall, g's

FIGURE 3-1.   FORCES AND VARIABLES CONSIDERED IN MONONOBE-
OKABE EQUATION FOR EARTHQUAKE-INDUCED
LATERAL EARTH PRESSURES (Mononobe, 1929;
Okabe, 1926)

- The pressure distribution from the Mononobe-Okabe
  equation (assumed to be linearly increasing with depth)
  has been shown from comparisons with small-scale test
  results to be incorrect, even for soils above the water
  table (Seed and Whitman, 1970).

In some instances, the above limitations have been recognized
and alternative procedures for computing earthquake-induced lateral
pressures have been developed. For example, effects of dynamic
porewater pressures have, in some design procedures, been repre-
sented as equivalent pseudostatic water pressures applied by
fully saturated or partially saturated backfill (Matsuo and
O'Hara, 1965; Seed and Whitman, 1970). In other procedures, an
alternative harmonic analysis procedure by Scott (1973b) has been
used, that represents the soil as a one-dimensional shear beam
attached to a rigid or flexible wall through horizontal springs
that represent soil/wall interaction. Techniques are also avail-
able to estimate earthquake-induced lateral pressures for cohesive
soil conditions, assuming dynamic increases in lateral pressures
to be proportional to free-field deformation, with an upper limit
equal to the passive pressure (Taylor and Indrawan, 1981). However,
the Mononobe-Okabe equation, despite its limitations, is the pre-
dominant technique in use today for computation of earthquake-
induced lateral pressures for port and harbor retaining wall
structures.

3.2.2 DYNAMIC WATER PRESSURE

The pressure exerted by the water on the seaward side of
port and harbor retaining-wall structures could affect the
behavior of such structures during earthquakes. For example,
there is evidence that a reduction in these water pressures
during earthquakes has contributed to the resulting failure of
many quay wall structures (Seed and Whitman, 1970; Okamoto, 1973).

Despite the possible importance of these dynamic water pressures, they are usually ignored in current design practice for port and harbor facilities (Table 3-1). Where such pressures are considered, they are most typically represented using an expression developed for dam/reservoir systems by Westergaard (1933). The pressures derived in this classic work are based on the assumptions that (1) the dam is rigid, infinitely long, and has a vertical upstream face; (2) the reservoir extends to infinity in the upstream direction; and (3) effects of surface waves are ignored. Solutions were developed by Westergaard for hydrodynamic water pressures, including effects of the compressibility of the water, for the case of harmonic ground motions in a horizontal direction perpendicular to the dam axis (Fig. 3-2). Westergaard's results show the hydrodynamic pressures to be of opposite phase to the ground acceleration, and therefore are equivalent to inertia forces from an additional mass moving with the dam. The magnitude of this mass is dependent on the frequency of the harmonic ground motions.

Various investigators have examined the applicability of Westergaard's approach, and a comprehensive summary of these examinations is provided by Chopra (1967). Basically, they show that (1) the use of a single effective mass (shown by Westergaard to be frequency-dependent) may not fully describe the hydrodynamic response to earthquake excitations, which are typically wide-band processes; and (2) Westergaard's solution is valid only for excitation frequencies less than the fundamental frequency of the reservoir.

In summary, hydrodynamic water pressures are seldom considered in the design of retaining-wall structures at ports and harbors. Furthermore, in those instances when such pressures are considered, they are most typically represented using the effective mass
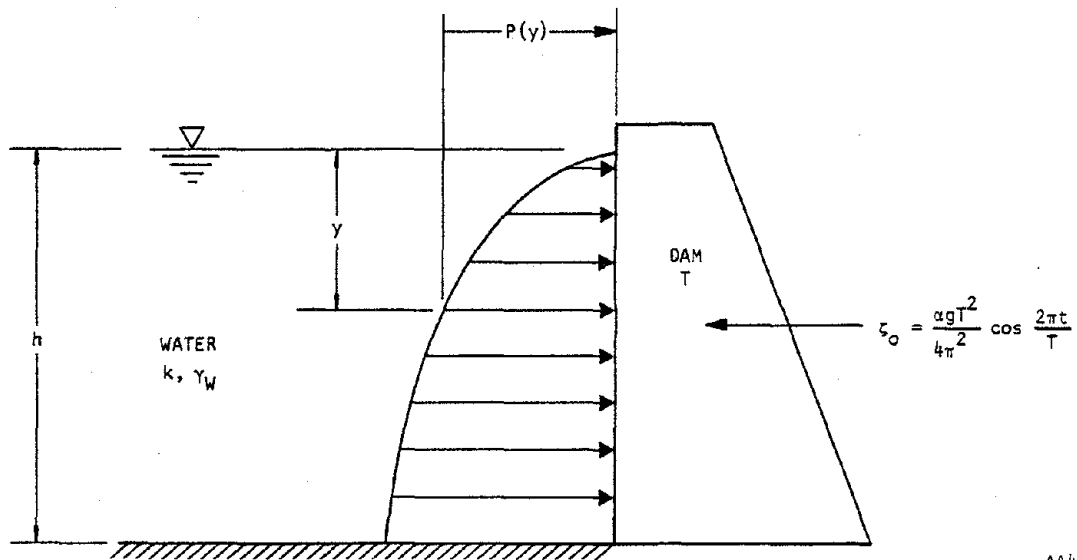
AA451

Variables:

P(y) = Hydrodynamic water pressure at depth y

h = Depth of reservoir

k = Bulk modulus of water

γ_W = Unit weight of water

α = Amplitude of harmonic acceleration of dam, g's

T = Natural period of dam

$\zeta_o(t)$ = Motion of dam

FIGURE 3-2. FORCES AND VARIABLES CONSIDERED IN WESTERGAARD (1933) APPROACH FOR COMPUTING EARTHQUAKE-INDUCED HYDRODYNAMIC PRESSURES

concepts of Westergaard, which have certain limitations that the designer should keep in mind. It is noted that, in this regard, significant progress has been made in the representation of hydrodynamic pressures in dynamic analysis techniques; this progress has been made primarily through linear finite element substructuring approaches, although some nonlinear techniques have also been developed (see Chapt. 4).

3.2.3 EARTHQUAKE EFFECTS ON BEARING CAPACITY

During an earthquake, the bearing capacity of the soil under-lying gravity-type structures at ports and harbors may be affected in three ways. First, because of the horizontal component of the applied seismic excitations, the structure may be subjected to tipping that could increase the pressures underlying its toe, causing them to exceed the ultimate bearing capacity of the soil medium. Second, porewater pressure buildup in loose, saturated, cohesionless soil materials could reduce their bearing capacity, even if no tipping of the structure takes place. Finally, for unsaturated soils (or saturated clays) not subject to porewater pressure buildup, strain-rate effects could result in a slight increase in bearing capacity.

In general, such earthquake-related effects on the bearing capacity of the soil medium are seldom considered directly (Table 3-1), although effects of porewater pressure buildup are considered indirectly through liquefaction assessments (see Sec. 3.2.6). Where such effects are considered, they are generally based on engineering judgment in which a slight increase or decrease relative to static conditions is considered, depending on the particular soil conditions at the site.

3.2.4 LATERAL RESISTANCE OF PILES TO SEISMIC EFFECTS

Piles are widely used foundation support elements at port and harbor facilities, not only for piers but for quay walls and bulkheads as well. In a seismic design sense, they function to mobilize the deeper soil deposits in resisting the effects of the structural vibrations (in the case of piers) or of lateral displacements (in the case of quay walls or sheet-pile bulkheads), which may be particularly significant in the event of porewater pressure buildup. The ability of piles to carry out this function is dependent on (1) suitably designing the cross section, end conditions, embedment depth, orientation, and spacing of the piles so they can transmit the seismic loads and mobilize the underlying soils; and (2) considering the possible effects of porewater pressure buildup and liquefaction, which could reduce the effective embedment depth of the piles and increase the applied lateral loads. In current design practice for port and harbor facilities, the effects of earthquakes on the design of pile supports are either neglected or, if considered, are represented as pseudostatic loads in conjunction with conventional static pile design procedures. Although techniques are available to represent porewater pressure and dynamic effects in the seismic design of piles (e.g., Finn and Martin, 1980), these techniques are seldom applied in current practice.

Both batter piles and vertical piles are used as foundation support systems at port and harbor facilities. Batter piles have been shown to be desirable as support at anchors for sheet-pile bulkheads, as a means for resisting lateral displacements of the sheet pile due to porewater pressure buildup in the soil medium (See Chapts. 2 and 5). Experience from past earthquakes has shown them to be less desirable for use at piers where, because of their significant lateral stiffness, they transmit large lateral seismic forces which have resulted in severe damage to pile caps

and decking (Arno and McKinney, 1973; Margason, 1975). Vertical piles, which are more flexible laterally, are therefore more suit-able as pier foundation supports and are probably somewhat less desirable as anchors for sheet-pile bulkheads, because of their reduced resistance to lateral forces applied to the bulkhead.

3.2.5 EARTHQUAKE-INDUCED SLOPE INSTABILITY

The evaluation of slope stability can be important in the design of port and harbor facilities, particularly in the case of gravity-type quay walls or trestle-type piers with small retaining walls (JPHRI, 1980). In current seismic design practice for port and harbor facilities, pseudostatic methods are most widely used to evaluate the safety of the facility during earthquakes (Table 3-1). These methods represent the seismic effects on a potential slide mass in terms of an equivalent static horizontal force acting at the centroid of the mass; this force is computed as the product of a seismic coefficient (i.e., the horizontal acceleration of the slide mass in g's) and the weight of the slide mass (Fig. 3-3). The factor of safety against sliding of the mass is then computed by summing moments from its seismic force, its weight, and its shear and/or frictional resistance along the assumed slip surface (Terzaghi, 1950; Seed, 1979b). In most design applications, a seismic coefficient ranging from 0.1 to 0.15 is used.

The pseudostatic techniques, as summarized above, have the significant limitation of not accounting for the time-varying effects of the intensity and direction of the response of this soil mass. Therefore, as described by Seed (1979b), such tech-niques should be used only under the following very limited conditions which have been identified from evaluations of field
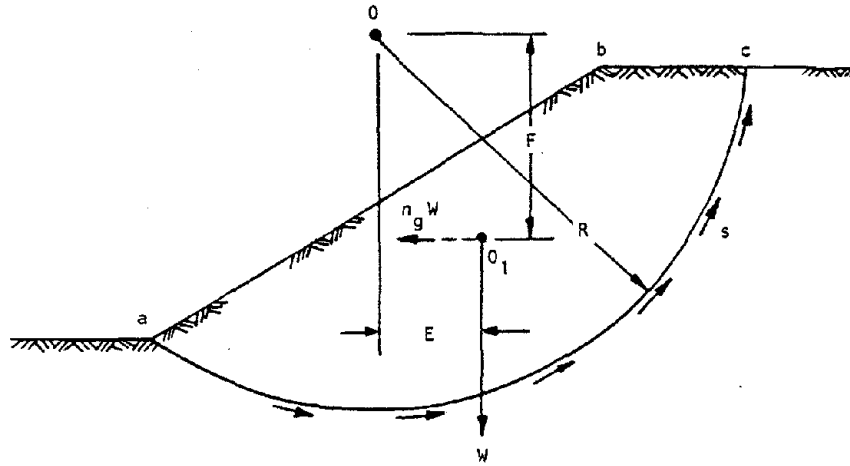
Variables:

n_g = Peak horizontal acceleration, g's

W = Weight of soil mass defined by slip circle

R = Radius of slip circle

s = Shear resistance along slip circle

R,F = Moment arms

FIGURE 3-3.   PSEUDOSTATIC METHOD FOR EVALUATING EARTHQUAKE-INDUCED SLOPE INSTABILITIES (Seed, 1979b)

performance of embankments and from comparisons with results from separate analyses by Makdisi and Seed (1978).

- The criteria shown in Table 3-2 are followed

- The soils do not lose more than 15% of their initial strength due to the earthquake shaking and the associated displacements, nor do they build up large porewater pressures.

On the basis of these conditions, the engineer should assess the applicability of pseudostatic methods at a particular site, in accordance with the following considerations (Seed, 1979b):

- Based on prior field and laboratory experience, the second condition given above limits the use of the pseudostatic approach to certain types of soil (e.g., many clayey soils, dry sands, some dense saturated sands) for which large strength losses due to seismic effects are generally not a problem.

- In case of doubt, careful laboratory studies will invariably provide a basis for an appropriate engineering decision concerning the applicability of the pseudostatic approach.

- Some soils, which might be vulnerable to the development of large porewater pressures and some strength loss under conditions of strong shaking, may show little evidence of these effects under less intense shaking; i.e., the applicability of the pseudostatic approach must be evaluated by considering the design levels of shaking as well as the soil type.

TABLE 3-2. SEED (1979b) CRITERIA FOR APPLICABILITY
OF PSEUDO-STATIC APPROACH FOR EVALUATING
EARTHQUAKE-INDUCED SLOPE INSTABILITY*

Earthquake Magnitude	Design Criteria
6.5	FS = 1.15 for seismic coefficient of 0.1
8.5	FS = 1.15 for seismic coefficient of 0.15

*Applicable only for slopes comprised of soils which do not
build up large porewater pressure due to earthquake shaking
nor show more than 15% strength loss (usually cohesive
soils such as clays, silty clays, sandy clays, or very
dense cohesionless soils) based on acceptable deformations
due to earthquake shaking and crest acceleration less than
0.75g.

The above discussion indicates that, at port and harbor sites dominated by loose saturated cohesionless soils where earthquake-induced porewater pressure buildup and corresponding strength losses could occur, the applicability of pseudostatic approaches is questionable, particularly if the site may be subjected to strong ground shaking or if large embankment heights are involved. In view of this, the following alternative and more reliable approaches could conceivably be used at port and harbor facility sites, but, in fact, are seldom applied in current design practice for such facilities:

- Newmark (1965) Approach. In this approach, slope failure is presumed to be initiated and movements begin to occur if the inertia forces on a potential slide mass are sufficiently large to overcome the yield resistance of the soil (Fig. 3-4a); also, movements would stop when the inertia forces were reversed. Thus, by computing an acceleration at which inertia forces are sufficiently high to initiate yielding, and integrating the effective acceleration in excess of this yield acceleration as a function of time, velocities and displacements of the slide mass can be determined (Fig. 3-4b). This approach is most useful when yield accelerations can be reliably determined, which includes situations where porewater pressures do not change significantly during the ground shaking (Seed, 1979b).

- Dynamic Analysis. This approach (Table 3-3a) involves the use of finite element analyses of the embankment stresses induced by the seismic excitations and by static conditions. The states of stress obtained from these analyses are applied to embankment soil samples
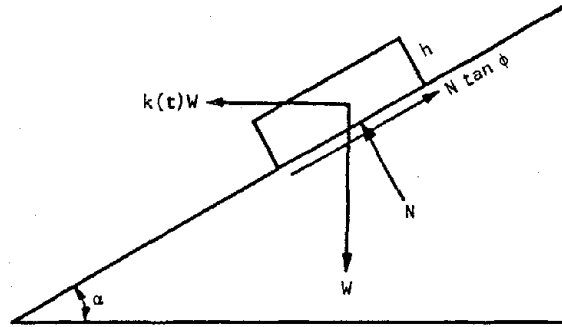
(a) Forces on sliding block
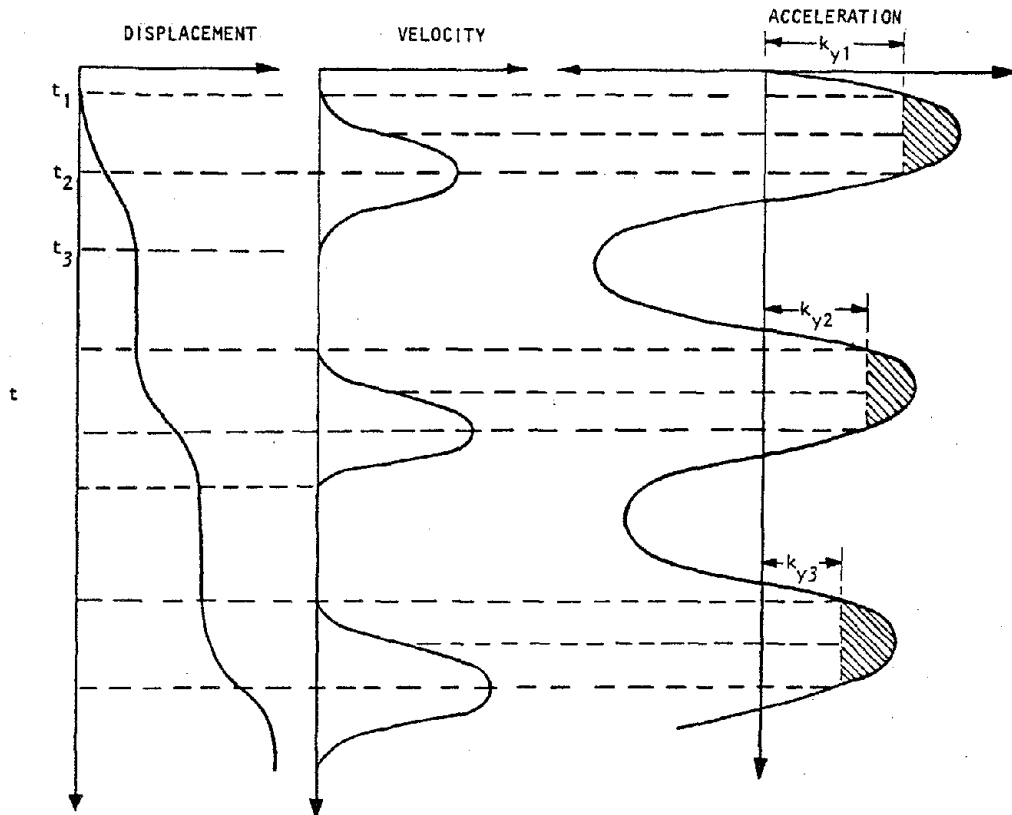
(b) Integration of effective acceleration
    time history

FIGURE 3-4. NEWMARK (1965) APPROACH FOR EVALUATING
EARTHQUAKE-INDUCED SLOPE INSTABILITIES

TABLE 3-3. DYNAMIC ANALYSIS PROCEDURE FOR EVALUATING EARTHQUAKE-INDUCED SLOPE INSTABILITY

Step Number	Description
1	Determine the cross section of the dam to be used for analysis.
2	Determine, with the cooperation of geologists and seismologists, the maximum time history of base excitation to which the dam and its foundation might be subjected.
3	Determine, as accurately as possible, the stresses existing in the embankment before the earthquake; this is probably done most effectively at the present time using finite element analysis procedures.
4	Determine the dynamic properties of the soils comprising the dam, such as shear modulus, damping characteristics, bulk modulus, or Poisson's ratio, which determine its response to dynamic excitation. Since the material characteristics are nonlinear, it is also necessary to determine how the properties vary with strain.
5	Compute, using an appropriate dynamic finite element analysis procedure, the stresses induced in the embankment by the selected base excitation.
6	Subject representative samples of the embankment materials to the combined effects of the initial static stresses and the superimposed dynamic stresses and determine their effects in terms of the generation of porewater pressures and the development of strains. Perform a sufficient number of these tests to permit similar evaluations to be made, by interpolation, for all elements comprising the embankment.
7	From the knowledge of the pore pressures generated by the earthquake, the soil deformation characteristics and the strength characteristics, evaluate the factor of safety against failure of the embankment either during or following the earthquake.
8	If the embankment is found to be safe against failure, use the strains induced by the combined effects of static dynamic loads to assess the overall deformations of the embankment.
9	Be sure to incorporate the requisite amount of judgment in each of Steps 1 to 8 as well as in the final assessment of probable performance, being guided by a thorough knowledge of typical soil characteristics, the essential details of finite element analysis procedures, and a detailed knowledge of the past performance of embankments in other earthquakes.

(a)   Step-by-step procedure (Seed et al., 1975a)

Dam	Date of Earthquake	Maximum Acceleration	Predicted Performance	Actual Performance	Reference
Sheffield	1925	≅0.2 g	Failure by sliding	Failure by sliding	Seed et al., 1969
Lower San Fernando	1971	≅0.5 g	Major upstream slide	Major upstream slide	Seed et al., 1973
Upper San Fernando	1971	≅0.5 g	No failure-- large downstream movement	No failure-- large downstream movement	Serff et al., 1976
Dry Canyon	1952	≅0.1 g	Small deformation--some cracking	Small deformation--some cracking	Lee and Walters, 1972
Lower Franklin	1971	≅0.2 g	No damage	No damage	Seed et al., 1973
Silver Lake	1972	≅0.2 g	No damage	No damage	Seed et al., 1973
Fairmont	1971	≅0.2 g	No damage	No damage	Seed et al., 1973
Chabot	1906	≅0.4 g	No damage	No damage	Makdisi et al., 1978

(b)   Comparisons with prior field observations of earth dam behavior (Seed, 1979b)

in laboratory tests to measure the development of pore-
water pressures and strains in the embankment (Seed
et al., 1975a). The most recent techniques of this
type may involve studies of simultaneous porewater
pressure buildup and dissipation during the ground
shaking, as discussed in Chapter 4. This is the most
complete and reliable approach now available, and has
produced excellent correlation with observed field
behavior during past earthquakes (Table 3-3b).

In summary, pseudostatic techniques are the predominant
approach in the current design practice for assessing potential
earthquake-induced slope instabilities at port and harbor sites.
These techniques, however, have important limitations particularly
where porewater pressure effects may be important. Alternative
and more reliable techniques involving increased degrees of
sophistication in the representation of dynamic phenomena are
available, but are seldom used in port and harbor design
applications.

3.2.6 LIQUEFACTION ASSESSMENTS

It is only in the assessment of the potential for earthquake-
induced liquefaction at port and harbor facilities that dynamic
analysis is now routinely carried out (Table 3-1). However, even
this is a relatively recent development and a potential major
problem exists at many ports and harbors because possible lique-
faction has been essentially ignored in past seismic design
practice. Two different types of liquefaction assessment proce-
dures in common use--one involving site response analyses and the
other using simplified procedures--are summarized in this section.

3.2.6.1 Procedures Incorporating Site Response Analyses

The basic liquefaction assessment procedures that incorporate
site response analyses are described by Seed (1979a). The steps
in this procedure are summarized in Table 3-4 and warrant the
following comments:

- As shown in Step 2 of Table 3-4, dynamic site-response
  analyses are most typically one dimensional in current
  practice, and therefore do not consider effects of soil/
  structure interaction, irregular topography, etc. which
  are often important for port and harbor facilities.
  In Chapter 4, dynamic analysis techniques are described
  that can represent these effects and can be readily
  incorporated into the overall liquefaction assessment
  procedure shown in Table 3-4.

- The need for Step 5 results from the fact that cyclic
  triaxial tests are believed to be a rather imperfect
  representation of the actual loading conditions to
  which elements of soil in the field are subjected
  during earthquakes. Cyclic simple shear tests provide
  a better, although still imperfect, representation of
  field loading conditions, but, at the time of the
  original studies that led to the procedure given in
  Table 3-4, cyclic simple shear tests were much more
  difficult to conduct. Therefore, routine testing has
  primarily involved cyclic triaxial tests, with the
  results of these tests corrected to field conditions
  on the basis of research studies using cyclic simple
  shear tests (see Seed and Peacock, 1971). The factor
  C_r, which is used to reduce the stresses causing
  liquefaction in cyclic triaxial tests to those causing
  liquefaction in cyclic simple shear tests (or, more
  strictly, to those stresses estimated to cause lique-
  faction in the field) was initially believed to be a

TABLE 3-4. LIQUEFACTION EVALUATION PROCEDURE INCORPORATING
SITE RESPONSE ANALYSES (Pyke, 1982)

Step	Original Procedure	Possible Modifications (1982)
1	Select one or more appropriate acceleration histories.	
2	Conduct one-dimensional response analysis using "equivalent linear" procedures.	Use nonlinear response analysis and/or account for drainage. Incorporate effects of soil/structure interaction and irregular topography and layering.
3	Compute the equivalent number of uniform cycles in layers of interest.	
4	Conduct cyclic triaxial tests to determine cyclic stresses causing liquefaction.	Always use intact samples: conduct constant-height, cyclic simple shear tests.
5	Correct results of laboratory tests to field conditions using $C_r = 0.6$.	Correct as a function of age, overconsolidation ratio, pre-straining, soil type, and degree of disturbance.
6	Compare stresses computed in Step 3 to those causing liquefaction.	
7	--	If factor of safety exceeds 1, read pore pressure ratio from standard charts as a function of N/N_{ℓ} (see Sec. 4.2.3.2.2).

function of relative density but typically had a value of about 0.6. This factor is commonly called the simple shear correction factor. Further background regarding the use of laboratory test procedures to assess liquefaction potential at port and harbor sites is provided in Chapter 4. In addition, Chapter 4 describes the use of empirical methods, based on field observations of earthquake-induced site behavior, as a supplement to laboratory test procedures or as an alternative if laboratory test data are not available.

- The approach shown in Table 3-4 constitutes a total stress approach in which porewater pressure effects are not included in the dynamic analysis of the earthquake-induced soil stresses. Alternative approaches are (1) effective stress methods in which porewater pressure effects are incorporated into the analysis of the soil stresses; and (2) probabilistic methods in which the effects of uncertainties in defining the seismic input and/or the system material properties are systematically represented. Total stress methods are most widely used in current practice and are the only fully developed procedure now available for incorporating soil/structure interaction and irregular topography in the liquefaction evaluation. Each of these procedures is described and evaluated in Chapter 4.

3.2.6.2 Simplified Procedures

Two different types of simplified procedures for evaluating liquefaction potential were developed by Seed and Idriss (1971) and are widely used in current design practice for port and harbor facility sites. The first type of simplified procedure (Table 3-5)

TABLE 3-5.   SIMPLIFIED LIQUEFACTION EVALUATION
            PROCEDURE (Seed and Idriss, 1971;
            Pyke, 1982)

Step	Original Procedure	Possible Modifications (1982)
1	Fix ground surface peak acceleration.	
2	Compute average cyclic stresses in layers of interest using Equation 3-1.	Use site-specific data on r_d.
3	Determine equivalent number of uniform cycles as function of magnitude.	Use Seed et al. (1975b).
4	Determine stress ratio causing liquefaction in cyclic triaxial tests from standard data.	Use more recent data, including Japanese data.
5	Correct results of laboratory tests to field conditions using $C_r = 0.6$.	Correct as a function of age, overconsolidation ratio, prestraining, soil type, and degree of disturbance or method of sample preparation.
6	Compare stresses computed in Step 2 to those causing liquefaction.	
7	--	If factor of safety exceeds 1, read pore pressure ratio from standard charts as a function of N/N_ℓ (see Sec. 4.2.3.2.2).

follows essentially the same steps as the procedure described in Section 3.2.6.1, but eliminates the need to conduct site response analyses and cyclic triaxial tests. In this, Seed and Idriss suggested that, as an alternative to site-response analyses, the average shear stress at any depth of interest, τ_{av}, could be computed from the surface peak acceleration in g's, a_{max}, by means of the following expression:

$$\tau_{av} = 0.65 \, a_{max} \, \sigma_v \, r_d \tag{3-1}$$

where σ_v is the total overburden stress at the depth of interest and r_d is a depth-reduction factor provided by Seed and Idriss. They also provided typical equivalent numbers of cycles as a function of earthquake magnitude that could be used in conjunction with the average cyclic shear stress to describe the loading due to earthquake shaking. The resistance to liquefaction was estimated from typical cyclic triaxial test data as a function of the median particle size of the soil (D_{50}) and relative density (D_r) and application of the simple shear correction factor.

Seed and Idriss showed that this simplified procedure provided a reasonable fit to observations of both the occurrence and the nonoccurrence of liquefaction during previous earthquakes; then, using the Gibbs and Holtz (1957) relationship between relative density and Standard Penetration Test (SPT) blowcounts, they constructed a chart showing the potential for liquefaction as a function of blowcount for given values of the surface peak acceleration. Direct use of this chart therefore constituted a simplified procedure of the second kind and, moreover, represented the first state of development of an empirical procedure based solely on field tests and field observations of the occurrence of liquefaction in previous earthquakes (Pyke, 1982). Because the form of the chart for evaluating liquefaction potential directly

in terms of SPT blowcount has since changed, the steps involved
in using it are not described here, but instead are given in
Chapter 4 in terms of the most current procedures of this type,
as described by Seed and Idriss (1981).

3.3   STRUCTURE SPECIFIC CONSIDERATIONS

In this section, seismic design considerations are summarized
for various structures that exist at ports and harbors. The
particular structure types discussed in this context are gravity-
type quay walls, sheet-pile bulkheads, and piers.

3.3.1   GRAVITY-TYPE QUAY WALLS

3.3.1.1   Types

There are three classes of gravity-type quay walls, namely
(1) cast-in-place block-type; (2) precast block-type; and
(3) caisson-type. The cast-in-place block-type quay walls are
placed where soil conditions are firm and where construction under
reasonably dry conditions can be carried out. Precast block-type
quay walls can be placed on firm or soft soil conditions; they
involve relatively simple construction techniques that are not
hampered by the presence of shallow seawater or ground water.
Caisson-type quay walls are typically constructed where water
is deep.

In general, block-type quay walls are more susceptible
to seismic effects than are caisson-type quay walls; they are
particularly susceptible to earthquake-induced sliding between
layers of blocks, which is seldom addressed in current design
practice. Of the two classes of block-type quay walls, the
cast-in-place block type walls have generally sustained less
damage during prior earthquakes, because of the construction-
related requirement that they be placed on firm soil.

3.3.1.2 Seismic Design Considerations

Seismic forces generally considered in the design of gravity-type quay walls include lateral earth pressure and the inertia force of the wall. Dynamic water pressures should also be considered although, in fact, they are typically ignored in current practice (Sec. 3.2.2).

When subjected to these seismic forces, the quay walls are designed to avoid overturning and excessive tilting and sliding, although some horizontal wall movement is tolerated. In this, possible earthquake-induced sliding along the quay wall base, as well as sliding due to slope instabilities (Sec. 3.2.5), are design considerations. Earthquake effects on the bearing capacity of the soils underlying the quay walls are seldom considered in current practice (Sec. 3.2.3).

The effects of lateral earth pressure, while important for each of the classes of gravity-type quay walls, are particularly important for caisson-type quay walls because of their height. In Japan, attempts are sometimes made to reduce these lateral pressures by cement grouting of the backfill. Also, the stability of caisson-type quay walls under these lateral pressures can be increased by such measures as widening the base of the wall, using pile supports, partially embedding the wall in the under- lying soil medium, and replacing underlying weak soil materials with sandy soils that have an increased bearing capacity.

3.3.2 SHEET-PILE BULKHEADS

Important seismic loads for the design of sheet-pile bulk- heads include lateral pressures applied through the backfill and hydrodynamic pressures applied by the ocean water. As discussed in Section 3.2, these lateral pressures are most typically repre- sented using the Mononobe-Okabe equation, and hydrodynamic water pressures are seldom represented.

The design of the embedment depth and cross section of the sheet pile is generally carried out using standard static design procedures directed toward insuring an adequate factor of safety against toe failure and insuring an adequate bending resistance of the sheet pile under the applied seismic loads. Static design procedures are also used to design the tie rod based on its tensile resistance to the seismic loads. Porewater pressure effects are seldom considered in these design applications.

Perhaps the most critical element of the sheet-pile bulkhead that relates to seismic effects is the anchor, which may be comprised either of a wall or of a sheet pile. Experience from past earthquakes shows that the principle earthquake-induced failure mode of sheet-pile bulkheads has been insufficient anchor resistance, due primarily to installation of the anchor at shallow depths where the backfill is most susceptible to a loss of strength due to porewater pressure buildup and liquefaction. Therefore, the design of anchor systems to resist these seismic effects is particularly important, and may be enhanced through the use of deeply embedded piles and/or sheet piles. Unfortunately, the designs of the anchors to resist the seismic loads is typically based on static earth pressure theories in which possible porewater pressure effects are neglected.

Another anchor failure mode shown from past earthquakes to be important is a loss of anchor resistance due to insufficient distance between the anchor and the bulkhead wall. This type of failure occurs when all or part of the dynamic passive pressure zone of the anchor falls within the dynamic active pressure zone for the wall, resulting in a loss or reduction in the passive pressure resistance of the anchor. Therefore, when designing sheet-pile bulkheads, care should be taken to provide sufficient distance between the anchor and the wall, with due regard to

3-26

possible effects of porewater pressure buildup and other earthquake-related dynamic phenomenae on the extent of these active and passive pressure zones.

3.3.3 PIERS

When compared to gravity-type quay walls and sheet-pile bulkheads, piers have suffered much less extensive damage during prior earthquakes. This is because piers, which are aboveground and are constructed of piles with platform decks for docking purposes, are relatively lightweight and are not subjected to lateral soil pressures of the type applied to quay walls and bulkheads. The seismic design of pier structures is typically based on pseudostatic lateral forces, computed in a manner analogous to that for conventional buildings (e.g., UBC, 1979).

The simplest type of pier is the trestle-type, which is pile supported and sometimes built with small retaining walls at sloping sites having soils unfavorable for the construction of gravity-type quay walls or bulkheads. Past design practice for such piers has seen the wide use of batter piles, in addition to vertical piles, presumably to provide a greater stiffness in resisting the lateral loads that might be encountered during the structure life. However, experience from prior earthquakes has shown that the configuration and large lateral stiffness of batter piles has caused severe damage to pile caps and decking of pier structures (Arno and McKinney, 1973; Margason, 1975). For this reason, vertical piles, which have a greater lateral flexibility, are now preferred over batter piles in current seismic design practice for pier structures. Some design considerations for vertical piles as well as batter piles are summarized in Section 3.2.4.

3.4 SUMMARY OF RESULTS

This chapter shows that seismic effects are often not nearly as important a design consideration for port and harbor facilities as would be desirable, in view of the extensive damage to such facilities that has occurred during prior earthquakes. The seismic design provisions that do exist typically address some of the potential earthquake-induced phenomena in a simplified pseudo-static manner and ignore many of the others. Dynamic analysis is now routinely used only for liquefaction assessment. The possible role of dynamic analyses as a means for substantially improving the reliability of port and harbor facility seismic design provisions is examined in Chapter 4 and illustrated in Chapter 5.

CHAPTER 4

DYNAMIC ANALYSIS PROCEDURES

4.1 BACKGROUND DISCUSSION

4.1.1 ROLE OF DYNAMIC ANALYSIS

The seismic design of many major structures (e.g., earth dams, bridges, nuclear power plants, etc.) has included the use of modern dynamic analysis techniques as an integral part of the design process. For such structures, dynamic analysis has represented the principal vehicle for assessing the integrity of the structures under the prescribed seismic shaking, as well as for evaluating the response and stability of the surrounding soil medium. It would seem appropriate that dynamic analysis procedures should fulfill a similar function for port and harbor facilities, particularly in view of their extreme susceptibility to earthquake-induced damage (Chapt. 2) and the limited seismic provisions in current design practice for such facilities (Chapt. 3).

The implementation of dynamic analysis involves five main steps, all of which require the use of sound judgment during their execution. In this, it is particularly important to check that the results obtained and conclusions drawn from each step are consistent with engineering experience and practice. The steps for analysis of ports and harbors are:

1. The measurement of reliable dynamic properties of the surrounding soil materials in the laboratory, including their strain-dependent stiffness and damping characteristics and the cyclic stress states that lead to significant porewater pressure buildup under simulated in-situ conditions.

2.   The selection of an analytical procedure that is con-
     sistent with the ability to provide reliable input
     data and to interpret analytical results.

3.   The development of an appropriate model of the specific
     soil/structure system that well represents its response
     characteristics of principal importance for design.

4.   The analysis of the dynamic response of the soil and
     structure and the potential for porewater pressure
     buildup in the soil medium.

5.   The utilization of the dynamic analysis results in the
     design process, with due regard for the approximations
     inherent in the analytical procedure and the uncertain-
     ties in the description of the seismic input and the
     soil/structure system.

Keeping this overall process in mind, this chapter addresses one
aspect of the process--the analytical procedures appropriate for
application to port and harbor facilities.

4.1.2 ANALYSIS PROCEDURE REQUIREMENTS

     As has been shown in Chapter 2, the behavior of port and
harbor facilities is significantly affected by the surrounding
soil medium, and a major portion of the damage induced in such
facilities can be tied to porewater pressure buildup and the
resulting large scale liquefaction and sliding that has occurred
in the loose-to-medium-dense saturated soil deposits that often
prevail at port and harbor sites. Therefore, a meaningful dynamic
analysis procedure must account for these soils effects and, in
view of this, should satisfy the following requirements:

1.   Through a soil/structure interaction analysis that
     accounts for the geometry and material properties of

facilities. To do this, the remainder of the chapter is divided
into three main sections that describe three main types of dynamic
analysis techniques. The first of these sections addresses deter-
ministic total stress methods. Such methods, as applied in
accordance with Requirements 1 and 2, first compute the soil/
structure system response neglecting porewater pressure effects;
then, the resulting soil shear stresses are used as input to a
separate liquefaction analysis of the site. Therefore, the
soil/structure system response analysis and liquefaction analysis
necessary to satisfy Requirements 1 and 2 are not fully coupled
when used in the context of a total stress method. Nevertheless,
deterministic total stress methods presently represent the most
readily adaptable approach for analyzing port and harbor facili-
ties at this time and are therefore emphasized in this chapter.

The last two sections of the chapter address deterministic
effective stress methods and probabilistic methods--which are
both still under development and are therefore representative of
possible future directions for dynamic analysis of port and harbor
facilities. Deterministic effective stress methods that satisfy
Requirements 1 and 2 would compute the soil/structure system
response including porewater pressure effects; i.e., unlike total
stress methods, the soil/structure system response analysis
(Requirement 1) and the liquefaction analysis (Requirement 2)
would be fully coupled in such effective stress methods. However,
effective stress methods incorporating the two-dimensional or
three-dimensional procedures necessary to carry out such coupled
analyses are still in an initial stage of evolution; i.e., nearly
all of the current effective stress methods are based on free-
field site response analyses using one-dimensional procedures.

Probabilistic methods, which are the last of the dynamic
analysis procedure addressed in this chapter, offer the signifi-
cant benefits of systematically representing the uncertainties

4-4

that exist in defining seismic input motions and material proper-
ties. Although certain elements of such methods can be applied
at this time, further development of probabilistic approaches
is required before they can be used on a routine basis.

4.2   DETERMINISTIC TOTAL STRESS METHODS

In the context of Requirements 1 and 2 for the seismic
analysis of port and harbor facilities, total stress methods
can be considered as being comprised of the following three
steps: (1) use of a dynamic analysis technique to compute the
soil/structure system response, without considering the effects
of porewater pressure buildup and dissipation as the earthquake
progresses; (2) conversion of the irregular soil stress time
histories computed in Step 1 to equivalent cyclic stresses; and
(3) comparison of these earthquake-induced cyclic shear stresses
to critical shear stresses for the various soil layers, in order
to assess the potential for liquefaction at the site. The above
definition of total stress methods is identical to that used in
conventional dynamic liquefaction analyses of soil deposits
(Sec. 3.2.6) except that, in Step 1, the coupled response of
the soil/structure system (including states of stress in the
structure as well as the surrounding soil) is now computed,
instead of the free-field response of the soil medium. State-
of-the-art techniques for carrying out each of the above steps
are summarized and evaluated in the subsections that follow.

4.2.1   STEP 1:   SOIL/STRUCTURE SYSTEM RESPONSE ANALYSIS

In this subsection, the soil/structure interaction analysis
techniques assessed for use in analyzing port and harbor facili-
ties are grouped according to the way that the stress/strain
characteristics of the soil deposits are represented. Accordingly,

three groups of techniques are presented--corresponding to linear, equivalent linear, and fully nonlinear soil material models. The basic computational techniques involved in equivalent linear and nonlinear analyses are applicable to effective stress as well as total stress analyses, although effective stress analyses also require provisions for the development and dissipation of excess porewater pressures. These additional provisions are discussed in Section 4.3. Linear analysis techniques are not considered applicable to port and harbor facility sites because of their inability to represent effects of the strain-dependence of the soil material properties--which are particularly important at port and harbor sites. Therefore, these methods are summarized herein only for purposes of completeness.

4.2.1.1 Linear Methods

Linear soil/structure interaction analysis techniques, as the name suggests, incorporate a linear elastic model of the soil and structure. There are two types of such techniques now available. The first type--termed direct methods--is the most widely used in current practice, and is characterized by its determination of the dynamic response of the soil and structure simultaneously (e.g., Bathe et al., 1974; SDC, 1979; McAuto, 1980). In this, both the soil and structure are most typically represented by a finite element model (Fig. 4-1a), although other modeling procedures (e.g., finite difference) can be used. Seismic input motions are applied to such models along a subsurface boundary of the soil medium. Special energy-absorbing procedures should be employed at the artificial subsurface soil boundaries to minimize unwanted reflections and simulate radiation damping, although no such procedures are yet available that perform this function in a fully satisfactory way in all cases. It is noted that direct methods, as defined in this way, are not limited to linear techniques; in fact, all equivalent linear and nonlinear techniques are also classed as direct methods.
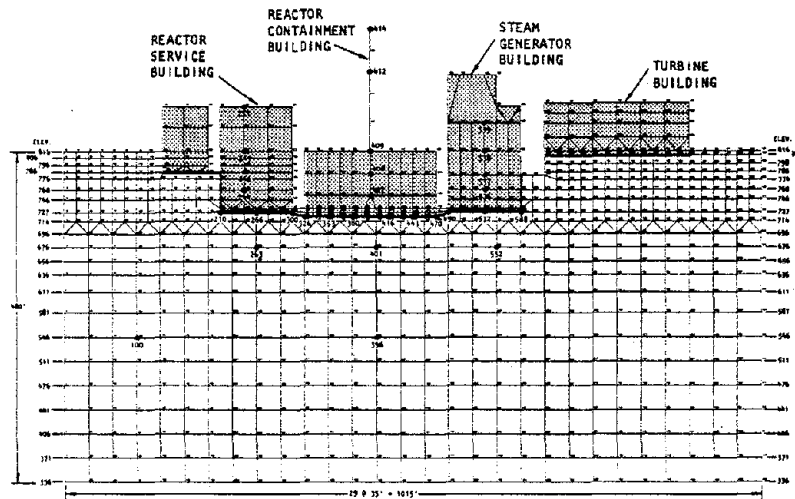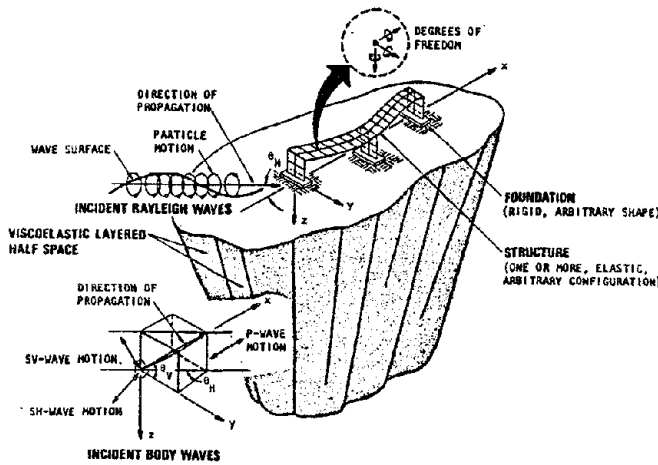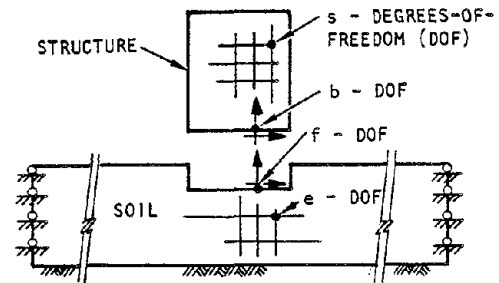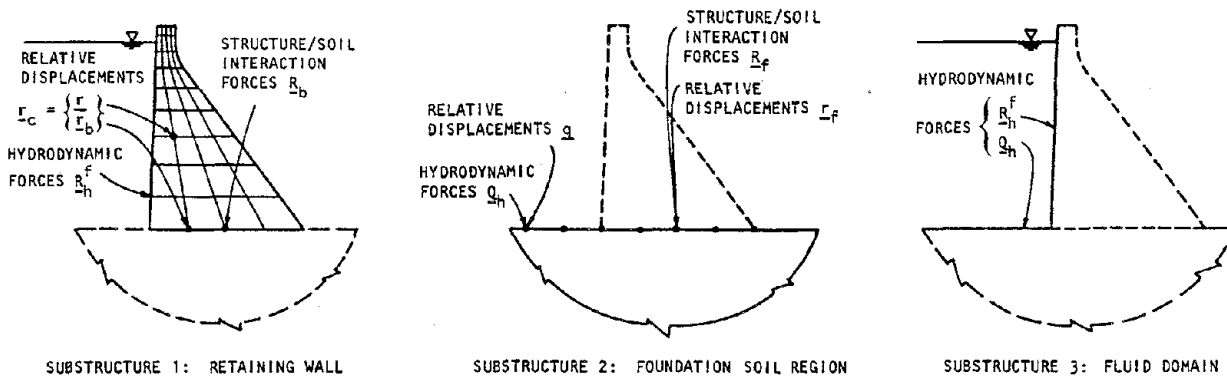
The second type of linear soil/structure interaction analysis technique is the substructure method. Unlike the direct method, where the dynamic response of the soil/structure system is computed in one step, the substructure method reduces the soil/structure interaction problem to a sequence of substructures, separately analyzes the response characteristics of each substructure, and then superimposes these results to obtain the combined response of the soil/structure system. Because substructure techniques are based on the principle of superposition, they are limited to linear analyses.

The most common substructure techniques typically represent the superstructure as a finite element model and the foundation/ soil system either as a continuum (e.g., Werner et al., 1979; Wong and Luco, 1980) or as a separate finite element model (e.g., Gutierrez and Chopra, 1978). The techniques using continuum foundation/soil system models (Fig. 4-1b) have the advantage of being able to represent radiation damping exactly and three-dimensional effects in a relatively economical manner; however they cannot yet accommodate irregular embedded foundations, irregular topography, or irregular soil layering. The substructure methods involving finite element foundation/soil models do not have the latter limitation, but are more costly to implement and require the use of approximate energy-absorbing boundary conditions to simulate radiation damping.

Another type of substructure approach that is of particular interest for port and harbor structures are the techniques that incorporate hydrodynamic effects in the analysis of retaining-wall/soil/water systems (e.g., quay walls). Such techniques treat this system as being comprised of two substructures--the backfill/wall and the fluid domain--coupled through the hydro-dynamic forces and continuity conditions at the face of the wall

(Fig. 4-1c). As developed by Prof. Chopra and his associates at the University of California, these techniques have represented the backfill and wall as a finite element model and the fluid domain either as a continuum (if the domain has simple geometry) or as a finite element model (if the wall face is sloped or the fluid domain irregular). Effects of water compressibility and interaction between the water and the underlying soil can be approximated in these methods (e.g., Chakrabarti and Chopra, 1974; Chopra and Chakrabarti, 1981; Hall and Chopra, 1982).

4.2.1.2 Equivalent Linear Methods

Over the past several years, a family of soil/structure interaction analysis techniques have been developed at the University of California at Berkeley that utilize an equivalent linear model for the soil medium together with a limited number of elastic structure element types. Such methods are very important in current practice because they represent a simplified approach for incorporating the effects of the strain-dependent properties of the soil medium.

To summarize equivalent linear methods, this subsection is divided into four main parts. The first part describes the basic equivalent linear model and its application. The final three parts summarize the family of dynamic finite element programs that use the equivalent linear model. These summaries are limited to the deterministic analysis techniques QUAD-4, FLUSH, and SASSI. A probabilistic approach using the equivalent linear model, PLUSH, is summarized in Section 4.4.1.

4.2.1.2.1 *Description of Basic Model*

In the equivalent linear soil model, the soil is represented as a linear viscoelastic material whose stiffness and energy dissipation characteristics are introduced by using an equivalent shear

modulus, G, and an equivalent damping ratio, λ (Fig. 4-2a); these correspond to the real and imaginary parts respectively of the complex modulus representation (i.e., $G^* = G(1 + 2i\lambda)$) in a hysteretic material model (SW/AA, 1980). Each of these parameters can vary with the depth of the soil layer and the strain level within the layer. Guidelines for defining the strain-dependence of these parameters are provided in the form of curves built into the FLUSH code that were developed by Seed and Idriss (1970) and relate shear modulus and damping to shear strain for different soil materials (Fig. 4-2b). It is noted that the amplitudes of these curves can be adjusted by the engineer, using a multiplicative constant that accounts for differences in relative densities, static shear strengths, etc., represented by the curves relative to those of the actual site soil materials being analyzed. Also, the engineer is free to incorporate completely different curves if he desires, although this is seldom done in practice.

The implementation of the equivalent linear approach is an iterative process. In this, shear moduli and damping values are first estimated for each soil element in the model. Then the analysis is carried out using these properties, and acceleration and shear strain time histories are computed throughout the soil/ structure model. From these time histories, effective shear-strain amplitudes are estimated in each soil element as the product of the maximum strain and a numerical factor (usually about 0.6) provided by the user. Curves similar to those in Figure 4-2b are then consulted to see if the shear moduli and damping values used in the response evaluation are compatible with the characteristic strains developed. If the soil properties are not compatible, these curves are used to provide improved values of shear moduli and damping for the next iteration and the process is repeated until convergence has occurred, usually witin three to five iterations. The response from the last iteration is considered to correspond to the strain-dependent response.

DEFINITION: COMPLEX MODULUS FOR HYSTERETIC MATERIAL: $G^* = G(1 + 2i\lambda)$

WHERE

G = SECANT SHEAR MODULUS

λ = DAMPING RATIO = $\dfrac{A_L}{4\pi A_T}$

A_L = AREA OF LOOP

A_T = AREA OF TRIANGLE

SHEAR STRESS

G_1

G_2

LOCUS OF TIPS OF HYSTERESIS LOOPS

SHEAR STRAIN

SHEAR STRAIN AMPLITUDE
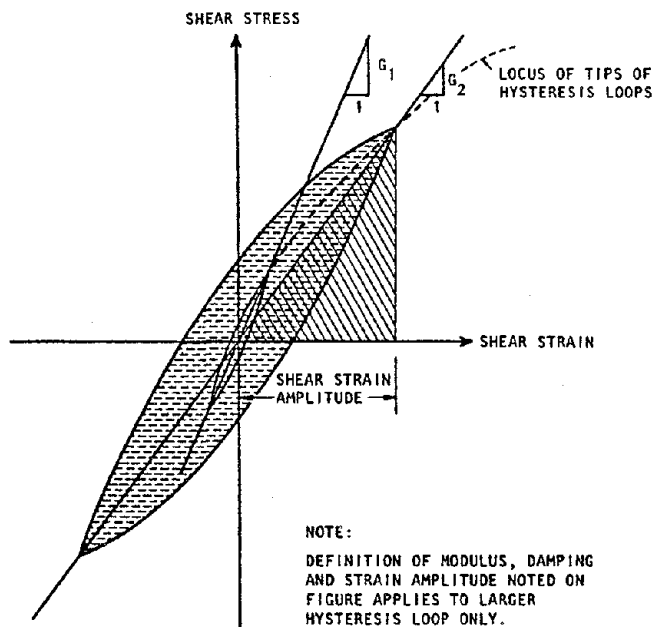
NOTE:
DEFINITION OF MODULUS, DAMPING AND STRAIN AMPLITUDE NOTED ON FIGURE APPLIES TO LARGER HYSTERESIS LOOP ONLY.

(a) Definition of shear modulus and damping ratio

COHESIONLESS SOILS

SATURATED CLAYS
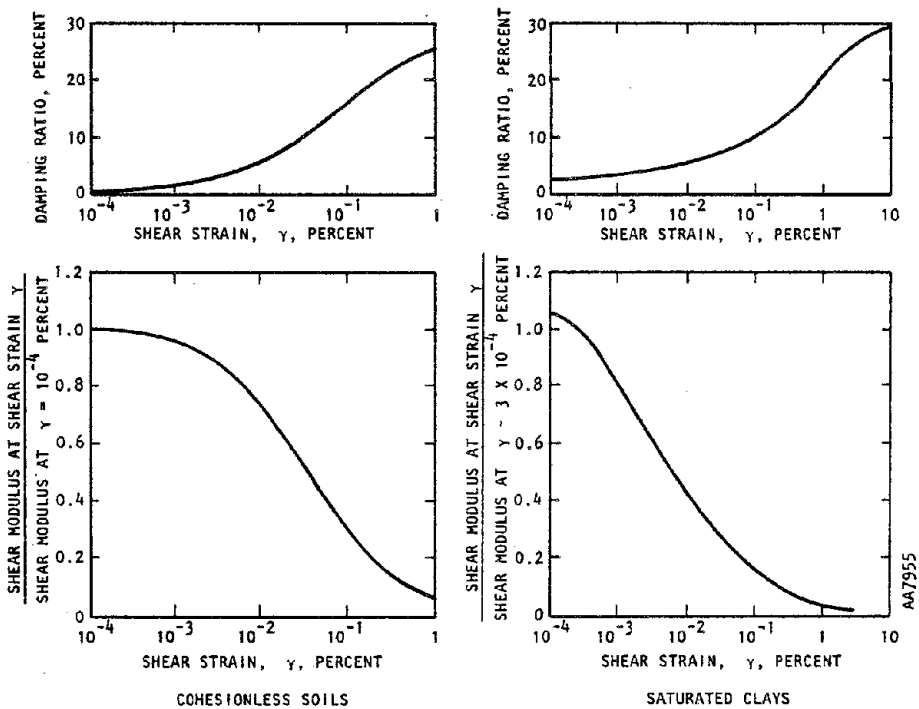
(b) Typical curves used to define strain-dependent properties (Seed and Idriss, 1970)

FIGURE 4-2. EQUIVALENT-LINEAR SOIL MODEL

In practice, the application of equivalent linear methods in a total stress approach may include the following additional considerations:

- If curves such as those shown in Figure 4-2b are developed from undrained laboratory tests, then the effects of excess porewater pressures in reducing the soil stiffness may be approximated through the use of shear modulus vs. strain curves for a number of cycles consistent with the equivalent number of cycles antici-pated from the ground shaking (Fig. 4-3).

- Field conditions involving irregular topography, sloping soil layers, or proximity to large structures may result in gravity-induced initial shear stresses on horizontal planes (Fig. 4-4). Such shear stresses, which represent initial conditions existing prior to the cyclic loading from the earthquake, have been shown (1) to reduce the tendency for excess porewater pressures to develop under undrained cyclic loading; and (2) to increase the tendency for permanent displacements upon subsequent earthquake-induced ground shaking. In the equivalent linear total stress approach, these initial shear streses are estimated using separate nonlinear static finite element analyses (e.g., Duncan and Chang, 1970; Clough and Duncan, 1971). Results from these analyses are then used to define initial conditions for the cyclic laboratory tests carried out under Step 3 of the total stress approach, to determine the liquefaction potential for the site (Sec. 4.2.3.2).

$$G = K_2\sigma_m^{1/2}$$

σ_m = MEAN EFFECTIVE STRESS, psf

N = EQUIVALENT NUMBER OF CYCLES

INCREASING N

SHEAR STRAIN, γ, PERCENT
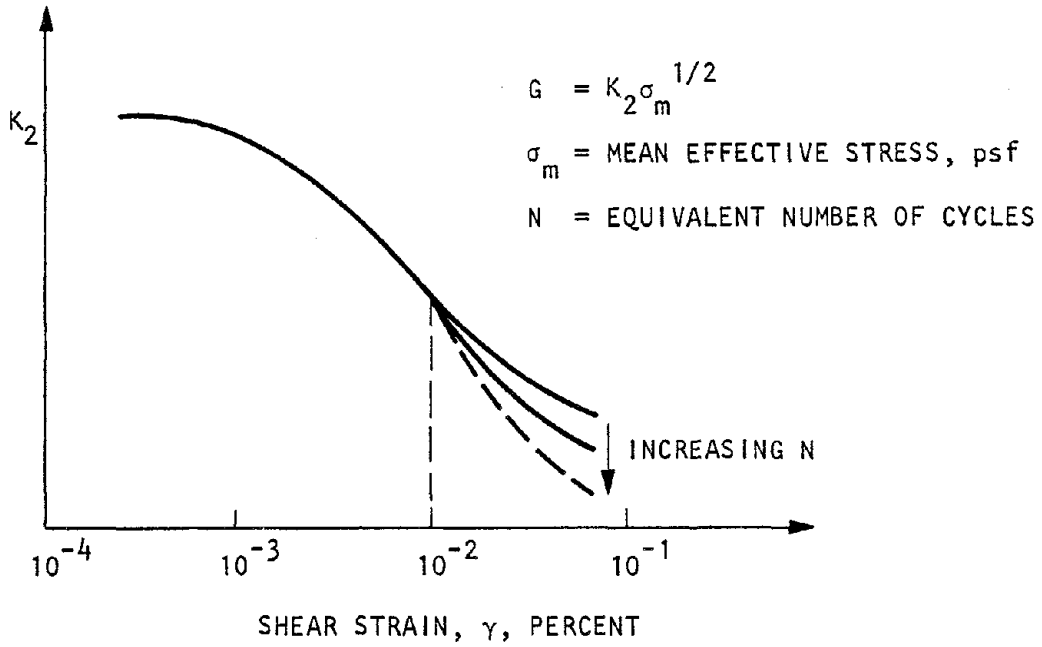
FIGURE 4-3. EFFECT OF EQUIVALENT NUMBER OF CYCLES ON STRAIN-DEPENDENT SHEAR MODULUS FOR SANDS
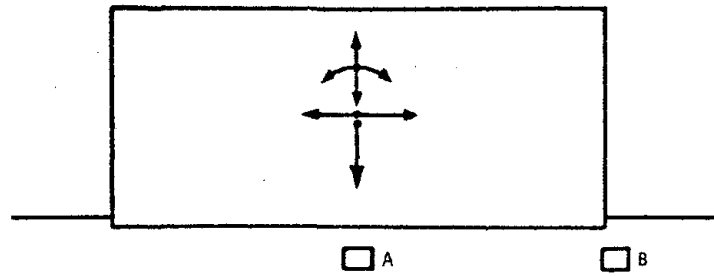
(a)   Ocean floor structure
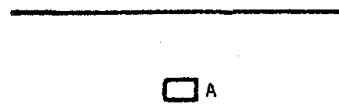
(b)   Earthquake loading   (c)   Earthquake loading
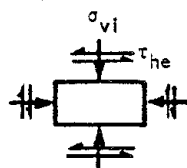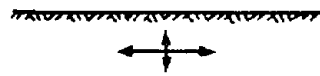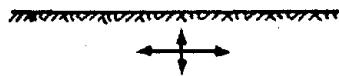
(d)   Element A (no initial   (e)   Element B (initial
      shear stresses)   shear stresses)
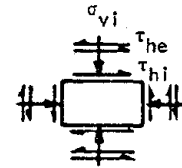
FIGURE 4-4.   STRESS CONDITIONS FOR SOIL ELEMENTS IN CYCLIC
              LOADING ENVIRONMENTS (Seed, 1979a)

4.2.1.2.2 *QUAD-4 Dynamic Analysis Procedure*

The first of the family of dynamic finite element codes that utilizes the equivalent linear model and features variable damping (i.e., separate representation of damping in each soil element) is QUAD-4 (Idriss et al., 1973). This code has the following features:

- Two-dimensional soil/structure system analyses are carried out in which both the soil and structure are represented as an assemblage of quadrilateral elements.

- Seismic input motions are assumed to arise from vertically propagating shear waves (for horizontal motions) or vertically propagating P-waves (for vertical motions). The effects of horizontal and vertical seismic input motions are analyzed separately, rather than simultaneously.

- The control motion approach for analyzing the soil/ structure system response is used (Seed et al., 1975c). This approach is comprised of (1) defining free-field seismic input motions as "control motions" applied at a specified location within the soil grid and consisting of an acceleration time history of appropriate intensity, frequency content, and duration; (2) deconvolving these control motions to obtain corresponding motions at the base of the finite element grid; and (3) using these base motions as input to the soil/structure system analysis (Fig. 4-5).

- The system damping matrix is derived by assembling element damping matrices which are defined in a Rayleigh damping form. The Rayleigh damping coefficients for each element are defined in terms of its strain-dependent damping ratio and the fundamental frequency of the soil/structure system.
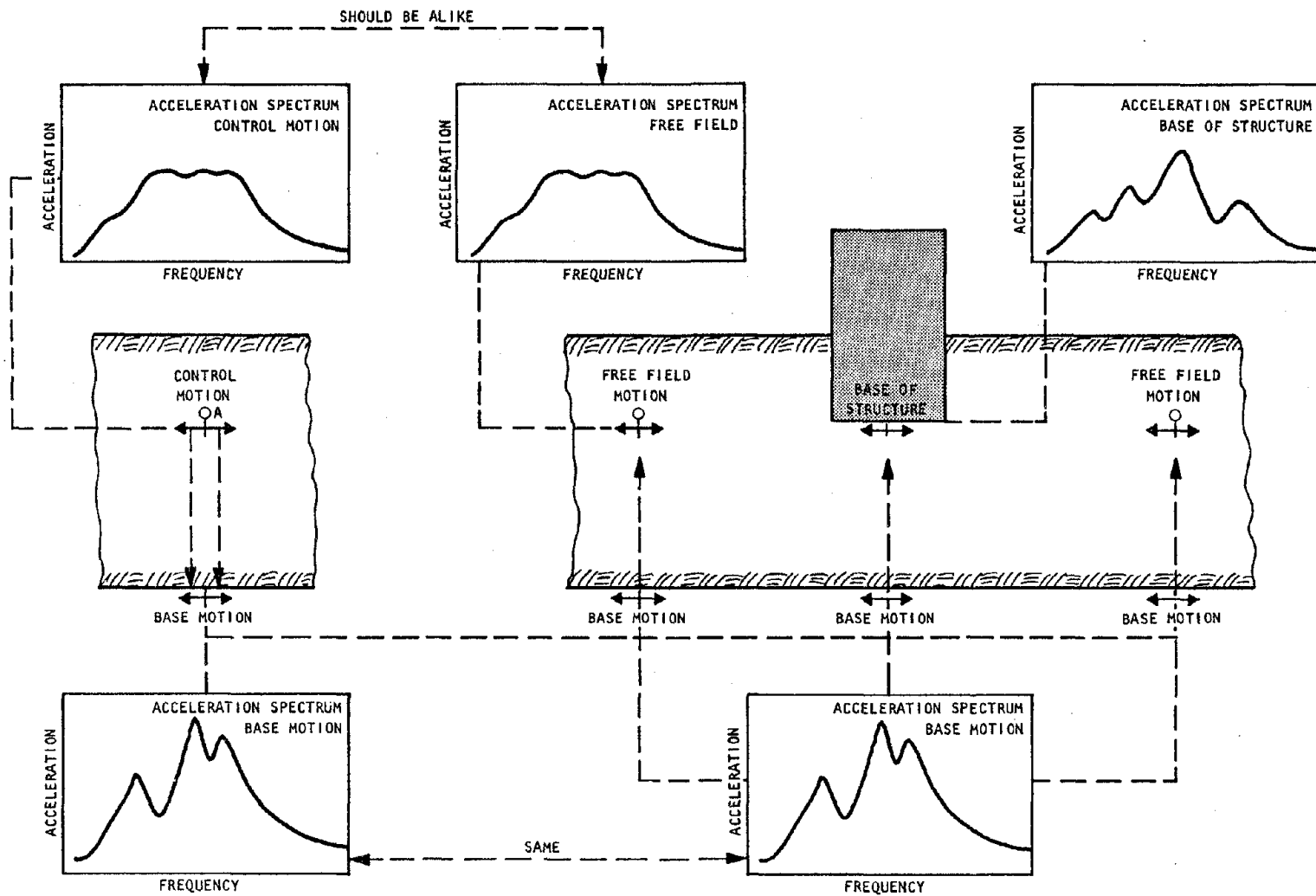
(a) Soil deposit model   (b) Finite element model of soil/structure system

FIGURE 4-5. SCHEMATIC REPRESENTATION OF CONTROL MOTION METHOD
(Seed et al., 1975c)

- At the start of each cycle of the equivalent linear analysis, the system stiffness matrix and damping matrix are assembled (based on shear moduli and damping ratios consistent with the current strain level for each element) together with the system mass matrix. The resulting system of equations of motion are then numerically integrated using step-by-step procedures to obtain the response time history for the entire system.

QUAD-4 is significant because it is the only member of this family of equivalent linear finite element programs that operates in the time domain. However, it has certain limitations, the most important of which are:

- The damping representation in QUAD-4 severely overdamps the higher modes of response, and is not consistent with the theoretically correct definition of the element damping ratio in terms of the complex modulus of a hysteretic material (Fig. 4-2a).

- No energy-absorbing boundary conditions are included in QUAD-4.

- The availability of only quadrilateral elements leads to inefficiencies in modeling structures.

Because of these important limitations, QUAD-4 was essentially superseded by the subsequent development of the FLUSH code as described in the subsequent paragraphs, although QUAD-4 is still occasionally used in practice today. It is noted that both QUAD-4 and FLUSH have additional limitations related to (1) the necessity of using a rigid base to the soil grid, which leads to uncertainties when modeling deep soil sites; (2) the inability to address horizontal and vertical input motions simultaneously; and

(3) the restriction to considering only vertically propagating body waves. These latter limitations have only recently been eliminated through development of the SASSI code.

4.2.1.2.3 *FLUSH Code Dynamic Analysis Procedure*

The FLUSH code (Lysmer et al., 1975) was developed shortly after QUAD-4, and has certain important advantages over its predecessor. First, it utilizes a complex modulus representation of the equivalent linear soil parameters, thereby removing the inconsistencies in the damping representation that exist in QUAD-4. In addition, energy-absorbing boundary conditions along the side boundaries of the grid and beam elements for modeling structures have been added. Finally, the calculations are carried out in the frequency domain using Fast Fourier Transform techniques, which offer important computational efficiencies over the QUAD-4 time-domain numerical integration approach. Because of these features, FLUSH code is perhaps the most widely used soil/ structure interaction approach in practice today.

The FLUSH code is based on the use of one of two types of two-dimensional finite element models to represent the soil/ structure system; in each type, the models are comprised of beam and quadrilateral elements, feature energy-absorbing boundaries to simulate the infinite lateral extent of the soil medium, and consider excitations only from vertically propagating body waves. The first type of model corresponds to a conventional plane strain model (Fig. 4-6a) in which average properties for a unit slice of the soil/structure system is represented. The second type is a modified two-dimensional model in which three-dimensional wave propagation effects are simulated through the use of in-plane viscous dampers attached to each node point of the soil medium (Fig. 4-6b). This model is based on a slice of the soil/structure
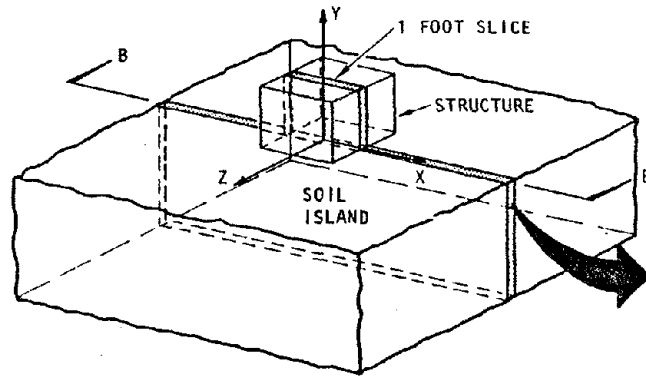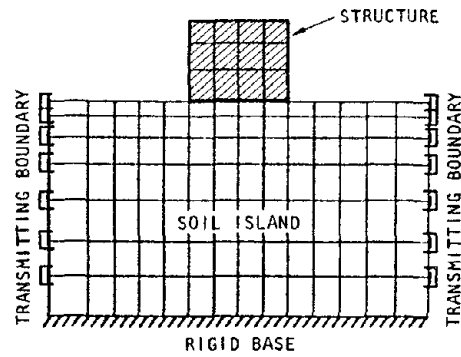
(a) Plane strain model
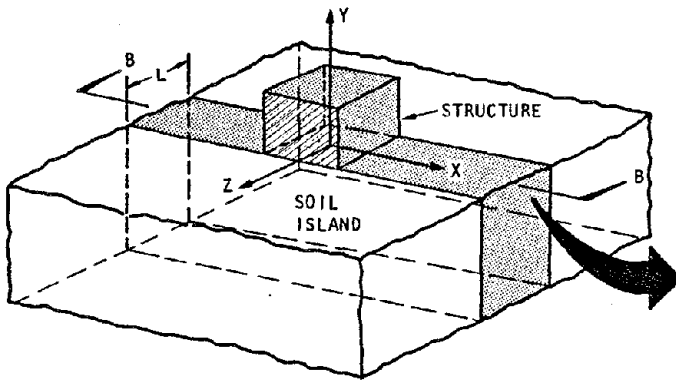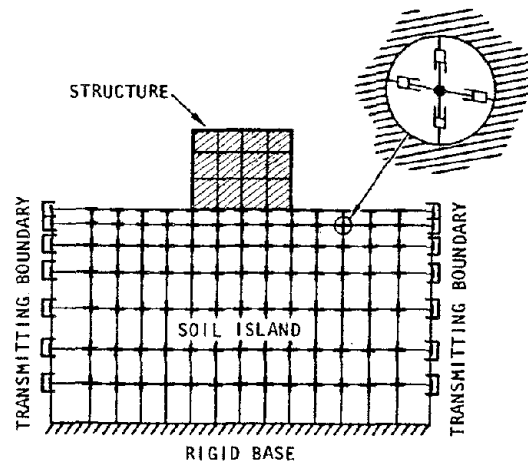
(b) Modified two-dimensional

FIGURE 4-6. SOIL/STRUCTURE SYSTEM MODELING PROCEDURES USED IN *FLUSH* CODE (Lysmer et al., 1975)

system whose width is equal to the out-of-plane width of the struc-
ture. It is noted that the in-plane viscous dampers in FLUSH code,
as well as the energy-absorbing boundaries, are based on the
assumption of horizontal soil layers over the entire length of
the grid.[*]

For either of the above two-dimensional models, the control
motion method (Fig. 4-5) is deployed. In this, input motions are
defined along a rigid base of the soil grid that represents an
interface between the soil and the underlying rock. Either hori-
zontal or vertical motions, but not both simultaneously, can be
considered and are either specified directly at the rigid base or
are computed by deconvolving control motions specified at the
ground surface or at some specified location in the upper soil
layers. Once the input motions are specified in this manner,
Fourier transform techniques are used to transform the equations
of motion from the time domain to the frequency domain, and the
response of the soil/structure system is computed as the product
of its frequency-response functions and the various harmonic
signals that comprise the input motions. The resulting system
response in the time domain is then obtained as the inverse
Fourier transform of the above product. This process is repeated
for each iteration cycle required for the equivalent linear
analysis.

---

[*] For some cases (e.g., for dynamic analyses of quay walls, sheet-
pile bulkheads, etc.) the conditions of horizontal soil layering
over the entire length of the grid may not be satisfied. Because
this violates the conditions on which the energy-absorbing
boundaries and in-plane viscous dampers are based, care and
judgment must be exercised in using these features of FLUSH
code. For example, it may be appropriate to (1) extend the
lateral boundaries of the grid so as to minimize the effects
of the energy-absorbing boundaries in the region of interest;
and (2) either eliminate the in-plane viscous dampers and use
the plane strain modeling approach (Fig. 4-6a) or, where this
option is not physically meaningful, use properties of the
viscous dampers that are representative of the soil properties
in the region of interest.

4.2.1.2.4 *SASSI Code Dynamic Analysis Procedure*

The most recent development in this family of equivalent linear dynamic analysis techniques is the SASSI code (Lysmer et al., 1981). This code has the following significant advancements over its predecessors.

- The site is horizontally layered and comprised of viscoelastic layers over a viscoelastic half-space. (Therefore, the prior limitations associated with the presence of a rigid boundary at the base of the soil grid have been eliminated.)

- The seismic environment consists of an arbitrary three-dimensional superposition of arbitrarily incident body waves (P- and S-waves) and surface waves (R- and L-waves). (Therefore, the prior limitations associated with considering only vertically incident body waves have been eliminated).

- The structure(s) can be represented by fully three-dimensional finite element models connected to the soil at several points within the embedded part of the structure. (Therefore the prior limitations associated with the use of a two-dimensional soil/structure model have been eliminated.)

Within the above context, SASSI code can analyze embedded structures with flexible basements, structure/soil/structure interaction, effects of torsional ground motions, pile foundations, etc. in a much more complete manner than its predecessors. SASSI also has the features of (1) being modular (so that individual parts of the analysis can be performed separately and complete reanalysis is not necessary if the structure or seismic environment are changed); (2) operating in the frequency domain (which

enhances the computational efficiency of the code); and (3) in addition to seismic excitations, having a capability of considering external forces acting directly on the structure (e.g., impact loads, wave forces, loads from rotating machinery, etc.). It should be noted, however, that for a number of these problems, other soil properties in addition to those defining its behavior in shear, may be important, but are not directly considered by the equivalent linear model.

The primary feature of the SASSI code is a substructuring method termed the flexible volume method (Tabatabaie-Raissi, 1982). According to this approach, interaction occurs at all nodes of the embedded part of the structure, so that the mass, stiffness, and damping matrices of the structure are reduced by the corresponding properties of the excavated mass of soil (Fig. 4-7a). The resulting analysis procedure involves the following steps:

- Site Response Problem--In this phase of the analysis the free-field motions due to any combination of arbitrarily incident body or surface waves, are computed at the soil layer interfaces where the structure(s) are connected.

- Impedance Problem--This second step of the analysis corresponds to the computation of the impedance matrix (i.e., dynamic stiffness matrix) for the interaction node points in the soil. This step is carried out by applying a unit harmonic horizontal and vertical force once at each layer interface in an axisymmetric soil model, and then computing the corresponding harmonic displacements at the other interaction nodes (Fig. 4-7b). This results in the complete dynamic flexibility matrix (for all of the interaction node point degrees of freedom) which is inverted to obtain the impedance matrix (Tajirian, 1981).
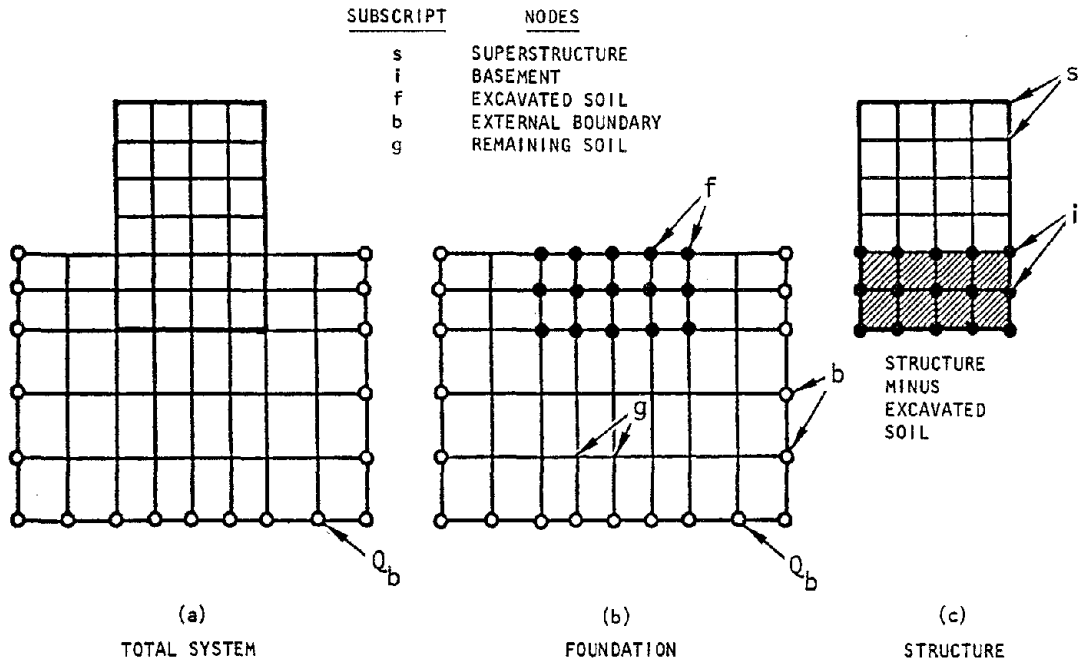
(a) Substructuring of interaction model
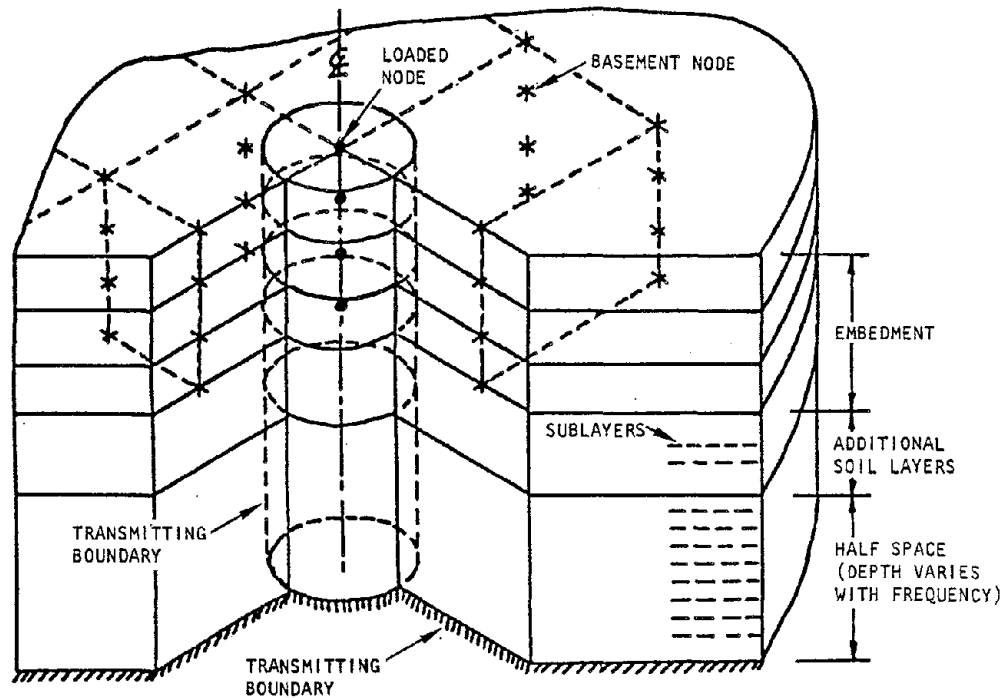
(b) Axisymmetric model for impedance analyses

FIGURE 4-7. *SASSI* CODE (Lysmer et al., 1981)

- **Structural Problem**--This final phase of the analysis involves forming the complex frequency-dependent stiffness matrix and load vector for the soil/structure system. This stiffness matrix, formed by subtracting the corresponding matrix for the excavated soil and adding the impedance matrix obtained as described above, is then inverted to obtain the structural response.

The current (mid-1982) status of the SASSI code is that it has only recently been installed on a public CRAY computer system, and no users manual is yet available. Therefore, at present, there is very little experience among earthquake engineers with the use of this code. For this reason, although SASSI is undoubtedly the state of the art of this family of equivalent linear methods, further application of the code will be required to further assess its particular capabilities.

4.2.1.3 <u>Nonlinear Methods</u>

4.2.1.3.1 *General Description*

A third technique for carrying out dynamic soil/structure interaction analyses in a total stress approach is through the use of nonlinear finite element methods.[*] Such methods differ from the equivalent linear methods just described in that the soil properties are changed as necessary at each time step in accordance with the nonlinear constitutive relations for each soil element, and can incorporate such phenomena as gravity

---

[*]Nonlinear two-dimensional and three-dimensional finite difference methods are also available but are typically not widely used in soil/structure interaction analyses because of (1) their difficulty in representing structures; and (2) technological advances in finite element methodologies which have substantially improved their computational efficiency and storage requirements.

effects, separation or sliding along soil/structure interfaces, effects of irregular topography and soil layering, and permanent distortions. Nonlinear methods of analysis can therefore represent general levels of stress, strain, and deformation induced by the ground shaking, as well as the transient fluctuations in these quantities with each cycle of the applied seismic excitation.

4.2.1.3.2 *Constitutive Laws*

A central aspect of the nonlinear methods of analysis is the constitutive laws that are used. These laws represent the fact that (1) soils are not a linear material, and instead involve rather complex nonlinear relationships between stress and strain; and (2) in addition to exhibiting nonlinear behavior, many soils show varying degrees of viscosity as well. Accordingly a brief summary of some of the types of models used to represent various aspects of this behavior is provided below.

a. Mathematical Functions and Mechanical Models

In this approach, particular stress/strain curves are fit through the use of (1) mathematical expressions, which may be based in part on nonlinear elasticity theory, or (2) models comprised of systems of mechanical elements. This approach is conceptually simple and is popular because of the relative ease with which experimental data can be fit; however, it is typically restricted in application to particular loading paths. Examples of techniques that employ this basic approach are:

●   Mathematical Functions (Fig. 4-8a). In such techniques, mathematical expressions based on hyperbolic relations (e.g., Duncan and Chang, 1970; Hardin and Drnevich, 1971) or the Ramberg-Osgood equation (Liou et al., 1977) are used to define the initial loading curve, and the Masing (1926) rules serve to represent the hysteresis

R-8122-5395

$$\frac{\tau}{\tau_y} = \frac{\tau_c}{\tau_y} + \frac{\gamma - \gamma_c}{\gamma}\left[\frac{1}{1 + \left|\frac{\gamma - \gamma_c}{n\gamma_y}\right|}\right]$$

$$\frac{\varepsilon - \varepsilon_o}{2\varepsilon_y} = \frac{\sigma - \sigma_o}{2\sigma_y} + \alpha\left|\frac{\sigma - \sigma_o}{2\sigma_y}\right|^r$$

$$\frac{\varepsilon}{\varepsilon_y} = \frac{\sigma}{\sigma_y} + \alpha\left|\frac{\sigma}{\sigma_y}\right|^r$$
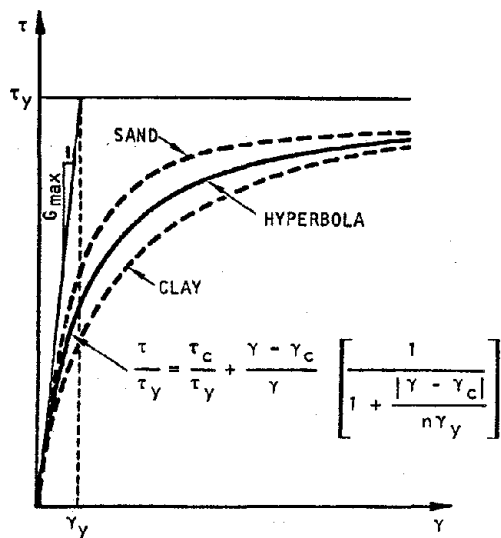
DEFINITION OF TERMS
IN HYPERBOLIC MODEL
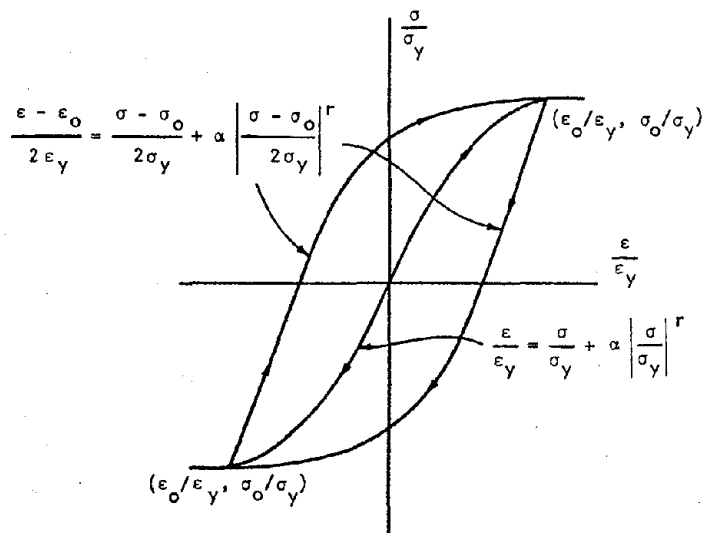
RAMBERG-OSGOOD HYSTERESIS LOOPS
INCORPORATING MASING RULES

(a)   Mathematical functions
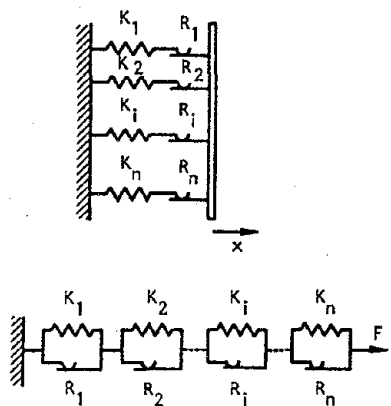
(b)   Iwan models
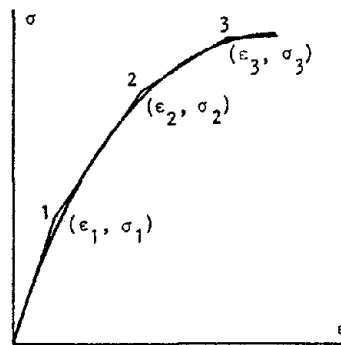
(c)   Simplified form of variable
modulus model

FIGURE 4-8.   NONLINEAR CONSTITUTIVE LAWS USING MATHEMATICAL
FUNCTIONS AND MECHANICAL MODELS (Pyke, 1979,
Christian and Desai, 1977)

4-26

loop. Various alternative procedures for extending these basic models to better represent irregular cyclic loading phenomena have been suggested (e.g., Pyke, 1979).

● Mechanical Models (Fig. 4-8b). The most common models of this type for soil analysis are described by Iwan (1967) and are comprised of linear-spring/Coulomb-slider building blocks assembled either in parallel or in series. As noted by Pyke (1979), mechanical models of this type are particularly well suited to one-dimensional analyses, but can be extended to two-dimensional or three-dimensional applications within the framework of plasticity theory.

● Variable Modulus Models (Fig. 4-8c). Models of this type empirically fit test data by defining tangent moduli for the range of stress encompassed by the data, and the appropriate modulus to be used during any load increment. In the context of the plasticity theory discussed below, such models are equivalent to defining a completely arbitrary plastic yield function that fits the test data, and then using some simplified, nonrigorous procedure to force the material to satisfy the yield function.

b.   Plasticity Models

This type of soil model describes limiting stress states in the plastic region of the soil behavior--i.e., the region beyond which there is no unique relationship between stress and strain. Such models are characterized by a yield function and a flow rule (Fig. 4-9). A yield function, often expressed in terms of stress invariant, defines conditions of limiting equilibrium within a plastic region, beyond which additional strain is accompanied by

MOHR-COULOMB $\phi = 0$

$\sigma_1 = \sigma_2 = \sigma_3$

TRESCA $\phi = 0$

$-\sigma_3$

$-\sigma_2$

$-\sigma_1$

i) Mohr-Coulomb
(linearized form)

$-\sigma_3$

$\sigma_1 = \sigma_2 = \sigma_3$

$-\sigma_2$

$-\sigma_1$

ii) Mohr-Coulomb
(general form)

$-\sigma_3$ DRUCKER-PRAGER $\phi = 0$

VON MISES
$\phi = 0$

$-\sigma_2$

$-\sigma_1$

iii) Drucker-Prager
(linearized form)

$-\sigma_3$

$\sigma_1 = \sigma_2 = \sigma_3$

$-\sigma_2$

$-\sigma_1$

iv) Drucker-Prager
(general form)
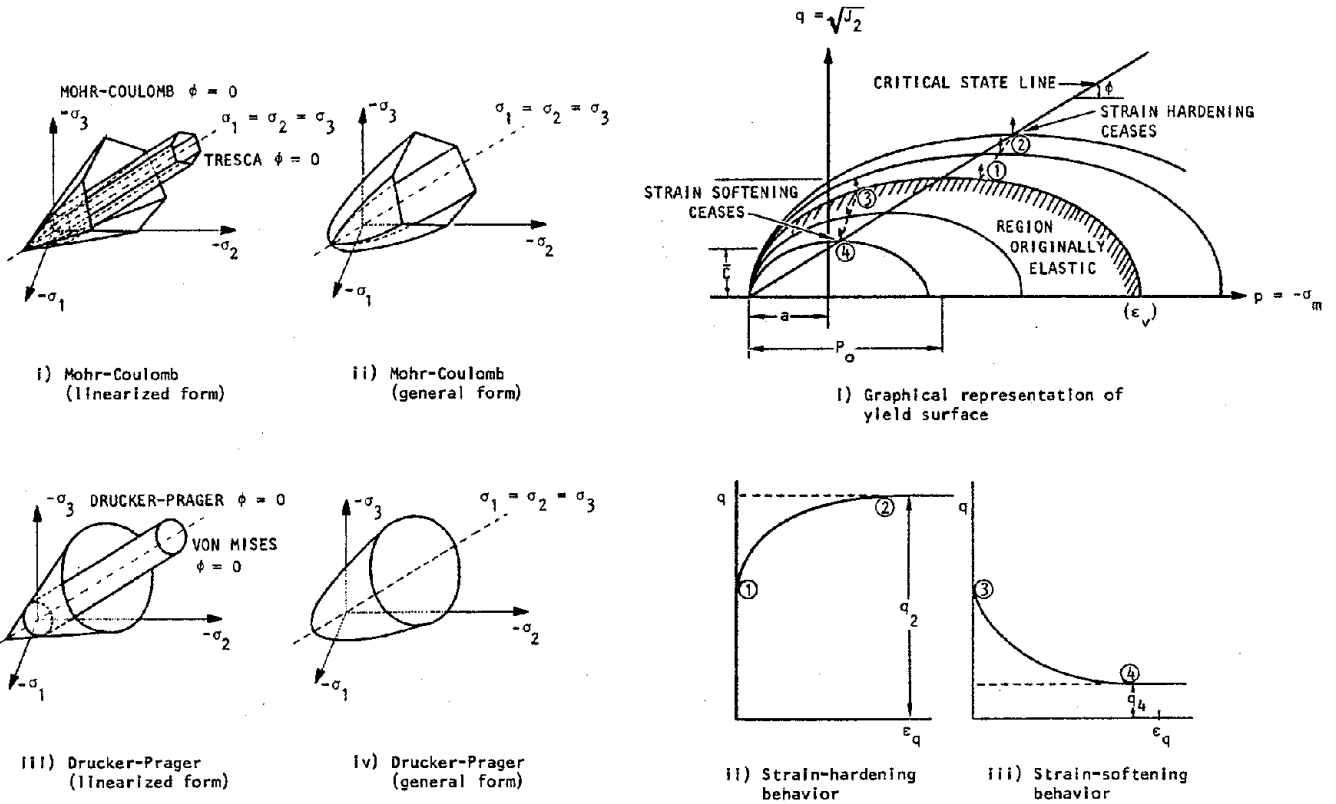
(a) General and linearized yield surfaces in principal-stress space

$q = \sqrt{J_2}$

CRITICAL STATE LINE ϕ

STRAIN HARDENING CEASES

②

①

STRAIN SOFTENING CEASES

③

④

REGION ORIGINALLY ELASTIC

$\bar{c}$

$p = -\sigma_m$

(ε_v)

a

P_0

I) Graphical representation of yield surface

q

②

q_2

①

ε_q

q

③

④

q_4

ε_q

ii) Strain-hardening behavior

iii) Strain-softening behavior

$\sqrt{J_2'}$

FAILURE ENVELOPE

ASSOCIATED FLOW RULE
$\dot{\varepsilon}^P$

E

CAP

ASSOCIATED FLOW RULE
$\dot{\varepsilon}^P$

A   B   P
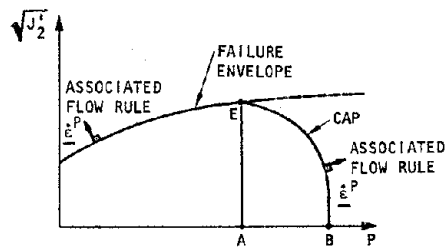
(c) Typical yield surface in the cap model

$-\sigma_3$

$\sigma_1 = \sigma_2 = \sigma_3$

a

$-\sigma_2$

$-\sigma_1$
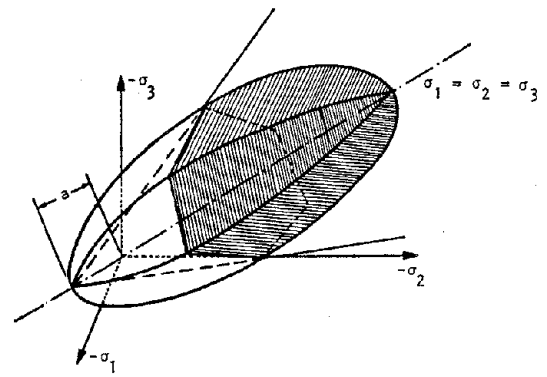
iv) Generalization corresponding to Mohr-Coulomb critical surface

(b) Critical-state strain-hardening or strain-softening yield surface

FIGURE 4-9. NONLINEAR CONSTITUTIVE LAWS USING THEORY OF PLASTICITY (Zienkiewicz and Humpheson, 1977, Sandler et al., 1976)

much reduced (or zero) stress increments. When a load increment results in a stress state that lies outside of this yield surface (i.e., the surface defined by the yield function), a flow rule is used to determine the elastic and plastic portions of the deformation. In general, the yield surface changes shape or translates whenever yield occurs; this type of behavior is characterized as work hardening or work softening. Examples of plasticity models used in modeling of geologic media are the classical approaches based on Von-Mises, Mohr-Coulomb, and Drucker-Prager criteria; critical state concept models including the cap models (Sandler et al., 1976), Cambridge models (Lade, 1979), and models based on variations of this concept (e.g., Prevost, 1977); and endochronic models (e.g., Bazant and Krizek, 1976).

c.   Viscoelastic Models

Models of this type describe the behavior of materials that relax in a time-dependent manner, following an initial response that is purely elastic. Unlike elasto-viscoplastic models (described subsequently) there is no minimum stress level for such relaxation to occur. Linear viscoelastic models are a special case for which the parameters defining the time-dependent behavior are constant. Generally, these parameters will be functions of time-dependent stress or strain.

d.   Viscoplastic Models

This type of soil model may be considered as a generalization of the viscoelastic model to incorporate the concepts of a yield condition. Stress relaxation will occur only when the yield condition is exceeded. Following any load increment that results in a stress state that exceeds the yield condition, the stress relaxes, according to a defined time-dependent relationship, until the yield condition is exactly satisfied. The concepts of a yield

function and a flow rule that defines the elastic and inelastic portions of the time-dependent deformation are the same as for elastoplastic materials.

4.2.1.3.3 *Computational Techniques*

In nonlinear methods of analysis, a step-by-step integration technique is required to obtain the desired response histories of the soil/structure system. The integration technique used is an important consideration in such analysis techniques since it defines the number of arithmetic operations, the amount of data to be handled, and the time step required for stability and accuracy of the numerical results.

Many integration methods are currently in use but they can be classified into two groups. One group is referred to as the "implicit method" in which equilibrium is expressed at node points by a system of coupled equations in which the unknown quantities are the generalized displacements, velocities, and accelerations. The solution of a coupled system of equations requires formulation of global stiffness, damping, and mass matrices and the inversion of a matrix whose order is the same as the number of equations. The global stiffness matrix, and possibly the damping matrix are updated at each time step to represent nonlinear behavior.

A second group of integration techniques is known as the "explicit method," in which equilibrium between external, internal, and inertia forces is expressed at node points by a system of uncoupled or near-coupled equations. It is possible to write these equations without formulating stiffness, mass, or damping properties at the global level. Nonlinear behavior is represented by updating the internal forces, which incorporate the material constitutive laws, at each time step.

From a cost-effectiveness viewpoint, the implicit methods are usually more stable and hence can tolerate larger step sizes. However, they require more core space because of the need to manipulate the global stiffness matrix, and they also require more time per step because the solution of a set of simultaneous equations is involved in each step. In contrast, the explicit methods usually require much smaller step sizes for numerical stability, but they require smaller core size and involve less calculation and hence run time per step.

4.2.1.3.4 *Assessment of Nonlinear Analysis Procedures*

The features of several nonlinear dynamic analysis procedures are summarized in Table 4-1 and comparisons between several nonlinear and equivalent linear procedures are given in Table 4-2. These tables illustrate the wide range of nonlinear procedures that are available and that, in addition to highly refined soil modeling capabilities, many of the procedures incorporate (1) a wide range of structure element types; (2) the ability to accommodate arbitrarily phased seismic input motions applied along the grid boundaries; and (3) a fully three-dimensional capability. Therefore, these nonlinear procedures represent the most sophisticated techniques now available for carrying out soil/ structure interaction analyses.

Despite these significant analytical advantages, nonlinear dynamic analysis procedures have certain practical disadvantages for application to port and harbor facilities in a total stress context. One such disadvantage is the high computation costs of such analysis procedures, which precludes their use in parametric analysis to account for uncertainties in input parameters. Other disadvantages pertain to the difficulty that can exist in measuring many of the required nonlinear soil parameters from routine soil testing, and in the time and level of training required to apply these complex analysis procedures.

TABLE 4-1.   NONLINEAR FINITE ELEMENT ANALYSIS PROCEDURES

Items for Comparison	ANSYS (DeSalvo and Swanson, 1979)	TRANAL (Baylor, Bieniek, and Wright, 1974)	MARC (Marc, 1979)	NASTRAN (McCormick, 1979)	ADINA (Bathe, 1978)
Static Analyses	Linear, thermal, plastic, buckling, creep Nonlinear material properties and geometry	None	Linear, thermal Nonlinear material properties and geometry	Linear, buckling, thermal Nonlinear material properties and geometry	Linear, thermal Nonlinear material properties and geometry
Eigenvalues and Eigenvectors	Yes	No	Yes	Yes (3 methods, restartable, complex roots)	Yes
Dynamic Analysis	Modal (linear) Nonlinear Transient Implicit Harmonic response	Nonlinear Step-by-step Explicit	Linear and nonlinear Step-by-step Implicit Explicit Modal	Linear and nonlinear Step-by-step Implicit	Linear and Nonlinear Step-by-step Implicit Explicit
Element Types Truss Beam Plate and Flat Shell Curved Shell Solid Two-Dimensional Special	Yes Yes Yes Yes Yes Yes Pipe and fluid elements	No No No No Yes No No	Yes Yes Yes Yes Yes Yes Concrete pipe and fluid elements	Yes Yes Yes Yes Yes Yes Substructures Pipe and fluid elements	Yes Yes Yes Yes Yes Yes Fluid elements
Loading Nodal Point Member Gravity Initial Stress/Strain	Yes Yes Yes Yes	Yes Yes Yes No	Yes Yes Yes Yes	Yes Yes Yes Yes	Yes Yes Yes Yes
Kinematic Boundary Conditions for Dynamic Analysis	Displacement, velocity, and acceleration	Displacement	Displacement	Displacement, velocity, and acceleration Energy-absorbing boundary conditions	Displacement
Maximum Number of Node Points	Dynamically allocated (D.A.)	D.A.	D.A.	D.A.	D.A.
Maximum Number of Elements	D.A.	D.A.	D.A.	D.A.	D.A.
Maximum Half-Bandwidth	Wavefront technique	D.A.	D.A.	D.A. (active column technique)	D.A.
Maximum Number of Load Cases	D.A.	D.A.	D.A.	D.A.	D.A.
Maximum Number of Materials	D.A.	D.A.	D.A.	D.A.	D.A.
Maximum Number of Cross Sections	D.A.	D.A.	D.A.	D.A.	D.A.
Graphic Output Grid or Mesh Plot Mode Shapes Time History Response Spectra Contour Plot	Yes Yes Yes Yes Yes	Yes No Yes No No	Yes Yes Yes Yes Yes	Yes Yes Yes Yes Yes	No No No No No
Automatic Mesh Generation	Yes	Yes	Yes	Yes	Yes
Bandwidth Minimization	Wavefront technique	Not applicable	Yes	Yes	No
Constrained DOF (slaving)	Yes	No	Yes	Yes	Yes
Special Features	Early conversion of cartesian to cylindrical or polar coordinates Large deflections Interactive mode of computation Extensive output graphics	Bonding and debonding capability Subcycle integration capability	Extensive output graphics	Sparse matrix methods Extensive output graphics Executive control	

AA10464

TABLE 4-2. MAJOR FEATURES OF NONLINEAR AND EQUIVALENT LINEAR COMPUTER CODES

Code	Soil Properties	Type	Element Types	Large Strain Capability	Energy-Absorbing Boundary	Seismic Input	Strongly Nonlinear Interface	3-D Effects	Structure-Structure Interaction
TRANAL	Nonlinear	Explicit Time Domain, Finite Element	Continuum	Yes	No	General	Yes	Yes	Yes
STEALTH	Nonlinear	Explicit Time Domain, Finite Difference	Continuum	Yes	Yes	General	Yes	Yes	Yes
SAP 7	Nonlinear	Implicit Time Domain, Finite Element	Continuum, Structural	Yes	No	General	No	Yes	Yes
NONSAP	Nonlinear	Implicit, Time Domain, Finite Element	Continuum, Structural	Yes	No	General	No	Yes	Yes
DYNA3D	Nonlinear	Explicit Time Domain, Finite Element	Continuum	Yes	No	General	Yes	Yes	Yes
FLUSH	Equivalent Linear	Implicit, Frequency Domain, Finite Element	Continuum, Structural	No	Yes	Rigid Bedrock Shaking, Vertically Propagating Body Waves	No	No	Yes
SASSI	Equivalent Linear	Implicit Frequency Domain, Finite Element	Continuum Structural	No	Yes	General	No	Yes	Yes

In view of these considerations, it would appear difficult to justify the expense and effort required for a nonlinear total stress analysis of the soil/structure system response for port and harbor facilities, particularly since the potentially significant effects of porewater pressures are not even considered. However, in the framework of effective stress methods where such porewater effects are incorporated, the use of nonlinear techniques for port and harbor facility analyses appears more appropriate. The applicability of nonlinear methods in this way is described in Section 4.3.

4.2.1.4 Applicability of Various Techniques to Analysis of Port and Harbor Facilities

A summary of the advantages and limitations of the use of existing linear, equivalent-linear, and nonlinear soil/structure interaction techniques in total stress analyses of port and harbor facilities is provided in Table 4-3. This table indicates that

- Linear methods are judged to be inapplicable to port and harbor facilities because they cannot represent the strain-dependence of the surrounding soil material properties.

- Nonlinear methods represent the most complete and rigorous approach for analyzing soil/structure interaction effects. However, practical limitations probably preclude their use in total stress applications at this time. Such methods appear most appropriate for use in an effective stress framework for analyzing port and harbor facilities (Sec. 4.3).

TABLE 4-3. APPLICABILITY OF SOIL/STRUCTURE INTERACTION TECHNIQUES
TO TOTAL STRESS ANALYSES OF PORT AND HARBOR FACILITIES

Approach	Advantages	Limitations
Linear	Simplicity and reduced costs of analyses. Substructure techniques available that incorporate hydro-dynamic effects.	Linear representation of soil material properties probably pre-cludes application of these techniques to analyses of port and harbor facilities, for which strain-dependence of soil proper-ties is important.
Equivalent Linear	Simplest and most cost-effective approach available for considering strain-dependence of soil proper-ties. Recently developments in this family of codes (SASSI) are three-dimensional, and can consider arbitrarily incident seismic waves. Energy absorbing boundary condi-tions included.	Techniques based on horizontally layered sites leads to some uncer-tainty when applied to port and harbor sites with irregular topography. Hydrodynamic effects and permanent displacements not computed.
Nonlinear	Most complete and advanced approach for representing strain-dependence of soil properties. Permanent dis-placements, gravity effects and separation at soil/structure inter-face can be represented. Some tech-niques available that include hydro-dynamic effects.	Costly and difficult to apply. Soil parameters required for some nonlinear models not readily obtained from routine laboratory tests. Energy-absorbing boundary conditions typically not included.

● Although equivalent linear methods have some limita-
tions when applied to port and harbor facilities,
they appear to be the most practical approach now
available for use in dynamic total stress analyses
of such facilities.

● The use of any of the methods indicated in Table 4-3
require the use of sound engineering judgment when
applying the methods and interpreting their results.

4.2.2   STEP 2:   DETERMINATION OF EQUIVALENT CYCLIC STRESS HISTORIES

Once the structural and soil responses are determined in
Step 1 including soil/structure interaction effects, the next
step in the deterministic total stress approach is to convert
the resulting irregular soil shear stress histories to equivalent
cyclic stresses. These cyclic stresses are used in Step 3 to
assess the liquefaction potential of the site.

The principal approach now available for obtaining equivalent
cyclic stresses is empirical and has been developed by Seed et al.
(1975b). This involves a weighting procedure in which each cycle
of an irregular shear stress history is assigned a weighting
factor based on a standard weighting curve developed from labora-
tory test data. In this way, the irregular shear stress history
computed from Step 1 at any location in the soil medium is
converted to an equivalent number of uniform stress cycles at
some preselected cyclic stress level, usually $0.65 \ \tau_{max}$ (where
τ_{max} is the maximum shear stress computed at the given soil
location).

The key aspect of this approach is the determination of the
weighting curve. To obtain this curve, Seed et al. used large
scale simple shear test data relating cyclic stress ratio to the

number of cycles to cause initial liquefaction, as obtained by
DeAlba et al. (1976). By observing that the shapes of these
curves are similar to those from other simple shear test results
and are not strongly affected by relative density or confining
pressure, Seed et al assumed that the DeAlba et al. curve for a
relative density of 65% has a shape that is representative of the
shear stress vs. number of cycle curve for any sand at any confin-
ing pressure. This is plotted as the solid curve corresponding
to initial liquefaction in Figure 4-10a. Then, to obtain a corre-
sponding weighting curve for soils safe from liquefaction, Seed
et al. assumed a condition whereby (1) the shear stress to cause
liquefaction in one cycle is a factor of 1.5 times the maximum
shear stress developed during the ground shaking; and (2) this
factor gradually reduces to a value approaching 1.0 as the number
of cycles becomes large. From this, the dashed curve in Fig-
ure 4-10a was developed by Seed et al. as a general weighting
curve for a nonliquefied state that defines an equivalent number
of cycles at any stress level and for all site conditions and
ground motions. A corresponding curve specifically oriented
toward defining an equivalent number of cycles at a particular
cyclic stress level of 0.65 τ_{max}, is provided in Figure 4-10b.

Once the weighting curve is defined, the conversion of an
irregular shear stress history to an equivalent number of cycles
at any cyclic stress level is straightforward. For example, if
a cyclic stress level of 0.65 τ_{max} is selected, it is necessary
simply to count the number of peaks in the irregular stress
history at each stress level (expressed as a fraction of τ_{max})
and multiply this number of peaks by a conversion factor obtained
from Figure 4-10b. This provides the equivalent number of cycles
at 0.65 τ_{max} for that stress level. Repeating this process for
all stress levels and summing the results provides the total
number of cycles for the entire stress history. This process
is illustrated in Figure 4-11.
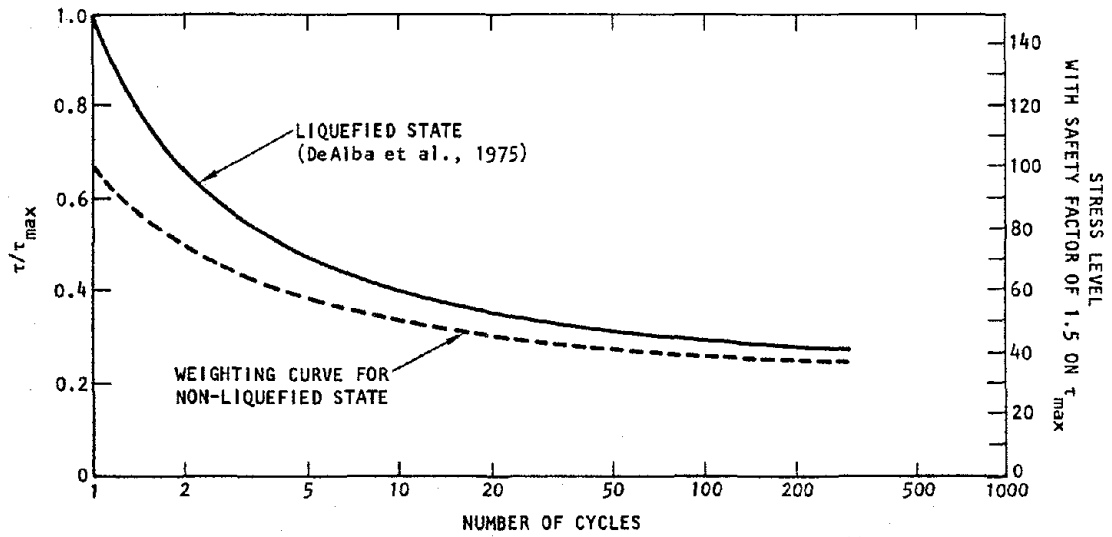
(a) Derivation of general weighting curve
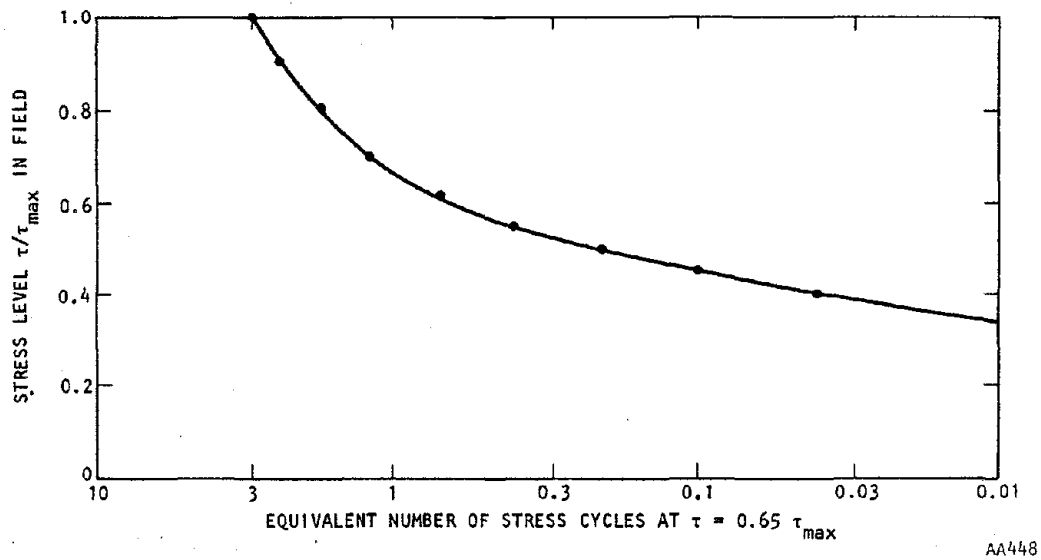
(b) Weighting curve for cyclic stress
     level of $0.65\tau_{max}$

FIGURE 4-10. EMPIRICAL PROCEDURE FOR OBTAINING EQUIVALENT
CYCLIC SHEAR STRESSES (Seed et al., 1975b)

ORION BLVD. RECORD, N-S COMP., SAN FRANCISCO EARTHQUAKE, 1971
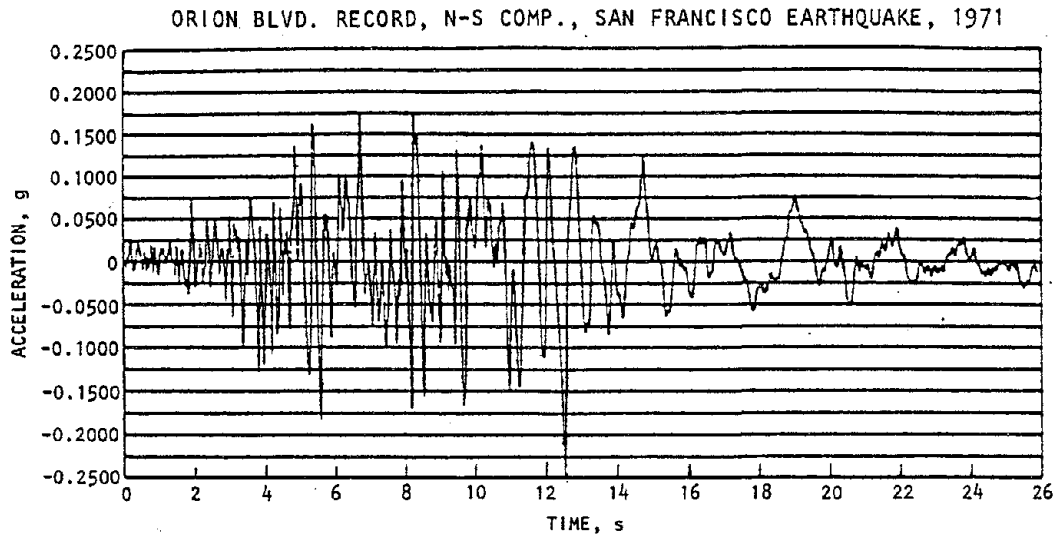
Stress Level: Fraction of τ_{max}	Above Horizontal Axis			Below Horizontal Axis		
	Number of Stress Cycles	Conversion Factor	Equivalent No. of Cycles at 0.65 τ_{max}	Number of Stress Cycles	Conversion Factor	Equivalent No. of Cycles at 0.65 τ_{max}
τ_{max}	--	--	--	1	3.00	3.00
0.95 τ_{max}	--	--	--	--	--	--
0.90 τ_{max}	--	--	--	--	--	--
0.85 τ_{max}	--	--	--	--	--	--
0.80 τ_{max}	--	--	--	--	--	--
0.75 τ_{max}	--	--	--	--	--	--
0.70 τ_{max}	2	1.20	2.40	2	1.20	2.40
0.65 τ_{max}	1	1.00	1.00	2	1.00	2.00
0.60 τ_{max}	--	--	--	2	0.70	1.40
0.55 τ_{max}	6	0.40	2.40	--	--	--
0.50 τ_{max}	1	0.20	0.20	3	0.20	0.60
0.45 τ_{max}	1	0.10	0.10	2	0.10	0.20
0.40 τ_{max}	2	0.04	0.08	3	0.04	0.12
0.35 τ_{max}	1	0.02	0.02	6	0.02	0.12
0.30 τ_{max}	--	--	--	--	--	--
		Total	6.20		Total	9.84
	Average number of cycles at 0.65 τ_{max} = 8.0					

AA452

FIGURE 4-11.   EVALUATION OF EQUIVALENT UNIFORM CYCLIC STRESS SERIES FOR ORION BLVD. RECORD, N-S COMPONENT (Seed et al., 1975b)

It is noted that the Seed et al. (1975b) approach, as summarized in the above paragraphs, represents the primary technique now used for obtaining equivalent cycles in conjunction with a *deterministic* analysis. Alternative procedures based on cumulative damage laws in a *probabilistic* framework have also been employed and are summarized in Section 4.2.1.

4.2.3 STEP 3: ASSESSMENT OF LIQUEFACTION POTENTIAL OF SITE

The final step in the total stress method of analysis of port and harbor facilities is the evaluation of the liquefaction potential at the facility site. This involves the development of data that define critical cyclic stress conditions that lead to liquefaction at the site, and the comparison of these data with the earthquake-induced stresses obtained from Steps 1 and 2. Two approaches are available for providing critical stress data: (1) empirical methods, based on observations of the performance of sand deposits during prior earthquakes; and (2) experimental methods, which involve the laboratory testing of soil samples from the site to determine critical stress conditions that lead to liquefaction. Because both of these general approaches warrants consideration in conjunction with total stress evaluations of port and harbor site liquefaction potential, their applicability to this problem is described in the summaries that follow.

4.2.3.1 Empirical Method

Empirical methods are based on the compilation of extensive field data from prior cases involving known field behavior and site conditions and estimated or measured ground motions. From these compilations, combinations of those conditions shown by the field data to correspond to the occurrence or nonoccurrence of liquefaction are identified, from which lower bound conditions for the onset of liquefaction at a particular site can be defined.

The principal work in the compilation of field data and the development of empirical methods has been carried out by Professor H.B. Seed and his associates. The first work along these lines was described by Seed and Idriss (1971), and subsequent expansions in the field data base and in experimental programs that have provided important insights into the phenomena of liquefaction. This has led to improved empirical data of the type used most recently by Seed and Idriss (1981).

The most important features of these recent empirical methods are the data base, the soil representation, and the applicability of the present empirical procedures. These are summarized in the subsections that follow, together with a description of how the procedure can be used with the Step 1 and Step 2 dynamic analysis results.

4.2.3.1.1 *Data Base*

An important feature of the empirical methods is the significant field data on which they are based. The Seed-Idriss (1981) methods are based on data from Japan and also from the United States (Alaska and California), Chile, and most recently from China, Guatemala, and Argentina. These represent a substantial data base reflecting a range of earthquake conditions under which the occurrence or nonoccurrence of liquefaction was observed.

4.2.3.1.2 *Soil Representation*

The characteristics of the soil layer under investigation are represented in the empirical methods using Standard Penetration Test (SPT) blowcounts. In this, it is recognized that the SPT blowcounts: (1) may not be an appropriate index of the liquefaction characteristics of soils; and (2) may be strongly dependent on the particular boring and sampling procedures used for its determination. Nevertheless, ample field data for

indicating liquefaction potential are presently available only in terms of SPT blowcounts, although this situation will undoubtedly change with time as other index parameters are determined for soils whose liquefaction resistance has been established by actual earthquakes.[*]

The Seed-Idriss (1981) procedures use equivalent SPT blow-counts that correspond to an overburden pressure of 1 ton/sq ft. To obtain such blowcounts, procedures are provided to correct the actual measured blowcounts to account for various factors related to the material properties, confining pressure, overburden pressure, and layer depth (Table 4-4). Furthermore, these equiva-lent SPT blowcounts presume certain standard field test procedures; any deviations from these procedures should be considered in making additional corrections to the measured blowcounts, in accordance with the judgment of the engineer.[†]

4.2.3.1.3 *Present Empirical Procedure*

The present form of the Seed-Idriss (1981) empirical approach is intended for use when no information is available on the nature of the shear stress histories in the soil, and all that is known about the ground shaking is the peak free-field acceleration at the ground surface and the magnitude of the earthquake. There-fore, the simplified procedures summarized below are used to

---

[*]Such other in situ index parameters that can be correlated with soil liquefaction characteristics include cone penetration resistance, electrical properties, shear wave velocity, etc.

[†]The standard test procedures presumed by Seed and Idriss entail: (1) the use of a rope and drum system, with two turns of the rope around the drum, to lift the falling weight; (2) drilling mud to support the sides of the hole; (3) a relatively small diameter hole, approximately 4 in. in diameter; and (4) pene-tration resistance measured over the range 6 in. to 18 in. penetration into the ground.

TABLE 4-4.   CORRECTIONS TO SPT BLOWCOUNTS FOR USE IN EMPIRICAL LIQUEFACTION ANALYSIS TECHNIQUE (Seed and Idriss, 1981)

Effect	Empirical Correction
Energy Loss in Drive Rods	For soils at depths less than 10 ft, multiply measured N values (blowcounts) by 0.75
Overburden Pressure	Correct measured blowcounts to an effective overburden pressure of 1 ton/sq ft through the expression $$N_1 = C_N \cdot N$$ where N = original measured blowcounts, C_N = function of effective overburden pressure at depth of penetration test (see adjacent figure, Marcuson and Bieganovsky, 1976), and N_1 = equivalent blowcounts corresponding to effective overburden pressure of 1 ton/sq ft
Grain Size Distribution of Sands	If $D_{50} > 0.25$ mm, use N_1 values as determined above. If silty sands and silts plotting below A-line and with $D_{50} < 0.15$ mm, use $$N_1 = N_1 \text{ (as determined above)} + 7.5$$
Confining Pressure	If the confining pressure exceeds 1.5 tons/sq ft, reduce the stress ratio causing liquefaction to allow for the reduction due to increased confining pressure. Such reductions may be determined by laboratory tests or on the basis of experience.
Clay Content and Water Content for Clayey Soils	If the clay content (determined by 0.005 mm) > 20%, consider the soil nonliquefiable. If the water content of any clayey soil (clay, sandy clay, silty clay, clayey sand, etc.) < 0.9 LL, consider the soil nonliquefiable.

(Adjacent figure in Overburden Pressure cell: plot of C_N (0 to 1.6) versus EFFECTIVE OVERBURDEN PRESSURE, kips per sq ft (0 to 10), showing curves for D_r = 40 TO 60% and D_r = 60 TO 80%)

estimate cyclic stress ratios for use in the liquefaction assessments. Extension of this present approach to accommodate soil shear stresses obtained from dynamic analysis is described in Section 4.2.3.1.4.

With this as background, the present Seed-Idriss approach first computes a free-field cyclic stress ratio from the following formula:

$$\frac{\tau_h}{\sigma_v'} = 0.65 \frac{a_{max}}{g} \frac{\sigma_v}{\sigma_v'} r_d \tag{4-1}$$

where

τ_h = Cyclic shear stress

σ_v' = Initial effective overburden stress acting at the location of interest prior to the earthquake

σ_v = Total overburden stress acting at the location of interest

a_{max} = Peak acceleration at ground surface

g = Acceleration of gravity

r_d = Stress reduction faction that accounts for the effect of the depth of the location of interest below the ground surface (Seed and Idriss, 1971)

The development of the present form of the empirical curves involved the use of Equation 4-1 to compute a cyclic shear stress ratio at the numerous sites throughout the world where peak accelerations were either measured or estimated and where it was known whether or not liquefaction occurred. These cyclic stress ratios and the corresponding modified SPT blowcounts were then plotted and, from a compilation of numerous data of this type, a family of curves was developed that, for a range of earthquake

magnitudes, defined critical combinations of cyclic stress ratio and modified SPT blowcounts representative of lower bound conditions for the onset of liquefaction. The most recent family of curves of this type, as developed by Seed and Idriss (1981), is shown in Figure 4-12a. An example correlation of the particular Seed-Idriss curve for magnitude 7.5 earthquakes with recent field data from China, Central and South America, and Japan is shown in Figure 4-12b.

It is important to note in this approach that the earthquake magnitude is considered by Seed and his associates to be representative of the number of stress cycles which, of course, is also an important variable for defining the onset of liquefaction.[*] In fact, in their most recent work that led to the curves shown in Figure 4-12a, Seed and Idriss considered the data from magnitude 7.5 earthquakes to be a baseline, because of the significant amount of data at that general magnitude level that had recently been obtained. Then, to obtain corresponding curves at other magnitude levels, Seed and Idriss used the following procedure:

1. From prior statistical analyses of strong motion data by Seed et al. (1975b), in which magnitude was correlated with equivalent number of stress cycles (obtained from measured peak acceleration and Eq. 4-1), an equivalent number of stress cycles at each given magnitude level was established (Fig. 4-13a).

---

[*]Prior statistical studies have shown that the duration of strong shaking increases with earthquake magnitude (e.g., Trifunac and Brady, 1975). Since the number of stress cycles will also increase with increasing duration, Seed and his associates have used the earthquake magnitude as a means of representing the number of stress cycles in their empirical approach.
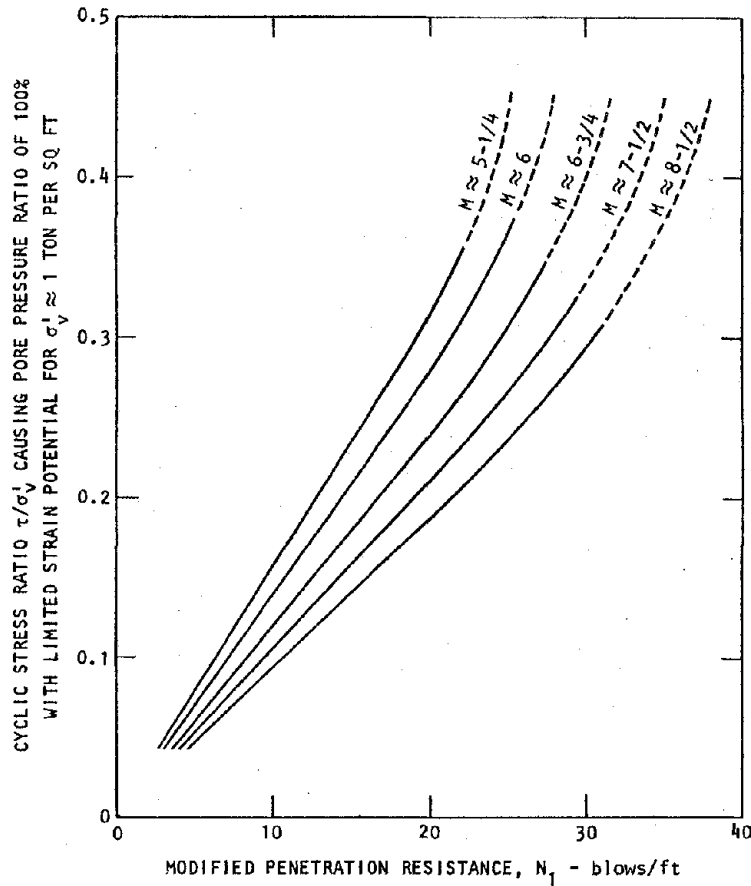
(a) Chart for evaluation of liquefaction potential for different magnitude earthquakes
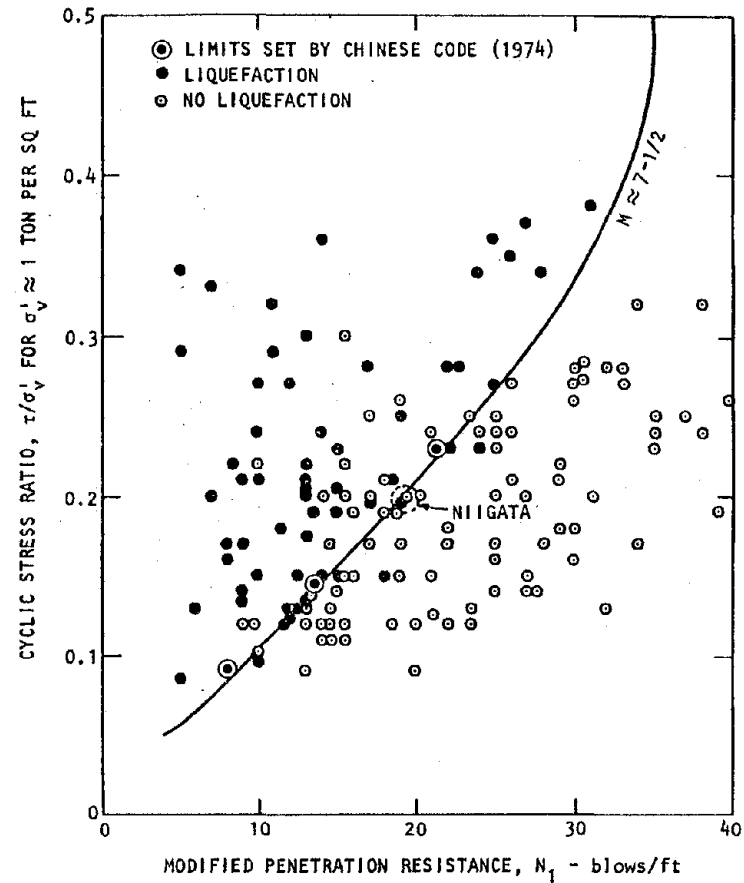
(b) Correlation between field liquefaction behavior of sands ($D_{50} > 0.25$ mm) under level ground conditions and standard penetration resistance (all data)

FIGURE 4-12. EMPIRICAL LIQUEFACTION ANALYSIS TECHNIQUE (Seed and Idriss, 1981)
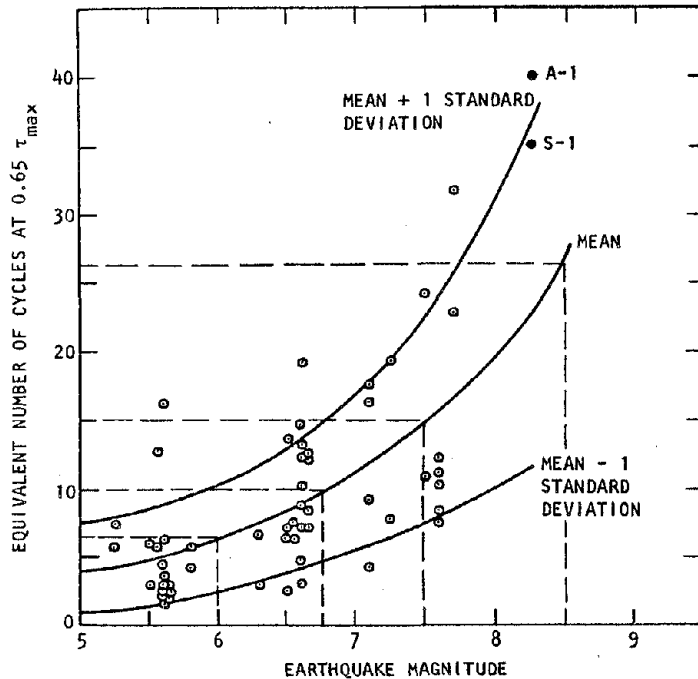
(a) Statistical correlations of magnitude vs. equivalent number of shear stress cycles

EQUIVALENT NUMBER OF CYCLES AT 0.65 τ_{max}

MEAN + 1 STANDARD DEVIATION

MEAN

MEAN - 1 STANDARD DEVIATION

• A-1
• S-1

EARTHQUAKE MAGNITUDE
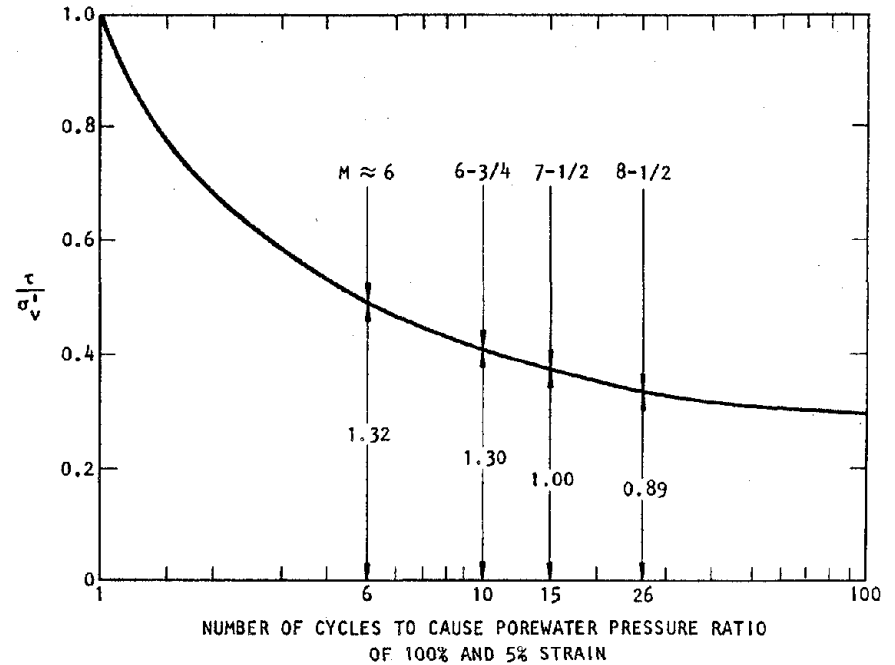
(b) Basis for scale factors for various earthquake magnitudes

$\dfrac{\tau}{\sigma'_v}$

M ≈ 6   6-3/4   7-1/2   8-1/2

1.32   1.30   1.00   0.89

NUMBER OF CYCLES TO CAUSE POREWATER PRESSURE RATIO OF 100% AND 5% STRAIN

Earthquake Magnitude	No. of Representative Cycles at 0.65 τ_{max}	$\dfrac{\left(\dfrac{\tau_{av}}{\sigma'_v}\right)_{M\ =\ Variable}}{\left(\dfrac{\tau_{av}}{\sigma'_v}\right)_{M\ =\ 7.5}}$
8-1/2	26	0.89
7-1/2	15	1.0
6-3/4	10	1.13
6	6	1.32
5-1/4	2-3	1.5

(c) Computation of scale factors

FIGURE 4-13. DEVELOPMENT OF SCALE FACTORS FOR SEED-IDRISS (1981) FAMILY OF LIQUEFACTION CURVES

AA453

2. From laboratory tests which established critical combina-
    tions of cyclic stress ratio and number of cycles to
    cause liquefaction, cyclic stress ratios were defined
    for each number of stress cycles defined for the
    various magnitude levels in Step 1 (Fig. 4-13b).

3. Ratios were computed of the cyclic stress ratio
    established in Step 2 for each magnitude level to the
    cyclic stress ratio established for magnitude 7.5.
    These ratios corresponded to the factors by which the
    Seed-Idriss liquefaction curve for magnitude 7.5 was
    scaled to obtain the curve for each of the other
    magnitude levels (Fig. 4-13c).

4.2.3.1.4 *Extension of Procedure to Accommodate Dynamic Analysis Results*

Under the total stress dynamic analysis procedure being
described herein for port and harbor facilities, the earthquake-
induced cyclic stress ratio and equivalent number of cycles has
been obtained from the first two steps of the procedure. These
results can be used with the following modified form of the Seed-
Idriss (1981) empirical procedure to assess the liquefaction
potential at the port and harbor facility site:

●   From Steps 1 and 2 of the dynamic analysis procedure,
    obtain the equivalent number of cycles, N_{eq}, of
    earthquake-induced stress at 0.65 τ_{max} for a given
    location within the site.

●   It is now desired to use the Seed-Idriss approach to
    construct critical liquefaction curves for this

particular condition of N_{eq} cycles. To do this, the following procedure is carried out (Fig. 4-14):

a. As in the original Seed-Idriss procedure, use their liquefaction curve for magnitude 7.5 as a baseline, except now consider this curve to correspond to 15 cycles of stress (which is the average number of stress cycles shown by Seed et al. (1975b) to correspond to this magnitude level).

b. Use the curve in Figure 4-13b to define the critical cyclic stress ratio for N_{eq} cycles and for 15 cycles.

c. Compute a scale factor as the ratio of these two sets of critical cyclic stress ratios. Use this ratio to scale the Seed-Idriss liquefaction curve for 15 cycles (i.e., magnitude 7.5) to obtain the liquefaction curve for N_{eq} cycles.

● Plot the earthquake-induced cyclic stress obtained from the dynamic analysis, together with the modified penetration resistance at the particular location of the stress computation, within the set of axes containing the above Seed-Idriss liquefaction curve for N_{eq} cycles. Assess the liquefaction potential at that location, based on where the earthquake results fall relative to this liquefaction curve.

● Alternately, read off the cyclic stress ratio required to cause liquefaction in N_{eq} cycles for the appropriate modified penetration resistance, and divide this by the cyclic stress ratio corresponding to a cyclic shear stress of $0.65 \, \tau_{max}$, in order to obtain a factor of safety against liquefaction.

FROM RESULTS OF SEISMIC ANALYSIS
(STEPS 1 AND 2):

0.65 τ_{max} (CYCLIC STRESS RATIO)

N_{eq} (NUMBER OF CYCLES)

MODIFIED PENETRATION
RESISTANCE AT LOCATION
OF STRESS COMPUTATION,
MP_i

$\frac{\tau}{\sigma_v'}$

$\left(\frac{\tau}{\sigma_v'}\right)_{N_{eq}}$ CYCLES

$\left(\frac{\tau}{\sigma_v'}\right)_{15}$ CYCLES

N_{eq}

NUMBER OF CYCLES TO CAUSE POREWATER PRESSURE
RATIO OF 100% AND 5% STRAIN

SCALE FACTOR:

$$S.F. = \frac{\left(\frac{\tau}{\sigma_v'}\right)_{N_{eq}}}{\left(\frac{\tau}{\sigma_v'}\right)_{15}}$$

CYCLIC STRESS RATIO τ/σ_v' CAUSING PORE PRESSURE
RATIO OF 100% WITH LIMITED STRAIN POTENTIAL
FOR $\sigma_v' = 1$ TON PER SQ FT

LIQUEFACTION
CURVE FOR N_{eq}
CYCLES,
$(L.C.)_{15}$ x S.F.

$\frac{0.65\ \tau_{max}}{\sigma_v'}$

SEED-IDRISS
LIQUEFACTION
CURVE FOR 15
CYCLES,
$(L.C.)_{15}$

MP_i

MODIFIED PENETRATION RESISTANCE, blows/ft

AA449

FIGURE 4-14.   ASSESSMENT OF LIQUEFACTION POTENTIAL USING SEED-IDRISS (1981)
EMPIRICAL PROCEDURE WITH DYNAMIC ANALYSIS RESULTS

4.2.3.2 Methods Based on Laboratory Tests

A second approach for evaluating the liquefaction potential of the soil materials at port and harbor facility sites is through the use of laboratory cyclic load tests of the site soil materials. A brief summary of the historical development of current laboratory testing techniques, and a description of current test procedures is provided in the paragraphs that follow. For more detailed information, the reader is referred to the excellent summary papers that exist in this area (e.g., Seed, 1979a; Finn, 1981 and 1982) and to the various references cited below.

4.2.3.2.1 *Development of Test Procedures*

The objective of laboratory cyclic test procedures is to measure the potential for liquefaction of soil samples under conditions that represent as closely as possible the field conditions of the soil medium during the earthquake shaking. This requires the use of careful samping techniques as well as state-of-the-art testing techniques by experienced and capable engineers with a due regard for the various factors that influence the liquefaction characteristics of sandy soil materials.

a. Basic Testing Techniques

Initially, cyclic triaxial tests were used to evaluate the liquefaction potential of sands (Seed and Lee, 1966), although it was subsequently realized that cyclic simple shear tests provide a better representation of the loadings on elements of soil (Seed and Peacock, 1971). At that time, however, cyclic simple shear tests were thought to be difficult to conduct, and appropriate test apparatus was not widely available. As a result, routine soils testing for liquefaction assessments continued to be carried out using cyclic triaxial tests, but with an appropriate simple shear correction factor, C_r, to make these test results

representative of those under simple shear conditions (or more strictly to conditions in the field).[*]

At the present time, the use of cyclic simple shear tests has become more routine, particularly in view of the recent realization that undrained loadings could be simulated in constant-height cyclic simple shear tests (Pickering, 1973; Moussa, 1975); however, cyclic triaxial tests are still most widely used in current practice. For either type of test, procedures are now available for correcting test results to account for membrane compliance (Martin et al., 1975 and 1978).

b.   Summary of Research Programs

Since the initial development of the above laboratory test procedures, considerable research has been directed toward gaining insight into the factors affecting the liquefaction characteristics of soils. This has provided an improved understanding of liquefaction phenomena, and a corresponding improved basis for interpreting and carrying out laboratory tests. Results from these investigations are summarized in Table 4-5 and show that only one of the factors investigated--that of multidirectional shaking--resulted in a reduced resistance to liquefaction. Of the remaining factors, it has been shown that increases in relative density, preparation of samples by tamping or vibration

---

[*]In this, the relationship between cyclic stress ratios for simple shear tests to those from cyclic triaxial tests is expressed as

$$\left(\frac{\tau_h}{\sigma_v'}\right)_{\text{simple shear}} = C_r\left(\frac{\sigma_{dc}}{2\sigma_3}\right)_{\text{triaxial}}$$

where τ_h is the cyclic shear stress on the horizontal plane, σ_v' is the effective overburden pressure, and σ_{dc} and σ_3 are the cyclic deviator stress and the ambient pressure respectively from the cyclic triaxial test.

TABLE 4-5.   FACTORS INFLUENCING LIQUEFACTION POTENTIAL — SUMMARY OF
RESEARCH PROGRAMS (Seed, 1979a; Finn, 1981; Pyke, 1982)

Factor	Investigators	Results
Sample Size	DeAlba et al. (1976)	Large-scale simple shear tests on samples prepared by pluviation showed that early results from cyclic simple shear tests on smaller samples were generally correct.
Multidirectional Shaking in Simple Shear Tests	Pyke et al. (1974) Seed et al. (1975d) Ishihara and Yamazaki (1980)	Under multidirectional shaking or stress conditions, porewater pressures build up faster than under unidirectional shaking, and the cyclic stress ratio required to cause liquefaction is about 15% less for multidirectional shaking.
Method of Sample Preparation and Soil Structure	Pyke (1974) Ladd (1974, 1977) Mulilis et al. (1975)	The characteristics of saturated sands under cyclic loading are significantly influenced by sample preparation. To illustrate this, it has been shown that preparation of samples by tamping or vibration, as opposed to pluviation, tends to increase their resistance to liquefaction. Different structural arrangements of the sand grains due to different sample preparation methods have led to markedly different porewater pressure development characteristics.
Relative Density	Castro and Poulos (1977) and many others	The resistance of soil samples to liquefaction is increased substantially with increasing relative density.
Grain Characteristics	Wong et al. (1975) Finn (1981) Tokimatsu and Yoshimi (1981)	When corrected for system compliance, laboratory test values of cyclic stress ratio causing initial liquefaction in clean sands are not sensitive to variations in mean grain diameter. However, finer grained soils (silty sands and silts) are more resistant to liquefaction than are clean sands for the same apparant relative density, and clays are considered to have no potential for liquefaction.
Previous Strain History	Finn et al. (1970) Seed et al. (1977) Ishihara and Okada (1978)	An increased resistance to liquefaction occurs when small cyclic shear strains are applied to a saturated undrained sand sample and drainage is not allowed to occur.
Lateral Pressure Coefficient and Overconsolidation	Seed and Peacock (1971) Ishihara and Takatsu (1979) Finn and Bhatia (1980)	Cyclic stress ratios required to cause liquefaction are significantly increased by the overconsolidation ratio OCR and by the coefficient of lateral pressure at rest, K_o.
Geologic Age	Ohsaki (1969) Casagrande (1976) Youd and Hoose (1977)	The resistance of soil samples to liquefaction is increased with increasing geologic age.

(as opposed to pluviation), prestraining, sustained consolidation, and geologic age all tended to increase the resistance to lique-faction. Grain size effects on the liquefaction resistance of clean sands has been shown to be small; however finer grained soils (silty sands and silts) have been shown to be more resistant to liquefaction than are clean sands at the same state of compactness. Effects of sample size on liquefaction resistance have been shown to be small, as indicated by comparisons of results from large scale simple shear tests (using samples prepared by pluviation) with those from simple shear tests on smaller samples.

c. Effects of Initial Shear Stresses

As previously noted in Section 4.2.1.2, the effects of initial static shear stresses on horizontal planes, which occur due to the departure of the site from level ground conditions or due to the presence of large structures, may, in some cases, be important for port and harbor facilities as well as for earth structures. In general, it has been established that the presence of these initial shear stresses will tend to increase the resistance to liquefaction (Lee and Seed, 1967; Vaid and Finn, 1979). However, porewater pressure buildup and liquefaction is a potential problem even in the presence of initial shear stresses (Seed, 1979a) but, despite this, relatively little attention has been given to the effects of such stresses on the potential for liquefaction of soil deposits. Indeed, most of the research projects summarized in Table 4-5 and in the preceding paragraph have been based on level ground conditions (with no initial shear stresses) although the general trends from these studies would appear to hold when significant initial shear stresses are present. In practice, porewater pressure effects on soils with initial shear stresses are evaluated either using cyclic simple shear tests with initial static stress conditions (Finn and Byrne, 1976) or, more commonly,

by cyclic triaxial tests on anisotropically consolidated samples
with an appropriate simple shear correction factor (Lee and Seed,
1967).

d.   Definition of Simple Shear Correction Factor

The simple shear correction factor, C_r for cyclic triaxial
tests (as defined earlier in this subsection), is dependent on
whether the sands are isotropically consolidated (corresponding
to level ground conditions) or anisotropically consolidated
(corresponding to conditions leading to significant initial shear
stresses on horizontal planes). For anisotropically consolidated
cyclic triaxial tests, C_r has generally been taken to have a
value of about 1.0, when K_c (the anisotropic consolidation
ratio) is 1.5 or greater (Pyke, 1982). The remaining discussion
corresponds to the more commonly considered level grounds condi-
tions with isotropic consolidation (K_c = 1.0).

During the initial development of cyclic triaxial test proce-
dures for isotropic consolidated sands, C_r was considered to be
dependent primarily on relative density and to have a value of
about 0.6. Since then, values of C_r proposed by Finn et al.
(1971), Seed and Peacock (1971), and Castro (1975) have ranged
from 0.55 to 1.0, depending on the coefficient of lateral pres-
sure at rest, K_o (Table 4-6). Subsequent comparisons by DeAlba
et al. (1976) of cyclic triaxial and simple shear test results for
normally consolidated sands ($K_o \cong 0.4$) and for a range of relative
densities have shown C_r to be about 0.63 (Fig. 4-15), although
this value varied slightly with the number of cycles. In view of
the agreement between these various investigators, the original
assumption of C_r = 0.6 appears reasonable for freshly deposited,
normally consolidated sands, although it should be noted that the
effects on C_r of several of the factors listed in Table 4-5 have
not yet been evaluated. For overconsolidation sands, studies more

TABLE 4-6. ESTIMATES OF SIMPLE SHEAR CORRECTION FACTOR, C_r, FOR LEVEL GROUND CONDITIONS (Seed, 1979a)

Source	Equations	C_r for $K_o = 0.4$	C_r for $K_o = 1.0$
Finn et al. (1971)	$C_r = (1 + K_o)/2$	0.7	1.0
Seed and Peacock (1971)	Varies	0.55 - 0.72	1.0
Castro (1975)	$C_r = 2(1 + 2K_o)/(3\sqrt{3})$	0.69	1.15
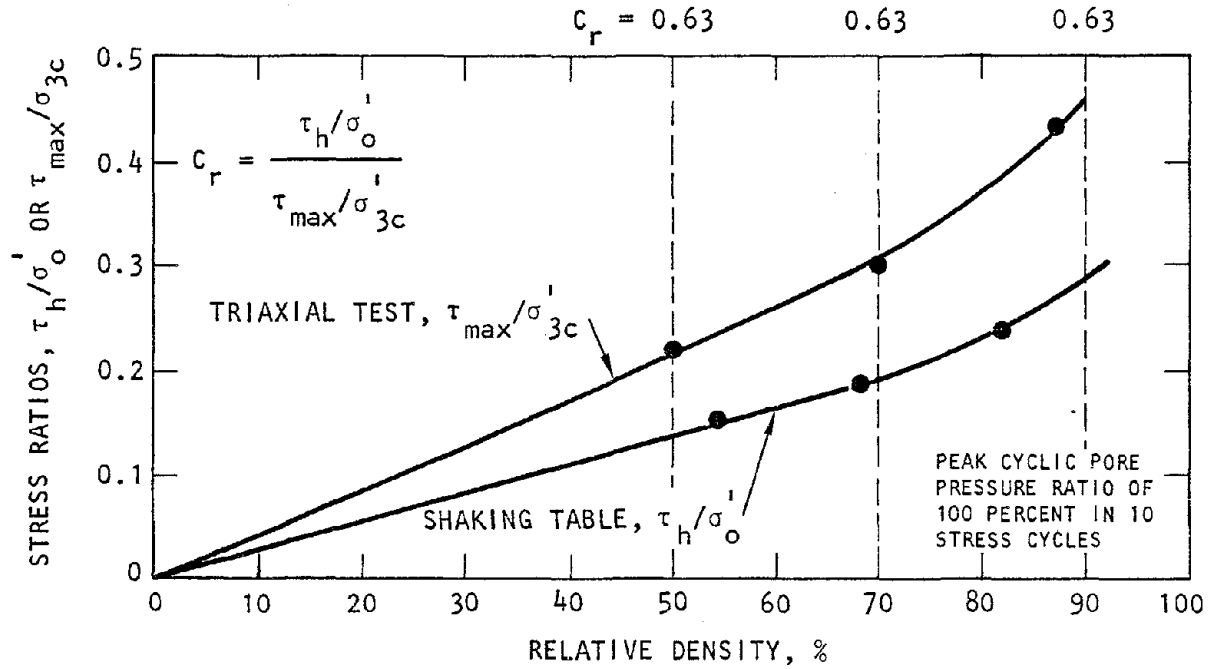
FIGURE 4-15. ESTIMATES OF C_r FROM COMPARISON OF SHAKING TABLE AND TRIAXIAL TEST RESULTS FOR LEVEL GROUND CONDITIONS (DeAlba et al., 1976)

recent than those shown in Table 4-6 have shown that effects of overconsolidation in increasing the resistance to liquefaction are even greater than had been previously assumed (Ishihara and Takatsu, 1979; Finn and Bhatia, 1980). From these studies, the ratio of the cyclic stress ratio causing liquefaction of clean sands for overconsolidated samples to that for normally consolidated samples appears to be about 1.4 for an Overconsolidation Ratio (OCR) of 2 and about 2.0 for an OCR of 4. Ishihara et al. (1978a) had previously shown that the effect of overconsolidation is even more significant for sands with fines than for clean sands.

d. Sampling and Handling

The effects of sampling and handling of the soil specimens can be very important and should be considered in the interpretation of laboratory test data. Prior studies have shown that the beneficial effects of prestraining, and also presumably of overconsolidation and sustained consolidation, tend to be erased by even the most careful sampling, and that the effect of sample disturbance is invariably to reduce the resistance to liquefaction, whatever the changes in sample density. Thus, while it is desirable to test only samples that have been obtained by the most careful sampling and handling procedures, even then the results may be conservative.

In the last few years, there has been considerable improvement in techniques for minimizing sample disturbance, and there is evidence that these improvements may well reduce the effects of sample disturbance noted above (Seed et al., 1982). Good sampling practice for potentially liquefiable sands that are saturated (i.e., are below the water table) now involves either draining before shipping or freezing (Walburg, 1978; Ishihara et al., 1978b; Singh et al., 1979). Freezing has the significant

advantage that extraction and setting up of test specimens in the laboratory becomes much easier, and the possibility of disturbance at this stage is essentially eliminated (Singh et al., 1982; Pyke, 1982). For the case of new fills, where one cannot start with samples of in-situ material, samples should generally be prepared in the laboratory using the "moist tamping" procedure (Ladd, 1977) and allowance should be made for the expected effects of aging.

4.2.3.2.2 *Application of Test Procedures*

As previously discussed, a dynamic analysis of port and harbor facilities within a total stress framework involves three main steps, in which Steps 1 and 2 are directed toward obtaining earthquake-induced structure stresses as well as cyclic shear stresses at appropriate locations in the soil medium; these stresses include the effects of soil/structure interaction, the topography of the site, etc. The soil cyclic shear stresses obtained from these dynamic analyses, as well as static states of shear stress obtained from static analyses (if warranted by site conditions), serve as input to the laboratory test evaluations of the liquefaction potential at the site (Step 3). The use of laboratory tests in this manner is outlined in Figures 4-16 and 4-17 and is described in the paragraphs that follow.

a. Laboratory Testing

The first step in this procedure involves the conducting of the laboratory tests to determine the cyclic shear stresses causing liquefaction of the test samples (Step A, Fig. 4-16). These tests would be conducted at various levels of cyclic stress, τ_{cy}, or of cyclic stress ratio τ_{cy}/σ_v' causing failure as a

INPUT
• Earthquake induced cyclic shear stresses from dynamic analysis of soil/structure system, τ_h
• Static shear stresses, if warranted by conditions at site, from static analysis of soil/structure system

LABORATORY TEST PROCEDURES		
Step	Conventional Procedure	Possible Extensions or Modifications (1982)
A. Conduct laboratory tests to determine cyclic shear stresses causing liquefaction of soil samples, τ_{cy}	Use cyclic triaxial tests	Always use intact samples. Conduct constant height simple shear tests. Account for any initial static shear stresses that may be present before the earthquake (Seed et al., (1975a).
B. Correct laboratory test results to field conditions	Use simple shear correction factor $(C_r) \cong 0.6$ for $K_c = 1.0$, and $C_r \cong 1.0$ for $K_c \geq 1.5$	Correct as a function of geologic age, overconsolidation ratio, prestraining, soil type, and degree of disturbance.
C. Determine potential for liquefaction at site	Compute Factor of Safety as: $$F.S. = \frac{\tau_{cy} \text{ (from Step B)}}{\tau_h \text{ (from analyses)}}$$	If F.S. > 1, one can estimate the pore-water pressure ratio from standard curves as a function of N/N_ℓ (Fig. 4-17). Alternatively, instead of using F.S., one can evaluate liquefaction potential using cumulative damage concepts (Donovan, 1971).

FIGURE 4-16. USE OF LABORATORY TEST PROCEDURES IN TOTAL STRESS DYNAMIC ANALYSIS OF PORT AND HARBOR FACILITIES (Pyke, 1982)

LEGEND

u_g = POREWATER PRESSURE

σ'_{v_o} = INITIAL EFFECTIVE STRESS

N = NUMBER OF STRESS CYCLES APPLIED DURING EARTHQUAKE

N_ℓ = NUMBER OF STRESS CYCLES REQUIRED TO CAUSE INITIAL LIQUEFACTION

AVERAGE

PORE PRESSURE RATIO, $r_u = u_g/\sigma'_{v_o}$

CYCLE RATIO, N/N_ℓ
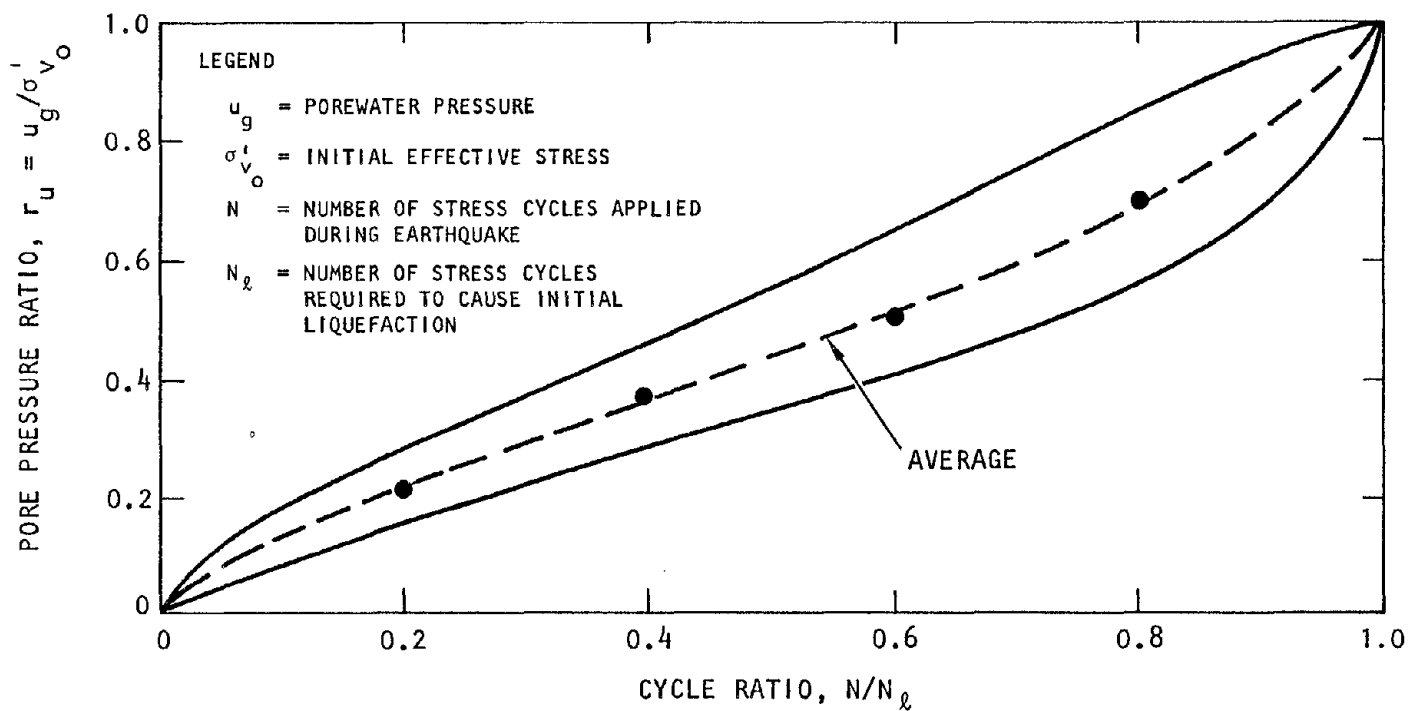
FIGURE 4-17.   RATE OF POREWATER PRESSURE BUILDUP IN CYCLIC SIMPLE SHEAR TESTS (after DeAlba et al., 1976)

function of the number of cycles of loading (Fig. 4-18)[*]. In this, "failure" in laboratory tests may be taken as "initial liquefaction"--defined either in terms of stresses (i.e., when the excess porewater pressure first equals the confining pressure, σ_v') or in terms of strains (usually when the peak-to-peak axial strain first reaches 0.10 in cyclic triaxial tests or when the peak-to-peak shear strain first reaches 0.15 in cyclic simple shear tests).

As indicated in Figure 4-18, the above laboratory tests are most typically carried out using cyclic triaxial procedures although, as previously noted, recent developments have seen an increased use of cyclic simple shear tests. Such tests should incorporate the effects of any initial static shear stresses on horizontal planes that may be significant. The presence of such stresses, which occur under slopes or heavy structures, substantially complicates the laboratory test program. For these conditions, several sets of laboratory tests with different initial shear stresses must be conducted to cover the range of initial stress states shown to exist by static analyses of the type described in Section 4.2.1.2.1. The subsequent procedures used for modifying these test results to represent field conditions should be similar to those used for earth dams (Seed et al., 1975a; Seed, 1979b).

b. Laboratory Test Correction

The second step in the use of laboratory tests to evaluate the potential for liquefaction at port and harbor sites involves

---

[*]When preparing results of the type shown in Figure 4-18, it is often convenient to normalize the cyclic shear stress causing failure by the confining pressure; however there are conditions for which this normalizaton is not appropriate and for which separate plots of cyclic shear stress vs. cycles to failure must be developed for a range of confining pressures (Pyke, 1982).
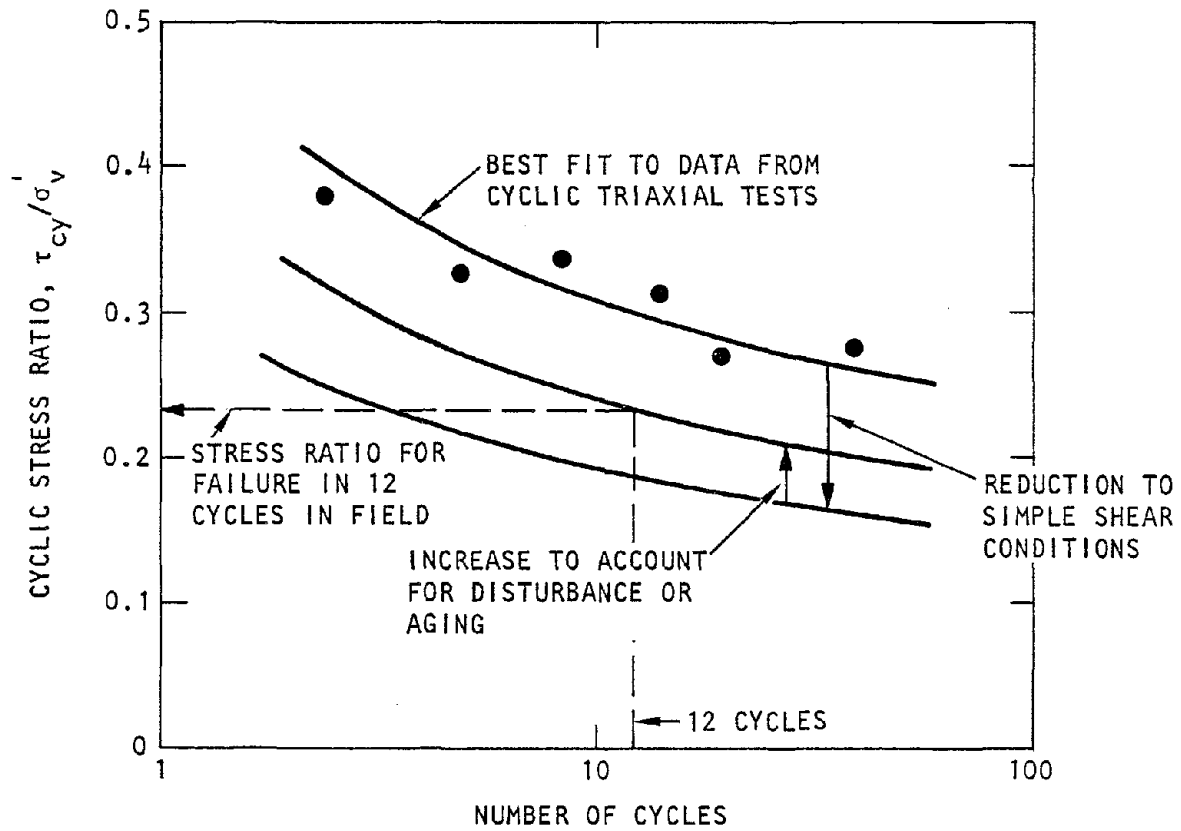
FIGURE 4-18. USE OF LABORATORY TEST RESULTS TO ASSESS
LIQUEFACTION POTENTIAL FOR LEVEL GROUND
CONDITIONS (Pyke, 1982)

the correction of the laboratory test results from Step A to correspond to field conditions (Step B, Fig. 4-16). The conventional approach for making such corrections is through the use of a simple shear correction factor (C_r) of about 0.6 in conjunction with cyclic triaxial testing, as discussed previously. However, with the availability of the extensive results from the research programs summarized previously, corrections to cyclic triaxial or cyclic shear test data can be made to account for such factors as geologic age, overconsolidation ratio, prestraining, soil type, and degree of disturbance.

c. Evaluation of Liquefaction Potential

The final step in this laboratory test procedure involves evaluation of the liquefaction potential of the port and harbor facility site (Step C, Fig. 4-16). The conventional procedure for carrying this out involves a two-step process for each soil location at which the evaluation is to be carried out. First, for the number of shear stress cycles obtained from the dynamic analysis results for that location, the curve from the laboratory test results (Fig. 4-18) is used to obtain the cyclic stress or cyclic stress ratio causing liquefaction (including, of course, the appropriate corrections to represent field behavior). This quantity is then divided by the corresponding stress or stress ratio from the dynamic analysis results, and the resulting ratio is termed the Factor of Safety against liquefaction (F.S.); i.e., if F.S. > 1, the soil at the location in question can be considered safe from liquefaction. It is noted that, in the determination of F.S., the cyclic shear stress or stress ratio from the dynamic analysis is most typically considered to be 0.65 τ_{max}, where τ_{max} is the maximum dynamic shear stress computed at the location in question.

Other techniques are available as supplements or alternatives to the above definition of Factors of Safety to indicate the liquefaction potential for the site. For example, for cases where F.S. > 1, it is possible to use experimentally developed normalized curves of the type shown in Figure 4-17 to evaluate the extent of the porewater pressure buildup (DeAbla et al., 1976). Also, as an alternative to the use of F.S. as described above, some investigators have used cumulative damage concepts based on an analogy between Miner's fatigue law and the cyclic behavior of saturated sands to estimate liquefaction potential (e.g., Donovan and Singh, 1978). This approach is described within the framework of probabilistic methods in Section 4.4.

4.2.3.3 Discussion of Methods

In this discussion of total stress methods of dynamic analysis of port and harbor facilities, two techniques--empirical and experimental--have been described for assessing whether the facility site will liquefy due to the computed earthquake-induced cyclic stress field. It is clear that both methods have important advantages; i.e., the empirical results provide valuable information from prior field observations of earthquake behavior, while the experimental results from laboratory testing consider the measured liquefaction characteristics of the actual soil materials at the site. However, both methods contain uncertainties as well--examples of such uncertainties are the use of SPT blowcounts in the current empirical approaches and the effects of sample disturbance in the laboratory test method. Therefore, judgment must be exercised in the use of either approach, although it would seem there is much to be gained from the use of both approaches at port and harbor facility sites.

Seed (1979a) has considered this same issue and provides the following valuable perspective that underscores the desirability for considering results from past field observations as well as from laboratory tests.

It would seem that the design engineer confronted with the need to evaluate the cyclic mobility or liquefaction potential of a deposit (under level ground) has two basic choices if he considers it appropriate to neglect the possible effects of drainage occurring during the period of cyclic stress application:

1. To calculate the stresses induced in the ground by the design earthquake...and to compare these stresses with those required to cause liquefaction of representative samples in the laboratory.... (In this procedure) the main problem will lie in correctly assessing the characteristics of the in-situ deposit from laboratory tests performed on even good quality undisturbed samples.... Two approaches are available: (a) to take the best possible undisturbed samples and then try to reconstruct their true field characteristics by subjecting them to a stress path designed to reproduce their in-situ condition or (b) to allow for sample disturbance effects by reasonable judgment.

2. To be guided by the known field performance of sand deposits correlated with some measure of in-situ characteristics, such as the standard penetration test....

It would be imprudent to ever neglect the guidance to be derived from records of past experience and this should always be considered in any site evaluation.... It is also apparent that considerable judgment is required whichever method is used. In the best situations it would hopefully be possible to obtain reasonable agreement on the potential for liquefaction using both of the available approaches. However, without the exercise of considerable judgment or a serious attempt to recreate the in-situ characteristics, the direct use of laboratory test data from tests on even "undisturbed" samples of moderately dense to dense deposits seems likely to lead to over-design in most cases.

4.3 DETERMINISTIC EFFECTIVE STRESS METHODS

4.3.1 GENERAL DISCUSSION

The preceding section has described in some detail the use of deterministic total stress methods for dynamic analysis of port and harbor facilities. As described, these methods do not incorporate effects of porewater pressure buildup and dissipation during the dynamic analysis. This important limitation is, however, overcome by a second and more complex dynamic analysis technique--deterministic effective stress methods.

Effective stress methods have experienced considerable development in recent years and are based on the premise that soil behavior is fundamentally controlled by effective stress rather than by total stress. For port and harbor facility analysis, these methods would involve: (1) use of laboratory tests of soil specimens to determine the necessary material para-meters for the effective stress soil model; and (2) a dynamic analysis that utilizes these measured material parameters to compute the soil/structure system response, including porewater pressure buildup and dissipation. Unlike total stress methods, which assess liquefaction potential through comparisons of dynamic response results with data from laboratory cyclic tests and/or empirical methods, effective stress methods assess lique-faction potential directly from the computed soil/porewater response. Of course, it will always be prudent to use empirical methods as an independent verification of any effective stress analysis.

At present, effective stress methods are primarily available as one-dimensional site response analysis techniques that treat the case of vertically propagating shear waves in a horizontally layered site. Such techniques cannot be used to analyze the

dynamic response of port and harbor facilities--where the presence
of the structure and the irregular topography that often exists
near such facilities will cause a departure from the idealized
conditions of vertically propagating shear waves. Therefore, for
port and harbor sites, one-dimensional effective stress techniques
can only be used to estimate free-field site response character-
istics in regions of the site away from the structure. To analyze
the soil/structure system response, two-dimensional or three-
dimensional techniques are required.

Although two-dimensional or three-dimensional effective
stress methods are not generally available, the desirability
of developing such methods has been recognized by geotechnical
engineers, and work is proceeding in this area (e.g., Ferritto,
1981; Finn, 1982).[*] For particular application to port and
harbor facilities, it is recognized that such methods will be
important for the following reasons:

- For many port and harbor facilities, the geometry of
  the adjacent backfill and subsurface soil deposits is
  such that drainage paths are relatively shorter than,
  for instance, large earth dams. It is therefore more
  important that the effects of dissipation of porewater
  pressure, as well as the buildup of porewater pressure,
  be considered in the analysis of such facilities.

---

[*]A two-dimensional effective stress soil model is essentially
a special case of a general three-dimensional model; hence
implementation of a three-dimensional analysis presents no new
difficulties. However, because three-dimensional analyses are
much more costly, two-dimensional analyses will be used in most
practical applications.

- As the strength and duration of the ground shaking
  increases, the influence of porewater pressure effects
  on the response of saturated cohesionless soil deposits
  that often comprise port and harbor sites will also
  increase. Therefore, for such cases, properly conceived
  and applied effective stress methods should provide
  increasingly improved representations of the port
  and harbor facility response, when appropriate two-
  dimensional or three-dimensional techniques become
  readily available.

In summary, effective stress methods can provide certain
important benefits when used for the seismic analysis of port and
harbor facilities. Unfortunately, because such methods are not
yet generally available in two-dimensional or three-dimensional
form, they must still be considered as being under development
with regard to port and harbor facility applications. In view
of this, the objective of this section is to provide information
pertinent to the future development of effective stress methods
suitable for seismic analyses of port and harbor facilities.

4.3.2 BASIC CONCEPTS

The development of effective stress methods for analyzing
the behavior of soil materials is the cornerstone of modern
soil mechanics. Pioneering work in this area was carried out
by Terzaghi (1923) who described the effect of porewater presure
on the strength and deformation of saturated porous media, and
developed a one-dimensional consolidation model that described
the compaction of the soil matrix under applied load and the
development and dissipation of excess porewater pressure. Biot
(1941) extended Terzaghi's effective stress concept to allow for
consideration of a three-dimensional stress state. His generalized

consolidation theory can be represented using two governing equations--a storage equation (which is an expression of mass balance and force equilibrium) and a constitutive equation (describing the mechanical behavior of the soil matrix). These equations are expressed in terms of the unknown porewater pressure and volumetric strain, with coupling between mechanical and fluid flow occuring through the compressibility of the fluid and the soil matrix.

Basic consolidation theory involves several simplifying assumptions, including (1) a fully saturated soil medium comprised of a linear elastic soil skeleton with incompressible soil that undergoes infinitesimal strains and has a porosity that varies linearly with effective pressure; and (2) a compressible fluid medium with a constant bulk modulus, a volume that varies linearly with porewater pressure, and a fluid flow that is governed by Darcy's Law. Subsequent development of effective stress methods has built on the basic concepts inherent in these initial simplified methods, while incorporating insights and data gained from numerous experimental investigations of porewater pressure buildup leading to liquefaction. This work, summarized by Seed (1979a) and Finn (1981) and also in Section 4.3.3 of this report, has led to current effective stress methods with the following characteristics:

- The effective stress methods are primarily one dimensional; very few two-dimensional methods have been developed and these are not readily available at this time.

- The strain dependence of the soil matrix material properties is now considered using nonlinear material models or, less commonly, equivalent linear models.

- The methods often incorporate empirical models to represent effects of several soil/fluid parameters, based on results from experimental programs. The empirical parameters needed to define these models are often not readily obtainable from conventional cyclic testing procedures.

- Various methods for coupling the behavior of the soil matrix and the porewater are employed, ranging from loosely coupled to fully coupled techniques. These are described further in Section 4.3.3.

4.3.3 CURRENT PROCEDURES

With the preceding discussion as background, some representative current effective stress procedures will now be described. In view of the significant development of effective stress methods that is presently taking place, it is not possible to describe all of the procedures now available. Therefore, selected procedures that are recognized within the earthquake engineering and geotechnical engineering community are summarized, so as to indicate the general state of the art in this area.

Both one-dimensional effective stress methods (which are predominant in current practice) and two-dimensional methods (which are largely under development) are summarized in the paragraphs that follow. For each of these, two subsets of effective stress methods--representative of loosely coupled and fully coupled soil/porewater behavior--are described. Basically, loosely coupled methods make use of two distinct models--one to describe the dynamic mechanical behavior and the other to describe porewater flow (Fig. 4-19a). Coupling between these two models may be achieved in several ways, and may incorporate various levels of interaction between mechanical and porewater flow
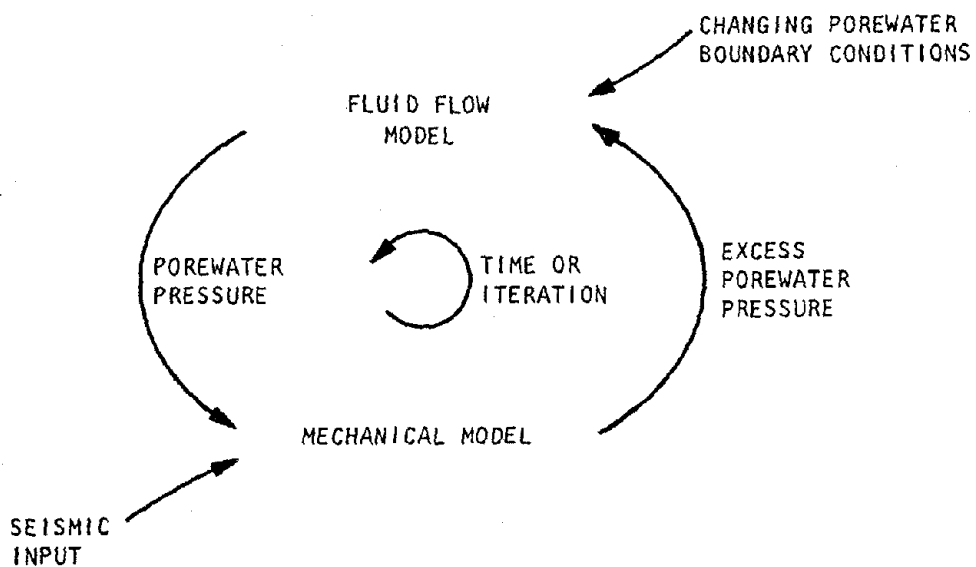
(a) Loosely-coupled soil/porewater behavior
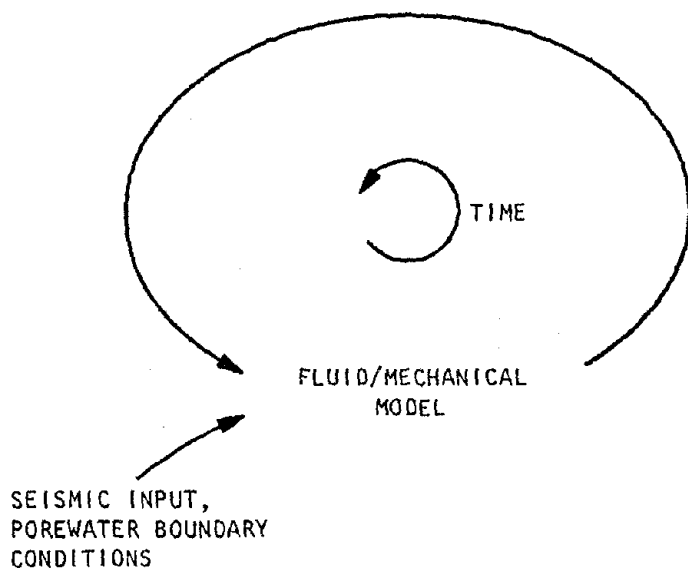
AA469

(b) Fully-coupled soil/porewater behavior

FIGURE 4-19. TYPES OF EFFECTIVE STRESS METHODS

phenomena. Fully coupled methods, on the other hand, treat the soil and porewater as a two-phase mixture and develop equations that govern the behavior of that mixture (Fig. 4-19b). These equations include all possible interactions between the two phases, and hence couplings between mechanical and porewater flow phenomena. Various alternative computational schemes are summarized in Table 4-7 for both the loosely coupled and fully coupled methods.

4.3.3.1 One-Dimensional Loosely Coupled Methods

Two prominent members of this class of effective stress methods are those developed by Martin and Seed (1979) and by Finn et al. (1977). These methods represent examples of the iterative and time-marching approaches respectively, as summarized in Table 4-7 for the loosely coupled methods.

4.3.3.1.1 *Martin and Seed (1979) Approach*

The Martin-Seed approach for carrying out effective stress analyses involves the following simplified procedure:

1. Use the MASH code (Martin and Seed, 1978a) to carry out a nonlinear dynamic total stress analysis of the seismic response of the soil deposit over the entire duration of the ground shaking.[*] In this initial dynamic response calculation, the effects of porewater pressure on the soil response are neglected.

---

[*]Although the MASH code is used with APOLLO in the particular applications by Martin and Seed, any other appropriate nonlinear dynamic analysis techniques could also be used.

TABLE 4-7.   CURRENT EFFECTIVE STRESS METHODS

Method	Basic Concept	Computational Approaches
Loosely Coupled	Makes use of two distinct models--one to describe dynamic mechanical behavior and the other to describe porewater flow	Iterative Approach. Involves the use of an iterative cycle comprised of separate mechanical and porewater flow analyses (using separate computer codes) that each extend over the entire duration of the shaking. In this, the input parameters for one analysis are progressively modified based on output from the other, and the complete analyses are repeated until convergence is achieved. For this case, the computational cycle in Figure 4-19a is simply an iteration, in which no time marching of the iteration cycle is involved and there is no continuous interaction considered between the mechanical and porewater flow behavior (e.g., Sec. 4.3.3.1.1). Time-Marching Approach. Involves the consideration of a series of shorter time periods that comprise the total duration of shaking. In this, the mechanical and porewater flow models can be used iteratively within each time period, so that satisfactory convergence is achieved before proceeding to the next time period. As the time periods become very small, the need for iteration is eliminated and the mechanical and porewater flow models essentially track each other through time. For this case, the computation cycle in Figure 4-19a is essentially a time period (e.g., Sec. 4.3.3.1.2).
Closely Coupled	Soil and porewater are represented as a two-phase mixture, and equations governing the behavior of that mixture are defined	Several methods are possible for implementing the computation cycle for closely coupled methods (Fig. 4-19b). One such method could involve recalculating each part of the behavior of the system in a sequential manner. In this, the use of very short time steps would eliminate the need for iteration (e.g., see Sec. 4.3.3.4.1). Alternatively, a single set of equations defining the system behavior may be used (e.g., Sec. 4.3.3.2.1). For this case, some iteration may be required.to achieve a completely consistent state before moving on to the next time step. Whichever method is used, the analysis should still be considered fully coupled, since all interaction between the two phases of the mixture are incorporated within the equations governing the system behavior.

2. Convert the irregular soil response time histories from Step 1 to an equivalent number of cycles at an appropriate cyclic stress level, usually 0.65 τ_{max} (see Sec. 4.2.2).

3. Use the results from Step 2 as input to the APOLLO code (Martin and Seed, 1978b), which computes the rate of porewater pressure generation during the seismic excitation, and the corresponding time history of porewater pressure within each layer of the soil deposit. Use APOLLO to then compute the effective stress time history in each soil layer, and the resulting time history of the reduction in shear modulus (assumed proportional to the square root of the effective stress).

4. Carry out a second MASH code dynamic analysis of the seismic response of the soil deposit over the entire duration of shaking, incorporating the porewater pressure, effective stress, and modulus reduction histories from Step 3.

5. Recycle Steps 1 through 4 until reasonable convergence is attained between results of successive cycles.

The main elements of the above procedure are the MASH and APOLLO codes. The MASH code is a nonlinear finite element technique that incorporates the Davidenkov model to simulate the nonlinear soil behavior under seismic excitation. The one-dimensional porewater flow code, APOLLO, incorporates built-in empirical relationships between (1) the undrained porewater

pressure ratio and the cycle ratio, N/N_ℓ^*; and (2) the compressibility of the sand and the porewater pressure ratio and relative density.

4.3.3.1.2 *Finn et al. (1977) Approach*

Finn et al. (1977) describe a nonlinear effective stress approach for the dynamic analysis of dry or saturated sands that is the basis for the computer code named DESRA. The approach consists of a procedure for dynamic analysis, a specific nonlinear stress-strain law, and a method for computing volume changes and porewater pressures. When used in the effective stress mode for the analysis of saturated sands, the increase in porewater pressure within each soil layer during each time step of integration is computed using parameters that describe the volume change and rebound characteristics of the soil (Martin et al., 1975); the effective stress state in each soil layer is thereby modified appropriately for the next time step. This modification in effective stress, in turn, leads to a corresponding modification in the tangent shear modulus for each soil layer, which is a function of the mean effective stress. These modifications in shear moduli are incorporated into the step-by-step numerical integration of the nonlinear equations of motion for the soil deposit.

4.3.3.2 One-Dimensional Fully Coupled Methods

Two representative methods that fall in this class are those described by Ghaboussi and Dikmen (1979) and by Katsikas and Wylie (1982). These are summarized in the paragraphs that follow.

---

*In this, N is the total number of equivalent cycles of stress that result from the ground shaking (from Step 2 of the Martin-Seed procedure) and N_ℓ is the number of cycles necessary to cause initial liquefaction at that same cycle stress level.

4.3.3.2.1 *Ghaboussi and Dikmen (1979) Approach*

The Ghaboussi-Dikmen approach for carrying out effective stress treats saturated sands as a two-phase medium; the two phases are the porous deformable granular soil solid and the porewater. Using Biot's (1961) dynamic theory of saturated porous solids as a starting point in conjunction with a finite element approach, coupled equations of motion are developed for defining the displacements of the fluid relative to the solid. This approach is implemented in a computer code named LASS-3.

The LASS-3 methodology by Ghaboussi and Dikmen comprises a one-dimensional approach for analyzing the response of horizontally layered saturated sand site subjected to multidirectional shaking. Features of the soil/fluid model are as follows:

- The soil material model is nonlinear and incorporates isotropic and kinematic hardening, an associated flow rule, and a shear strength that is independent of the direction of the resultant shear stress.

- The model of the fluid phase is developed using Darcy's Law to represent the flow of porewater through the porous soil material, and linear consitutuve relation- ships to define fluid pressure in terms of normal strain.

- The solid soil material and the fluid phase are coupled through volumetric strains.

- Initial liquefaction is assumed to occur when a loading/ unloading stress path, defined in terms of shear stress and effective normal stress, approaches a Mohr-Coulomb failure surface. The loading portion of this stress path has the form of a quarter of an ellipse in stress

space; in unloading, the effective stress is assumed
constant until the previous maximum or minimum value
of shear-stress/effective-stress ratio is reached,
after which the stress path becomes elliptic again but
at a new reduced initial effective stress level. This
loading/unloading stress path is intended to reflect
that successive cycling tends to reduce the effective
stress level for each new cycle.

4.3.3.2.2 *Katsikas and Wylie (1982) Approach*

The effective stress approach developed by Katsikas and
Wylie (1982) incorporates a model whose principal parts represent
one-dimensional propagation of shear waves through the solid
matrix of the soil and pressure waves through the porewater.
These two wave propagation phenomena are coupled through the
volumetric soil deformation. Features of the Katsikas-Wylie
model are (1) inelastic representation of shear wave propagation
through the soil skeleton; (2) coupling between the shear wave
and pressure wave propagation; (3) use of fundamental equations
of motion and continuity to represent porewater pressure develop-
ment and redistribution through the soil; and (4) association
of excess porewater pressure development with the inelastic
volumetric deformation of the soil matrix.

4.3.3.3 Two-Dimensional Loosely Coupled Methods

There is little information available at this time regarding
the existence of two-dimensional effective stress methods that can
be classed as loosely coupled. However, it would appear possible
to define such a technique by coupling: (1) an existing nonlinear
or equivalent linear soil/structure interaction analysis technique
that, by itself, does not incorporate porewater pressure effects;
and (2) any code that can be used to compute two-dimensional

porewater pressure generation and dissipation effects during earthquake or cyclic loading (e.g., GADFLEA, Booker et al., 1976). This loosely-coupled approach would involve a computational procedure with the following steps: (1) calculation of the soil/structure system response for a short segment of the total ground shaking; (2) use of the soil stresses obtained from this computation as input to the porewater pressure code, in which generated and redistributed porewater presures are obtained; (3) use of these porewater pressures to modify the effective stresses and the corresponding soil material parameters in the soil/structure system model; (4) use of these modified soil parameters as input to an analysis of the soil/structure system response over the next time segment; and (5) repeat of Steps 1 to 4 over successive time segments that comprise the entire duration of the ground shaking.

The process outlined above appears to represent a practical engineering approach for carrying out two-dimensional effective stress analyses of the seismic reponse of port and harbor facilities. However, the choice of a soil/structure interaction technique for use in this process warrants discussion. In this, considering that a loosely coupled effective stress approach involves certain simplifications pertaining to the modeling of the fluid flow and the fluid/soil coupling, a soil/structure interaction approach consistent with these simplifications should use either equivalent linear soil models or simple nonlinear models. The more highly refined nonlinear soil models appear more appropriate for use in the context of two-dimensional fully coupled effective stress methods (Sec. 4.3.3.4) where the incorporation of porewater pressure effects is more complete.

The use of equivalent linear methods for modeling soil/structure interaction effects in a two-dimensional effective stress framework also requires further comment. In a total

stress context, such methods were shown to represent a practical and consistent approach for carrying out soil/structure interaction analysis (Sec. 4.2.1.4). However, for use in a loosely coupled effective stress analysis, the methods presently have drawbacks, in that the frequency-domain approaches that represent the state of the art for equivalent linear techniques (e.g., FLUSH and SASSI) are inefficient for use in this particular process; i.e., analysis techniques that perform in the time domain and have a restart capability are required. Unfortunately, the existing time-domain equivalent linear approach, QUAD-4, does not have a restart capability and, furthermore, does not have a satisfactory representation of soil damping (Sec. 4.2.1.2.2). Therefore, some further development is required before the type of analysis summarized above can be undertaken using equivalent linear methods.

4.3.3.4 Two-Dimensional Fully Coupled Methods

The relatively limited amount of work to date involving the development of two-dimensional fully coupled methods is represented by the procedures of Zienkiewicz et al. (1978 and 1980) and Prevost (1981), and is summarized in the paragraphs that follow.

4.3.3.4.1 *Zienkiewicz et al. (1978 and 1980)*

Zienkiewicz et al. (1978, 1980) describe an effective stress method based on the use of an explicit finite element method for representing the dynamic, nonlinear behavior of an undrained soil. The key component of the method is the soil liquefaction model that is used to describe the volumetric densification of the soil that occurs during cyclic loading, and hence the increase in porewater pressure. The problem of developing a fully nonlinear model of the soil skeleton behavior that describes progressive decrease in volume during cyclic loading is avoided by separating

nonlinear behavior into two parts; that due to basic material non-
linearity and that which constitutes the cumulative volumetric
change. The former part is described by an elastoplastic model
that utilizes a Mohr-Coulomb type yield criterion, with a non-
associated flow rule that eliminates volumetric straining during
plastic flow. The second part of the nonlinear model consists of
an empirical description of the so-called autogeneous volumetric
strain that accompanies cyclic loading. This description defines
the autogeneous volumetric strain in terms of the total strain
path length and two sets of material constants, derived from
undrained cyclic simple shear tests, that describe behavior
before and after initiation of soil liquefaction.

Although the earlier work by Zienkiewicz et al. (1978) might
be described as loosely coupled and representative of only undrained
conditions, the subsequent work (Zienkiewicz et al., 1980) has
incorporated coupled equations for a saturated porous medium
under dynamic conditions. These, of course, consist of equations
of motion for the soil-fluid mixture and fluid flow continuity
conditions. Although this later work enabled drained conditions
to be represented, the authors observed that under most conditions
undrained behavior could usually be assumed.[*] The two methods
described by Zienkiewicz et al. share a common empirical descrip-
tion of the autogeneous volumetric strain. The validity of this
empirical description rests on the assumption that the length of
the strain path can be used to uniquely define the autogeneous
volumetric strain. The question arises, as with other models, as
to whether the simple load path followed during laboratory cyclic
shear tests is sufficient to define the in-situ behavior of a
soil that may be subjected to much more complex, nonuniform load
histories.

---

[*]This assumption may not be valid for port and harbor sites
(Sec. 4.3.1).

4.3.3.4.2 *Prevost (1981) Model*

The method proposed by Prevost (1981) makes use of coupled field equations obtained by viewing the soil as a multiphase medium consisting of an elastic porous skeleton and viscous fluids and by using the continuum theory of mixtures (Truesdale and Toupin, 1960; Atkin and Crane, 1976a,b; Hart, 1981). This theory incorporates the requirements of mass balance, momentum balance, and nonlinear constitutive relationships for the coupled soil/porewater system, in accordance with a repetitive computational cycle that recalculates each part of the behavior of the system in a sequential manner. The general nonlinear problem is treated in a piecewise linear manner, in which the properties of the porous soil skeleton are considered to be time independent and both the porewater and the soil grains are assumed to be incompressible.

The most interesting feature of this model is the treatment of plastic flow, which is defined by a set of yield surfaces that translate in stress space and change in size in a manner that reflects a blend of isotropic and kinematic hardening and the past stress-strain history. Specification of the model parameters requires the definition of the initial size and position of the yield surfaces and associated plastic moduli, the size and change of plastic moduli as a function of load and elastic shear and bulk moduli. These parameters may be derived from conventional monotonic axial and cyclic-strain controlled simple shear tests. The model does not, however, include cyclic degradation effects that are necessary to describe soil liquefaction.

The Prevost model is currently intended for studying soil consolidation under static and cyclic loading conditions in which inertia terms may be neglected. Since, as noted above, there is also no description of soil densification due to cyclic loading

the model is presently unsuited to investigation of soil liquefaction. However, the mixtures theory approach upon which the model is based does provide a consistent theoretical basis for development of a complete coupled effective stress model.

4.3.4 FUTURE DEVELOPMENT

This section has summarized basic concepts of effective stress methods as well as some of the methods that are used in current earthquake engineering practice. It remains to discuss some possible directions for further development of effective stress methods so that they may become more applicable to port and harbor facility applications.

Future development of effective stress methods for port and harbor facility analyses should be primarily directed toward techniques for two-dimensional or three-dimensional analysis of both the loosely coupled and fully coupled types. The development of loosely coupled methods (Sec. 4.3.3.3) is of most importance, even though such methods involve certain approximations in the soil/porewater modeling. They represent a practical approach with important benefits over total stress methods. Further development of the more fundamental fully coupled methods, such as described by Zienkiewicz and Prevost (Sec. 4.3.3.4), is also justified. Though such methods may not become tools for routine engineering design of port and harbor facilities, they do provide a means of evaluating the consequences of the approximations made during less rigorous analyses.

Analytical development of effective stress methods, although important, must be carried out within a practical framework and with due regard to the following considerations:

- Costs of Analyses. The engineering time and computer costs associated with the use of such effective stress methods may be high.

- <u>Measured Data</u>. There could be uncertainty involved in the measurement of many of the soil/fluid material parameters required as input to such methods; in accounting for effects of sample disturbance, site inhomogeneity, etc. when measuring the required material parameters; and in developing field or laboratory test data suitable for verifying the methods.

- <u>Practical Application</u>. The application of such effective stress methods and interpretation of their results will probably require a special level of training and experience on the part of the engineer using the methods.

In addition to these considerations, it should also be noted that the basic requirement of any analytical method is that it should serve to develop the engineering judgment on which sound engineering decisions can be based. In view of this, development of effective stress methods should not outstrip our ability either to provide reliable input data for the use of such methods, or to apply and interpret their results. Future development of effective stress methods should therefore be comprised of the following three types of programs: (1) experimental programs--that provide an improved basis for identifying significant soil parameters, for measuring their values representative of field conditions, and for interpreting their effects on the liquefaction process; (2) analytical programs--that use these experimental programs as a means for developing and enhancing two-dimensional and three-dimensional analysis procedures suitable for application to port and harbor facilities; and (3) education--so that engineers involved in port and harbor facility designs can properly obtain the required experimental measurements, apply the effective stress methods, and interpret their results.

4.4 PROBABILISTIC METHODS

The deterministic analysis techniques described in the previous sections, do not account for the considerable uncertainties that exist in defining the input motions and soil properties required for such analysis. Effects of such uncertainties can best be represented through the use of probabilistic methods, which provide results in terms of the probability level associated with the occurrence of a given event (such as a given state of stress in the structure, the occurrence of liquefaction, etc). Such probabilistic methods are a topic of considerable interest and research within the earthquake engineering community although, because they are now still under development, they are not yet widely used in current practice.

Because of their potential importance as a future approach for the analysis of port and harbor facilities, the features of some representative probabilistic analysis techniques pertaining to their applicability to ports and harbors are briefly summarized in this section. More extensive summaries are available elsewhere (e.g., Christian, 1980) and the reader is referred to such summaries as well as to the references cited in the paragraphs that follow. The summary contained herein is broken down into subsections that deal with soil/structure interaction analyses, liquefaction analyses, combined analyses that include soil/ structure interaction and liquefaction, and an assessment of the current and future applicability of probabilistic methods to port and harbor facilities.

4.4.1 SOIL/STRUCTURE INTERACTION ANALYSIS

The use of probabilistic techniques for soil/structure interaction analyses falls into the general category of random vibrations methods as described by Crandall and Mark (1963) and further developed for earthquake engineering and soil dynamic

problems by Vanmarcke (1976, 1977). Such techniques are characterized by the use of frequency-dependent power spectral density functions as a means for calculating the probability of exceedance of the response at particular locations within the system being analyzed.

To date, there has been only limited development of probabilistic techniques for carrying out earthquake-induced soil/ structure interaction analyses. The PLUSH code, as recently developed by Romo-Organista et al. (1980), represents the most widely recognized approach of this type in current practice, and is therefore briefly described in the following paragraphs. It is noted that this approach features a probabilistic definition of the seismic input and a deterministic treatment of the soil/ structure system properties.

The PLUSH code represents an extension of the FLUSH code (Sec. 4.2.1.2.3) so as to perform probabilistic analyses of soil/structure systems subjected to seismic excitation. As shown in Figure 4-20a, PLUSH retains certain key features of FLUSH, such as (1) beam and quadrilateral elements; (2) transmitting boundaries at the sides of the soil grid; (3) in-plane viscous dampers attached to each soil node point to simulate three-dimensional wave propagation; (4) a deconvolution procedure to obtain rigid base input motion from specified control motions; (5) excitation from vertically propagating body waves; and (6) equivalent linear soil model with the same iterative process as in FLUSH code. The main differences between PLUSH and FLUSH are:

1. Input Motion Definition. FLUSH uses acceleration time histories whereas PLUSH uses a median design response spectrum or equivalent power spectral density function.
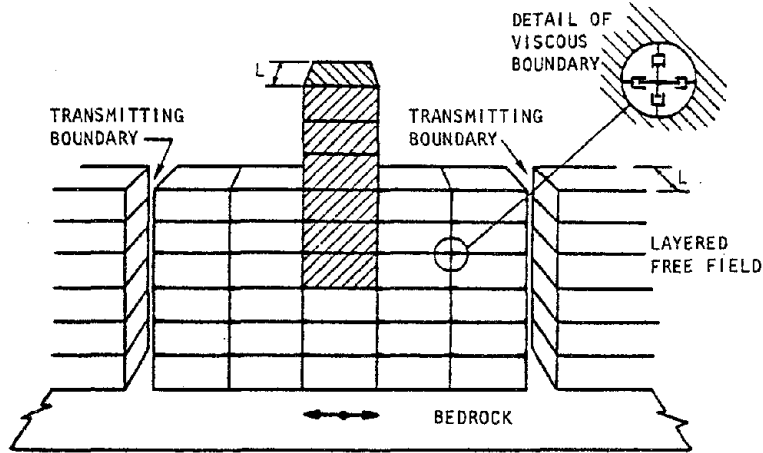
(a)   Soil-structure model
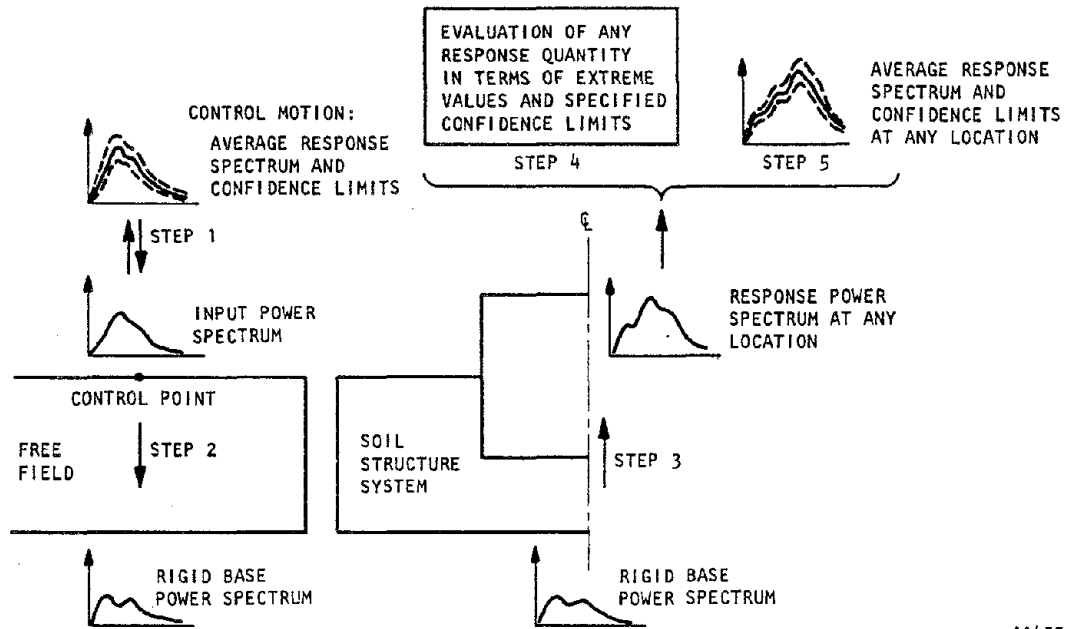
(b)   Seismic analysis procedure

FIGURE 4-20. FEATURES OF *PLUSH* CODE (Romo-Organista et al., 1980)

2. Response Definition. FLUSH computes a deterministic
response at any locations in the grid, whereas PLUSH,
which considers an infinite ensemble of input motions,
furnishes probabilistic estimates of the system response
at any location.

The basic analysis technique used in PLUSH (Fig. 4-20b) is
summarized as follows:

1. Control Motion. From the specified control motion mean
response spectrum and confidence limits, obtain the
corresponding input power spectrum.

2. Base Motions. Use deconvolution techniques to convert
the input power spectrum to an equivalent power spectrum
at the rigid base of the soil grid.

3. Output Power Spectra. Using a frequency analysis tech-
nique in conjunction with the finite element model and
the base motions from Step 2, obtain the response power
spectra at specified locations within the soil/structure
system.

4. Extreme Values of Response. Use the above output power
spectra in conjunction with first passage probability
concepts (Vanmarcke, 1972) to obtain extreme values
corresponding to specified confidence limits of response
quantities such as accelerations, moments, stresses, etc.
It is important to note that this step can be extended
to develop complete probability density functions for
any of these response quantities.

5. <u>System Response Forms</u>. Apply the output power spectra from Step 3 to single-degree-of-freedom systems with various frequencies and dampings to obtain system response spectra, in terms of specified confidence limits.

4.4.2 LIQUEFACTION ANALYSIS PROCEDURES

In recent years, there have been several techniques developed for analyzing the probability of occurrence of earthquake-induced liquefaction at a given site. Some representative techniques of this type are briefly summarized below.

4.4.2.1 Cumulative Damage Approach

The cumulative damage approach, as developed by Donovan (1971), uses probabilistic techniques for estimating the number of equivalent cycles for various stress levels, together with Miner's fatigue law to evaluate the cumulative effects of these stress cycles on the liquefaction potential at the site (Fig. 4-21). This approach can be applied in conjunction with either (1) shear stresses computed from a dynamic analysis (probabilistic or deter-ministic) or (2) distributions of earthquake induced stress cycles inferred from statistical analyses of recorded earthquake motions.

This basic approach predicts liquefaction to occur when

$$\sum_i \frac{n_i}{N_i} > 1 \qquad (4\text{-}2)$$

where N_i is the number of equivalent cycles at the <u>ith</u> shear stress level that by itself would cause liquefaction, and n_i is the number of equivalent cycles at the <u>ith</u> stress level that is induced by the seismic excitation. The quantity N_i can be

(a) Actual irregular   (b) Equivalent uniform
     cyclic stresses   stress cycles, N_{eq}

(c) Miners damage   (d) Equivalent cycle
     potential   method
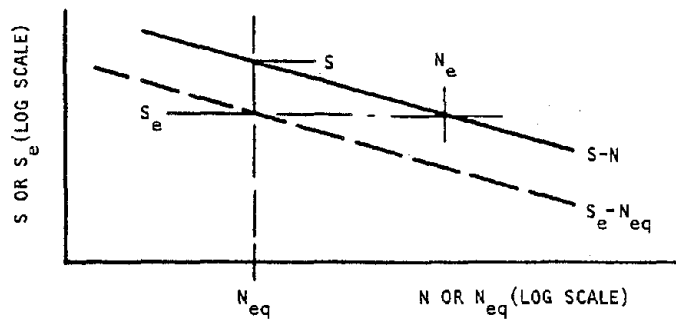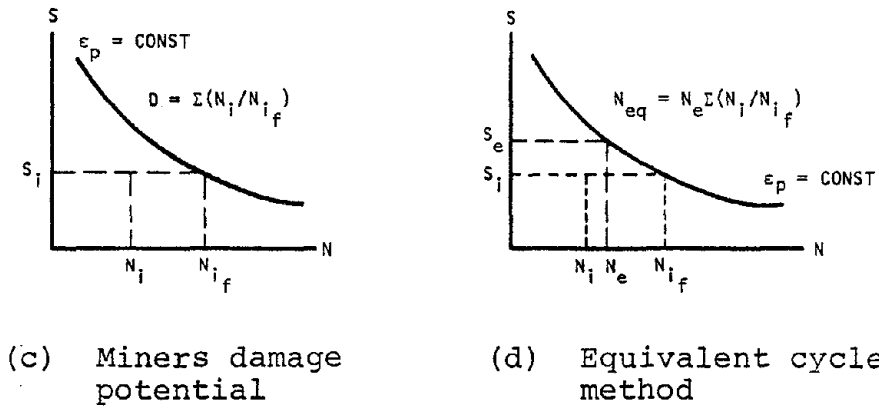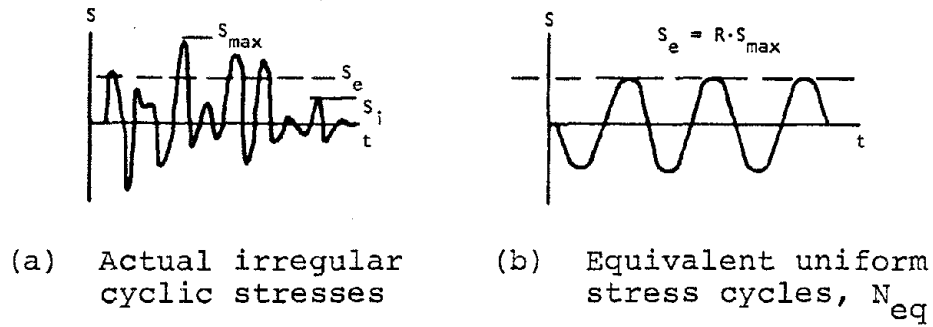
(e) S-N data on log-log scales

FIGURE 4-21. CUMMULATIVE DAMAGE AND EQUIVALENT CYCLE
              CONCEPTS (Annaki and Lee, 1977)

obtained from standard laboratory test procedures. The determination of the quantity n_i involves the following steps:
(1) estimate the total number of cycles, C_T, as the ratio of the duration of strong shaking* to an estimated site period;
(2) assuming the shear stresses to follow a Rayleigh distribution, determine the probability of occurrence of the <u>ith</u> shear stress level, $P(\tau_i)$; and (3) obtain n_i as the product of C_T and $P(\tau_i)$. It is noted that, if a dynamic analysis of the soil/structure system response (or the site response) is available, then the Rayleigh distribution for the shear stress in the soil at any location, as required under Step 2 above, can be obtained directly from the dynamic analysis results. However, if no such dynamic analysis results are available, the Rayleigh distribution is obtained from an estimate of the peak acceleration (assuming acceleration to be directly proportional to shear stress) and a "sigma ratio" (defined as the ratio of the peak shear stress to the rms shear stress, and derived from statistical analyses of earthquake data, again assuming direct proportionality between acceleration and shear stress).

The basic cumulative damage approach has been used by Donovan and Singh (1978) to develop liquefaction criteria for the Trans-Alaska pipeline, and has been applied to various other case studies by Valera and Donovan (1977). In addition to Donovan and his co-workers, other investigators have also used the cumulative damage as a means for assessing liquefaction potential. Faccioli (1973) used a starting point for a liquefaction analysis based on cumulative damage considerations that was similar to that of Donovan; however Faccioli used a somewhat different probabilistic approach based on statistical moments of earthquake data. Annaki and Lee

---

*In Donovan's approach, the Hsuid et al. (1969) definition of duration of strong shaking has been adopted although conceptually, any other existing definition could be used.

(1977) applied the cumulative damage approach in conjunction with laboratory test data and, from this, concluded that the cumulative damage approach is valid for dealing with irregular loading effects on soils. More recently, Sato and Der Kiureghian (1982) applied the cumulative damage approach in conjunction with life-line systems of extended length; in this, they addressed lique-faction effects in terms of a "transition distance"--defined as the maximum epicentral distance that results in a unit value of the cumulative damage ratio (as defined in Eq. 4-2).

4.4.2.2 Methods Based on Seismic Risk Concepts

A second group of probabilistic methods for assessing lique-faction potential considers (1) the probability of liquefaction at a site for a given level of ground shaking; and (2) the probability of occurrence of all possible levels of ground shaking. Step 1 involves an evaluation of the liquefaction potential of the soil materials at the site, and may involve the use of laboratory test data and/or empirical data from field observations of soil behavior under seismic excitations. Step 2 involves consideration of the seismicity, geology, and tectonics of the region surrounding the site.

The various methods that have been developed to carry out liquefaction analyses may differ widely according to how Steps 1 and 2 are interpreted. To illustrate this, two approaches that feature differing interpretations of these steps are summarized in the paragraphs that follow.

4.4.2.2.1 *Yegian and Whitman (1978)*

The Yegian-Whitman approach carries out Step 1 above through the use of empirical data from field observations of the occurrence or nonoccurrence of liquefaction. These data are characterized in terms of a modified Standard Penetration Test

resistance and a site parameter dependent on the magnitude M, hypocentral distance R, vertical effective stress σ_v, and depth H. Yegian and Whitman then obtain a curve separating regions of liquefaction and nonliquefaction so as to minimize the number of misclassified points (Fig. 4-22a). From this, the Step 1 results characterizing the probability of liquefaction for a given level of ground shaking (herein characterized by M and R) are readily obtained using an assumed lognormal distribution of a "liquefaction potential index" defined in Figure 4-22. The Step 2 results, which herein involve computation of the probability of occurrence of an earthquake characterized by M and R, are obtained using conventional seismic risk analysis techniques. The final results, in terms of the total probability of liquefaction, are then obtained as the product of the Step 1 and 2 results, summed over all possible M and R values (Fig. 4-22b).

4.4.2.2.2 *Youd and Perkins (1978)*

The Youd-Perkins approach interprets Steps 1 and 2 in terms of a combination of regional maps termed a ground motion opportunity map and a ground failure susceptibility map. The ground failure opportunity map characterizes the opportunity for liquefaction in a given area as a function of the seismicity of the area and the rate of occurrence of ground motions sufficiently strong to produce liquefaction in susceptible materials (Fig. 4-23a); this map is obtained using seismic risk procedures. The ground failure susceptibility map, on the other hand, is derived deterministically based on qualitative evaluations of the properties of the geologic materials around the site, and whether they may be susceptible to liquefaction (Fig. 4-23b). The resulting combination of these maps shows the location of potentially liquefiable sediments as well as frequency of occurrence of ground motions sufficiently strong to induce liquefaction in these sediments (Fig. 4-23c).

LIQUEFACTION POTENTIAL INDEX, LPI

$$S_c = \frac{e^{0.5M_H}}{(R+16)\bar{\sigma}_v}$$

GROUND FAILURE

$\bar{S}_c$

NO GROUND FAILURE

CORRECTED SPT VALUES, N'

PROBABILITY OF LIQUEFACTION

DEPTH, ft
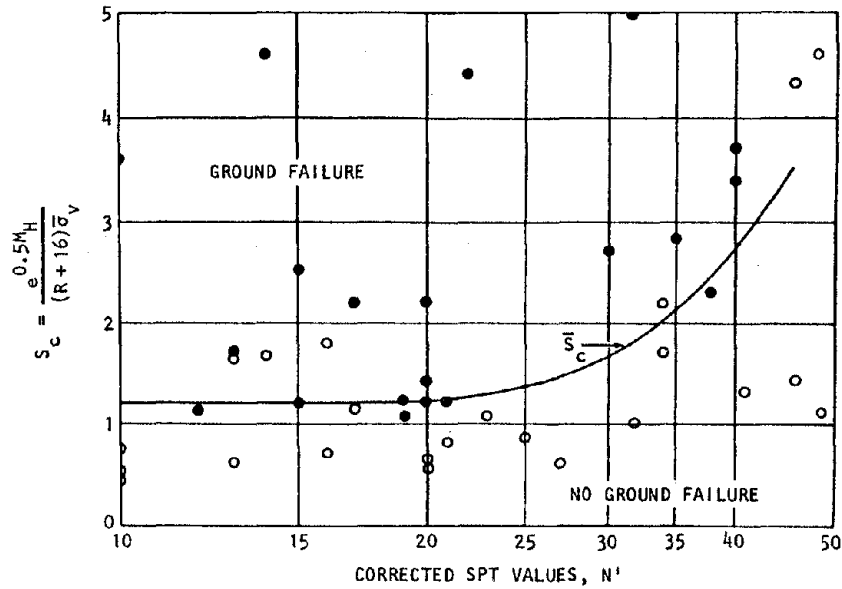
AVERAGE LPI

(a) Average strength parameter, $\bar{S}_c$
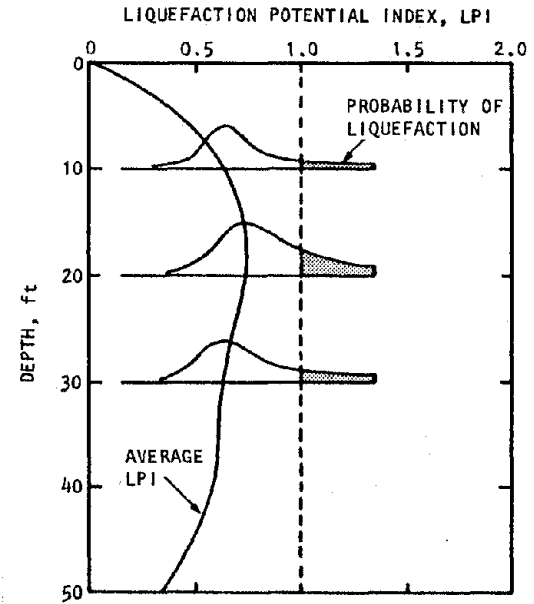
(b) Probability of liquefaction with depth

NOTE: $LPI = \dfrac{S_c (EARTHQUAKE)}{\bar{S}_c}$ (As defined in (a) above)

FIGURE 4-22. YEGIAN-WHITMAN (1978) APPROACH FOR ANALYZING PROBABILITY OF LIQUEFACTION
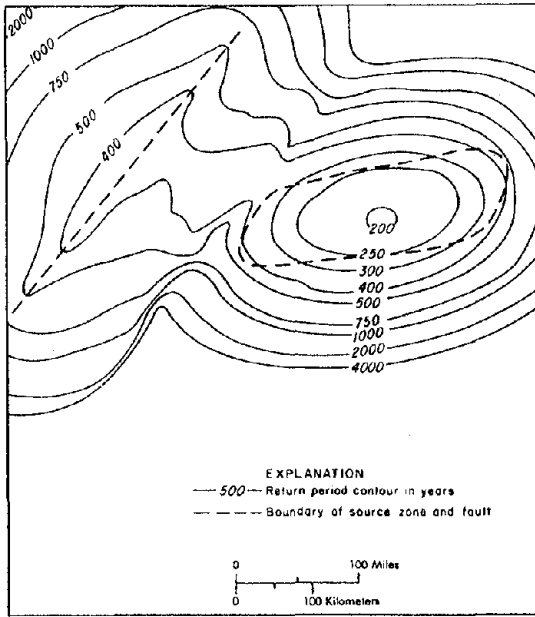
(a) Ground failure opportunity map (in terms of return periods)
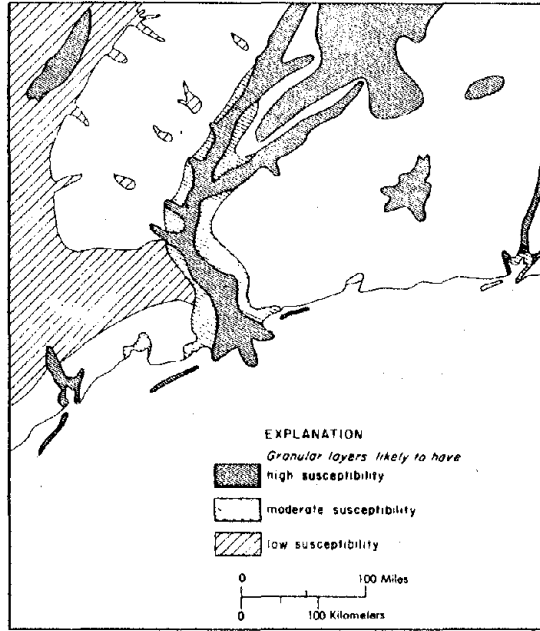
(b) Ground failure susceptibility map
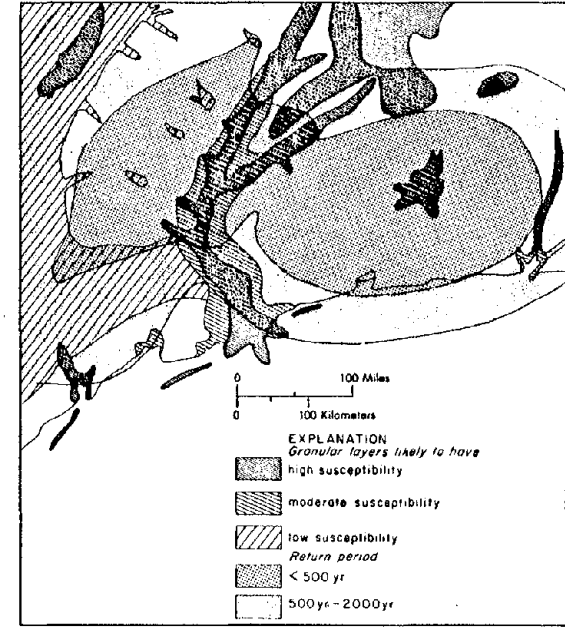
(c) Superposition of (a) and (b)

FIGURE 4-23. YOUD-PERKINS (1978) APPROACH FOR ANALYZING PROBABILITY OF LIQUEFACTION

4.4.2.3 Methods with Probabilistic Definitions of Soil Properties

Probabilistic liquefaction analysis techniques described in the preceding subsections are representative of the majority of probabilistic techniques now available in that they test the seismic excitation as random and the soil properties as deterministic. One of the few existing studies in which the soil properties are also assumed random is that of Haldar and Tang (1979). In this, all of the parameters used in the simplified liquefaction analysis procedure of Seed and Idriss (1971) are treated as random variables whose effects are described by their variances. Haldar and Tang then investigated the relative significance of the various parameters in the Seed-Idriss approach by determining the sensitivity of computed probabilities of liquefaction to different assumed levels of uncertainty in each of the parameters. Applications of their approach to historical records of site behavior during earthquakes show good agreement.

4.4.3 COMBINED SOIL/STRUCTURE INTERACTION AND LIQUEFACTION ANALYSIS

As previously noted, a complete dynamic analysis technique for port and harbor facilities should be able to represent two-dimensional response characteristics of the soil/structure system including an assessment of the potential for excess porewater pressure development and liquefaction in the soil materials that comprise the site. No such probabilistic approach of this type has yet been developed although, from the discussion in the previous subsections, at least one probabilistic technique with these features appears possible. This would involve what amounts to a total stress analysis procedure (in which porewater pressure effects on the soil/structure system response are neglected) and would be comprised of two main steps. The first of these steps

would use the PLUSH code (Sec. 4.4.1) to carry out a two-dimensional probabilistic analysis of the soil/structure system seismic response. From the results of this analysis, probability density functions for the shear stress states at various locations within the soil medium could be obtained (with relatively minor modifications of the present version of PLUSH), together with a probabilistic definition of the structure response. The second step in this approach would use these computed soil stress probability density functions in conjunction with a cumulative damage approach (Sec. 4.4.2.1) to estimate the probability of liquefaction at the site.

4.4.4 CURRENT AND FUTURE APPLICABILITY OF PROBABILISTIC APPROACHES

The previous subsections have briefly summarized the current state of the art regarding probabilistic techniques for evaluating the soil/structure system response and the potential for porewater pressure buildup and liquefaction at a site--which are the two main elements of a seismic analysis for port and harbor facilities. This summary has shown that (1) there is a wide range of techniques now available, although most of these feature a probabilistic treatment of the seismic input and a deterministic treatment of the soil properties; and (2) there is no probabilistic procedure yet used in current practice that treats both the soil/structure interaction and the liquefaction problems in the same analysis, although an approach combining the PLUSH code and cumulative damage procedures appears to be a possible first step in that direction.

From this, it is seen that, for application to port and harbor facilities, further development of probabilistic techniques that treat the combined soil/structure interaction and liquefaction problem would be desirable, incorporating improved procedures for treating the uncertainties in the soil properties

as well as the seismic input. These development efforts should consist of (1) experimental programs--directed toward developing the extended data base necessary for representing effects of the uncertainties in the soil properties; and (2) analytical programs-- directed toward developing practical and workable probabilistic methods for engineering applications, and toward addressing the considerable judgment factors often required in the practical application of probabilistic methods.

4.5 SUMMARY OF RESULTS

This chapter has evaluated the applicability of current dynamic analysis procedures as an engineering tool for enhancing and verifying the design of port and harbor facilities to resist strong earthquake motions. The evaluation process has considered the fundamental concepts on which various alternative methods are based, as well as the current state of development of each method. On this basis, the chapter has addressed deterministic total stress methods in some detail, since only these methods now treat the combined soil/structure interaction and liquefaction problem in a manner suitable for application to seismic analysis of port and harbor structures. However, deterministic effective stress methods and probabilistic methods are also described in the con- text of possible future directions for dynamic analysis of port and harbor facilities, when further development of these methods has taken place.

It has been noted in this chapter that the analytical procedure itself, is only part of the overall process inherent in carrying out a meaningful dynamic analysis for design purposes. This process actually involves five main steps which are (1) the measurement of reliable soils data; (2) the selection of an appropriate analysis procedure; (3) the development of a suitable model of the soil/structure system, (4) implementation of the

dynamic response calculations; and (5) utilization of the analysis results in the design process. The importance of exercising sound judgment during each of these steps, and of evaluating their results in accordance with experience and good engineering practice, cannot be overstated.

CHAPTER 5

ILLUSTRATIVE DYNAMIC ANALYSIS

5.1 OBJECTIVE AND SCOPE

In this chapter, a dynamic analysis of a port and harbor soil/structure system is carried out in order to illustrate the type of design information that can be obtained from such analysis. The analysis is carried out for a sheet-pile bulkhead structure and site in Japan, and the results of the analyses are used to indicate, for this particular structure and assumed seismic excitation (1) how the computed internal forces and moments in the structure compare with design values; (2) how the computed lateral pressures exerted by the soil onto the structure compare with those estimated from the Mononobe-Okabe equation; (3) the liquefaction potential of the site; and (4) how soil improvement techniques might affect the earthquake-induced behavior of this particular soil/structure system.

5.2 DESCRIPTION OF STRUCTURE AND SOIL CONDITIONS

5.2.1 STRUCTURE

The structure considered in these calculations is a sheet-pile bulkhead that is located at Nakano Wharf No. 4 in the Sendai Harbor in Japan (Fig. 5-1) and was shaken substantially during the Miyagi-Ken-Oki earthquake of June 12, 1978 (M_s = 7.4). The structure consists of a steel sheet pile supported by vertical steel pipes spaced at 5.25 ft that, in turn, are anchored by a tie-rod/H-beam system. An unreinforced concrete apron rests on the ground surface and extends from the sheet pile to beyond the anchor (Fig. 5-2). During the earthquake, the apron experienced cracking and settlement, but no other damage to this structural system was reported (Tsuchida et al., 1979).

N
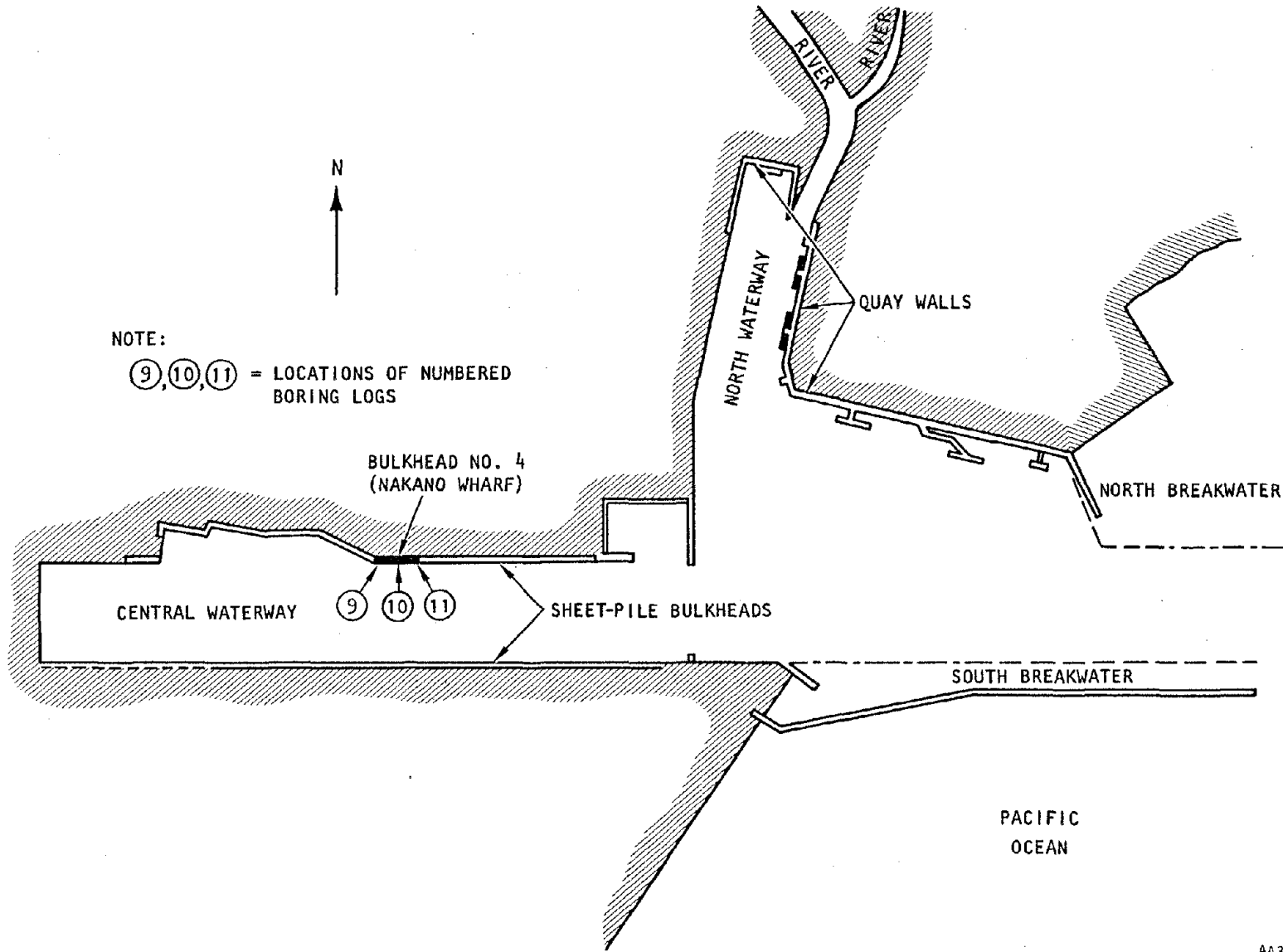
NOTE:

⑨,⑩,⑪ = LOCATIONS OF NUMBERED
BORING LOGS

BULKHEAD NO. 4
(NAKANO WHARF)

NORTH WATERWAY

QUAY WALLS

NORTH BREAKWATER

CENTRAL WATERWAY   ⑨ ⑩ ⑪   SHEET-PILE BULKHEADS

SOUTH BREAKWATER

PACIFIC
OCEAN

RIVER

RIVER

AA358

FIGURE 5-1.   SENDAI, JAPAN — HARBOR AREA (Tsuchida et al., 1979)

20m APRON WIDTH

16m

+3.3m

SEA WATER HIGH ▽ +1.4m
LEVELS LOW ▽ +0.4m

CONCRETE
APRON

TIE ROD
HIGH-STRENGTH
STEEL

STEEL H-BEAM
ANCHOR
(LENGTH = 12 m)

DESIGN WATERDEPTH -10.0m

-10.0 m

STEEL PIPE
SHEET-PILE S.T.K. 50
(LENGTH = 26.2m)

NOTE:

DIMENSIONS OF STRUCTURE ELEMENTS
GIVEN IN TABLE 5-1.

-24.0 m

0.0 m	BACKFILL ϕ = 30° γ = 1.8 γ'= 1.0
	SAND ϕ = 35° γ'= 1.0
-14.0 m	
	SILT C = 5.5 γ'= 0.6
-20.0 m	
	SAND ϕ = 25° γ'= 1.0
-25.0 m	
	SAND ϕ = 40° γ'= 1.0

NOTE:

ϕ = ANGLE OF INTERNAL
FRICTION

γ = DRY UNIT WEIGHT (t/m^3)

γ'= SATURATED UNIT
WEIGHT (t/m^3)

C = COHESION (t/m^2)

AA359

(a) Soil/structure configuration   (b) Soil profile

FIGURE 5-2. SHEET-PILE BULKHEAD NO. 4 AT NAKANO WHARF, SENDAI HARBOR, JAPAN
(Tsuchida et al., 1979)

5.2.2 SOIL CONDITIONS

Two sets of soil conditions are considered in this dynamic analysis. The first set corresponds to the actual soil conditions at this structure site, which are defined by Tsuchida et al. (1979) solely in terms of soil types, unit weights, friction angles, and Standard Penetration Test (SPT) blowcounts as provided in three adjacent boring logs (locations shown in Fig. 5-1). These logs (Fig. 5-3) show that the site is comprised of a single layer of fill underlain by saturated sands and silt. The low-water level of the sea is about 0.4 m above the bottom of the fill, and the high water level extends about 1 m higher; however, no information was available regarding the corresponding position of the water table in the soil relative to these levels.

The second set of soil conditions corresponds to the use of soil improvement techniques--i.e., deep compaction (e.g., vibro-flotation) techniques that are widely used to densify the soil materials at otherwise marginal sites (Mitchell and Kati, 1981). This consideration of soil conditions modified by soil improvement techniques has been motivated by the dramatic enhancements in resistance to liquefaction during earthquakes that has been observed in the past, primarily in Japan.[*] In view of these

_____

[*]For example, Watanabe (1966) observed that oil storage tanks constructed on loose saturated sands sustained considerable damage during the 1964 Niigata earthquake due to liquefaction of these sand layers, whereas adjacent tanks constructed on sands compacted by vibroflotation suffered only minor damage. Ohsaki (1970) observed similar comparisons between the response during the 1968 Tokachi-Oki earthquake of adjacent sites comprised of loose sands and sands compacted by vibroflotation. Similar trends, based on marked differences in behavior during the 1978 Miyagi-Ken-Oki earthquake of adjacent loose and compacted sand deposits at an oil tank site, were also observed by Ishihara et al. (1980), who then used laboratory tests and analyses to demonstrate that the resistance of sand deposits to liquefaction is markedly enhanced by vibroflotation.

ELEVATION, meters	TYPICAL PROFILE	ELEVATION, meters
+3.1	BACKFILL $\phi = 30°$ $\gamma = 1.8$ ① $\gamma' = 1.0$	+3.1
±0	SAND $\phi = 35°$ $\gamma' = 1.0$ ②	±0
-14.0		-5.0
	SILT $C = 5.5$ $\gamma' = 0.6$ ③	-10.0
-20.0		-15.0
	SAND $\phi = 25°$ $\gamma' = 1.0$ ④	-20.0
-25.0	SAND $\phi = 40°$ $\gamma' = 1.0$ ⑤	-25.0
-30.0		-30.0
	SAND ⑥	-35.0
		-40.0
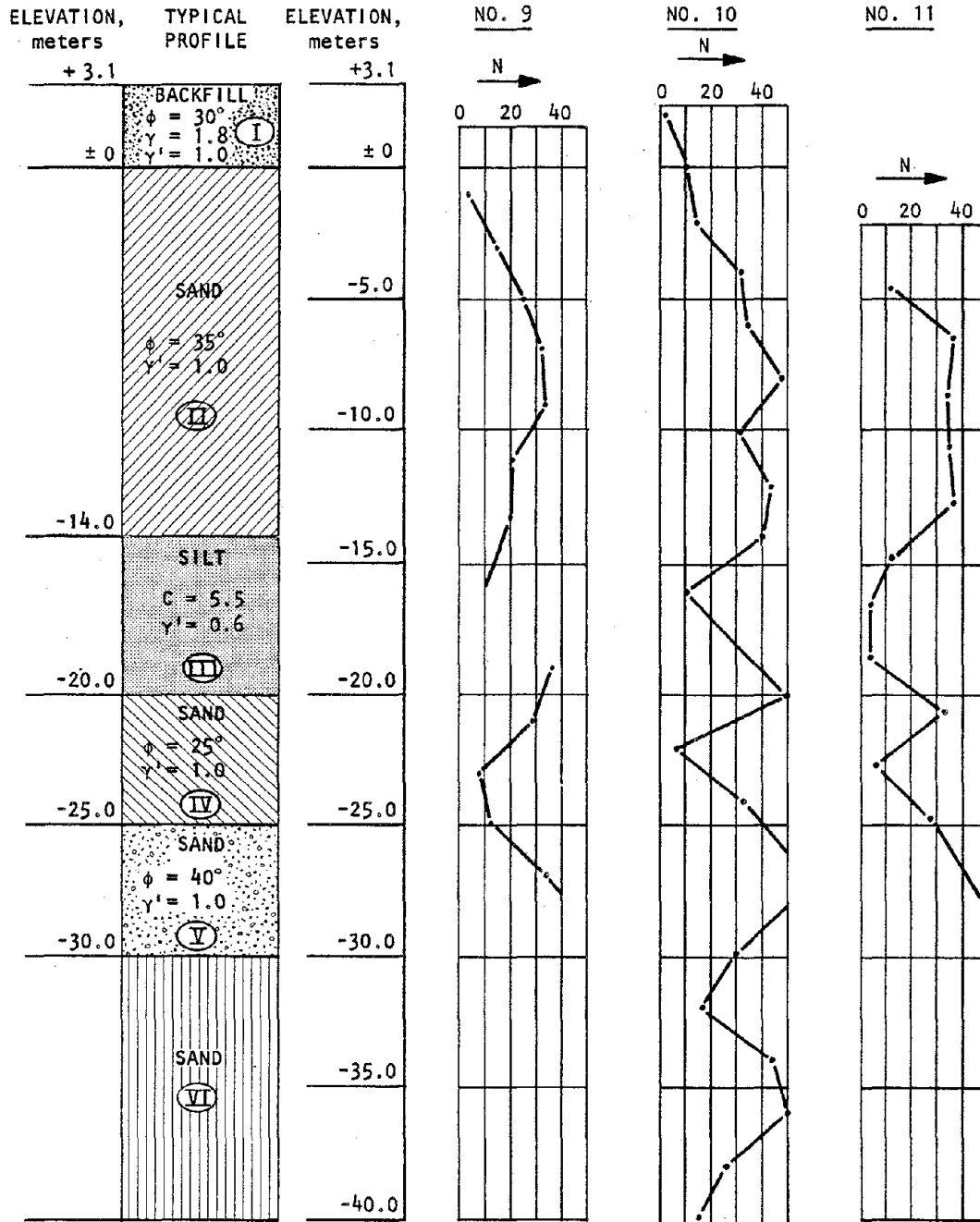
NOTE:
N = SPT BLOWCOUNTS
ϕ = ANGLE OF INTERNAL FRICTION
γ = DRY UNIT WEIGHT (t/m^3)
γ'= SUBMERGED UNIT WEIGHT (t/m^3)
C = COHESION (t/m^2)

AA362

FIGURE 5-3.   SOIL BORINGS IN VICINITY OF NAKANO WHARF NO. 4,
SENDAI HARBOR, JAPAN (Tsuchida et al., 1979)

observations, the results of this analysis will serve to indicate the effectiveness of soil improvement techniques in enhancing the liquefaction resistance at the site of this sheet-pile bulkhead. Estimates of the effects of these soil improvement techniques on the relative densities and the corresponding dynamic properties of the site soil materials are based on past experience according to procedures described in Section 5.5.3.2.

5.3 SEISMIC INPUT MOTIONS

Seismic input motions for these analyses were selected with an objective toward providing motions that were as close as possible to those experienced during the Miyagi-Ken-Oki earthquake by the sheet-pile bulkhead being investigated herein. Possible choices were limited to (1) motions recorded in the first floor of buildings in Sendai City, and to (2) free-field motion recorded at the Shiogama Harbor immediately north of the Sendai Harbor, which are among the strongest ever obtained at port and harbor regions in Japan. After some deliberation, the Shiogama Harbor records (Fig. 5-4) were selected because (1) these are truly free-field records whereas the motions recorded in the buildings at Sendai City are not; and (2) the locations and proximity of the Sendai and Shiogama Harbors relative to the earthquake epicenter are about the same. In particular, the North-South horizontal record and vertical record measured at Shiogama Harbor were used as seismic input motions for these analyses (for both the original and improved site condition cases) and these were deconvolved to obtain the corresponding base motions for each set of soil/structure system analyses.

As a final comment on these seismic input motions, it is noted that most strong motion instruments in Japan record over frequency ranges that do not extend to as high a frequency level as does that of instruments commonly used in the United States.
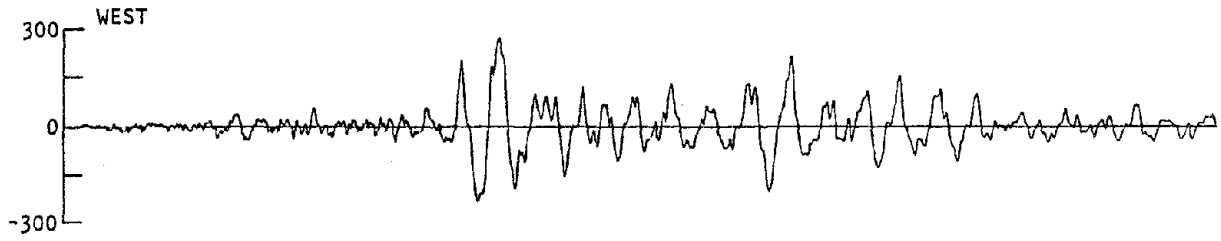
(a) Horizontal motions (east-west)
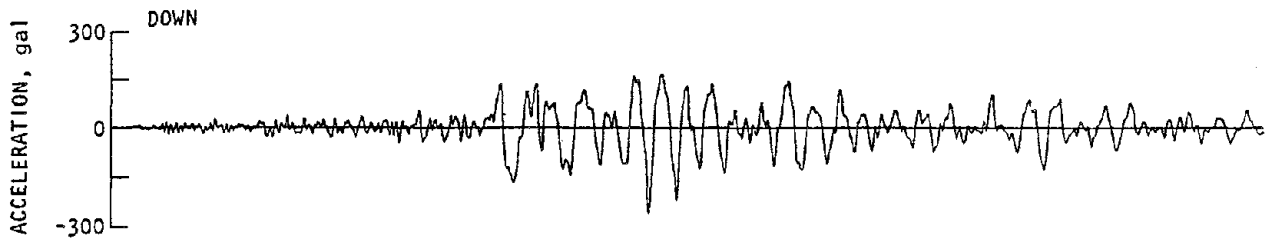
(b) Horizontal motions (north-south)
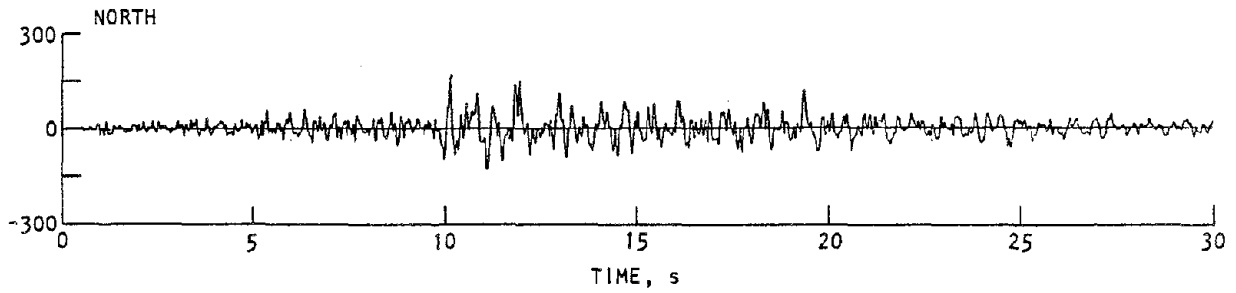
(c) Vertical motions

AA372

FIGURE 5-4. MOTIONS RECORDED AT SHIOGAMA HARBOR
(Mori and Crouse, 1981)

Furthermore, at higher amplitudes of shaking, the raw traces from Japanese instruments have an arc shape due to their being drawn by pens of constant radius and, in some cases, a slanting of the traces may occur due to the initial rest position of the pen arm not being parallel to the direction of paper movement (Brady, 1978). However, the particular Japanese records used in this study have been corrected for these as well as long period base-line shift effects, according to procedures described by Mori and Crouse (1981).

5.4 ANALYSIS PROCEDURE

The analysis procedure used herein corresponds to a deterministic total stress method, in which (1) a dynamic analysis procedure is used to compute the soil/structure system response, without considering the buildup of porewater pressure in the soil as the earthquake progresses; and (2) the soil shear stresses computed from this dynamic analysis are used to evaluate the potential for liquefaction at the site. Although total stress methods of this type do not consider porewater pressure effects during the dynamic analysis, they are the only techniques now readily available that can incorporate soil/structure interaction and the complete range of complex site geometries that might exist at port and harbor sites (Chapt. 4).

5.4.1 DYNAMIC ANALYSIS

The dynamic analysis of the bulkhead/soil system, corresponding to Step (1) above, is carried out using the FLUSH code (Lysmer et al., 1975). This code computes the two-dimensional response of a soil/structure system, in which the soil medium is comprised of homogeneous horizontal viscoelastic layers and is represented using an equivalent linear soil model. The system is subjected either to horizontal input motions from vertically propagating shear waves, or to vertical input motions from vertically propagating compression waves. These motions, applied

along a rigid base of the soil/structure grid, are typically
obtained by deconvolving a given ground surface record through a
one-dimensional model of the site profile. The applicability of
the FLUSH code to port and harbor facility analyses is discussed
in Section 4.2.1.2.3 of Chapter 4.

Results of these FLUSH code analyses are obtained in several
forms. First, shear stress histories are obtained at selected
locations within the soil grid, for use in assessing the liquefac-
tion potential of the site. Second, internal moments and forces
within the structure are used to obtain stresses and strains that
indicate whether structural damage could occur under the given
ground excitations. Third, lateral pressures computed in the
soil medium along its interface with the sheet pile are computed
for comparison with pressures computed using the Mononobe-Okabe
equation, which is the approach most widely used to define lateral
pressures for seismic design purposes (see Chapt. 3). Fourth, and
finally, motions and soil stresses computed within the soil/
structure system grid are compared to those from the free-field
one-dimensional deconvolution analyses to assess the importance of
soil/structure interaction and site geometry effects at this site.

5.4.2 EVALUATION OF LIQUEFACTION POTENTIAL

5.4.2.1 Overview of Liquefaction Evaluation Procedure

The procedure used in this illustrative dynamic analysis
to estimate the liquefaction potential at this particular site
involves (1) identifying locations within the soil medium at which
the potential for liquefaction is to be assessed, and obtaining
an appropriate definition of the shear stress at that location;
and (2) using these shear stresses and Standard Penetration Test
(SPT) data at the site, in conjunction with the Seed-Idriss (1981)
empirical procedures, to assess the liquefaction potential at
these locations. These empirical procedures are described in
Section 4.2.3.1 of Chapter 4.

The Seed-Idriss empirical approach is the only viable means for assessing liquefaction potential in these particular illustrative dynamic analyses, because of the absence of more complete site soils data from which alternative procedures incorporating laboratory tests can also be used. However, even where more complete soils data are available, this empirical approach is still valuable for use at an actual site because (1) it makes use of the extensive field observations of the actual behavior of soil sites during earthquakes; and (2) the more complete soils data obtained from established cyclic laboratory test procedures are prone to uncertainties due to sample disturbance. For these reasons, the empirical techniques used in these illustrative analyses are valuable as a means for supplementing the techniques using cyclic laboratory test data and, in fact, are the only possible methods that can be used when such well-defined soils data are not available.

5.4.2.2 Definition of Shear Stresses

Within the above framework, two different approaches are used to define shear stress input for the liquefaction assessment at the site of this sheet-pile bulkhead structure. The first corresponds to the use of soil shear stress histories obtained from the dynamic analysis results, and the conversion of these irregular stress histories to equivalent cyclic stress ratios through the use of the Seed et al. (1975b) procedures (see Sec. 4.2.2 of Chapt. 4). Then, as described in Section 4.2.3.1, these cyclic stress ratios, together with modified SPT resistances at the particular location being investigated, are used with a *modified* form of the Seed-Idriss (1981) results. In this, curves that separate conditions of liquefaction and nonliquefaction are developed, in terms of combinations of cyclic stress ratio and modified SPT resistance *for the particular number of stress cycles obtained from the computed stress histories.*

To supplement the above dynamic analysis results, a second approach for defining shear stress input is also included, and involves the use of the following expression for computing cyclic shear stress ratios:

$$\frac{(\tau_h)_{av}}{\sigma_v'} = \frac{0.65\ \tau_{max}}{\sigma_v'} = 0.65\ \frac{a_{max}}{g}\ \frac{\sigma_v}{\sigma_v'}\ r_d \qquad (5-1)$$

where

$(\tau_h)_{av}$ = Equivalent average cyclic stress in layer under consideration = $0.65\ \tau_{max}$, where τ_{max} is the peak shear stress

a_{max} = Peak ground acceleration

g = Acceleration of gravity

σ_v = Total overburden pressure in layer under consideration

σ_v' = Initial effective overburden pressure in layer under consideration

r_d = Depth-dependent stress reduction factor (Fig. 5-5)

This expression, which is drawn from the present Seed-Idriss (1981) empirical approach, is used to obtain cyclic stress ratios at various depths, through the use of the depth-dependent stress reduction factor, r_d (Fig. 5-5). These cyclic stress ratios, together with the modified SPT resistances at the depths under investigation, are used as input to the *present* form of the Seed-Idriss empirical results. This present form consists of curves *for various earthquake magnitudes* which define conditions of liquefaction and nonliquefaction in terms of combinations of cyclic stress ratio and modified SPT resistance. Therefore, in this second approach, the number of stress cycles is implicit in
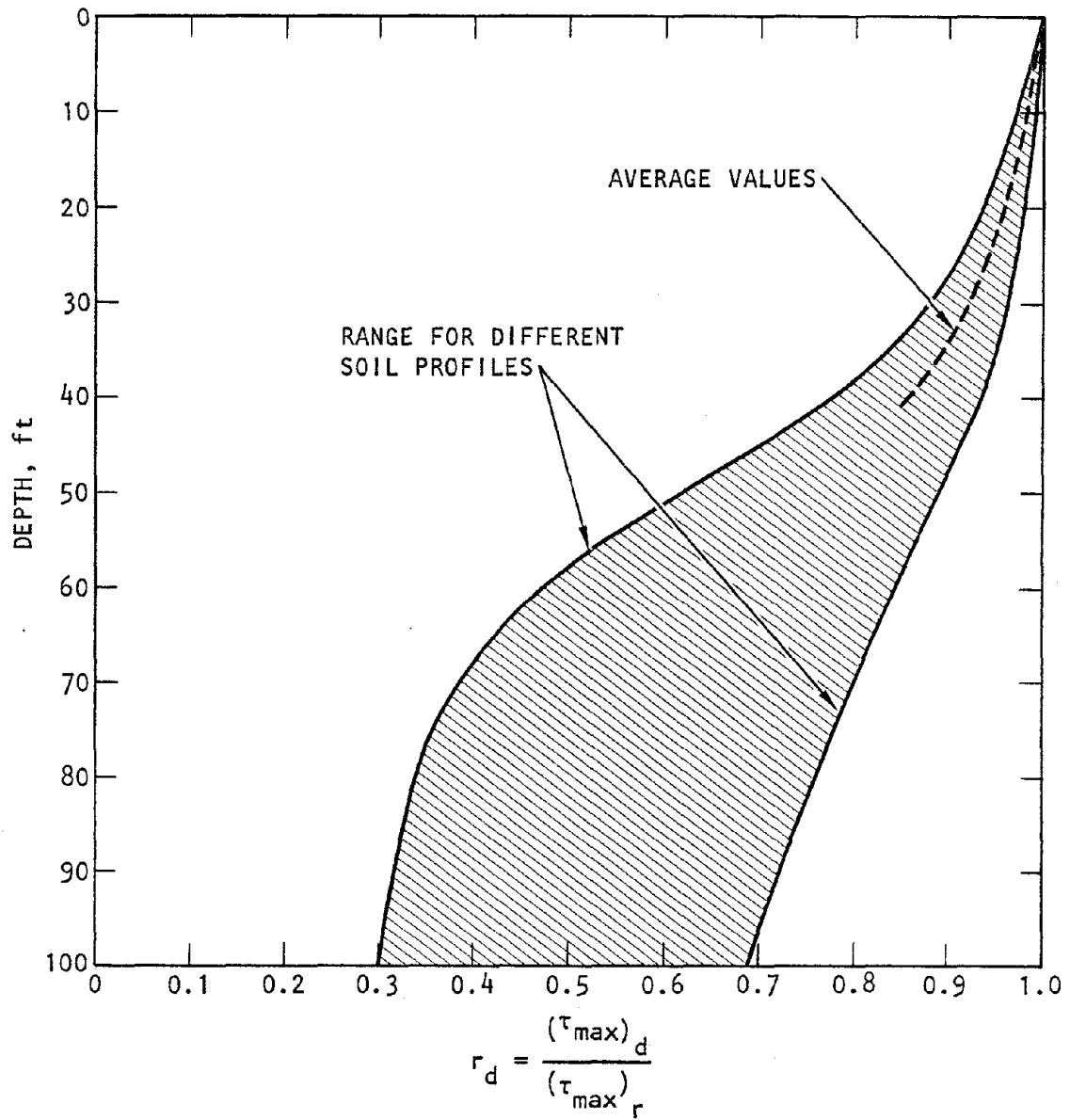
FIGURE 5-5.   RANGE OF VALUES OF r_d FOR DIFFERENT SOIL
PROFILES (Seed and Idriss, 1971)

the earthquake magnitude curves (see Sec. 4.2.3.1 of Chapt. 4).
For this illustrative analysis, the curve corresponding to magni-
tude 7.5, which is approximately the magnitude of the Miyagi-Ken-
Oki earthquake, is used.

There are two additional points to be made regarding the
determination of shear stress input for the evaluation of lique-
faction potential at this particular site. First, the use of
Equation 5-1 as a supplementary approach for estimating shear
stresses is in no way intended to represent a substitute for
dynamic analysis results. It is included here only so that,
through comparisons of the liquefaction evaluations obtained using
the dynamic analysis results vs. those obtained using Equation 5-1,
a measure of the adequacy of the use of Equation 5-1 may be
obtained for future applications where dynamic analysis may not be
possible. Second, it has been noted in Chapter 4 (Sec. 4.2.1.2.1)
that the departure of the site conditions from the ideal case of
infinitely long horizontal soil layers could lead to gravity-
induced initial shear stresses on horizonal planes. These initial
shear stresses could affect the soil response to a superimposed
cyclic stress condition and could reduce the rate of porewater
pressure generation due to cyclic stress applications (also see
Seed, 1979a). In practice, these initial shear stresses, when
judged to be significant, are estimated from static finite element
analyses and are incorporated into laboratory cyclic load tests
to assess the liquefaction potential at the site (see Chapt. 3
and Seed, 1979b). For this particular site, the limited soils
data precludes direct consideration of initial shear stress
effects; however judgment suggests that such effects would not be
important in this case, since the presence of the bulkhead during
placement of the soil behind the bulkhead should largely prevent
these initial shear stresses from developing. In view of this, it
is reasonable to assess the liquefaction potential in this illus-
trative example solely from the dynamic analysis results although,

in practice, the potential effects of initial shear stresses
should be evaluated on a case-by-case basis.

5.5   SOIL/STRUCTURE SYSTEM MODEL

5.5.1   FINITE ELEMENT GRID

The soil/structure system model used in this analysis is
shown in Figure 5-6.   This model consists of a two-dimensional
finite element grid with 148 node points, 104 soil elements,
22 structural beam elements, and 6 elements whose mass density
and elastic properties approximate the effects of the sea water.
The overall dimension of the grid is 265.6 ft (horizontal) by
149.8 ft (vertical) by 5.25 ft (normal to the plane of the
paper).[*]   The sea water level is assumed to be at the bottom of
the fill, which is approximately the low water level at this
structure location.   The base of the grid is rigid, and is the
location of the applied seismic excitations (Sec. 5.3).

The soil medium is comprised of six different materials that
correspond to the various sand and silt layers at the site.   The
base of the soil grid is rigid, and is the location at which the
horizontal and vertical seismic input motions are applied (sepa-
rately, not simultaneously in the same calculation).   In-plane
horizontal and vertical dashpots (not shown in Fig. 5-6) are pro-
vided at each soil node point to simulate out-of-plane radiation
damping effects, and energy-absorbing boundaries are employed
along each side boundary node point.   As previously noted in
Section 4.2.1.2.3, these in-plane viscous dampers and energy-
absorbing boundaries have been derived on the basis of horizontal

---

[*]This latter dimension corresponds to the spacing of the sheet-
pile supports and tie rod/H-beam anchor system (Fig. 5-2).
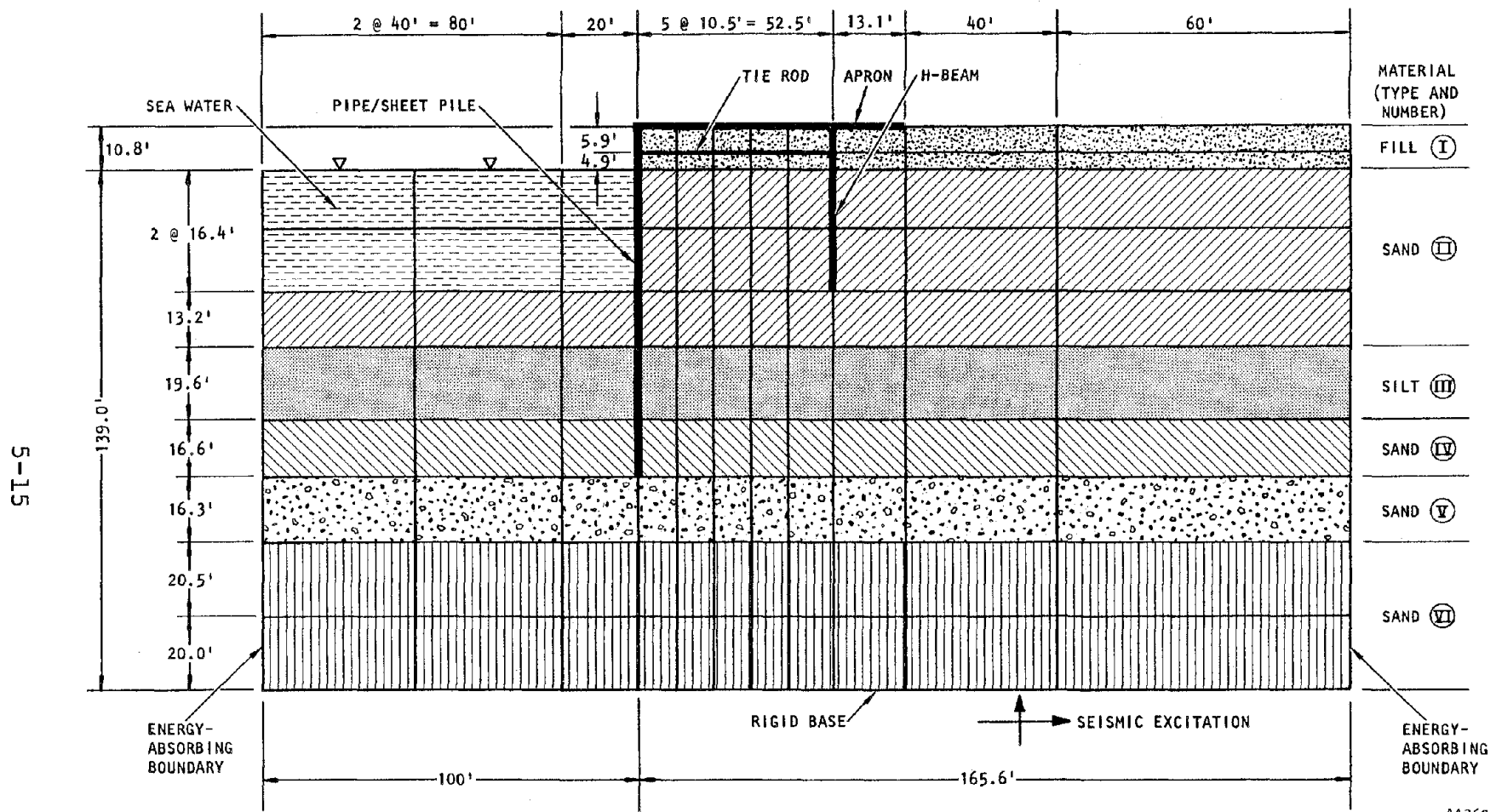
FIGURE 5-6.   FINITE ELEMENT MODEL

soil layering over the entire lateral extent of the grid. These
conditions do not hold over the depth of the sheet pile considered
in this analysis; i.e., water elements are used on one side of
the sheet pile and elements representing the soil backfill are
used on the other side. However, a satisfactory representation
of the system response is nevertheless provided in this analysis
by (1) extending the lateral boundaries of the soil grid a reason-
able distance away from the region of interest (which is the
region at the sheet-pile bulkhead location); and (2) using
in-plane dashpot coefficients for the layers along the depth of
the sheet pile that are representative of the soil backfill
properties.

The remainder of this section describes in more detail how
the structure was modeled and how the dynamic soil properties
were estimated.

5.5.2 STRUCTURE MODEL

The width of the finite element grid (5.25 ft) has been
selected to correspond to the spacing of the vertical pipes that
support the sheet pile, as well as the spacing of the tie-rod/
H-beam anchor which are connected to the vertical pipes (Fig. 5-2).
The overall model of the sheet-pile bulkhead is therefore com-
prised of four different beam element types that represent the
properties of its wall support system, apron, tie rod, and H-beam
anchor. The properties of these various structural elements are
given in Table 5-1.

5.5.3 SOIL MODEL

As previously noted, two sets of equivalent linear soil
models have been assumed for these illustrative dynamic analyses.
The first corresponds to the actual soil properties at the site,
as indicated by the various borings and the associated SPT blow-
counts obtained near the sheet-pile bulkhead structure (Fig. 5-3).

TABLE 5-1. PROPERTIES OF STRUCTURAL ELEMENTS IN FINITE ELEMENT GRID

Element	Dimensions	Material Properties			Section Properties		
		Modulus of Elasticity, psi	Poisson's Ratio	Unit Weight, pcf	Cross Sectional Area, ft²	Shear Area, ft²	Moment of Inertia, ft⁴
Sheet-Pile/ Pipe System	Pipe Diameter = 2.34 ft Wall Thickness = 0.0312 ft	3.0×10^7	0.25	490	0.2262	0.1131	0.1506
Concrete Apron	Thickness = 0.66 ft Width = 5.25 ft	3.0×10^6	0.15	150	3.460	2.318	0.0297
Tie Rod	Diameter = 0.164 ft	3.0×10^7	0.25	490	0.0211	0.0158	small
H-Beam	Total Depth = 1.274 ft Flange Width = 1.32 ft Web Thickness = 0.0492 ft Flange Thickness = 0.0492 ft	3.0×10^7	0.25	490	0.1877	0.0417	0.0546

AA396

5-17

R-8122-5395

The second soil model corresponds to properties assumed to result from application of deep compaction soil improvement techniques to the soil in the vicinity of the structure. In each of these soil models, the water table is assumed to occur at the top of the second row of fill elements which, in view of the lack of more definitive information (Sec. 5.2.2), allows for some reasonable fluctuation of the water table above the assumed sea water level (Fig. 5-7). The various soil models are described in more detail in the subsections that follow.

5.5.3.1 Model for Original Site Condition

The model for the original soil conditions at the structure site, before application of the deep compaction techniques, has been obtained by approximate techniques, based on SPT blowcounts in the absence of any direct measurement of dynamic soil properties in the field or in the laboratory. For the fill and sand layers, the procedure to obtain equivalent linear shear moduli involved the following:

- Define uniform SPT blowcount levels for each sand layer, based on an average of the blowcounts recorded over the depth of that layer in the three boreholes at the quay wall site. These are shown in Figure 5-7.

- Convert the SPT blowcounts to apparent relative density through the Gibbs & Holtz (1957) procedures (Fig. 5-8).

- For the apparent relative density for each layer obtained in this manner, utilize the appropriate curve of K_2 vs. shear strain as defined by Seed and Idriss (1970) (Fig. 5-9a).

- Compute the strain-dependent shear modulus for each layer as G (psf) $= 1000 K_2 \sqrt{\sigma_m'}$, where σ_m' is the mean effective stress in psf computed at the midheight of that layer (Fig. 5-7).
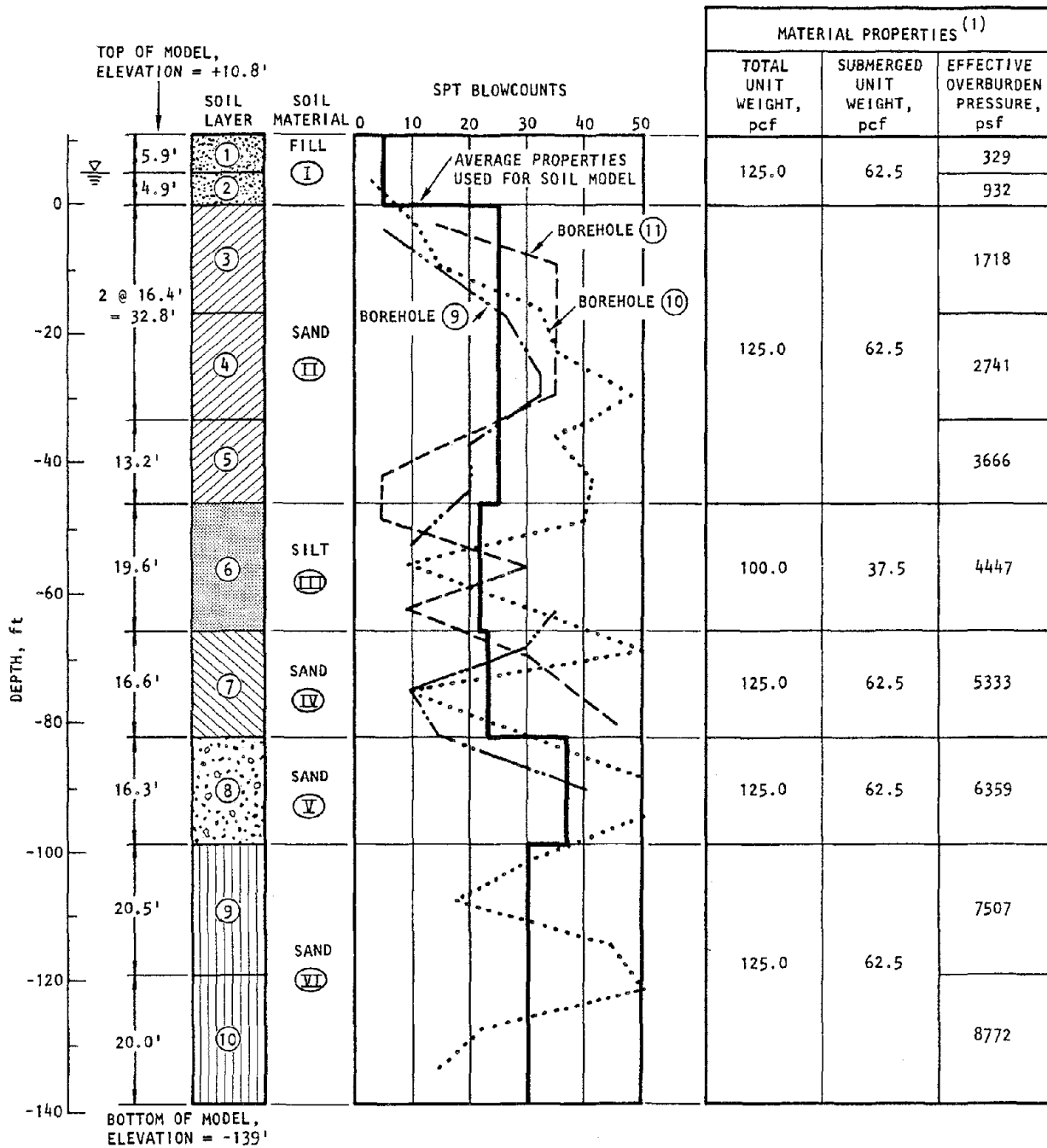
FIGURE 5-7. SOIL MATERIAL PROPERTIES FOR ORIGINAL SITE CONDITIONS CONSIDERED IN FINITE ELEMENT MODEL
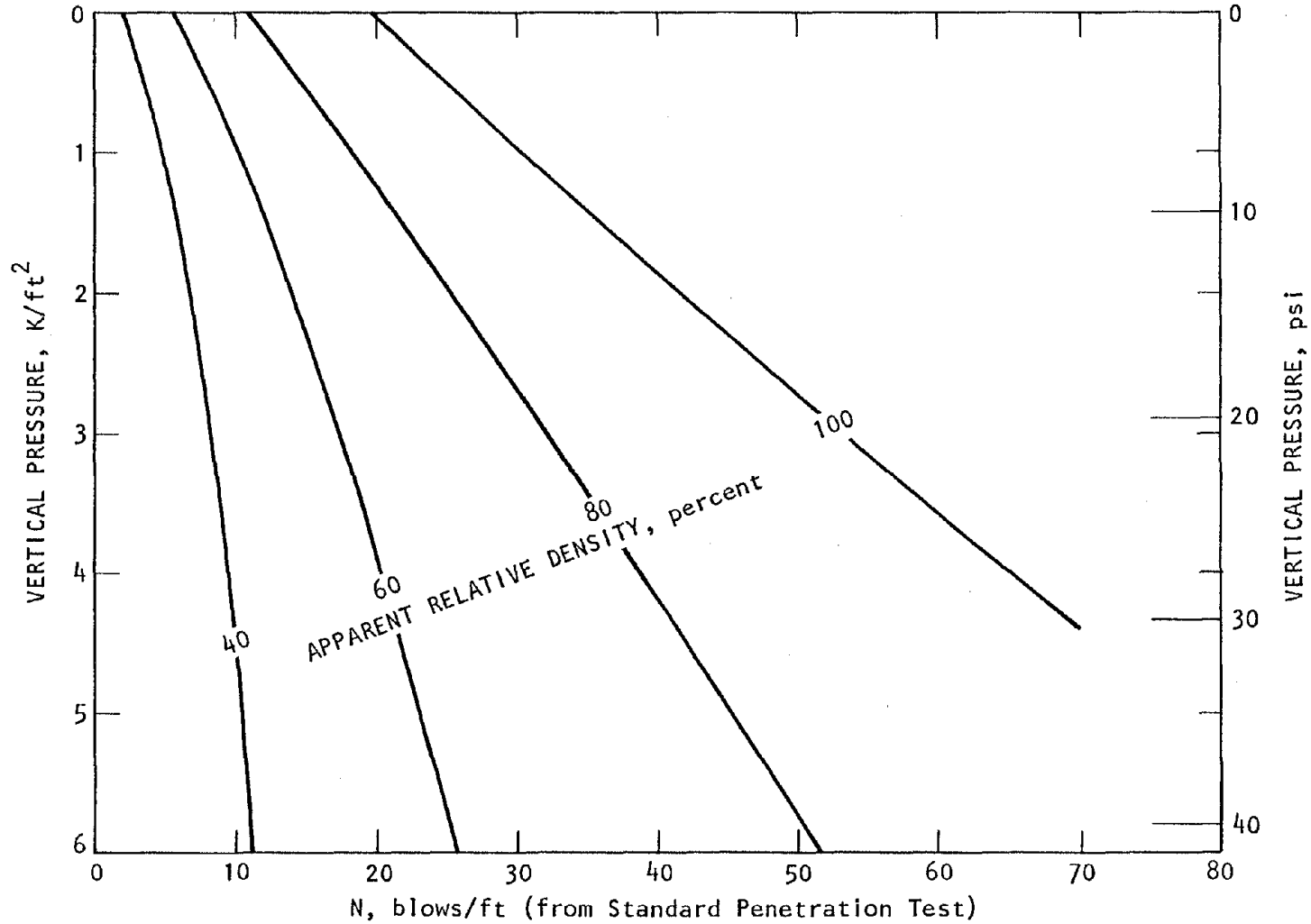
FIGURE 5-8. APPARENT RELATIVE DENSITIES CALCULATED FROM STANDARD
PENETRATION RESISTANCES (Gibbs and Holtz, 1957)
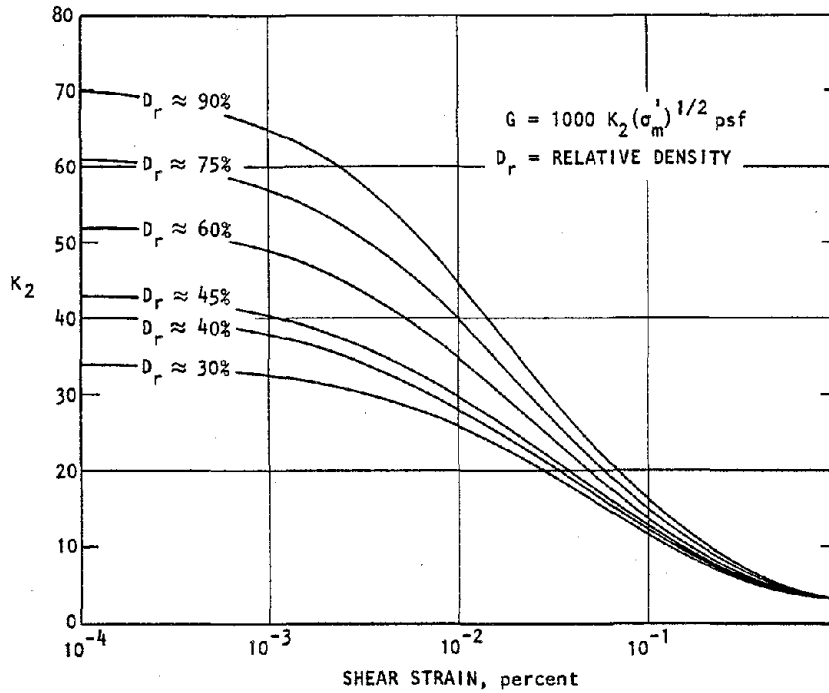
(a)   Shear moduli
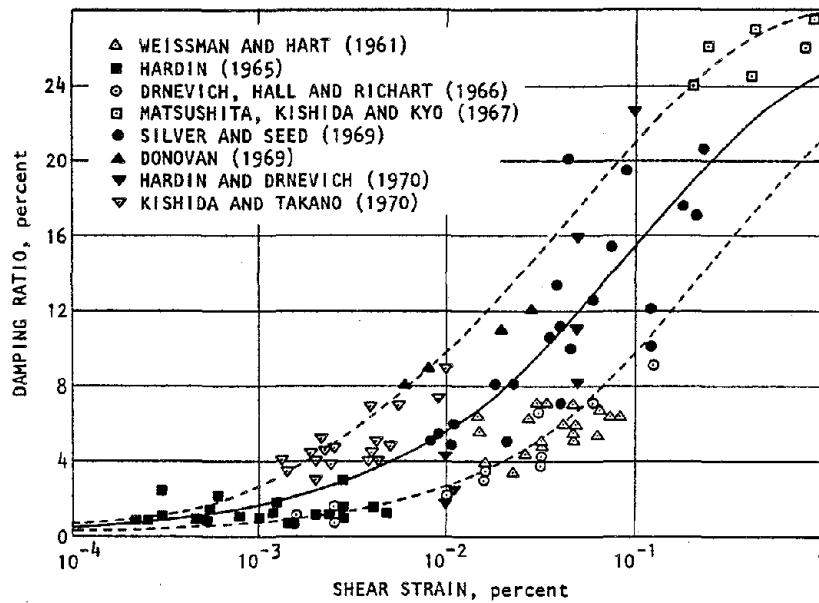
(b)   Damping ratios

FIGURE 5-9.   EQUIVALENT LINEAR DYNAMIC PROPERTIES FOR SANDS
(Seed and Idriss, 1970)

The strain-dependent damping ratios for the sands have been
assumed to correspond to the curve recommended by Seed and Idriss
(1970) (Fig. 5-9b). All other pertinent material properties for
the sand layers are given in Figure 5-7.

The definition of the dynamic properties of the silt layer
at this site was complicated by the lack of empirical test data
for silts, of the type shown in Figure 5-8 for sands. Therefore,
based on some early recommendations by Seed and Idriss (1970),
this silt layer was assumed to be a sand with a relative density
of 75% and with shear moduli modified by a factor of 0.7. The
strain-dependent damping curve for the silt layer was assumed
to be identical to that shown in Figure 5-9b for sands.

5.5.3.2 Model for Improved Site Conditions

As previously noted, a second set of site conditions was
considered in these analyses, in order to represent the use of
deep compaction soil improvement techniques to improve the prop-
erties of the soil materials. From past experience, it was
assumed that such techniques will increase the relative density
of the near-surface sand layers (within about 70 ft of the ground
surface) to a value of about 70%, regardless of the original rela-
tive density of these sand layers (Mitchell and Katti, 1981).
These soil improvement techniques were assumed to have no effect
on the relative density of the silt layer or the deeper sand
layers that exist at this site (Pyke, 1982). On this basis, the
following procedure was used to .define the soil model correspond-
ing to these improved conditions:

- For the fill and for each sand layer above the silt
  (Layers 1 through 5 in Fig. 5-7), the relative density
  was assumed to be increased to 70%.

- On this basis, new strain-dependent shear modulus curves were defined for each of these layers, based on the empirical data from Figure 5-9a and the mean effective stress for each layer. This mean effective stress as well as the strain-dependent damping ratios for each of these layers were assumed to be unchanged by the deep compaction techniques.

- New SPT blowcounts for these upper layers, necessary for use in the liquefaction evaluations, were obtained for each of these upper layers through the use of the Gibbs and Holtz (1957) procedures, in conjunction with an apparent relative density of 70% and the vertical pressure at the midheight of each layer (Fig. 5-8).

- The dynamic properties of the silt layer and the lower sand layers (Layers 6 through 10 in Fig. 5-7) were assumed to be unchanged from those of the original unimproved soil conditions.

5.6 RESULTS

5.6.1 FORM OF RESULTS

This section presents the results from the dynamic analyses of the sheet-pile bulkhead/soil system for two sets of soil conditions corresponding to (1) the original site conditions as described in Section 5.5.3.1 (Case 1); and (2) the modified site conditions corresponding to application of deep compaction soil improvement techniques, as described in Section 5.5.3.2 (Case 2). These results are presented in the form of computed motions, liquefaction assessments, lateral pressures along the bulkhead-wall/soil interface, and internal forces, moments, and stresses within the structure.

An important aspect of the results presented in the remainder of this chapter involves comparisons of the seismic response characteristics corresponding to the Case 1 (original) and Case 2 (improved) soil conditions. The comparisons presented are based on a total stress method of dynamic analysis which, as previously noted, does not represent effects of porewater pressure buildup on the computed response of the soil/structure system. In this, because the near-surface saturated soil layers in Case 1 exhibit much lower relative densities than for Case 2, the Case 1 system response to strong seismic excitations should be affected to a greater degree by these porewater pressure effects.[*] Therefore, it is expected that (1) these total stress analysis results will probably underestimate the differences in system response corresponding to the Case 1 and Case 2 soil conditions; and (2) because the porewater pressure effects neglected in these analyses will be less pronounced for the Case 2 soil conditions, its computed system response characteristics should be somewhat more representative than those obtained for the Case 1 conditions. These considerations should be kept in mind when interpreting the results presented in the remainder of this chapter.

5.6.2 COMPUTED MOTIONS

The horizontal and vertical motions at selected node points throughout the soil/structure grid were computed for both cases and were compared to each other and to the computed depth-dependent motions in the free field.[†] These motions, presented here as

---

[*] For example, for the case of undrained conditions, a porewater pressure buildup in the near-surface saturated soil layers will be more prominent in Case 1 than for Case 2. This, in turn, will result in a greater reduction in the mean effective stresses and in the corresponding equivalent linear shear moduli for these soil layers under Case 1 conditions (Fig. 5-9b).

[†] These subsurface free-field motions were obtained from a deconvolution of the measured ground surface motions through a soil column corresponding to the landward side of the sheet pile.

response spectra with a damping ratio of 0.05, are typified by
the results shown in Figures 5-10 through 5-13. These show that
(1) the computed motions corresponding to the original site condi-
tions (Case 1) are very similar to those corresponding to the
improved site conditions (Case 2);[*] and (2) the soil/structure
system motions are very similar to the free-field motions and are
therefore not sensitive to effects of soil/structure interaction
or site topography for the conditions represented by these analyses.

5.6.3 LIQUEFACTION ASSESSMENT

The approach used in these illustrative analyses to assess
the liquefaction potential at the site under its original soil
conditions (Case 1) and its improved soil conditions (Case 2) are
described in Section 5.4.2. Results from these assessments are
provided in the paragraphs that follow. It is noted that these
assessments are based only on the results from the horizontal
response analyses, since the vertical response analyses show
negligible shear stresses in the soil.

5.6.3.1 Cyclic Shear Stresses

As described in Section 5.4.2, two approaches are used to
provide shear stress input to the liquefaction assessments--the
first involves the use of results from the dynamic finite element
results and the second involves the use of Equation 5-1. In this
subsection, shear stresses obtained from the first approach
(i.e., from the dynamic finite element analysis) are presented.
This approach is used herein to assess the liquefaction potential
based on shear stresses computed in the saturated soil layers
beneath the midspan of the apron that extend to the bottom of the

---

[*]See comments in Section 5.6.1 regarding comparisons of the Case 1
and Case 2 response characteristics.
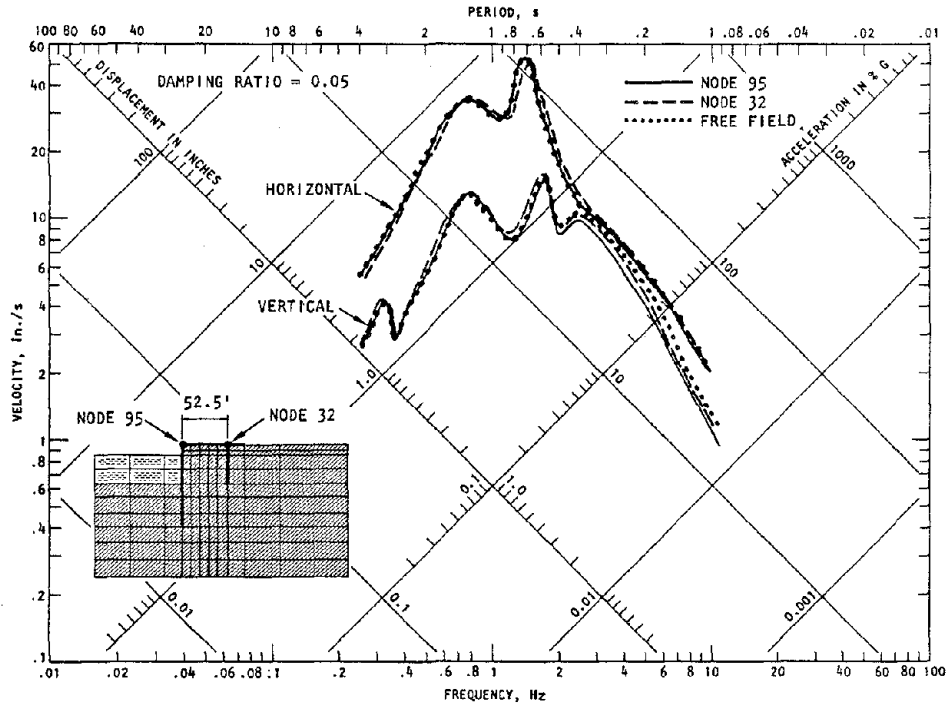
(a)   Case 1
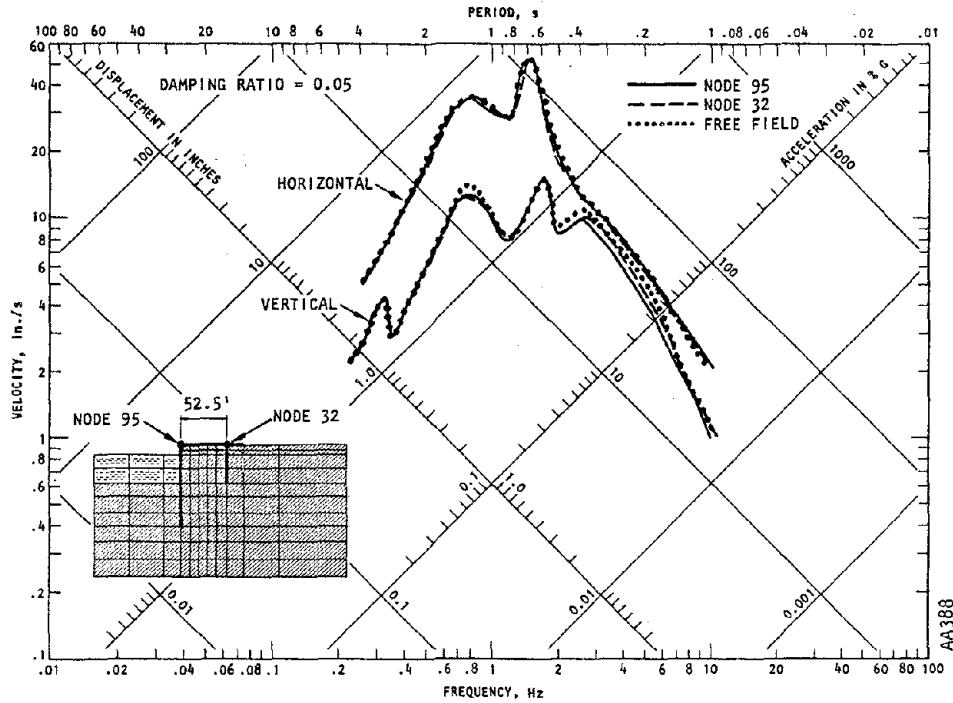
(b)   Case 2

FIGURE 5-10.   SPECTRA OF COMPUTED MOTIONS — TOP OF FILL
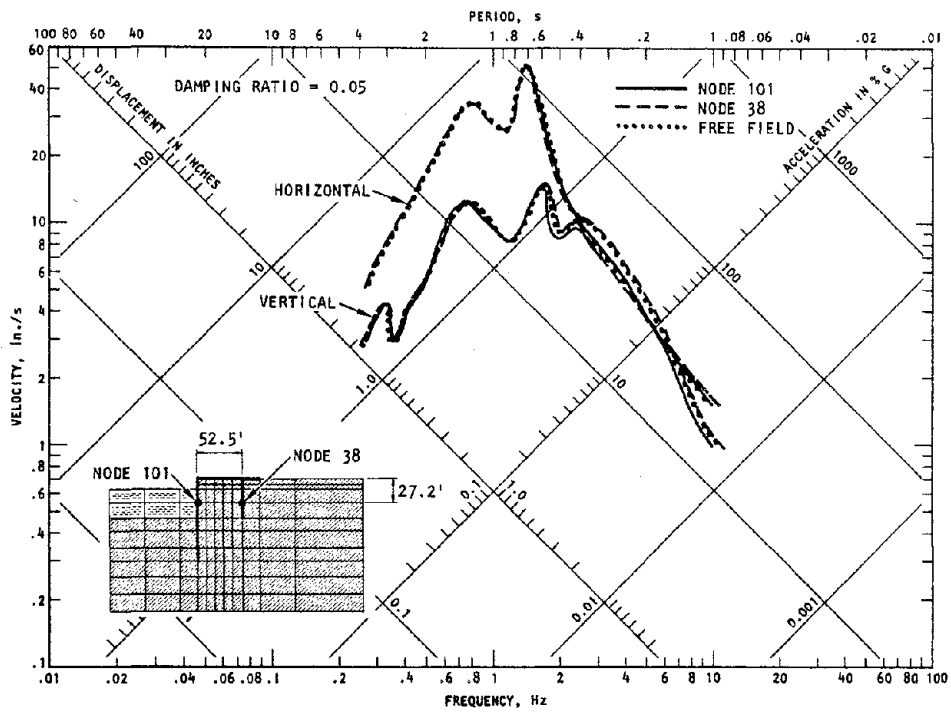
(a) Case 1
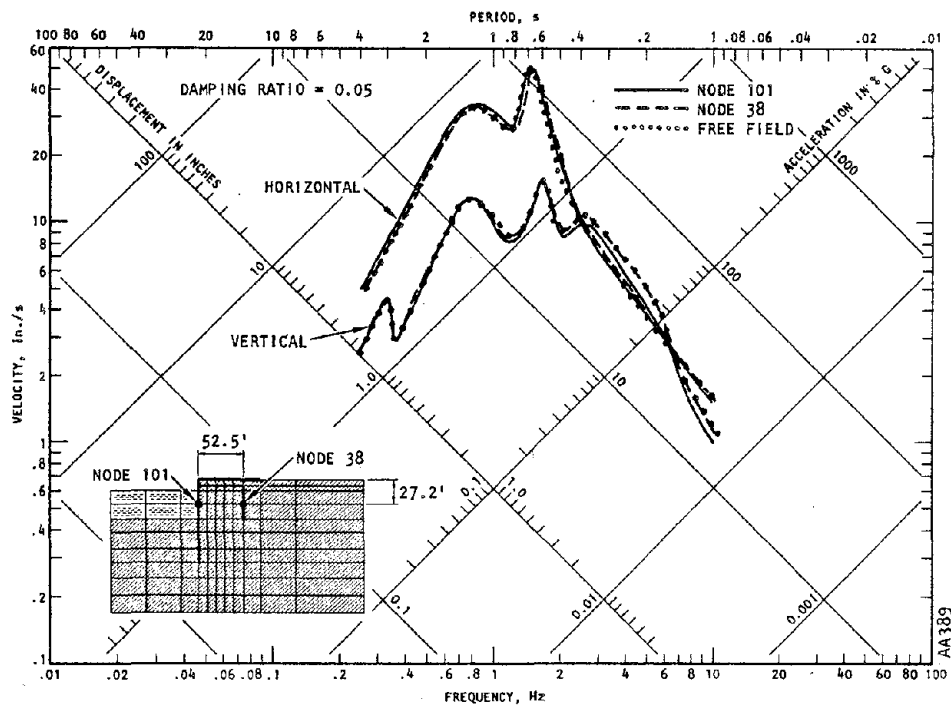
(b) Case 2

FIGURE 5-11.   SPECTRA OF COMPUTED MOTIONS — 27.2 FT BELOW
TOP OF FILL
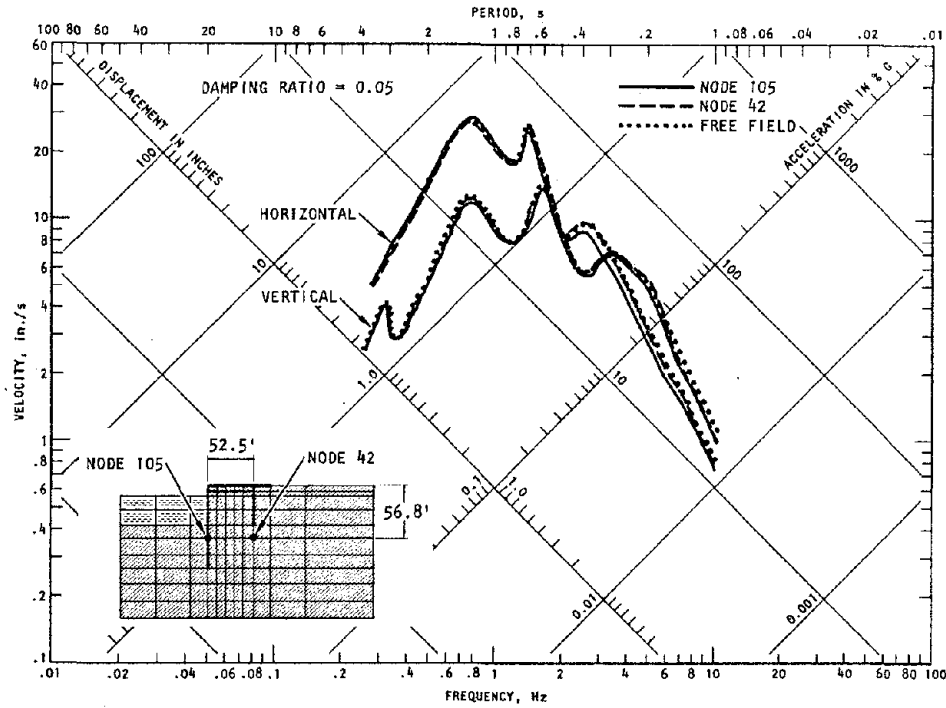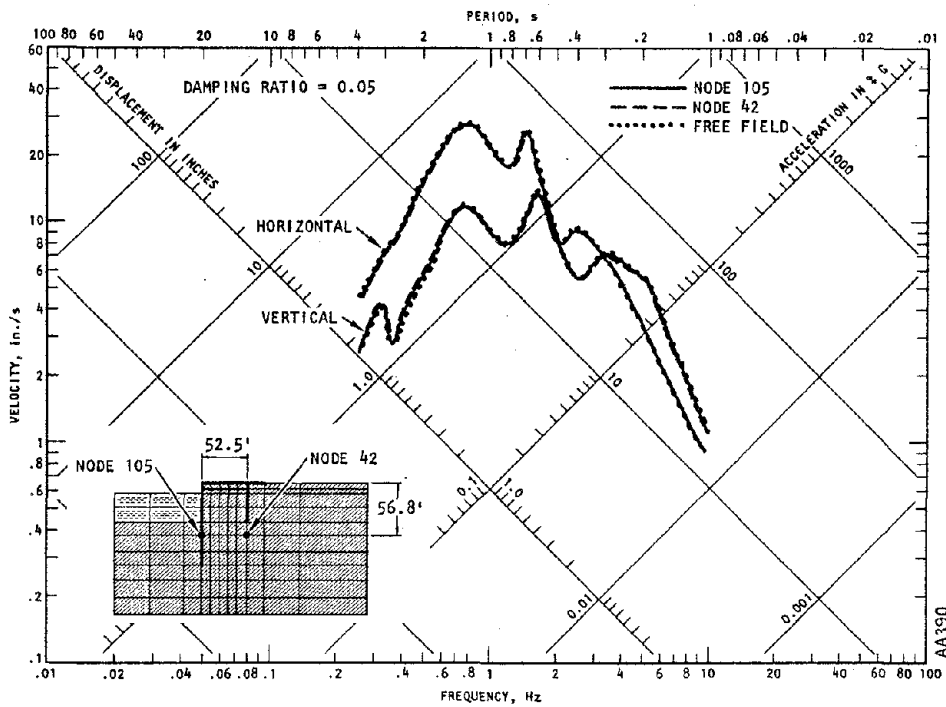
(a)   Case 1

(b)   Case 2

FIGURE 5-12.   SPECTRA OF COMPUTED MOTIONS — 56.8 FT BELOW
TOP OF FILL
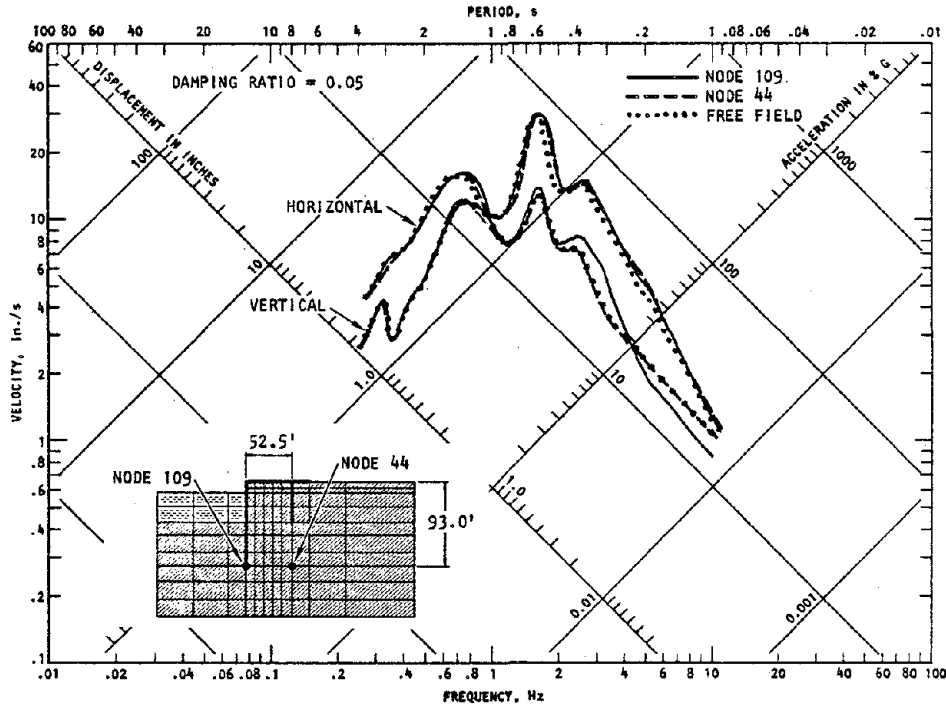
(a) Case 1
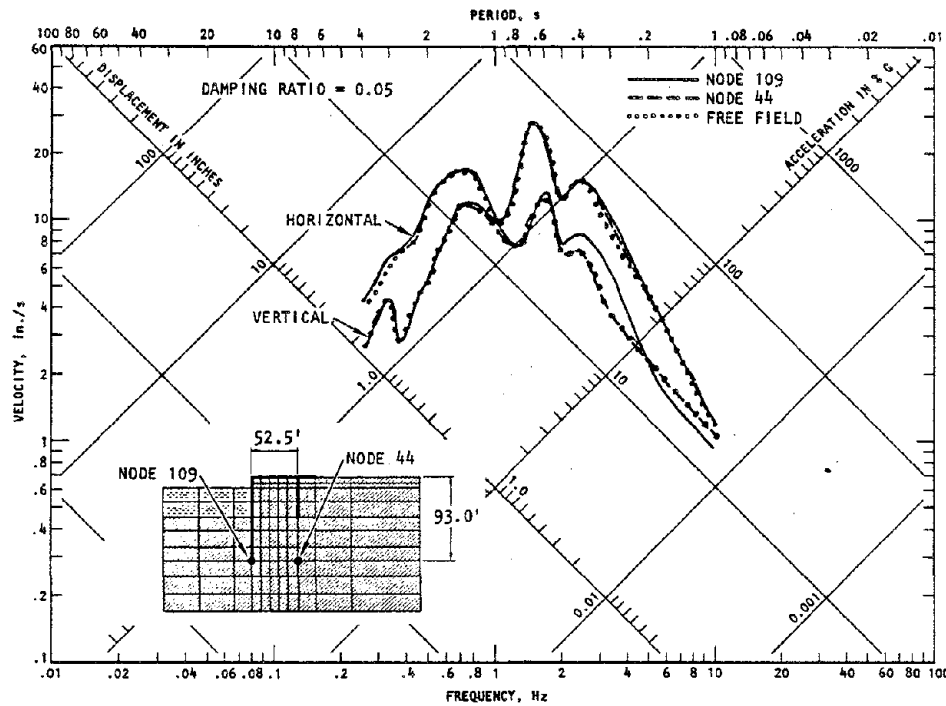
(b) Case 2

FIGURE 5-13. SPECTRA OF COMPUTED MOTIONS — 93.0 FT BELOW TOP OF FILL

sheet pile (i.e., at Elements 52 to 57 in Fig. 5-14). However, shear stresses have also been monitored at Element 51 in the fill material at this location (which is above the assumed position of the water table), and at Elements 71 to 77 (along the sheet-pile/ soil interface) to evaluate how the soil shear stresses are affected by differences in horizontal position.

Example shear stresses at these locations are given in Figure 5-15 and maximum soil shear stresses obtained at various locations in the finite element grid are listed in Table 5-2. These results show that the shear stresses computed from the finite element results are nearly the same for the Case 1 and Case 2 soil conditions.[*] The results also show that the near-surface maximum shear stresses in the soil vary with horizontal distance from the bulkhead wall and differ from free-field shear stresses computed from one-dimensional analyses. These differences are generally largest at Elements 71 to 77 (alongside the sheet pile) and are probably most attributable to surface topography effects, since soil/structure interaction should not be as significant for the relatively light and flexible structure considered in this analysis. At depths below about 27 ft, the peak shear stresses from the finite element analyses compare well with those from the one-dimensional free-field analyses.

The use of the Seed et al., (1975b) results to convert the irregular shear stress histories from the finite element analysis to equivalent cyclic shear stresses is illustrated in Figures 5-16 and 5-17. The cyclic shear stresses obtained in this manner are provided subsequently in Section 5.6.2.4, where the evaluation of the liquefaction potential for the site is described. Similarly,

___

[*] See comments in Section 5.6.1 regarding comparisons of the Case 1 and Case 2 response characteristics.
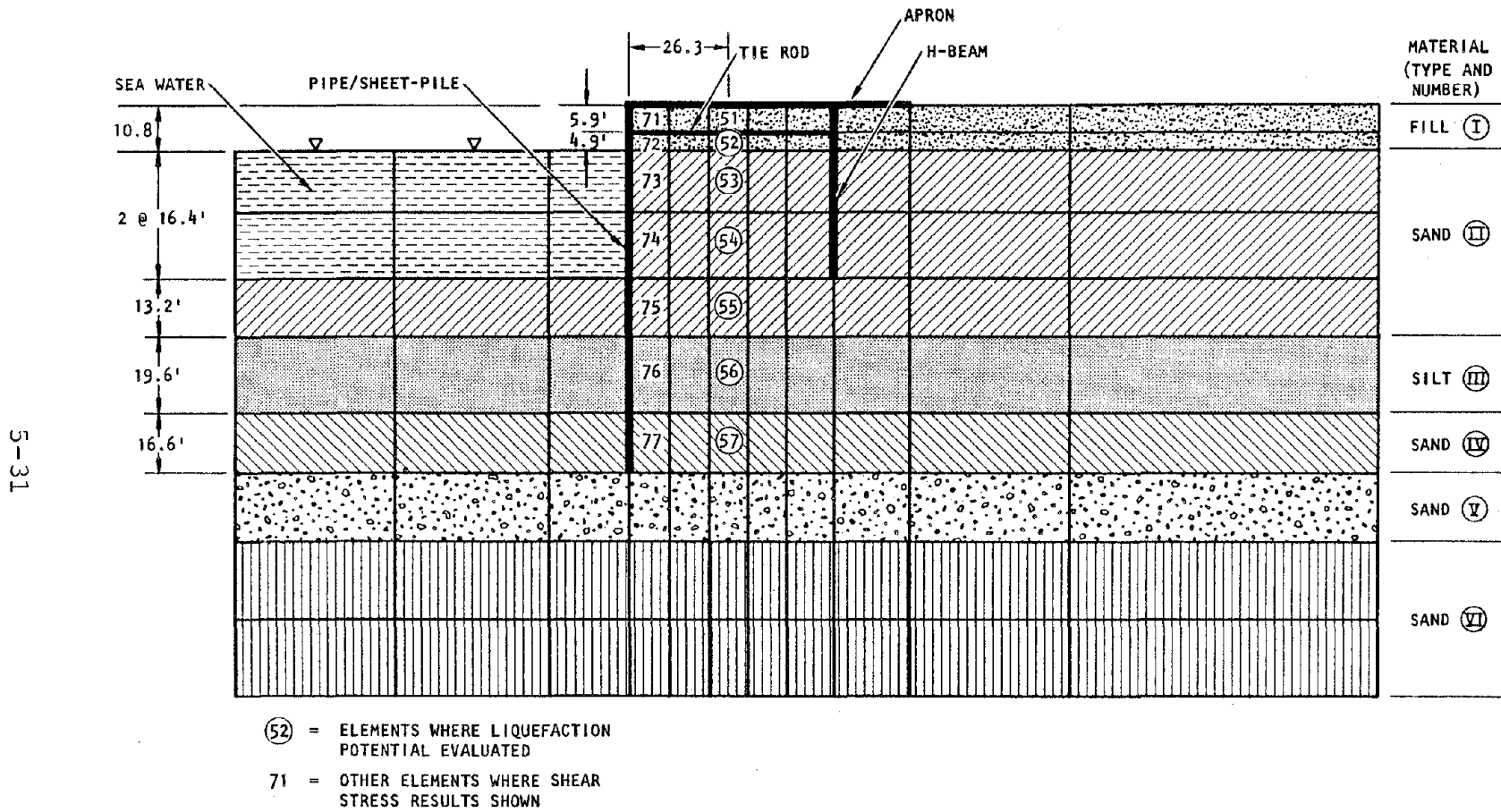
FIGURE 5-14. LOCATION OF ELEMENTS WHERE LIQUEFACTION
EVALUATION CARRIED OUT
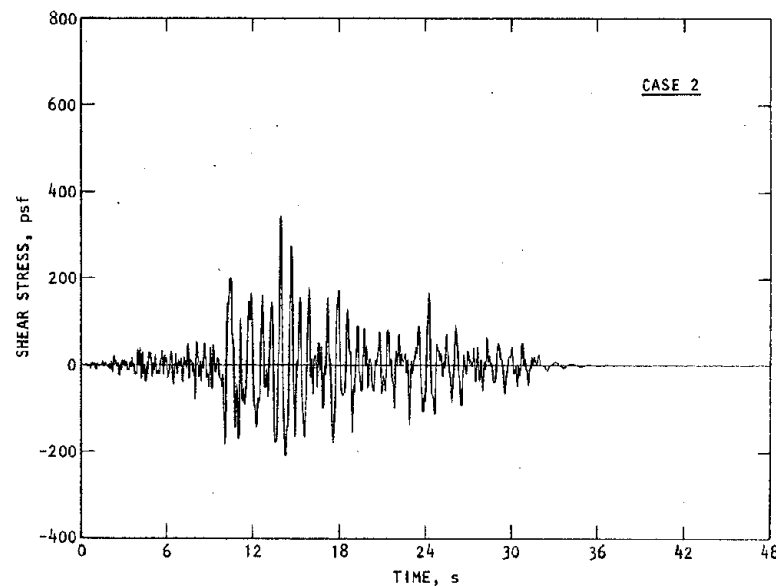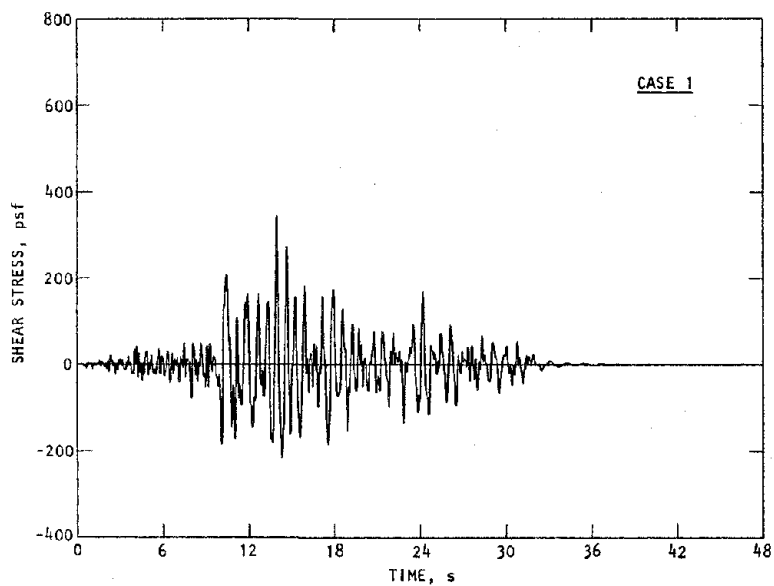
(a)   Element 52
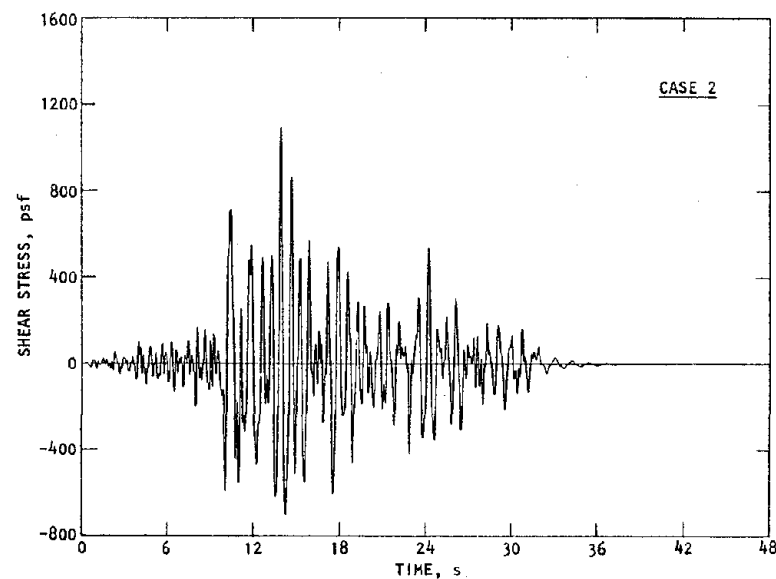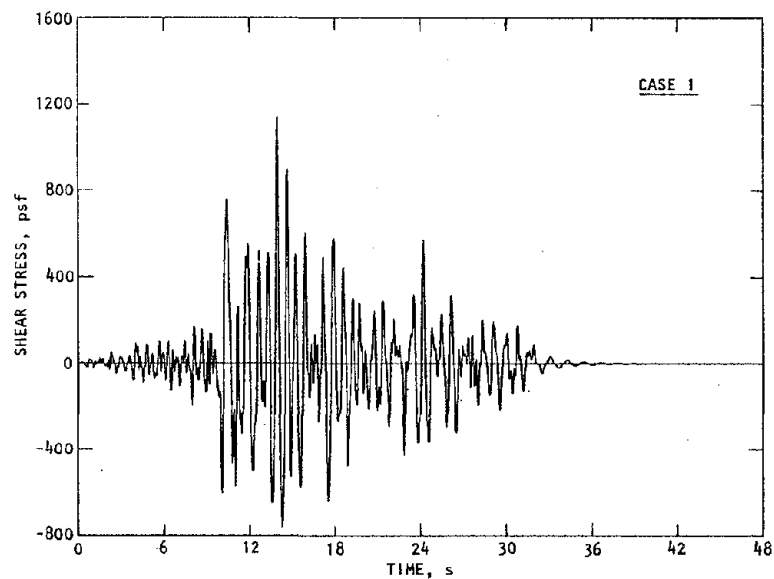
(b)   Element 54

AA377

FIGURE 5-15.   COMPARISON OF SHEAR STRESS HISTORIES FROM CASES 1 AND 2

TABLE 5-2. MAXIMUM SHEAR STRESSES IN SOIL FROM FINITE ELEMENT ANALYSIS

Case Number	Depth to Bottom of Layer, ft	Soil Shear Stress (free field) psf	Soil Shear Stress (Soil/Structure System)					
			Alongside Sheet Pile			26.3 ft Landward of Sheet Pile		
			Element No., Fig. 5-14	Shear Stress, psf	Ratio to Free Field Shear Stress	Element No., Fig. 5-14	Shear Stress, psf	Ratio to Free Field Shear Stress
1	5.9	105	71	138	1.31	51	236	2.25
	10.8	295	72	168	0.57	52	349	1.18
	27.2	655	73	520	0.79	53	685	1.05
	43.6	1155	74	1070	0.93	54	1150	0.99
	56.8	1410	75	1275	0.90	55	1380	0.98
	76.4	1500	76	1355	0.90	56	1460	0.97
	93.0	1485	77	1400	0.94	57	1430	0.96
2	5.9	104	71	120	1.15	51	229	2.20
	10.8	289	72	150	0.52	52	345	1.19
	27.2	650	73	490	0.75	53	655	1.01
	43.6	1150	74	1030	0.90	54	1100	0.96
	56.8	1395	75	1230	0.88	55	1330	0.95
	76.4	1460	76	1310	0.90	56	1400	0.96
	93.0	1480	77	1440	0.97	57	1455	0.98

τ_{max} = 1150 psf

$$\left.\begin{array}{l}\tau_{max} = 1150 \text{ psf} \\ \sigma'_o = 2741 \text{ psf}\end{array}\right\} 0.65 \ \tau_{max}/\sigma'_v = 0.272$$
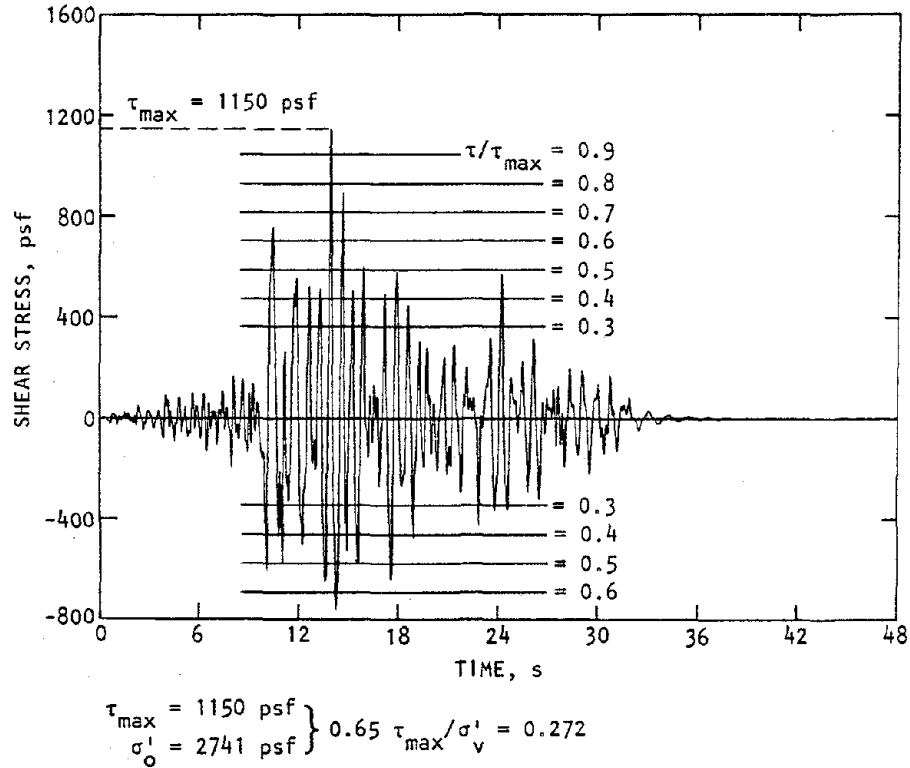
$\dfrac{\tau}{\tau_{max}}$	Positive			Negative		
	No. of Cycles	Conversion Factor (Fig. 5-16)	Equivalent Cycles at 0.65 τ_{max}	No. of Cycles	Conversion Factor (Fig. 5-16)	Equivalent Cycles at 0.65 τ_{max}
1	1	3	3.0			
0.95						
0.90						
0.85						
0.80						
0.75	1	1.5	1.5			
0.70						
0.65	1	1	1.0	1	1	1.0
0.60						
0.55						
0.50	2	0.2	0.4	3	0.2	0.6
0.45	2	0.1	0.2	1	0.1	0.1
0.40	5	0.04	0.2	3	0.04	0.12
0.35	1	0.02	0.02	1	0.02	0.02
0.30						
		Total	6.32		Total	1.84

Average No. of Cycles = 4.08

FIGURE 5-16. EXAMPLE DETERMINATION OF EQUIVALENT NUMBER OF STRESS CYCLES AT 0.65 τ_{max} (for Element 54, Case 1)
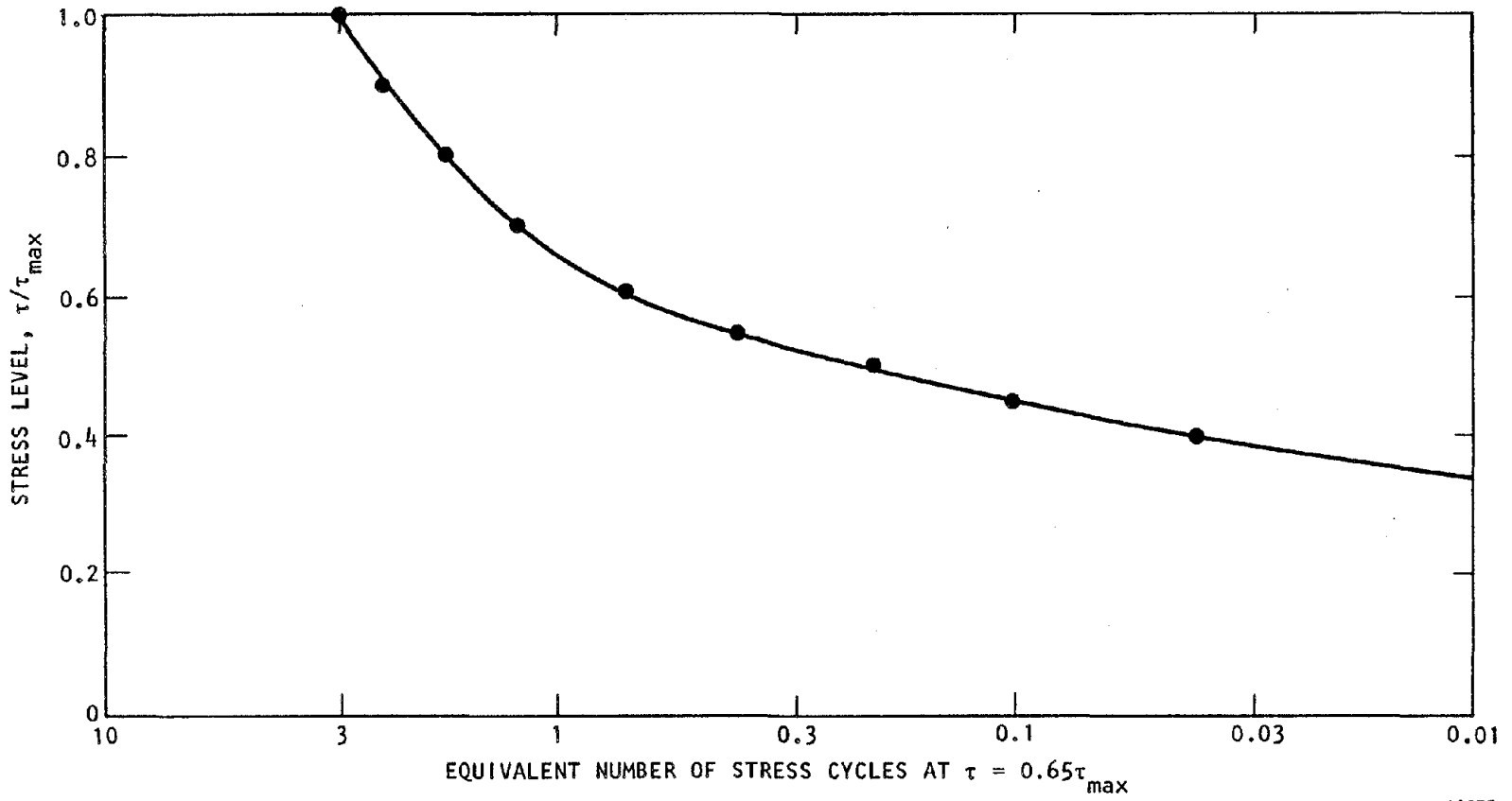
FIGURE 5-17.   EQUIVALENT NUMBER OF CYCLES AT $\tau = 0.65\tau_{max}$ FOR
                DIFFERENT STRESS LEVELS IN FIELD (Seed et al.,
                1975b)

AA375

cyclic shear stresses, obtained using Equation 5-1, are also provided in that section. In this, Equation 5-1 has been used to obtain shear stresses at depths corresponding to each of the element locations shown in Figure 5-14, so as to permit a comparison between the results of the two liquefaction assessment approaches considered in this analysis.

5.6.3.2 Modified Penetration Resistance

The Seed-Idriss (1981) empirical correlations of liquefaction potential represent the soil material characteristics in terms of the measured SPT resistance corrected to an effective overburden pressure of 1 tsf. This quantity is determined from the relationship

$$N_1 = C_N \cdot N$$

where N is the measured SPT resistance, N_1 is the corrected SPT resistance, and C_N is a function of the effective overburden pressure at the depth where the SPT was conducted (Fig. 5-18). The resulting values of N_1 at the elements being analyzed for the Case 1 and Case 2 soil conditions are shown in Tables 5-3 and 5-4. These tables show that the soil improvement techniques characterized in Case 2 result in a dramatic increase in the N_1 values for the fill (Element 52) and a noticeable but somewhat smaller increase in the N_1 values for the underlying sand layer; this can be contrasted with the essentially negligible effects of soil improvement on the soil/structure system motions and soil shear stresses (computed neglecting porewater pressure effects), as discussed previously.
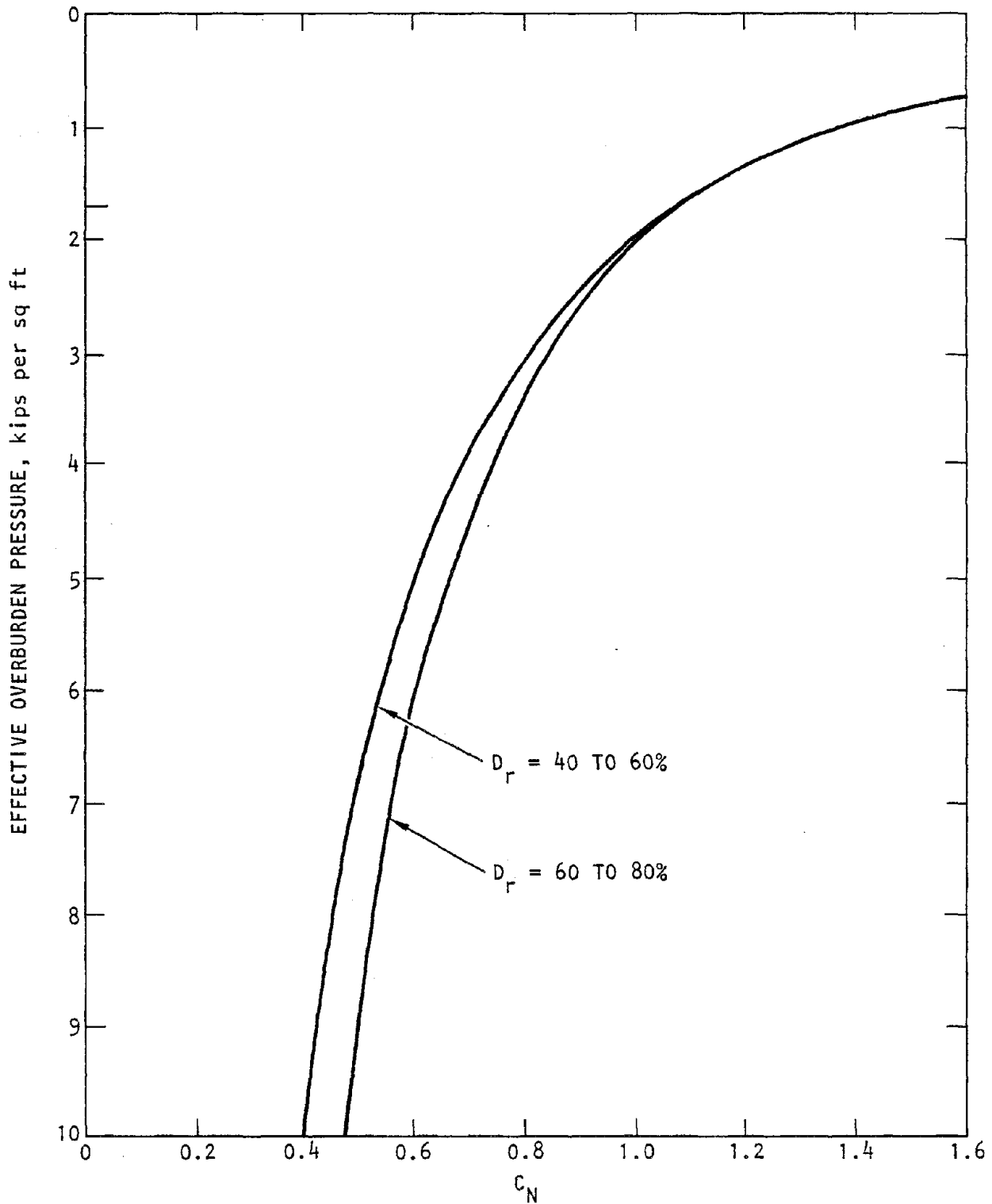
FIGURE 5-18.   RECOMMENDED CURVES FOR DETERMINATION OF C_N
BASED ON AVERAGES FOR W.E.S. TESTS (Seed
and Idriss, 1981)

TABLE 5-3. DATA FOR ASSESSING LIQUEFACTION POTENTIAL — CASE 1 CONDITIONS

Penetration Resistance					Average Cyclic Stress Ratio, $\dfrac{0.65 \tau_{max}}{\sigma'_v}$				
					From Soil/Structure System Finite Element Analysis			From Equation 5-1	
Element (Fig. 5-14)	N (Fig. 5-6)	σ'_v (ksf)	C_N (Fig. 5-18)	N_1 (C_N x N)	Peak Shear Stress, τ_{max} (ksf)	Average Cyclic Stress Ratio	Number of Cycles	Stress Ratio	Number of Cycles*
52	5	0.93	1.42	7.1	0.35	0.244	3.98	0.198	15
53	25	1.72	1.06	26.5	0.69	0.261	4.09	0.149	15
54	25	2.74	0.88	22.0	1.15	0.272	4.08	0.117	15
55	25	3.67	0.78	19.5	1.38	0.244	5.58	0.094	15
56	22	4.45	0.65	14.3	1.46	0.214	7.18	0.064	15
57	23	5.33	0.57	13.1	1.43	0.174	7.92	0.052	15

*For a magnitude 7.5 earthquake, 15 cycles of stress at 0.65 τ_{max} are assumed by Seed and Idriss (1981) to correspond to average conditions.

TABLE 5-4. DATA FOR ASSESSING LIQUEFACTION POTENTIAL — CASE 2 CONDITIONS

| Penetration Resistance | | | | | Average Cyclic Stress Ratio, $\dfrac{0.65\ \tau_{max}}{\sigma'_v}$ | | | | |
| | | | | | From Soil/Structure System Finite Element Analysis | | | From Equation 5-1 | |
Element (Fig. 5-14)	N (Fig. 5-6)	σ'_v (ksf)	C_N (Fig. 5-18)	N_1 (C_N x N)	Peak Shear Stress, τ_{max} (ksf)	Average Cyclic Stress Ratio	Number of Cycles	Average Cyclic Stress Ratio	Number of Cycles*
52	13	0.93	1.42	18.5	0.35	0.240	3.70	0.198	15
53	33	1.72	1.06	35.0	0.66	0.249	4.10	0.149	15
54	33	2.74	0.88	29.0	1.10	0.260	4.13	0.117	15
55	33	3.67	0.78	25.7	1.33	0.234	5.56	0.094	15
56	22	4.45	0.65	14.3	1.40	0.205	7.40	0.064	15
57	23	5.33	0.57	13.1	1.46	0.178	8.12	0.052	15

*For a magnitude 7.5 earthquake, 15 cycles of stress at 0.65 τ_{max} are assumed by Seed and Idriss (1981) to correspond to average conditions.

5.6.3.3 Evaluation of Liquefaction Potential

All data required for the evaluation of the liquefaction potential at the site using the Seed-Idriss empirical approach are summarized in Tables 5-3 and 5-4. These tables contain modified penetration resistances for each layer, average cyclic stress ratios and the corresponding number of stress cycles from the finite element analysis, and average cyclic stress ratios computed directly from Equation 5-1. As noted previously, the first liquefaction evaluation (from the finite element results) is based on the computed shear stresses from Elements 52 to 57 which, as shown in Table 5-2, are slightly higher than the free-field stresses at Element 52 and are comparable to the free-field stresses elsewhere. The second liquefaction evaluation is based on cyclic stress ratios computed from Equation 5-1, which requires only the peak free-field acceleration, and the layer overburden pressures and depth of the layer; it is independent of horizontal position within the site.

5.6.3.3.1 *Liquefaction Potential Using Cyclic Stress Ratios from Finite Element Analyses*

Section 5.6.3.1 has provided the shear stress time histories that were obtained from the finite element analyses, as well as the corresponding equivalent cyclic stress ratios and stress cycles. It remains to use this information in accordance with the Seed-Idriss (1981) empirical procedure to assess the liquefaction potential of the site.

To use this information in the most meaningful way, a slightly modified form of the Seed-Idriss procedure has been adopted. This modified form has been described in Chapter 4, and is summarized here in terms of the following steps:

- As in the present approach, assume that the cyclic stress ratio vs. modified penetration resistance curve

developed by Seed and Idriss for a magnitude 7.5 earth-
quake corresponds to a total of 15 stress cycles. (This,
in fact, is based on the prior statistical analysis of
strong motion accelerograms by Seed et al. (1975b) in
which earthquake magnitude vs. stress cycle correlations
were obtained, based on the assumption that cyclic shear
stress is directly proportional to peak acceleration).

- From the Seed-Idriss (1981) liquefaction curve relating
  shear stress ratio to critical number of stress cycles
  (i.e., number of cycles causing a porewater pressure
  ratio of 100% and a 5% strain), obtain the shear stress
  ratios corresponding to the number of cycles shown in
  Tables 5-3 and 5-4 to represent each of the shear stress
  time histories obtained from the finite element calcula-
  tions (Fig. 5-19).

- Obtain relative values of cyclic stress ratio corre-
  sponding to each of these numbers of stress cycles,
  by using the ratio of the ordinates of the curve in
  Figure 5-19 relative to the ordinate corresponding
  to 15 cycles. These ratios are shown directly in
  Figure 5-19 and are summarized in Table 5-5.

- By using these ratios to scale the Seed-Idriss liquefac-
  tion curve for 15 cycles (i.e., for an earthquake magni-
  tude of 7.5) obtain liquefaction curves that correspond
  to the particular number of stress cycles represented
  by each of the various shear stress histories from the
  finite element analyses. Such a family of curves for
  sands is shown in Figure 5-20.
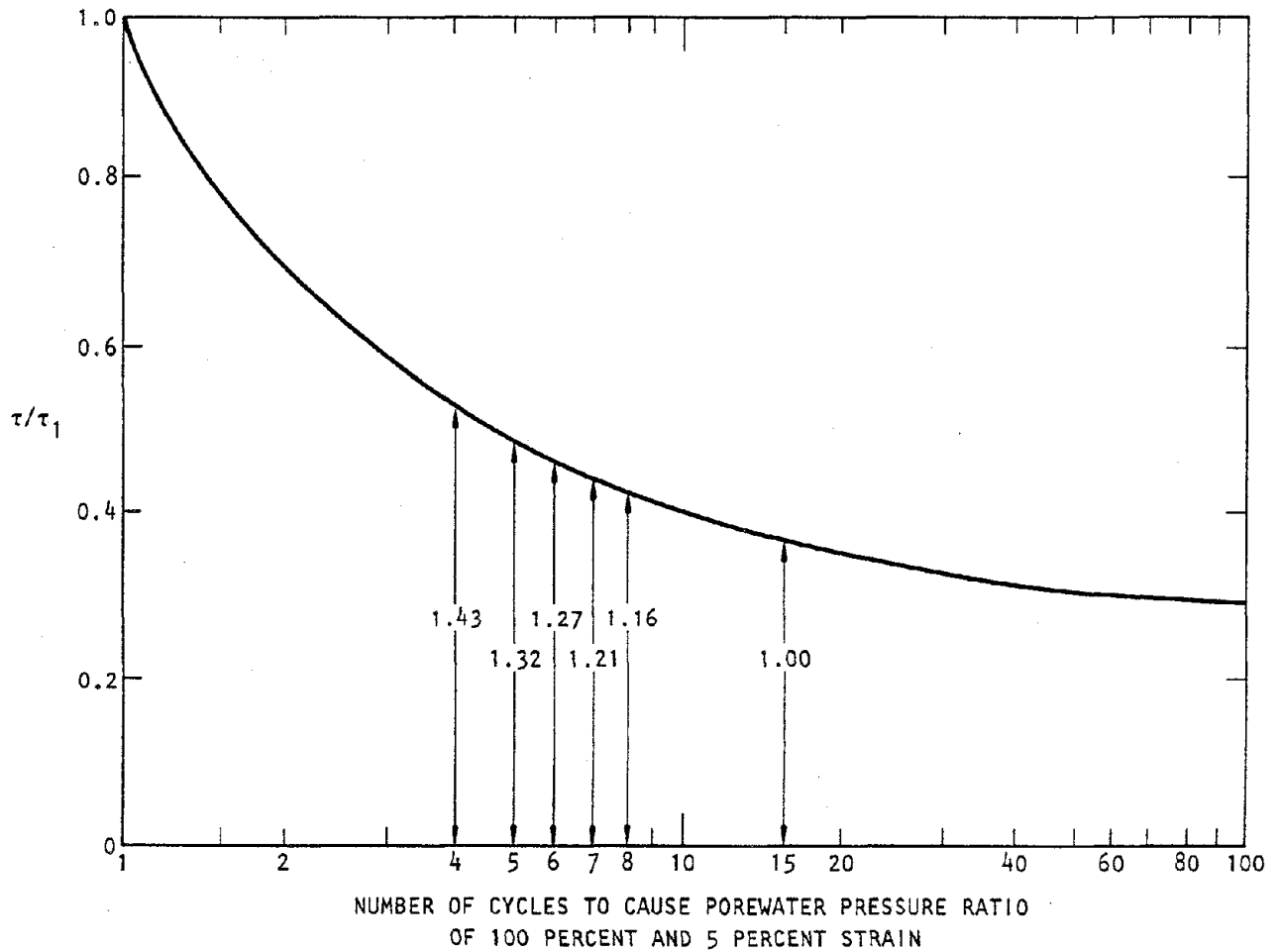
FIGURE 5-19.   REPRESENTATIVE RELATIONSHIP BETWEEN τ/τ_1
AND NUMBER OF CYCLES REQUIRED TO CAUSE
LIQUEFACTION (Seed and Idriss, 1981)

TABLE 5-5. BASIS FOR DETERMINATION OF CYCLIC STRESS
RATIO VS. MODIFIED PENETRATION RESISTANCE
RELATIONSHIPS FOR DIFFERENT NUMBERS OF
REPRESENTATIVE CYCLES AT $0.65\ \tau_{max}$

Number of Representative Cycles at $0.65\ \tau_{max}$, N_C	$\dfrac{\tau}{\tau_1}$ (Fig. 5-19)	$\dfrac{\left(\dfrac{\tau_{av}}{\sigma'_o}\right)_{N_C}}{\left(\dfrac{\tau_{av}}{\sigma'_o}\right)_{N_C\ =\ 15}}$
4	0.53	1.43
5	0.49	1.32
6	0.47	1.27
7	0.45	1.21
8	0.43	1.16
15	0.37	1.00
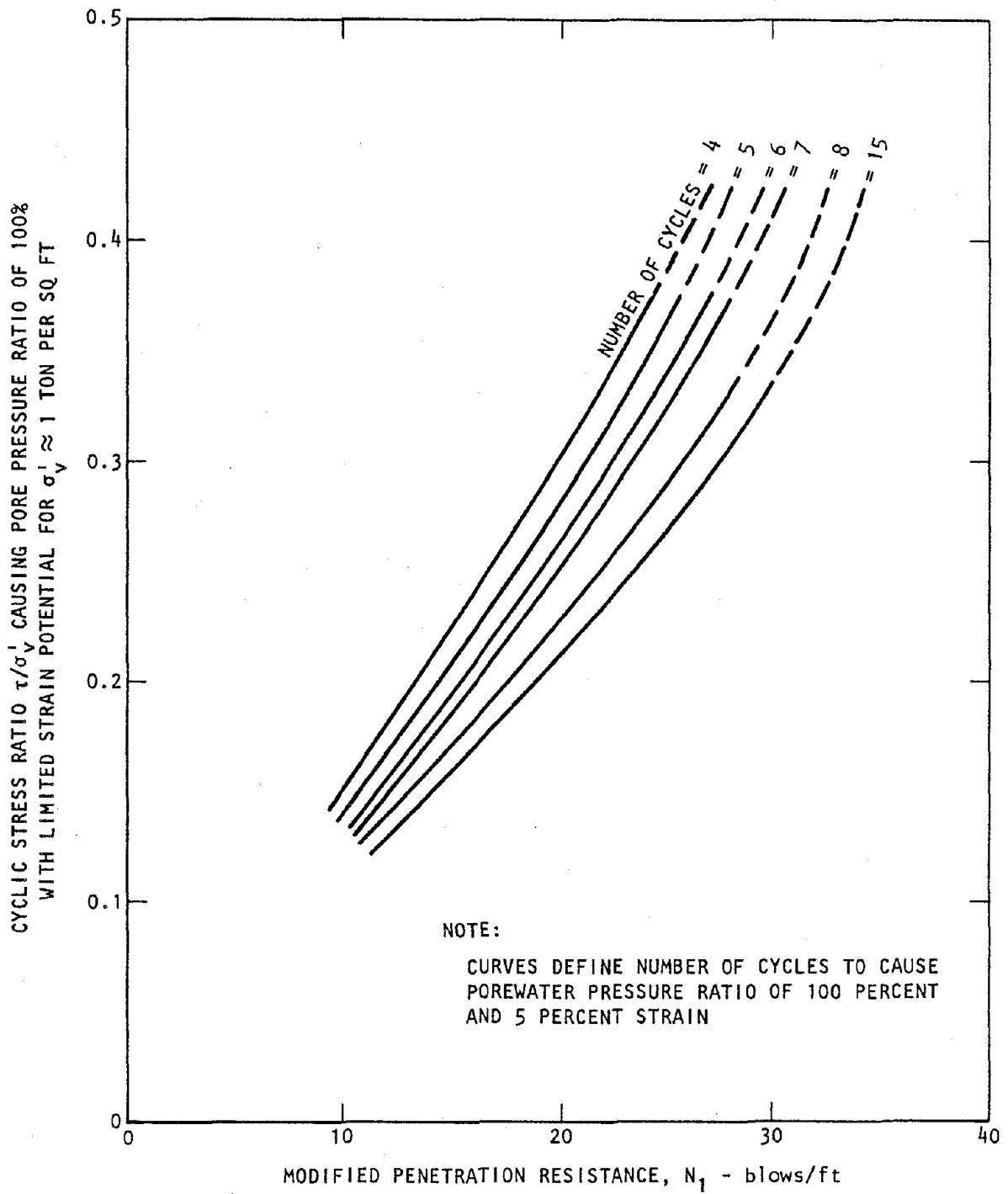
FIGURE 5-20. EVALUATION OF LIQUEFACTION POTENTIAL FOR
DIFFERENT NUMBERS OF STRESS CYCLES

The curves shown in Figure 5-20 are appropriate for use with the finite element analysis results since they are based on the actual number of cycles represented by the shear stress histories computed from these analyses. This can be contrasted with the present form of the Seed-Idriss curves which, for magnitude 7.5, (i.e., the magnitude corresponding to the ground motion data considered in this analysis), corresponds to 15 stress cycles--a number of cycles much greater than those represented by the computed shear stress histories. Thus, it is seen that the Seed-Idriss (1981) empirical procedures in their present form are intended for use in situations where nothing is known about the shear stresses within the site. However, when information on the shear stresses is available--such as computed shear stress histories as obtained from dynamic analyses of the type described here--the form of the Seed-Idriss results can be readily modified as described above to provide a suitable basis for comparison with the computed shear stress results.

The above procedure has been used to construct Seed-Idriss curves of critical cyclic stress vs. modified penetration resistance corresponding to four cycles of stress (the approximate number of stress cycles in Elements 52 to 54), five cycles and six cycles (which encompasses the number of cycles computed for Element 55), seven cycles (corresponding to Element 56) and eight cycles (the approximate number of cycles in Element 57). These sets of curves are plotted in Figures 5-21 and 5-22, for the Case 1 and Case 2 soil conditions respectively. Then, the conditions of cyclic stress ratio and modified penetration resistance for each element are plotted as points in the figure containing the Seed-Idriss curves with the appropriate number of stress cycles. When these element points fall above or adjacent to the Seed-Idriss curve, the soil at these element locations is judged to be vulnerable to liquefaction. If the points fall well below
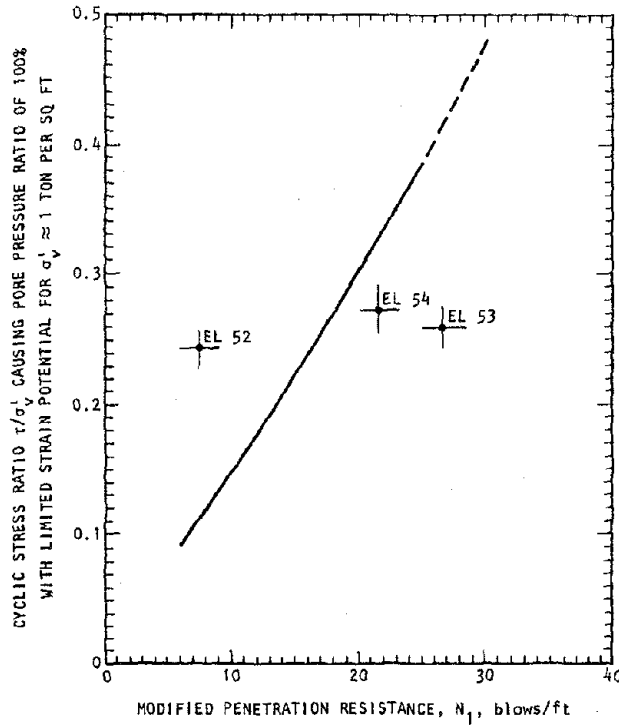
(a) Number of stress cycles = 4
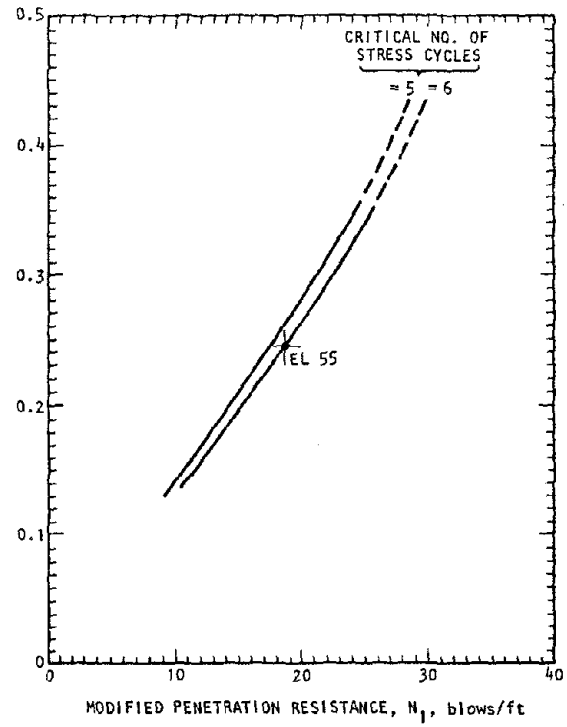
(b) Number of stress cycles = 5-6
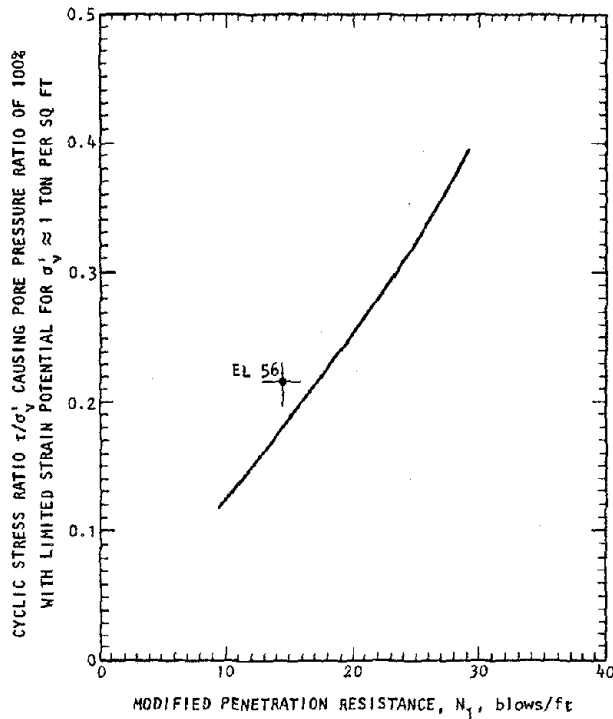
(c) Number of stress cycles = 7
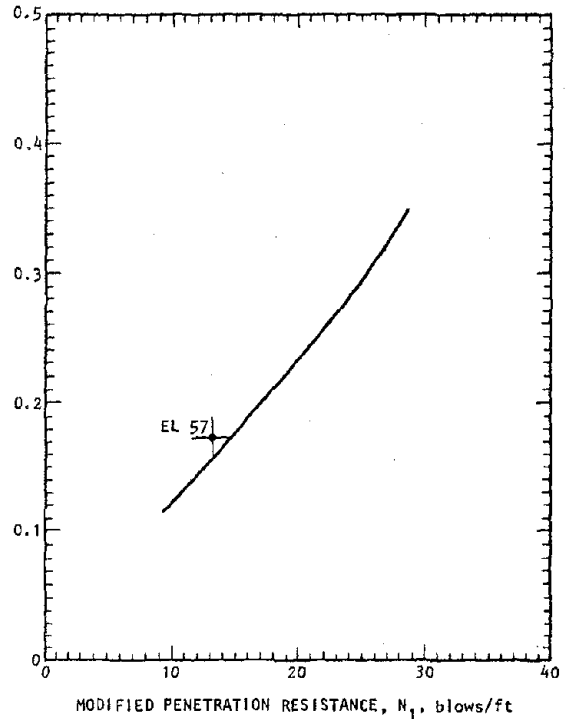
(d) Number of stress cycles = 8

FIGURE 5-21.   ASSESSMENT OF LIQUEFACTION POTENTIAL OF SITE USING STRESSES FROM FINITE ELEMENT RESULTS, CASE 1 CONDITIONS

(a) Number of stress
cycles = 4

(b) Number of stress
cycles = 5-6

(c) Number of stress
cycles = 7

(d) Number of stress
cycles = 8
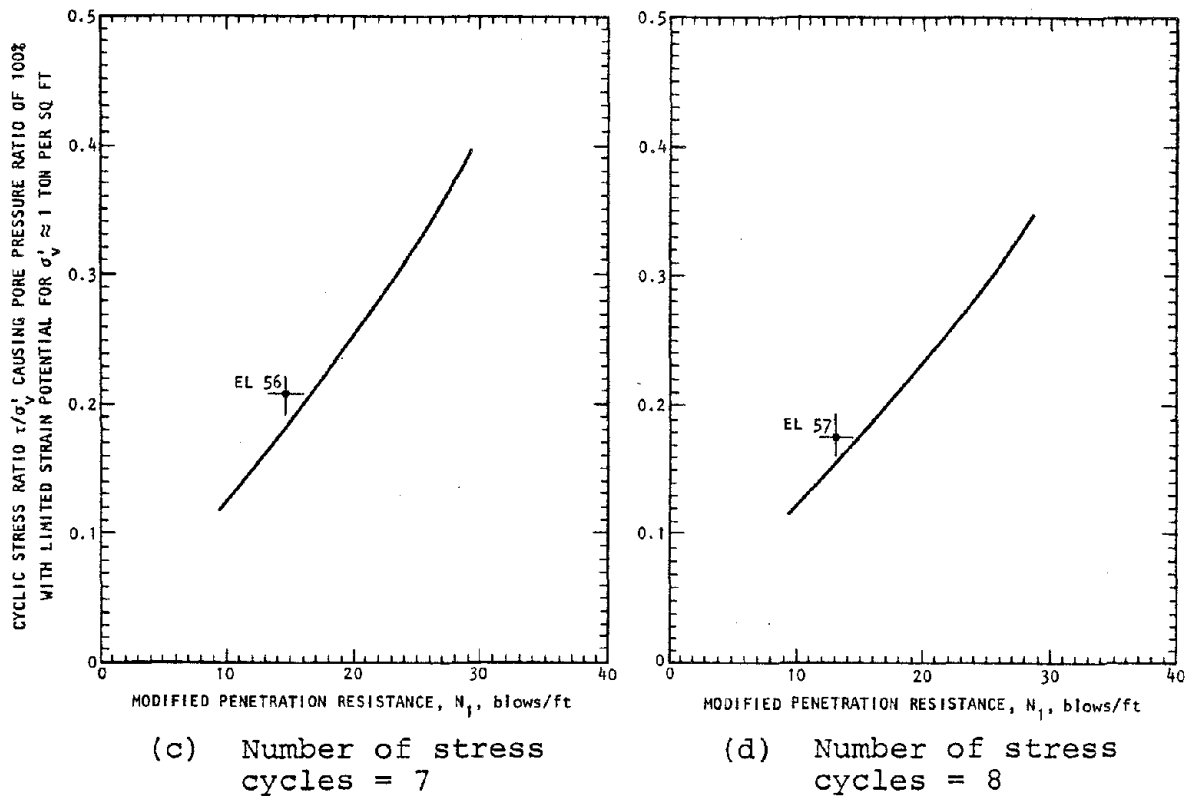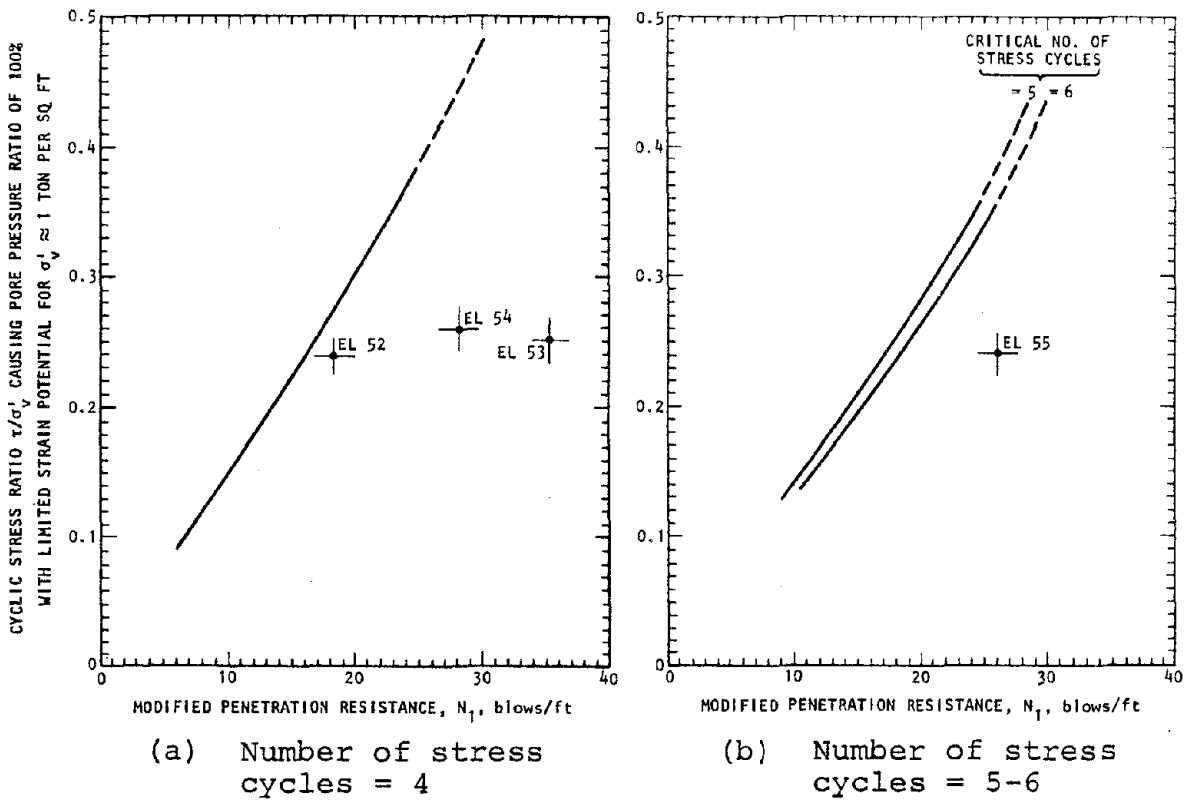
FIGURE 5-22. ASSESSMENT OF LIQUEFACTION POTENTIAL OF SITE
USING STRESSES FROM FINITE ELEMENT RESULTS,
CASE 2 CONDITIONS

in the Seed-Idriss curve, the soil at these element locations is judged safe from liquefaction. On this basis, the results shown in Figures 5-21 and 5-22 show the following trends:

● For the original (Case 1) soil conditions, the assumed saturated portion of the fill (Element 52) and the lower soil layers (Elements 55 to 57) are susceptible to lique-faction. The sand layer elements just below the fill (Elements 53 and 54) are shown to be marginally safe to safe from liquefaction, according to this assessment procedure (Fig. 5-21).

● The use of soil improvement techniques at this site (i.e., Case 2 conditions) results in a dramatic decrease in the susceptibility to liquefaction of the upper saturated soil layers (Elements 52 to 55); however, Element 52 is still shown to be only marginally safe from liquefaction. The susceptibility to liquefac-tion of the deeper soil layers (Elements 56 and 57) is unchanged from that observed in the Case 1 results, since these deeper layers are unaffected by the soil improvement procedures as represented in this analysis (Fig. 5-22).

5.6.3.3.2 *Liquefaction Potential Using Cyclic Stress Ratios from Equation 5-1*

The second approach used to assess the liquefaction potential of the site corresponds to the use of Equation 5-1 to compute cyclic shear stress ratios at selected depths. These are used with the original (rather than modified) Seed-Idriss (1981) curves, which are provided in terms of earthquake magnitude (rather than stress cycles). Results using this approach are

presented in Figure 5-23 for the Case 1 and Case 2 conditions. These results show the following trends:

- The Case 1 results (for the original soil conditions) indicate that only Element 52 (in the fill layer) will liquify, and that the underlying sand and silt layers are reasonably safe from liquefaction.

- The Case 2 results (for the improved soil conditions) show a dramatic improvement in the integrity of the soft fill layer represented by Element 52, although this layer is still seen to be marginal. As in Case 1, the underlying soil layers are shown by these results to be safe from liquefaction.

5.6.3.4 Assessment of Liquefaction Results

In this subsection, the above liquefaction results are assessed from the standpoint of (a) comparisons between the results of liquefaction assessment methods; (b) correlation of the results with the observed earthquake behavior of this sheet-pile bulkhead structure; and (c) effects of soil improvement techniques.

5.6.3.4.1 *Comparison of Liquefaction Assessment Methods*

Two methods of evaluating the liquefaction potential of this site have been used herein--one involves using cyclic stress ratios obtained from the finite element results while the other uses cyclic stress ratios computed from Equation 5-1. Tables 5-3 and 5-4 show that the cyclic stress ratios obtained from the finite element results are everywhere substantially larger than those from Equation 5-1, and the number of stress cycles is everywhere smaller. Bearing these differences in mind, the comparisons between the liquefaction results from the two sets

CYCLIC STRESS RATIO τ/σ'_v CAUSING PORE PRESSURE RATIO OF 100% WITH LIMITED STRAIN POTENTIAL FOR $\sigma'_v \approx 1$ TON PER SQ FT

0.5
0.4
0.3
0.2
0.1
0

EL 52
EL 53
EL 54
EL 55
EL 56
EL 57

10   20   30   40

MODIFIED PENETRATION RESISTANCE, N_1, blows/ft

(a) Case 1 results

0.5
0.4
0.3
0.2
0.1
0

EL 53
EL 52
EL 54
EL 55
EL 56
EL 57

0   10   20   30   40

MODIFIED PENETRATION RESISTANCE, N_1, blows/ft
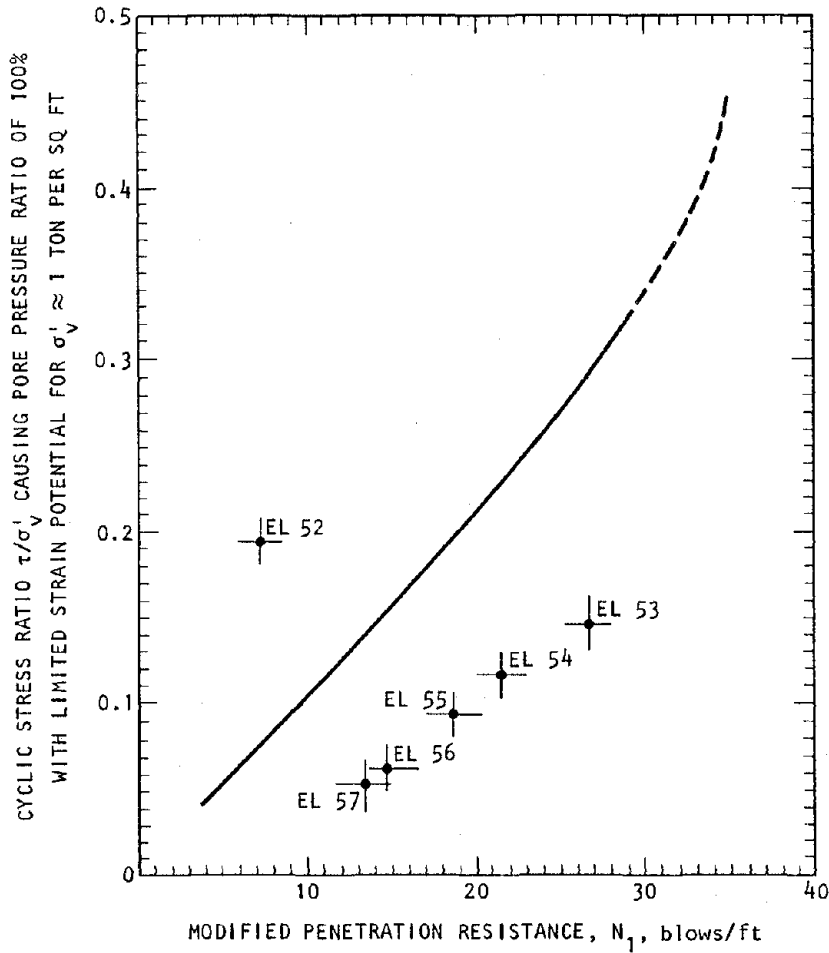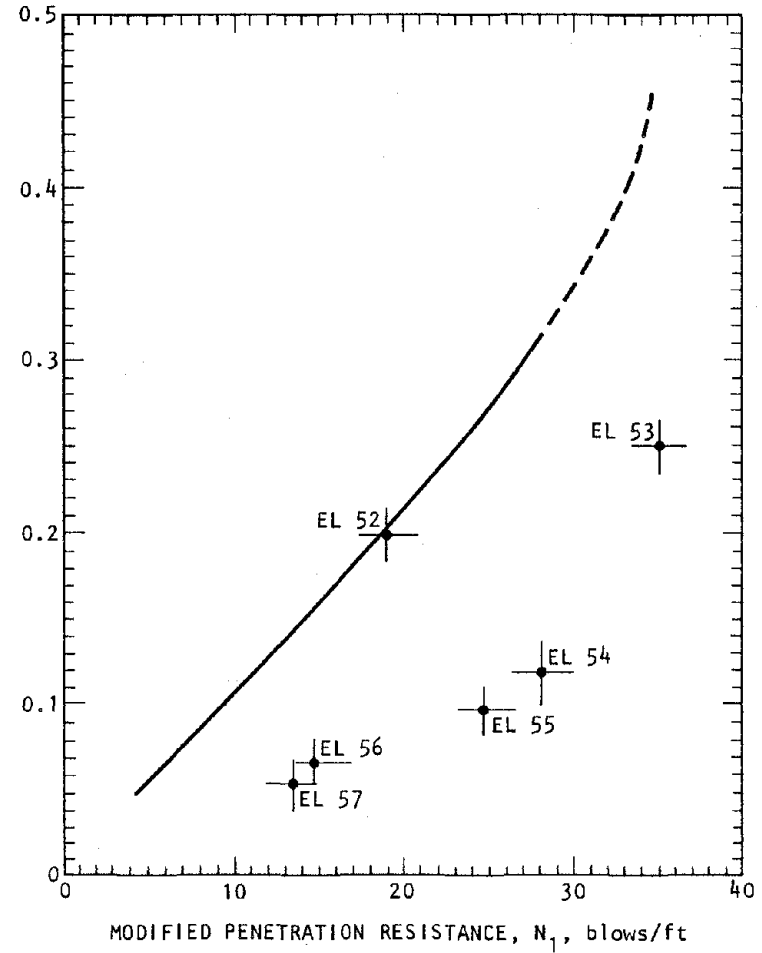
(b) Case 2 results

AA381

FIGURE 5-23.   ASSESSMENT OF LIQUEFACTION POTENTIAL OF SITE USING
STRESSES FROM EQUATION 5-1

of assessment procedures are summarized in Table 5-6 and indicate
the following trends:

- For the shallow soil layers (Elements 52 to 54), the
  results from the two sets of assessment procedures are
  generally qualitatively similar.

- For the deeper soil layers (Elements 55 to 57), the
  results from the two sets of results are often dis-
  similar. These differences can probably be related to
  the uncertainties that arise from the use of a single
  site-independent parameter (r_d as given in Fig. 5-5)
  to define the depth dependence of the cyclic shear
  stresses in Equation 5-1. As shown by the scatter
  bands in Figure 5-5, the uncertainty in defining r_d
  increases substantially with increasing depth, and is
  significant at the depths corresponding to Elements 55
  to 57.

- Where differences between the two sets of results exist,
  the procedure based on the finite element results tends
  to provide a more conservative assessment of liquefac-
  tion susceptibility.

These trends are based on the results for the particular conditions
considered in these illustrative dynamic analysis, and should not
be generalized to other conditions without further investigations.

5.6.3.4.2 *Correlation of Computations with Observed Behavior*

As noted earlier in Section 5.2, the concrete apron at the
sheet-pile bulkhead considered in this illustrative analysis
suffered cracking and settlement during the Miyagi-Ken-Oki earth-
quake. Clearly, this moderate degree of damage could have occurred
even in the absence of porewater pressure buildup at this site.

TABLE 5-6.   RESULTS FROM LIQUEFACTION EVALUATION

Location		Susceptibility to Liquefaction			
		Original Soil Conditions (Case 1)		Improved Soil Conditions (Case 2)	
Depth Below Ground Surface,* ft	Corresponding Element Number (Fig. 5-14)	Procedure Based on Finite Element Analysis (Fig. 5-21)	Procedure Based on Equation 5-1 (Fig. 5-23a)	Procedure Based on Finite Element Analysis (Fig. 5-22)	Procedure Based on Equation 5-1 (Fig. 5-23b)
8.35	52	Unsafe	Unsafe	Marginal	Marginal
19.0	53	Safe	Safe	Safe	Safe
35.4	54	Marginal-to-safe	Safe	Safe	Safe
50.2	55	Marginal	Safe	Safe	Safe
66.6	56	Unsafe	Safe	Unsafe	Safe
84.7	57	Unsafe	Safe	Unsafe	Safe

Note:

*Depth shown corresponds to distance from ground surface to midthickness of each soil element shown in Figure 5-14.

For example, contributing factors to this settlement and cracking could have included earthquake-induced consolidation of the unsaturated upper portion of the surface fill layer, as well as the lack of reinforcing steel in the apron. However, it is appropriate to also examine how this damage might have been related to the porewater pressure effects indicated by the analysis results. The extent of this porewater pressure buildup, which varies over the depth of the soil profile, could have contributed to the observed apron damage according to the following mechanism:

- Porewater pressure buildup--not only in the soil layers shown by the analysis to be susceptible to liquefaction but, to a lesser degree, in the other soil layers as well--could have resulted in an increase in the lateral pressure applied to the sheet pile. This, in turn, could have caused a lateral seaward movement of the sheet pile, and a resulting reduction in soil confinement. Near the ground surface, this reduced confinement could have permitted some lateral movement of the saturated portion of the fill (shown by the analysis to be susceptible to liquefaction) which could have led to settlement of the apron.

- In support of this hypothesis, it is appropriate to consider the differences in response characteristics between this sheet-pile bulkhead and an adjacent bulkhead structure. These two structures are similar, except for the anchor system of the adjacent structure which is supported on batter piles rather than vertical piles. In contrast to the bulkhead structure considered in this analysis, the adjacent structure was virtually

undamaged by the ground shaking during the Miyagi-Ken-Oki earthquake (see Sec. 2.16.3 of Chapt. 2). Although these differences in behavior are probably due, in part, to the somewhat denser soil conditions at the adjacent structure, the differences in anchor support systems between the two structures could also have been a factor. The batter-pile-supported anchor system of the adjacent bulkhead structure would have a greater resistance to the increased lateral pressures applied to the bulkhead due to porewater pressure buildup. This, in turn, would have reduced the corresponding lateral displacements of the bulkhead which, according to the hypothesis of the previous paragraph, would have reduced any detrimental effects on the bulkhead apron.

• Although no obvious evidence of liquefaction was mentioned in postearthquake inspections at this bulkhead site (Tsuchida et al., 1979), some occurrence of pore-water pressure buildup and liquefaction (as indicated by the analysis results) is plausible in view of the low penetration resistance of several of the soil layers and the strong shaking to which the site was subjected. In this regard, porewater pressure buildup contributing to settlement and cracking of the apron could have occurred without there being evidence of liquefaction of sufficient extent to warrant notice in a postearthquake inspection.

The important point from the above discussion is that the dynamic analysis results offer a plausible basis for interpreting the observed earthquake-induced damage to this sheet-pile bulkhead structure. Furthermore, as discussed in the subsection that follows,

the analysis results even show a possible remedy for the observed damage--involving the use of deep compaction soil improvement techniques to densify the site.

5.6.3.4.3 *Effects of Soil Improvement Techniques*

As a final aspect of the evaluation of these liquefaction results, the nature of the improvements due to the deep compaction soil improvement techniques, as represented by the Case 2 calculations, warrants reiteration. These calculations show that the soil improvement techniques result in a marked decrease in the susceptibility of the site to liquefaction, primarily because of the dramatic increase in the modified penetration resistance that results in the saturated soil layers near the ground surface. The calculations also show that the soil improvement techniques did not have any noticeable effect on the dynamic response of the soil/ structure system; in fact it was shown that the system motions and shear stresses were nearly the same for Cases 1 and 2. However, as indicated previously, the actual differences between the shear stresses and system response between Cases 1 and 2 could actually be somewhat greater than those indicated by the total stress analysis methods used herein, which do not account for the differing porewater pressure effects on the system response for these two cases. Therefore, the beneficial effects of soil improvement, which have been shown to be substantial even when porewater pressure effects on the system response are neglected, are probably underestimated to some degree by these analyses. These benefits are in line with the prior field observations in Japan (Watanabe, 1966; Ohsaki, 1970; Ishihara et al., 1980) as summarized in Section 5.2.2.

5.6.4 LATERAL PRESSURES ALONG SHEET-PILE/SOIL INTERFACE

As previously noted, the seismic design of quay walls, sheet-pile bulkheads, and other retaining wall structures at ports and harbors is typically based on pseudostatic lateral pressures computed from the Mononobe-Okabe (M-O) equation (Mononobe, 1929; Okabe, 1926; Seed and Whitman, 1970). The main assumptions behind the application of this equation have been described in Chapter 3 and will not be repeated here. However, in this section, the applicability of this equation is examined from a different standpoint--namely, through a comparison of the lateral pressures obtained using the M-O equation to those computed at the sheet-pile/soil interface from this finite element analysis. In these comparisons, dynamic lateral pressures induced only by the horizontal seismic excitations are included, since lateral pressures induced by the vertical seismic excitations are small.

The M-O equation defines not only the design levels of the earthquake-induced lateral pressures, but also the distribution of these pressures (as increasing linearly with increasing depth below the ground surface). Therefore, to evaluate each of these aspects of this design pressure definition, two sets of comparisons are shown between the M-O results and the dynamic lateral pressures computed from the finite element analysis. The first involves the distribution of dynamic pressures computed from the finite element results at specific instants in time, in order to compare these pressure distributions with the M-O results. The second comparison involves the envelopes of the dynamic lateral pressures, in order to show how the peak pressures computed from the finite element analysis compare with those from the M-O equation. In each comparison, the finite element results are provided in terms of both positive and negative dynamic pressures which, in practice, would be superimposed onto the corresponding static pressures when designing the sheet pile. Also, it is noted

that the lateral pressures computed from this dynamic analysis are consistent with those from the M-O equation, in that both sets of pressures neglect porewater pressure effects (see Chapt. 3).

Results of the first set of comparisons, involving dynamic lateral pressure distributions computed at specific instants in time for the Case 1 soil conditions, are shown in Figure 5-24. These results show that the dynamic pressure distributions from the finite element results differ markedly from the linearly varying pressure distribution represented by the M-O equation. This, of course, could have an important effect on the internal bending moments and shear forces obtained for purposes of the design of the sheet pile. The magnitudes of the pressures computed from the M-O equation are seen to exceed the finite element pressures at the specific instants of time shown in Figure 5-24.

Comparisons between the envelopes of the finite element dynamic pressures and the lateral pressures computed from the M-O equation are shown in Figure 5-25; tabulations of these finite element results are contained in Table 5-7. These show that (1) the dynamic lateral pressure envelopes computed corresponding to the Case 1 and Case 2 soil conditions are generally similar to one another;[*] and (2) the lateral pressures computed from the M-O equation bound the pressure envelopes from the finite element results.

5.6.5 STRUCTURE FORCES, MOMENTS, AND STRESSES

The final set of dynamic analysis results evaluates the integrity of the sheet-pile bulkhead structure by computing the internal forces, moments, and stresses generated in the structural

---

[*]See comments in Section 5.6.1 regarding comparisons of the Case 1 and Case 2 response characteristics.
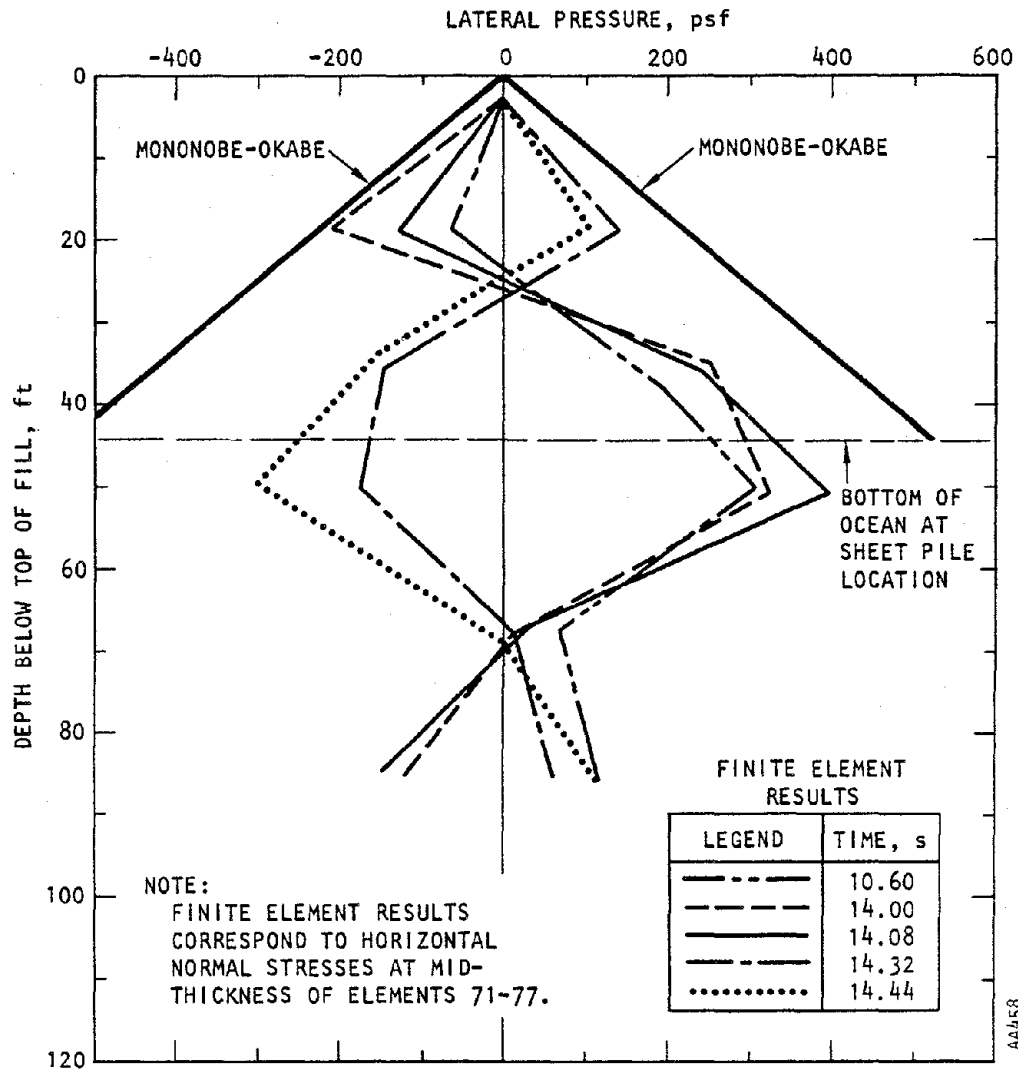
FIGURE 5-24. DYNAMIC LATERAL PRESSURE DISTRIBUTIONS
ALONG SHEET-PILE/SOIL INTERFACE AT
PARTICULAR INSTANTS OF TIME (Case 1 —
Soil Conditions)

LATERAL PRESSURE, psf

DEPTH BELOW TOP OF FILL, ft

OCEAN WATER LEVEL

MONONOBE-OKABE

BOTTOM OF OCEAN
AT SHEET PILE
LOCATION

MAXIMUM NEGATIVE
PRESSURE

MAXIMUM POSITIVE
PRESSURE

(a)   Case 1

LATERAL PRESSURE, psf

DEPTH BELOW TOP OF FILL, ft

OCEAN WATER LEVEL

MONONOBE-OKABE

BOTTOM OF OCEAN
AT SHEET PILE
LOCATION

MAXIMUM NEGATIVE
PRESSURE

MAXIMUM POSITIVE
PRESSURE

(b)   Case 2

FIGURE 5-25.   ENVELOPES OF DYNAMIC LATERAL PRESSURE ALONG
SHEET-PILE/SOIL INTERFACE

TABLE 5-7. PEAK LATERAL PRESSURES ALONG SHEET-PILE/SOIL INTERFACE
COMPUTED FROM FINITE ELEMENT ANALYSES

Element (see sketch below)	Maximum Positive Lateral Pressure				Maximum Negative Lateral Pressure			
	Case 1		Case 2		Case 1		Case 2	
	Peak Pressure, psf	Time, s	Peak Pressure, psf	Time, s	Peak Pressure, psf	Time, s	Peak Pressure, psf	Time, s
71	9.26	13.92	9.78	10.02	- 6.87	10.74	- 9.00	14.12
72	44.62	14.30	44.68	14.32	- 69.78	13.98	- 71.56	13.98
73	136.13	14.30	109.23	14.28	-201.04	13.96	-161.78	13.96
74	279.36	14.00	261.60	14.00	-196.09	10.10	-190.55	10.10
75	407.43	14.02	388.93	14.02	-304.82	14.42	-291.91	14.42
76	73.63	10.72	69.02	10.72	- 64.39	10.00	- 62.64	10.18
77	126.28	14.40	163.26	14.40	-144.53	14.02	-182.38	14.02
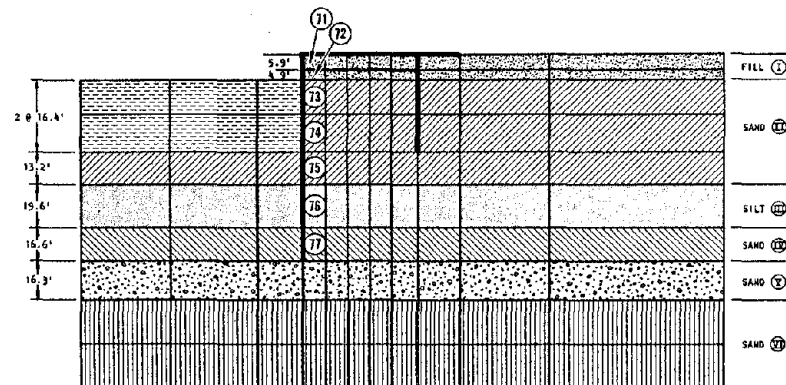
FINITE ELEMENT GRID

elements (Fig. 5-26) by the seismic excitations. These are pre-
sented in two different forms. First, Tables 5-8 and 5-9 contain
peak values of the axial forces, shear forces, and bending moments
within each structural element. These results show that (1) the
horizontal input excitations induce the largest shear forces and
bending moments in the H-beam anchor and the sheet pile, and
induce the largest axial forces in the tie rod; (2) the vertical
input excitations induce the largest axial forces in the H-beam
anchor and the sheet pile, and induce the largest shear forces
and bending moments in the concrete apron; (3) the internal struc-
ture forces and bending moments in the H-beam, the sheet pile, and
the concrete apron are very similar for the Case 1 and Case 2 site
conditions;[*] and (4) the most noticeable effects of the variation
in site conditions between Cases 1 and 2 are in the axial forces
in the tie rod, where it is seen that the Case 2 site conditions
(with the more dense and stiff upper fill and sand layers) gener-
ally reduce these axial forces relative to those from Case 1.

The second form of these results (Table 5-10) represents
estimates of normal stress induced in the structure by the axial
forces and bending moments. These are presented as sums of
absolute values of the normal stresses induced in the structure
by the peak axial forces and bending moments that result from the
horizontal and vertical response analyses. This method of presen-
tation was selected because (1) it corresponds to an upper bound
estimate of the normal stresses in the structure; (2) even within
a single analysis (for either horizontal or vertical input excita-
tions) the combined normal stresses due to axial loads and bending
moments are not directly provided by FLUSH code; and (3) the labor
that would be involved in obtaining these combined stresses was

---

[*]See comments in Section 5.6.1 regarding comparisons of the Case 1
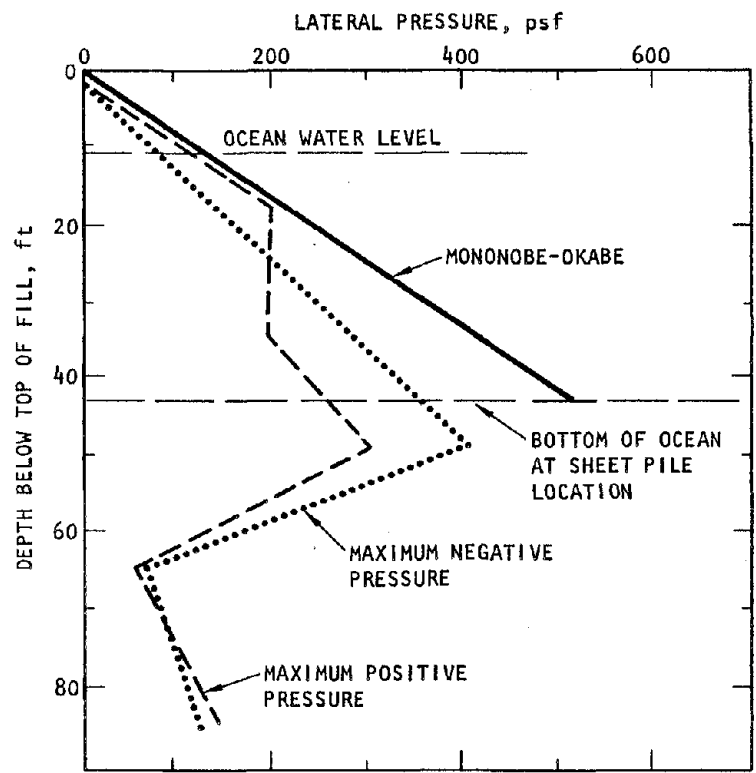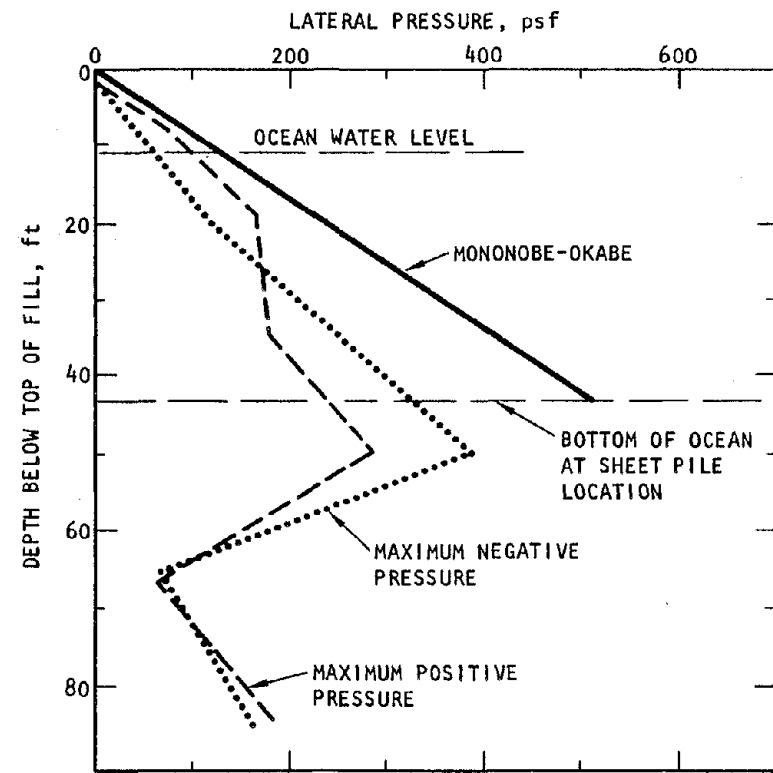and Case 2 response characteristics.
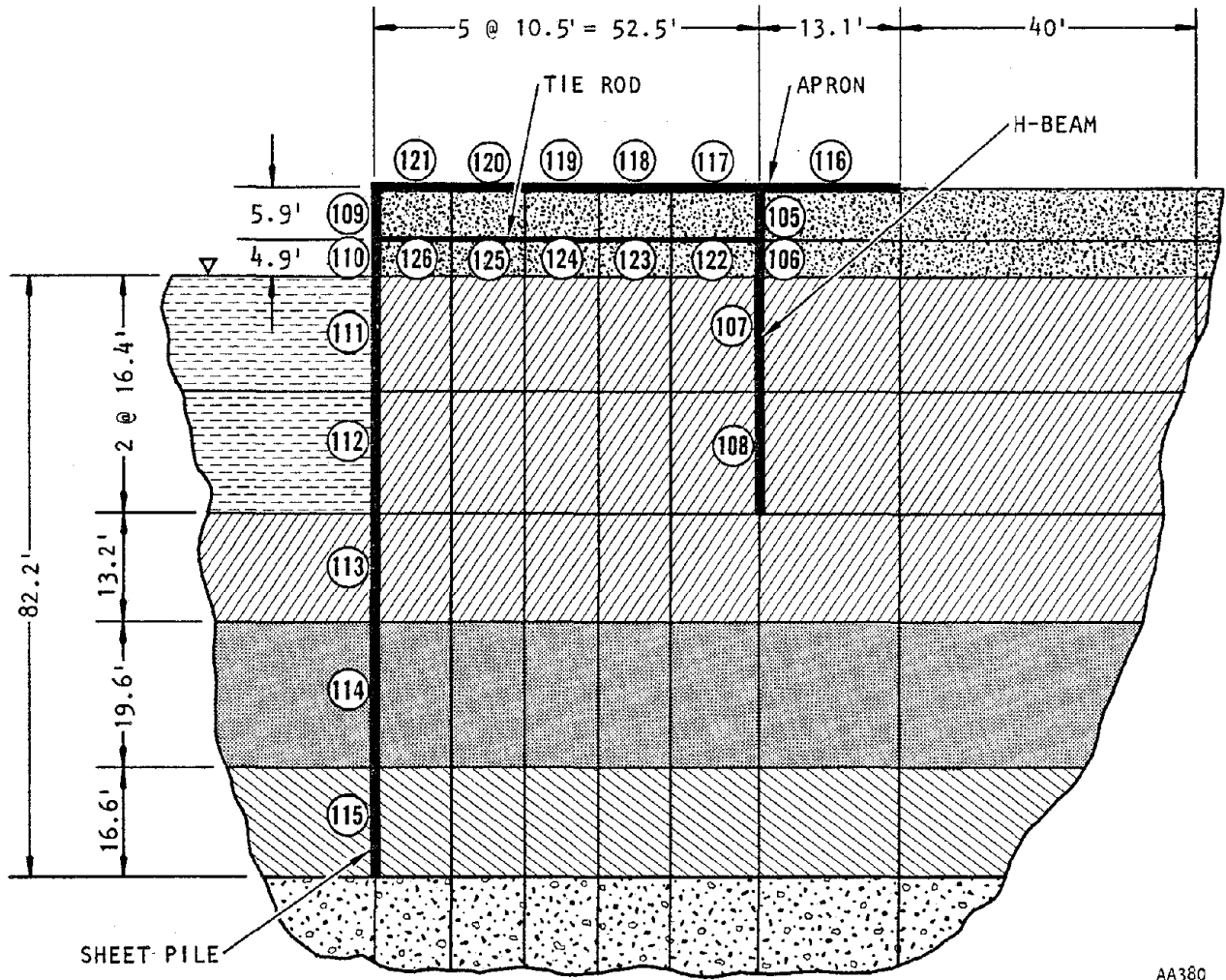
FIGURE 5-26. NUMBERING OF STRUCTURAL ELEMENTS
IN FINITE ELEMENT MODEL

TABLE 5-8.   PEAK FORCES AND MOMENTS — CASE 1 SITE CONDITIONS

Structural Element		Absolute Values of Peak Forces and Moments					
		From Horizontal Excitation			From Vertical Excitation		
Location	Number (see Fig. 5-26)	Axial Force, lb	Shear Force, lb	Bending Moment, lb-ft	Axial Force, lb	Shear Force, lb	Bending Moment, lb-ft
H-Beam Anchor (steel)	105	228	805	6,716	1,932	106	730
	106	153	2499	6,736	3,600	148	632
	107	202	1162	13,770	6,688	46	632
	108	292	840	13,770	9,856	small	129
Sheet Pile (steel)	109	235	687	4,678	1,523	99	1752
	110	797	1089	4,687	3,559	464	1777
	111	2,684	2351	37,970	14,350	182	1901
	112	9,055	1186	37,970	31,720	105	1901
	113	12,910	2902	54,390	39,230	151	1093
	114	10,810	5010	54,390	45,060	73	1093
	115	6,742	2666	44,260	39,070	20	336
Apron (concrete)	116	2,687	62	817	634	156	2046
	117	2,055	136	1166	933	70	1316
	118	2,358	30	268	1,559	28	870
	119	2,447	10	76	1,916	small	891
	120	2,148	8	135	1,876	55	891
	121	1,300	62	637	835	125	1619
Tie Rod (steel)	122	1,596	small	small	190	small	small
	123	938	small	small	158	small	small
	124	718	small	small	183	small	small
	125	628	small	small	243	small	small
	126	965	small	small	93	small	small

TABLE 5-9. PEAK FORCES AND MOMENTS — CASE 2 SITE CONDITIONS

Structural Element		Absolute Values of Peak Forces and Moments					
		From Horizontal Excitation			From Vertical Excitation		
Location	Number (see Fig. 5-26)	Axial Force, lb	Shear Force, lb	Bending Moment, lb-ft	Axial Force, lb	Shear Force, lb	Bending Moment, lb-ft
H-Beam Anchor (steel)	105	145	759	5,804	1,938	112	794
	106	174	1825	5,818	3,672	119	532
	107	204	1022	13,820	6,723	38	532
	108	317	843	13,820	9,798	6	103
Sheet Pile (steel)	109	258	789	4,971	1,640	89	1632
	110	616	693	4,976	3,960	336	1656
	111	1,985	2193	38,670	14,560	143	1649
	112	8,112	1083	38,670	31,740	102	1649
	113	12,070	2679	53,130	39,210	145	1038
	114	9,928	5570	56,050	45,620	70	1038
	115	6,099	3376	56,050	39,580	20	327
Apron (concrete)	116	2,885	42	550	768	155	2028
	117	2,420	93	790	1,137	58	1234
	118	2,772	21	186	1,897	22	857
	119	2,898	8	63	2,339	5	877
	120	2,550	8	144	2,275	47	877
	121	1,512	45	381	1,006	104	1482
Tie Rod (steel)	122	1,133	small	small	166	small	small
	123	650	small	small	124	small	small
	124	542	small	small	177	small	small
	125	535	small	small	259	small	small
	126	640	small	small	47	small	small

TABLE 5-10. UPPER BOUND ESTIMATES OF COMBINED NORMAL STRESSES

| Structural Elements | | | | Sum of Absolute Values of Peak Loads and Normal Stresses Induced by Horizontal and Vertical Input Excitations | | | | | | | | | |
| | | | | Case 1 | | | | | Case 2 | | | | |
Location	Area, A, in²	Section Modulus, S, in³	Element Number, (Fig. 5-26)	$\Sigma P^{(1)}$, lb	$\frac{\Sigma P}{A}$, psi	$\Sigma M_{max}^{(2)}$, lb-in.	$\frac{\Sigma M_{max}}{S}$, psi	$\frac{\Sigma P}{A} + \frac{\Sigma M_{max}}{S}$, psi	$\Sigma P^{(1)}$, lb	$\frac{\Sigma P}{A}$, psi	$\Sigma M_{max}^{(2)}$, lb-in.	$\frac{\Sigma M_{max}}{S}$, psi	$\frac{\Sigma P}{A} + \frac{\Sigma M_{max}}{S}$, psi
H-Beam Anchor (steel)	27	148	105	2,160	80	83,712	566	646	2,083	77	72,384	489	566
			106	3,753	139	83,880	567	706	3,846	142	72,480	490	632
			107	6,890	255	166,788	1127	1382	6,927	257	167,076	1129	1386
			108	10,148	376	166,788	1127	1503	10,115	375	167,076	1129	1504
Sheet Pile (steel)	33	222	109	1,758	53	77,160	348	401	1,898	58	79,236	357	415
			110	4,356	132	77,568	349	481	4,576	139	79,584	358	497
			111	17,034	516	478,452	2155	2671	16,545	501	483,828	2179	2680
			112	40,775	1236	478,452	2155	3391	39,852	1208	483,828	2179	3387
			113	52,140	1580	665,796	2999	4579	51,280	1554	650,016	2928	4482
			114	55,870	1693	665,796	2999	4692	55,548	1683	676,524	3047	4730
			115	45,812	1388	535,152	2410	3798	45,679	1384	676,524	3047	4431
Apron (concrete)	498	156	116	3,321	7	34,356	220	227	3,653	7	30,936	198	205
			117	2,988	6	29,784	191	197	3,557	7	24,288	156	163
			118	3,917	8	11,100	71	79	4,669	9	10,788	69	78
			119	4,363	9	11,592	74	83	5,237	11	11,280	72	83
			120	4,024	8	11,592	74	82	4,825	10	11,280	72	82
			121	2,135	4	27,072	174	178	2,518	5	22,356	143	148
Tie Rod (steel)	3	9	122	1,786	595	small	small	595	1,299	433	small	small	433
			123	1,096	365	small	small	365	774	258	small	small	258
			124	901	300	small	small	300	719	240	small	small	240
			125	871	290	small	small	290	794	265	small	small	265
			126	1,058	353	small	small	353	687	229	small	small	229

Note: (1) ΣP = Sum of absolute values of peak axial loads obtained from horizontal and vertical response analyses.

(2) ΣM_{max} = Sum of absolute values of peak bending moments obtained from horizontal and vertical response analyses. Values shown correspond to element location where this sum is maximum.

judged to be unwarranted in view of the approximations involved
in the use of separate horizontal and vertical response analyses
in the first place. In view of this, the upper bound normal
stresses shown in Table 5-10 are considered satisfactory for
purposes of assessing the integrity of the structure under the
applied seismic excitations. These results show that the upper
bound structure stresses are generally quite small when compared
with anticipated design levels, although those in the unreinforced
concrete apron are probably sufficient to have caused some cracking.
Table 5-10 also shows that the structure stresses are generally
similar for the Case 1 and Case 2 soil conditions, except for the
tie rod where the increased stiffness in the Case 2 upper soil
layers causes a reduced normal stress in the tie rod relative
to Case 1.[*]

5.7 SUMMARY OF RESULTS

In this chapter, a dynamic analysis of an actual sheet-pile
bulkhead that was shaken severely during the 1978 Miyagi-Ken-Oki
earthquake was carried out in order to illustrate the use of such
analyses during the seismic design of port and harbor facilities.
Results of this analysis showed that

- The calculations indicate that the site of this sheet-
  pile bulkhead is susceptible to porewater pressure
  effects. These effects, together with possible
  earthquake-induced settlement of the unsaturated loose
  fill above the water table, provide a plausible expla-
  nation for the observed damage to this structure from
  the earthquake--settlement and cracking of the apron.

---

[*]See comments in Section 5.6.1 regarding comparisons of the Case 1
and Case 2 response characteristics.

- Upper bound estimates of the earthquake-induced internal stresses in the structure (in the absence of porewater pressure effects) indicate these structure stresses to be very low when compared to anticipated design values, although the stresses in the apron are probably sufficient to have caused some cracking.

- Deep compaction soil improvement techniques, as represented in this analysis, substantially enhance the resistance of the upper portion of this site to porewater pressure buildup and liquefaction. This trend is in line with prior observations in Japan of the effects of soil improvement on the behavior of sand deposits during earthquakes.

- For these particular site conditions and seismic excitations, the dynamic analysis results produce lateral pressure distributions along the sheet-pile/soil interface that are markedly different from the pseudostatic pressure distributions computed from the Mononobe-Okabe equation and commonly used for design.

- Comparisons of the two-dimensional soil/structure system response with the one-dimensional free-field response showed that the peak shear stress in the near-surface regions of the soil backfill were affected by the topography of the site (and probably to a smaller degree by soil/structure interaction for this particular system). These effects on the soil/structure system response spectra and on the shear stresses in the deeper soil layers were much smaller.

REFERENCES

Agbabian Assoc. (AA). (1974) *Earthquake Vulnerability of Shipyard Facilities, Puget Sound Naval Shipyard, Phase 1 Study,* R-7518-2-3668. El Segundo, CA: AA, Dec.

----. (1976) *Earthquake Vulnerability of Shipyard Facilities, Puget Sound Naval Shipyard, Phase 2 Study,* R-7518-2-4163. El Segundo, CA: AA, Sep.

Amano, R. et al. (1956) "Aseismic Design of Quay Walls in Japan," *Proc. 1st Wld. Conf. Earthq. Eng.,* Berkeley, CA, Jun, Paper 32-1.

Annaki, M. and Lee, K.L. (1977) "Equivalent Uniform Cycle Concept for Soil Dynamics," *Jnl Geotech Eng. Div.,* ASCE, 103:GT6, Jun, pp 549-564.

Arno, N.L. and McKinney, L.F. (1973) "Harbor and Waterfront Facilities," *The Great Alaska Earthquake of 1964, Engineering.* Washington, DC: Nat'l. Acad. Sci., pp 526-643.

Atkin, R.J. and Craine, R.E. (1976) "Continuum Theories of Mixtures: Basic Theory and Historical Development," *Quart. Jnl of Math. and Appl. Math.,* 29, pp 209-244.

Bathe, K.J. (1978) *ADINA, A Finite Program for Automatic Dynamic Incremental Nonlinear Analysis,* Report 82448-1. Cambridge, MA: MIT, Dec.

Bathe, K.J. et al. (1974) *SAP IV, A Structural Analysis Program for Static and Dynamic Response of Linear Systems,* EERC 73-11. Berkeley: Univ. of Calif., Earthq. Eng. Res. Ctr, Apr.

Baylor, J.L.; Bieniek, M.P.; and Wright, J.P. (1974) *TRANAL: A 3-D Finite Element Code for Transient Nonlinear Analysis,* DNA-3501F. New York: Weidlinger Assoc., Jun.

Bazant, Z.P. and Krizek, R.J. (1976) "Endochronic Constitutive Law for Liquefaction of Sand," *Jnl Eng. Mech. Div.,* ASCE, 102:EM2, Apr, pp 225-238.

Belanger, D.P. (1973) "Port of Whittier," *The Great Alaska Earthquake of 1964, Engineering.* Washington, DC: Nat'l Acad. Sci., pp 1074-1107.

Biot, M.A. (1941) "Theory of Elasticity and Consolidation for a Porous Isotropic Solid," *Jnl Appl. Phys.*, 12, pp 155-164.

----. (1961) "Mechanics of Deformation and Acoustic Propagation in Porous Media," *Jnl Appl. Phys.*, 33:4, pp 1483-1498.

Booker, J.R. et al. (1976) *GADFLEA--A Computer Program for the Analysis of Pore Pressure Generation and Dissipation during Cyclic or Earthquake Loading*, EERC 76-24. Berkeley: Univ. of Calif., Earthq. Eng. Res. Ctr., Oct.

Brady, A.G. (1978) "Strong-Motion Earthquake Recordings," *Reconnaissance Report, Miyagi-Ken-Oki, Japan Earthquake, June 12, 1978*. Berkeley: Univ. of Calif., Earthq. Eng. Res. Inst., Dec, pp 15-28.

Casagrande, A. (1976) "On Liquefaction Phenomena: A Lecture to ENCOLD and the British Geotechnical Society, reported by P.A. Green and P.A.S. Ferguson," *Geotechnique*, 21:3.

Castro, G. (1975) *Liquefaction of Sands*. Harvard Soil Mechanics Series, No. 81.

Castro, G. and Poulos, S.J. (1977) "Factors Affecting Liquefaction and Cyclic Mobility," *Jnl Geotech. Eng. Div.*, ASCE, 103:GT6, Jun, pp 501-516.

Chakrabarti, P. and Chopra, A.K. (1974) "Hydrodynamic Effects in Earthquake Response of Gravity Dams," *Jnl Struct. Div.*, ASCE, 100:ST6, Jun, pp 1211-1224.

Chakrabarti, S. et al. (1978) "Seismic Design of Retaining Walls and Cellular Cofferdams," *Proc. ASCE Geotech. Eng. Div., Specialty Conf. on Earthq. Eng. and Struct. Dyn.*, Pasadena, CA, Jun, pp 325-341.

Chopra, A.K. (1967) "Hydrodynamic Pressures on Dams during Earthquakes," *Jnl Eng. Mech. Div.*, ASCE, 93:EM6, Dec, pp 205-223.

Chopra, A.K. and Chakrabarti, P. (1981) "Earthquake Analysis of Gravity Dams Including Dam-Water-Foundation Interaction," *Jnl Earthq. Eng. Struct. Dyn.*, 9:4, Jul-Aug, pp 363-383.

Christian, J.T. (1980) "Probabilistic Soil Dynamics: State-of-the-Art," *Jnl Geotech. Eng. Div.*, ASCE, 106:GT4, Apr, pp 385-397.

Christian, J.T. and Desai, C.S. (1977) "Constitutive Laws for Geologic Media," *Num. Meth. Geotech. Eng.*, eds. C.S. Desai and J.T. Christian. New York: McGraw-Hill, pp 65-115.

Clough, G.W. and Duncan, J.M. (1971) "Finite Element Analyses of Retaining Wall Behavior," *Jnl Soil Mech. Found. Div.*, ASCE, 97:SM12, Dec, pp 1657-1673.

Coulter, H.W. and Migliaccio, R.R. (1971) "Effects at Valdez," *The Great Alaska Earthquake of 1964, Geology.* Washington, DC: Nat'l Acad. Sci., pp 359-394.

Crandall, S.H. and Mark, W.D. (1963) *Random Vibration in Mechanical Systems.* New York: Academic Press.

DeAlba, P.A. et al. (1976) "Sand Liquefaction in Large-Scale Simple Shear Tests," *Jnl Geotech. Div.*, ASCE, 102:GT9, Sep, pp 909-927.

DeSalvo, G.J. and Swanson, J.A. (1979) *ANSYS, Engineering Analysis System, User's Manual.* Houston: Swanson Analy. Sys., Inc., Jul.

Depts. of the Army, Navy, and Air Force (DANAF). (1973) *Seismic Design for Buildings*, TM 5-809-10/NAV FAC P-355/AFM 88-3, Chapt. 13, Washington, DC, Apr.

Donovan, N.C. (1971) "A Stochastic Approach to the Seismic Liquefaction Problem," *Proc. 1st Intl. Conf. Appl. Statistics and Probab. Soil Struct. Eng.*, Hong Kong, Sep, pp 514-535.

Donovan, N.C. and Singh, S. (1978) "Liquefaction Criteria for Trans-Alaska Pipeline," *Jnl Geotech. Eng. Div.*, ASCE, 104:GT4, Apr, pp 447-462.

Duke, C.M. and Leeds, D.J. (1963) "Response of Soils, Foundations, and Earth Structures to the Chilean Earthquakes of 1960," *Bull. Seismol. Soc. Amer.*, 53:2, Feb, pp 309-357.

Duncan, J.M. and Chang, C.Y. (1970) "Nonlinear Analysis of Stress and Strain in Soils," *Jnl Soil Mech. Found. Div.*, ASCE, 96:SM5, Sep, pp 1629-1653.

Faccioli, E. (1973) "A Stochastic Model for Predicting Seismic Failure in a Soil Deposit," *Earthq. Eng. Struct. Dyn.*, 1:3, Jan-Mar, pp 293-307.

Ferritto, J.M. (1981) *Effective Stress Soil Models*, TM-51-81-12. Pt. Hueneme, CA: Naval Civil Eng. Lab., Aug.

Finn, W.D.L. (1981) "Liquefaction Potential: Developments Since 1976," *Proc. Intl. Conf. on Recent Adv. Geotech. Earthq. Eng. and Soil Dyn.*, St. Louis, Apr 26-May 3, pp 655-681.

Finn, W.D.L. (1982) "Dynamic Analysis and Liquefaction--Emerging Trends," *Proc. 3rd Intl. Earthq. Microzonation Conf.*, Seattle, WA, Jun 28-Jul 1, Vol. 2, pp 909-928.

Finn, W.D.L. and Bahtia, S.L. (1980) *Verification of Nonlinear Effective Stress Model in Simple Shear*, Preprint 80-250. Presented at ASCE Annual Conv., Florida, Oct.

Finn, W.D.L. and Byrne, P.M. (1976) "Liquefaction Potential of Mine Tailing Dams," *Proc. 12th Intl. Conf. on Large Dams*, Mexico City, Vol. 1, pp 153-176.

Finn, W.D.L. and Martin, G.R. (1980) "Offshore Pile Foundations in Sand under Earthquake Loading," *Applied Ocean Research*, 2:2, pp 81-84.

Finn, W.D.L. et al. (1970) "Effect of Strain History on Liquefaction of Sands," *Jnl Soil Mech. Found. Div.*, ASCE, 96:SM6, Nov, pp 1917-1934.

----. (1971) *Soil Liquefaction Studies using a Shaking Table, Closed Loop*. MTS Systems Corp., Fall/Winter.

----. (1977) "An Effective Stress Model for Liquefaction," *Jnl Geotech. Eng. Div.*, ASCE, 103:GT6, Jun, pp 517-533.

Gibbs, H.J. and Holtz, W.G. (1957) "Research on Determining the Density of Sands by Spoon Penetration Testing," *Proc. 4th Intl. Conf. on Soil Mech. and Found. Eng.*, London, Vol. 1, pp 35-39.

Ghaboussi, J. and Dikmen, S.U. (1979) *LASS-3, Computer Program for Seismic Response and Liquefaction of Layered Ground under Multi-Directional Shaking*, UILU-ENG-79-2012. Urbana: Univ. of Ill., Jul.

Gutierrez, J.A. and Chopra, A.K. (1978) "A Substructure Method for Earthquake Analysis of Structures Including Soil/Structure Interaction," *Jnl Earthq. Eng. Struct. Dyn.*, 6:1, Jan-Feb, pp 51-70.

Hakuno, M. (1968) *Harbor Facilities General Report on the Niigata Earthquake of 1964, Part 3: Damage to Civil Engineering Construction*, ed. H. Kawasumi. Tokyo: Tokyo Electrical Engineering College Press.

Haldar, A. and Tang, W.H. (1979) "Probabilistic Evaluation of Liquefaction Potential," *Jnl Geotech. Eng. Div.*, ASCE, 105:GT2, Feb, pp 145-163.

Hall, J.F. and Chopra, A.K. (1982) "Two-Dimensional Dynamic Analysis of Concrete Gravity and Embankment Dams Including Hydrodynamic Effects," *Jnl Earthq. Eng. Struct. Dyn.*, 10:2, Mar-Apr, pp 305-332.

Hardin, B.O. and Drnevich, V.P. (1972) "Shear Modulus and Damping in Soils: Design Equations and Curves," *Jnl Soil Mech. Div.*, ASCE, 98:SM7, Jul, pp 667-692.

Hart, R.D. (1981) "Application of Explicit Finite Difference Methods to Modeling Coupled Thermal-Mechanical-Hydraulic Behavior in Geologic Media," *Symp. Impl. Computer Proc. and Stress-Strain Laws in Geotech. Eng.*, Chicago, Aug.

Hayashi, S. et al. (1966) "Damage to Harbour Structures by the Niigata Earthquake," *Soils and Foundations* (Japan), 6:1, Jan.

----. (1975) "Recent Revision of Design Standards on Seismic Effects for Port and Harbour Structures," *Wind and Seismic Effects, 7th Joint Conf. U.S.-Japan Cooperative Program in Natural Resources*, Tokyo, May.

Idriss, I.M. et al. (1973) *QUAD-4: A Computer Program for Evaluating the Seismic Response of Soil Structures by Variable Damping Finite Element Procedures*, EERC 73-16. Berkeley: Univ. of Calif., Earthq. Eng. Res. Ctr.

Ishihara, K. and Okada, T. (1978) "Effects of Stress History on Cyclic Behavior of Sand," *Soils and Foundations* (Japan), 18:4, Dec, pp 31-45.

Ishihara, K. and Takatsu, H. (1979) "Effects of Overconsolidation and K_o Conditions on the Liquefaction Characteristics of Sands," *Soils and Foundations* (Japan), 19:4, Dec.

Ishihara, K. and Yamazaki, F. (1980) "Cycle Simple Shear Tests on Saturated Sands in Multi-Directional Loading," *Soils and Foundations* (Japan), 20:1, Mar.

Ishihara, K. et al. (1978a) "Effects of Overconsolidation on Liquefaction Characteristics of Sands Containing Fines," *American Society of Testing, Special Tech. Pub. 654*, pp 246-264.

----. (1978b) "Cyclic Strengths of Undisturbed Sands Obtained by Large Diameter Sampling," *Soils and Foundations* (Japan), 18:4, Dec.

Ishihara, K. et al. (1980) "Liquefaction Characteristics of Sand Deposits at an Oil Tank Site during the 1978 Miyagi-Ken-Oki Earthquake," *Soils and Foundations* (Japan), 20:2, Jun, pp 97-111.

Iwan, W.D. (1967) "On a Class of Models for the Yielding Behavior of Continuous and Composite Systems," *Jnl Applied Mech.*, 34:E3, Sep, pp 612-617.

Japanese Port & Harbor Res. Inst. (JPHRI). (1964, 1965) *Damage to Harbour Structures by the Niigata Earthquake*, Part I (1964) & II (1965). (in Japanese)

----. (1968) *Damage to Harbour Structures by the 1968 Tokachi-Oki Earthquake, The Investigation of the Tsunami Caused by the 1968 Tokachi-Oki Earthquake.* (in Japanese)

----. (1973) *The Damage to Port Structures and the Investigation of the Tsunami Caused by the Nemura Hanto Oki Earthquake on June 17, 1973.* (in Japanese)

----. (1980) "Earthquake Resistant Design for Quaywalls and Piers in Japan," *Earthquake Resistant Design for Civil Engineering Structures, Earth Structures and Foundations in Japan,* compiled by Japan Soc. of Civil Eng.

Kachadoorian, R. (1971) "Effects on the Alaska Highway System," *The Great Alaska Earthquake of 1964, Geology.* Washington, DC: Nat'l Acad. Sci., pp 641-703.

Katsikas, C.A. and Wylie, E.G. (1982) "Sand Liquefaction: Inelastic Effective Stress Model," *Jnl Geotech. Eng. Div.*, ASCE, 108:GT1, Jan, pp 63-81.

Kawakami, F. and Asada, A. (1966) "Damage to the Ground and Earth Structures by the Niigata Earthquake of June 16, 1964," *Soil and Foundations* (Japan), 6:1, Jan.

Kitajima, S. and Uwabe, T. (1979) *Analysis on Seismic Design in Anchored Sheet-Piling Bulkheads.* Japan Ports and Harbour Res. Inst., 18:1, Mar.

Kuribayashi, E. and Tazaki, T. (1979) "An Evaluation Study on Distribution-Characteristics of Property Losses Caused by Earthquakes," *Proc. JSCE*, 292, Dec, pp 75-81.

Ladd, R.S. (1974) "Specimen Preparation and Liquefaction of Sands," *Jnl Geotech. Eng. Div.*, ASCE, 100:GT10, Oct, pp 1180-1184.

Ladd, R.S. (1977) "Specimen Preparation and Cyclic Stability of Sands," *Jnl of Geotech. Eng. Div.*, ASCE, 103:GT6, Jun, pp 535-547.

Lade, P.V. (1979) "Cubical Testing Apparatus for Soil Testing," *Geotech. Testing Jnl*, ASIM, 1:2.

Lee, K.L. and Seed, H.B. (1967) "Dynamic Strength of Anisotropically Consolidated Sand," *Jnl Soil Mech. Found. Div.*, ASCE, 93:SM5, Sep, pp 169-190.

Lee, K.L. and Walters, H.G. (1972) "Earthquake Induced Cracking of Dry Canyon Dam," *Amer. Soc. Civ. Eng. Annual and Natl. Env. Eng. Mtg.*, Houston, Preprint No. 1794.

Lemke, R.W. (1971) "Effects at Seward," *The Great Alaska Earthquake of 1964, Geology*. Washington, DC: Nat'l Acad. Sci., pp 395-437.

Liou, C.P. et al. (1977) "Numerical Model for Liquefaction," *Jnl Geotech. Eng. Div.*, ASCE, 103:GT6, Jun, pp 589-606.

Long, E.L. (1973) "Earth Slides and Related Phenomena," *The Great Alaska Earthquake of 1964, Engineering*. Washington, DC: Nat'l Acad. Sci., pp 644-773.

Lysmer, J. et al. (1975) *FLUSH--A Computer Program for Approximate 3-D Analysis of Soil-Structure Interaction Problems*, EERC 75-30. Berkeley: Univ. of Calif., Earthq. Eng. Res. Ctr, Nov.

----. (1981) *SASSI: A System for Analysis of Soil-Structure in Interaction*. Berkeley: Univ. of Calif., Apr.

Makdisi, F.I. and Seed, H.B. (1978) "Simplified Procedure for Estimating Dam and Embankment Earthquake-Induced Deformations," *Jnl Geotech. Eng., Div.*, ASCE, 104:GT7, Jul, pp 849-867.

Makdisi, F.I. et al. (1978) "Analysis of Chabot Dam during the 1906 Earthquake," *Proc. ASCE Geotech. Eng. Div. Specialty Conf. on Earthq. Eng. and Soil Dyn.*, Pasadena, CA, Jun, pp 569-587.

MARC Analysis Res. Corp. (MARC). (1979) *MARC User's Manual*, Vols. A through E. Palo Alto, CA: MARC, Jul.

Marcuson, W.F. and Bieganousky, W.A. (1977) "Laboratory Standard Penetration Tests on Fine Sands," *Jnl Geotech. Eng. Div.*, ASCE, 103:GT6, Jun, pp 565-588.

Margason, E. (1975) "Pile Bending during Earthquakes," *Des., Constr., and Performance of Deep Foundations*, Seminar Series, ASCE Geotech. Group and Cont. Ed. Comm., San Francisco, Feb-Mar.

Martin, G.R. et al. (1975) "Fundamentals of Liquefaction under Cyclic Loading," *Jnl Geotech Eng. Div.*, ASCE, 101:GT5, May, pp 423-438.

----. (1978) "Effects of System Compliance on Liquefaction Tests," *Jnl Geotech. Eng. Div.*, ASCE, 104:GT4, Apr, pp 463-479.

Martin, P.P. and Seed, H.B. (1979) "Simplified Procedure for Effective Stress Analysis of Ground Response," *Jnl Geotech. Eng. Div.*, ASCE, 105:GT6, Jun, pp 739-758.

----. (1978a) *MASH--A Computer Program for the Nonlinear Analysis of Vertically Propagating Shear Waves in Horizontally Layered Deposits*, UCB/EERC-78/23. Berkeley: Univ. of Calif., Earthq. Eng. Res. Ctr.

----. (1978b) *APOLLO--A Computer Program for the Analysis of Pore Pressure Generation and Dissipation in Horizontal Sand Layers during Cyclic or Earthquake Loading*, UCB/EERC-78/21. Berkeley: Univ. of Calif., Earthq. Eng. Res. Ctr., Oct.

Matsuo, H. and O'Hara, S. (1965) "Dynamic Pore Water Pressure Acting on Quay Walls during Earthquakes," *Proc. 3rd Wld. Conf. on Earthq. Eng.*, New Zealand, Jan 22-Feb 1, V.1, p I-130.

Masing, G. (1926) "Eigenspannungen und Verfestigung beim Messing," *Proc. 2nd Intl. Cong. Applied Mech.*, pp 332-335.

McCormick, C.W. (ed.) (1979) *MSC/Nastran User's Manual*, Report MSR-39. Los Angeles: MacNeal-Schwandler Corp., May.

McDonnell-Douglas Automation Co. (McAuto). (1980) *STRUDL DYNAL User's Manual*. St. Louis: McAuto, Apr.

Mitchell, J.K. and Katti, R.K. (1981) "Soil Improvement: State-of-the-Art," *Proc. 10th Intl. Conf. Soil Mech. Found. Eng.*, Stockholm, Jun, Session 12, State-of-the-Art Report.

Mononobe, N. (1929) "Earthquake-Proof Construction of Masonry Dams," *Proc. World Eng. Conf.*, V.9, p 275.

Mori, A.W. and Crouse, C.B. (1981) *Strong Motion Data from Japanese Earthquakes*, Report No. SE-29. Boulder, CO: Nat'l. Oceanic and Atmos. Admin., Wld. Data Ctr. for Solid Earth Geophys., Dec.

Moussa, A.A. (1975) "Equivalent Drained-Undrained Shearing Resistance of Sand to Cyclic Simple Shear Loading," *Geotechnique*, 25:3, pp 485-494.

Mulilis, J.P. et al. (1975) *The Effects of Method of Sample Preparation on the Cyclic Stress-Strain Behavior of Sands*, EERC 75-18. Berkeley: Univ. of Calif., Earthq. Eng. Res. Ctr., Jul.

Newmark, N.M. (1965) "Effects of Earthquake on Dams and Embankments," *Geotechnique*, 15:2, Jun, pp 139-160.

Noda, S. and Hayashi, S. (1980) "Damage to Port Structures by the 1978 Miyagi-Ken-Oki Earthquake," *Proc. 7th Wld. Conf. on Earthq. Eng.*, Istanbul, Turkey, Sep, V.9, pp 415-423.

Noda, S. and Uwabe, T. (1975) *Seismic Disasters of Gravity Quay Walls*. Port and Harbour Res. Inst., Tech. Note No. 227. (in Japanese).

----. (1976) "Relation between Seismic Coefficient and Ground Acceleration for Gravity Quaywalls," *Proc. 8th US-Japan Conf. on Wind and Seismic Effects*, Gaithesburg, MD, May.

Okabe, S. (1926) "General Theory of Earth Pressure," *Jnl Japanese Soc. Civil Eng.*, 12:1.

Okamato, S. (1973) *Introduction to Earthquake Engineering*. New York: John Wiley & Sons.

Ohsaki, Y. (1969) "The Effects of Local Soil Conditions upon Earthquake Damage," *Proc. Spec. Sess. 1, 7th Intl. Conf. Soil Mech. Found. Eng.*, Mexico City.

----. (1970) "Effects of Sand Compaction on Liquefaction during the Tokachioki Earthquake," *Soil and Foundations* (Japan), 10:2, Jun, pp 113-128.

Pickering, D.J. (1973) "Drained Liquefaction Testing in Simple Shear," *Jnl Soil Mech. Found. Div.*, ASCE, 99:SM12, Dec, pp 1179-1184.

Pita, F.W. et al. (1982) "Seismic Design of Seattle Waterfront Facilities," *Jnl of Tech. Coun., ASCE*, 108:TC1, May, pp 24-33.

Prevost, J.H. (1977) "Mathematical Model for Static and Cyclic Undrained Clay Behavior," *Intl. Jnl Num. Anal. Meth. in Geomech.*, 1, pp 195-216.

----. (1981) "Nonlinear Anisotropic Stress-Strain-Strength Behavior of Soils," *Lab. Shear Strength of Soils*, ASTM STP-740.

Pyke, R.M. (1979) "Nonlinear Soil Models for Irregular Cyclic Loadings," *Jnl Geotech Eng., Div., ASCE*, 105:GT6, Jun, pp 715-726.

----. (1982) Personal communication to S.D. Werner (Feb-Sep).

Pyke, R.M. et al. (1974) *Settlement and Liquefaction of Sands under Multi-Directional Shaking*, EERC 74-2. Berkeley: Univ. of Calif., Earthq. Eng. Res. Ctr., Feb.

----. (1978) "Liquefaction Potential of Hydraulic Fills," *Jnl Geotech. Eng. Div., ASCE*, 104:GT11, Nov, pp 1335-1354.

Romo-Organista, M.P. et al. (1980) *PLUSH--A Computer Program for Probabilistic Finite Element Analysis of Seismic Soil/Structure Interaction*, EERC-77/01. Berkeley: Univ. of Calif., Earthq. Eng. Res. Ctr., Sep.

Sato, T. and Der Kiureghian, A. (1982) "Seismic Hazard Analysis of Lifelines Incorporating Soil and Geologic Effects," *Proc. 3rd Intl. Earthq. Microzonation Conf.*, Seattle, WA, *Jun 28-Jul 1*, Vol. 3, pp 1701-1711.

Scott, R.F. (1973a) "Behavior of Soils during the Earthquake," *The Great Alaska Earthquake of 1964, Engineering*. Washington, DC: Nat'l Acad. Sci., pp 49-72.

----. (1973b) "Earthquake-Induced Earth Pressure on Retaining Walls," *Proc. 5th Wld. Conf. on Earthq. Eng.*, Rome, Jun, Paper 202.

Seed, H.B. (1973) "Landslides Caused by Soil Liquefaction," *The Great Alaska Earthquake of 1964, Engineering*, Washington, DC: Nat'l Acad. Sci., pp 73-119.

----. (1979a) "Soil Liquefaction and Cyclic Mobility Evaluation for Level Ground during Earthquakes," *Jnl Geotech. Eng. Div., ASCE*, 105:GT2, Feb, pp 201-255.

Seed, H.B. (1979b) "Considerations in the Earthquake-Resistant Design of Earth and Rockfill Dams," *Geotechnique*, 29:3, pp 215-263.

Seed, H.B. and Idriss, I.M. (1967) "Analysis of Soil Liquefaction: Niigata Earthquake," *Jnl Soil Mech. and Found. Div.*, ASCE, 93:SM3, May, pp 83-108.

----. (1970) *Soil Moduli and Damping Factors for Dynamic Response Analysis*, EERC 70-10. Berkeley: Univ. of Calif., Earthq. Eng. Res. Ctr., Dec.

----. (1971) "Simplified Procedure for Evaluating Soil Liquefaction Potential," *Jnl Soil Mech. and Found. Div.*, ASCE, 97:SM9, Sep, pp 1249-1273.

----. (1981) "Evaluation of Liquefaction Potential of Sand Deposits Based on Observations of Performance in Previous Earthquakes: In-Situ Testing to Evaluate Liquefaction Susceptibility," *Amer. Soc. Civil Eng. National Conv.*, St. Louis, Preprint 81-544, Oct.

Seed, H.B. and Lee, K.L. (1966) "Liquefaction of Saturated Sands during Cyclic Loading," *Jnl Soil Mech. Found. Div.*, ASCE, 92:SM6, Nov, pp 105-134.

Seed, H.B. and Peacock, W.H. (1971) "Test Procedures for Measuring Soil Liquefaction Characteristics," *Jnl Soil Mech. and Found. Div.*, ASCE, 97:SM8, Aug, pp 1099-1119.

Seed, H.B. and Whitman, R.V. (1970) "Design of Earth Retaining Structures for Dynamic Loads," *Proc. 1970 Spec. Conf. on Lateral Stresses in the Ground and Design of Earth-Retaining Structures*, Jun, pp 103-147.

Seed, H.B. et al. (1969) "Analysis of Sheffield Dam Failure," *Jnl Soil Mech. and Found. Div.*, ASCE, 95:SM6, Nov, pp 1453-1490.

----. (1973) *Analysis of the Slides in the San Fernando Dams during the Earthquake of February 9, 1971*, EERC 73-2. Berkeley: Univ. of Calif., Earthq. Eng. Res. Ctr., Jun.

----. (1975a) "The Slides in the San Fernando Dams during the Earthquake of February 9, 1971," *Jnl Geotech. Eng. Div.*, ASCE, 101:GT7, Jul, pp 651-688.

----. (1975b) *Representation of Irregular Stress Time Histories by Equivalent Uniform Stress Series in Liquefaction Analyses*, EERC 75-29. Berkeley: Univ. of Calif., Earthq. Eng. Res. Ctr., Oct.

Seed, H.B. et al. (1975c) "Soil-Structure Interaction Analyses for Seismic Response," *Jnl Geotech. Eng. Div.*, ASCE, 101:GT5, May, pp 439-457.

————. (1975d) *Analysis of the Effects of Multi-Directional Shaking on Liquefaction Characteristics of Sands*, EERC 75-41. Berkeley: Univ. of Calif., Earthq. Eng. Res. Ctr., Dec.

————. (1976) "Pore-Water Pressure Changes during Soil Liquefaction," *Jnl Geotech. Eng. Div.*, ASCE, 102:GT4, Apr, pp 323-346.

————. (1977) "Influence of Seismic History on Liquefaction of Sands," *Jnl Geotech. Eng. Div.*, ASCE, 103:GT4, Apr, pp 257-270.

————. (1982) "Considerations in Undisturbed Sampling of Sands," *Jnl Geotech. Eng. Div.*, ASCE, 108:GT2, Feb, pp 265-283.

Serff, N. et al. (1976) *Earthquake Induced Deformations of Earth Dams*, EERC 76-4. Berkeley: Univ. of Calif., Earthq. Eng. Res. Ctr.

Shannon, W.L. and Hilts, D.E. (1973) "Submarine Landslide at Seward," *The Great Alaska Earthquake of 1964, Engineering*. Washington, DC: Nat'l. Acad. Sci., pp 144-156.

Shannon & Wilson and Agbabian Assoc. (SW/AA). (1980) *Evaluation of In-Situ Soil Damping Characteristics*, R-7339-4467. El Segundo, CA: Agbabian Assoc., Sep.

Singh, S. et al. (1982) "Undisturbed Sampling of Saturated Sands by Freezing," *Jnl Geotech. Eng. Div.*, ASCE, 108:GT2, Feb, pp 247-264.

System Develop. Corp. (SDC). (1979) *STARDYNE User's Manual*. Santa Monica, CA: SDC, Sep.

Tabatabaie-Raissi, M. (1982) *The Flexible Volume Method for Dynamic Soil-Structure Interaction*. Ph.D. dissertation, Univ. of Calif. at Berkeley.

Tajirian, F.F. (1981) *Impedance Matrices and Interpolation Techniques for 3-D Interaction Analysis by the Flexible Volume Method*. Ph.D. dissertation, Univ. of Calif. at Berkeley.

Tanaka, J.M. (1973) "Relocation of Valdez," *The Great Alaska Earthquake of 1964, Engineering*. Washington, DC: Nat'l Acad. Sci., pp 1108-1135.

Taylor, P.W. and Indrawan, Z. (1981) "A Simple Method of Estimating Seismic Pressure from Cohesive Soils against Basement Walls," *Proc. Intl. Conf. on Recent Advances in Soil Dyn. and Earthq. Eng.*, St. Louis, Apr, pp 241-244.

Terzaghi, K. (1923) Die Berechnung der Durchlassigkeitsziffer des Tones aus dem Verlauf der Hydrodynamischen Spannungserscheinungen, Sitznurngber. Akad. Wiss, Wien, 132, 125.

----. (1950) "Mechanisms of Landslides," *Engineering Volume of the Geological Survey of America*. Berkeley, CA.

Tokimatsu, K. and Yoshimi, Y. (1981) "Field Correlations of Sand Liquefaction with SPT and Grain Size," *Proc. Intl. Conf. on Recent Adv. Geotech. Earthq. Eng. and Soil Dyn.*, St. Louis.

Trifunac, M.D. and Brady, A.G. (1975) "A Study on the Duration of Strong Earthquake Ground Motion," *Bull. Seismol. Soc. Amer.*, 65:3, Jun, pp 581-626.

Truesdell, C. and Toupin, R.A. (1960) "The Classical Field Theories," *Handbuch der Physik, III*, 1. Berlin, Germany: Springer-Verlag, pp 226-793.

Tsuchida, H. and Noda, S. (1979) *Damage to Port Structures by the 1978 Miyagi-Ken-Oki Earthquake*, Preprint, 11th Joint Meeting U.S.-Japan Panel on Wind and Seismic Effects, UJNR, Tsukuba, Sep. (in Japanese.)

Tsuchida, H. et al. (1979) *The Damage to Port Structures by the 1978 Miyagi-Ken-Oki Earthquake*. Port and Harbour Res. Inst., Tech. Note No. 325.

----. (1980) "Analysis of Liquefactions during the 1978 Off Miyagi Prefecture Earthquake," *Proc. 7th Wld. Conf. on Earthq. Eng.*, Istanbul, Turkey, Sep, Vol. 3.

Uniform Building Code. (UBC). (1979) Whittier, CA: International Conf. of Building Officials.

U.S. Navy Facilities Engineering Comm. (USN). (1968-1971) *Design Manuals*, DM-7, DM-25, and DM-26. Washington, DC.

Vaid, Y.P. and Finn, W.D.L. (1979) "Static Shear and Liquefaction Potential," *Jnl Geotech. Eng. Div.*, ASCE, 105:GT10, Oct, pp 1233-1246.

Vaish, A.K. and Chopra, A.K. (1976) Closure to paper entitled "Earthquake Finite Element Analysis of Structure-Foundation Systems," *Jnl Eng. Mech. Div.*, ASCE, 102:EM5, Oct, pp 933-936.

Valera, J.E. and Donovan, N.C. (1977) "Soil Liquefaction Procedures--A Review," *Jnl Geotech. Eng., Div.*, ASCE, 103:GT6, Jun, pp 607-625.

Vanmarcke, E.H. (1972) "Properties of Spectral Moments with Applications to Random Vibrations," *Jnl Eng. Mech. Div.*, ASCE, 98:EM2, Apr, pp 425-446.

----. (1976) "Structural Response to Earthquake," *Seismic Risk and Engineering Decisions*. Amsterdam, Netherlands: Elsevier Pub. Co., Inc., pp 287-337.

----. (1977) "Random Vibration Approach to Soil Dynamics Problems," *The Use of Probabilities in Earthquake Engineering*, ASCE, pp 143-176.

Walberg, F.C. (1978) "Freezing and Cyclic Triaxial Behavior of Sands," *Jnl Geotech. Eng. Div.*, ASCE, 104:GT5, May, pp 667-671.

Wanatabe, T. (1966) "Damage to Oil Refinery Plants and a Building on Compacted Ground by the Niigata Earthquake and their Restoration," *Soil and Foundations* (Japan), 6:2, Mar, pp 86-99.

Werner, S.D. et al. (1979) "Structural Response to Traveling Seismic Waves," *Jnl Struct. Div.*, ASCE, 105:ST12, Dec, pp 2547-2564.

Westergaard, H.M. (1933) "Water Pressure on Dams during Earthquakes," *Trans. Amer. Soc. Civil Eng.*, 98, Paper No. 1835, pp 419-433.

Wong, H. and Luco, J.L. (1980) *Soil/Structure Interaction: A Linear Continuum Mechanics Approach (CLASSI)*. Los Angeles: Univ. of South. Calif.

Wong, R.T. et al. (1975) "Cyclic Loading Liquefaction of Gravelly Soils," *Jnl Geotech. Eng., Div.*, ASCE, 101:GT6, Jun, pp 571-583.

Wyss, M. and Brune, J.N. (1967) "The Alaska Earthquake of 28 March 1964: A Complex Multiple Rupture," *Bull. Seismol. Soc. Amer.*, 57:5, Oct, pp 1017-1023.

Yegian, M.K. and Whitman, R.V. (1978) "Risk Analysis for Ground Failure by Liquefaction," *Jnl Geotech. Eng. Div.*, *ASCE*, 104:GT7, Jul, pp 921-938.

Youd, T.L. and Hoose, S.N. (1977) "Liquefaction Susceptibility and Geologic Age," *Proc. 6th World Conf. on Earthq. Eng.*, *Vol. 6, Dynamics of Soil and Soil Structures*, New Delhi, Jan, pp 6-37 to 6-42.

Youd, T.L. and Perkins, D.M. (1978) "Mapping Liquefaction-Induced Ground Failure Potential," *Jnl Geotech. Eng. Div.*, *ASCE*, 104:GT4, Apr, pp 433-446.

Zienkiewicz, O.C. and Humpheson, C. (1977) "Viscoplasticity: A Generalized Model for Description of Soil Behavior," *Num. Method. Geotech. Eng.*, eds. C.S. Desai and J.T. Christian. New York: McGraw-Hill, pp 116-147.

Zienkiewicz, O.C. et al. (1978) "Nonlinear Seimic Response and Liquefaction," *Intl. Jnl. Num. Analyt. Meth. Geomech.*, 2, pp 381-404.

————. (1980) "Effective Stress Dynamic Modelling for Soil Structures Including Drainage and Liquefaction," *Proc. Intl. Symp. Soils under Cyclic and Trans. Loading, Swansea, Jan*, pp 551-554.